Radiotracer Studies of the Chlorination of γ-Alumina and the Catalytic Dehydrochlorination of 1,1,1 Trichloroethane.

This thesis is presented for the degree of

Doctor of Philosophy

by

JAMES THOMSON

Department of Chemistry
University of Glasgow
Glasgow G12 8QQ

November 1988.

To the memory of DARRELL THOMSON (8.4.77 - 3.10.85), a fine son, who was fatally injured in a road accident at the beginning of this work.

ACKNOWLEDGEMENTS

I would like to thank my supervisors Prof. G. Webb and Dr. J.M. Winfield (Glasgow University) for their help and guidance during my period of study at Glasgow University. I am also indebted to Dr. B. Webster (Glasgow University), Mr. R. MacRae and Mr. J. Buchanan (Computer Services) for their help and guidance during the quantum chemical studies. I would also like to thank my colleagues in the catalyst and fluorine groups for their friendship and many discussions chemical or otherwise.

Without the assistance provided by Mr. W. McCormick (glassblowing), Mr. T. Boyle, Mr. R. Spence and Mr. L. McGhee (technical assistance) this project would have been a more difficult task, and I would like to express my sincere appreciation for their various contributions.

I would also like to thank Mrs. Liz Hughes for her fast and efficient typing of this text.

Special thanks go to my wife Lynne, for her encouragement and support throughout the course of this work. The demonstratorship awarded to me by Glasgow University is also gratefully acknowledged.

CONTENTS

3.3 Experimental

5.3 Experimental

SUMMARY

The chlorination of calcined γ-alumina samples using anhydrous gaseous [^{36}Cl]-chlorine labelled hydrogen chloride, anhydrous gaseous [^{36}Cl]-chlorine labelled carbon tetrachloride, and anhydrous gaseous [^{14}C]-carbon labelled carbon tetrachloride has been studied together with the dehydrochlorination of 1,1,1 trichloroethane over the chlorine promoted γ-alumina surface at 293K.

The uptake of chlorine by the calcined γ-alumina materials in conjunction with the B.E.T areas of the calcined materials has shown that up to 50% more surface chlorine resulted from the carbon tetrachloride treatment of a given γ-alumina sample calcined above 373 K compared with the corresponding hydrogen chloride treatment.

It has been shown that treatment of the γ-alumina material with anhydrous gaseous hydrogen chloride resulted in labile surface chlorine. This treated surface was shown to be catalytically inactive towards the dehydrochlorination of 1,1,1 trichloroethane at 293K. Treatment of calcined γ-alumina with carbon tetrachloride at 500K resulted in two forms of surface chlorine being produced one of which was not labile and consisted of ~40% of the total chlorine present at the surface. Catalytic activity towards the dehydrochlorination of 1,1,1 trichloroethane at 293K was shown to occur at surface sites which possessed non-labile surface chlorine.

The labile properties of the catalytically inactive surface chlorine allowed the selective labelling of the

catalytically active site with [^{36}Cl]-chlorine. This selective labelling technique has shown that the dehydrochlorination reaction of 1,1,1 trichloroethane at 293K over the chlorine promoted γ-alumina surface was consistent with a concerted intramolecular dehydrochlorination mechanism.

Ab-initio SCF-UHF MO calculations using SV-321 G basis sets to cluster models of the aluminium environments present at the surface of γ-alumina suggest that the active site may consist of a co-ordinatively unsaturated dichlorinated aluminium environment. The SCF-UHF MO calculations showed that a stabilization of the LUMO orbital energy occurred by the addition of chlorine to the γ-alumina cluster model together with a lowering of the Fermi level of the cluster. The ab-initio calculations also show that the Brønsted acid character of a protonated cluster was enhanced by the addition of chlorine, as measured by the energy required to deprotonate the cluster, and that a strong Brønsted acid site required a near neighbour Lewis acid aluminium environment.

CHAPTER 1.

INTRODUCTION

Alumina is used as a support material in many industrial catalytic processes (1-2). Transition metal sulphides (Mo, W, Co, Ni etc)(3) supported on γ-alumina are catalytically active towards hydronitrogenation, hydrodesulphurisation, dehydrodeoxygenation or hydrodemetallation reactions of heavy petroleum fractions (4-5), whilst supported noble metals are used in reforming reactions (6-17). These catalysts are said to be bifunctional since both the metal and oxide components play active roles. Alumina is far from a passive inert support in these bifunctional catalysts (3,18).

The addition of chlorine to alumina enhances its activity for skeletal transformations of hydrocarbons. Chlorine promoted alumina is widely used as the acidic component of bifunctional reforming catalysts owing to its high selectivity for skeltal isomerization of alkene intermediates produced under reforming conditions (19-21). To produce a chlorine-promoted alumina catalyst active towards low temperature dehydration, dehydrohalogenation or isomerization reactions the chlorinating reagents must be able to donate two chlorine atoms and receive one oxygen atom in such a manner that the resulting oxygenated product is easily removed from the reaction zone (22). The chlorine-promoted γ-alumina possesses acid sites which are strong enough to degrade uninhibited chlorohydrocarbons at

room temperature. The degradation of uninhibited chlorohydrocarbons was previously known to take place on strong Lewis acid catalysts such as aluminium trichloride (23-24) or iron chloride (25).

1.1 Phases of Alumina

The catalytic behaviour of alumina is dependent upon the mode of preparation (26-35). There is only one stoichiometric oxide of aluminium (36), that is alumina, Al_2O_3. However this simplicity is compensated for by the existence of polymorphs and several hydrated species (37-44). Classification of the polymorphs based upon the crystallographic structures of the aluminas has been implemented (45).

Three distinguishing series are identified based on the close packed oxygen lattices with aluminium ions in octahedral and tetrahedral interstices. They are the α-series with hexagonal close-packed lattices schematically ABAB....., the β-series with alternating close-packed lattices schematically ABAC-ABAC or ABAC-CABA, and the γ-series with cubic-packed lattices schematically ABC ABC....

The sole representative of the α-series is α-alumina with aluminium atoms in the octahedral interstices, which is obtained in the form of stable Corundum or as the decomposition product of Diaspore (46). The β-series is represented by alkali or alkaline earth oxides containing β-alumina and the decomposition products of Gibbsite (χ and κ-alumina) which have a related structure (47). The γ-series is prepared from the decomposition products of the

hydroxides bayerite, nordstrandite and boehmite and this group is subsequently divided into γ- or low temperature groups (η- and γ-alumina), and the high temperature δ- or high temperature group (δ and θ-alumina)(48).

In this work we will investigate the properties of the low temperature phase of γ-alumina.

1.2 Preparation of γ-Alumina.

Well crystallized boehmite from which γ-alumina is obtained, is the end product of the aging process of aluminium hydroxide gel at pH>12 and at a temperature of 353K (49).

When an aqueous solution containing Al^{3+} ions is neutralized with ammonia, bulky amorphous precipitates containing large amounts of water are formed (36). The first precipitate is a gel-like substance which gives a diffuse X-ray powder diffraction diagram. The slurry from this precipitate is normally aged at temperatures between 313K and 353K at a pH>12 (49) for approximately 8 hours (50). If the aging process is prolonged, bayerite is formed, hence the particulars of this aging procedure are important in determining the properties of the final product. After aging the precipitate is filtered, washed and dried. The final operation in the preparation of γ-alumina consists of heating the solid at temperatures up to 873K.

During the thermal treatment, alumina passes through various states of hydration and several distinct

compounds are observed. The dehydration of the hydroxide, $Al_2O_3.3H_2O$; $Al(OH)_3$, involves three different compounds, gibbsite, bayerite, and nordstrandite. The particle size and crystallinity of gibbsite are usually greater than those of bayerite and nordstrandite and up to 25% boehmite is formed in gibbsite, whereas usually less than 5% boehmite is formed in bayerite and nordstrandite (51-53). Under vacuo the three hydroxides decompose at low temperatures to give the amorphous product, ρ-alumina which at higher temperatures converts to γ- or η-alumina and further into θ-alumina. The dehydration process of the hydroxides is shown schematically in figure 1.1.

The dehydration of the oxyhydroxides ($Al_2O_3.nH_2O$; n = 1 to 0 : For n = 1; AlO-OH) is dependent on its crystallinity. Well crystallized boehmite comprising of crystal sizes 71μm, decomposes according to the sequence:-

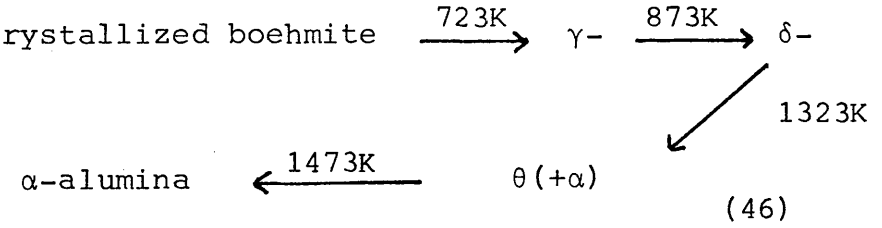

(46)

The δ-phase is strongly dependent upon the crystallinity of the boehmite and on any impurities present. If the boehmite is less crystalline, the formation of the δ-phase is retarded in favour of the formation of the θ-phase.

The important compoundsfor catalyst supports or promoted catalysts are the η- and γ-aluminas. They represent supports with high surface areas and thermal

Figure 1.1

Dehydration sequences of aluminium hydroxide.
{refs. 43 - 45}

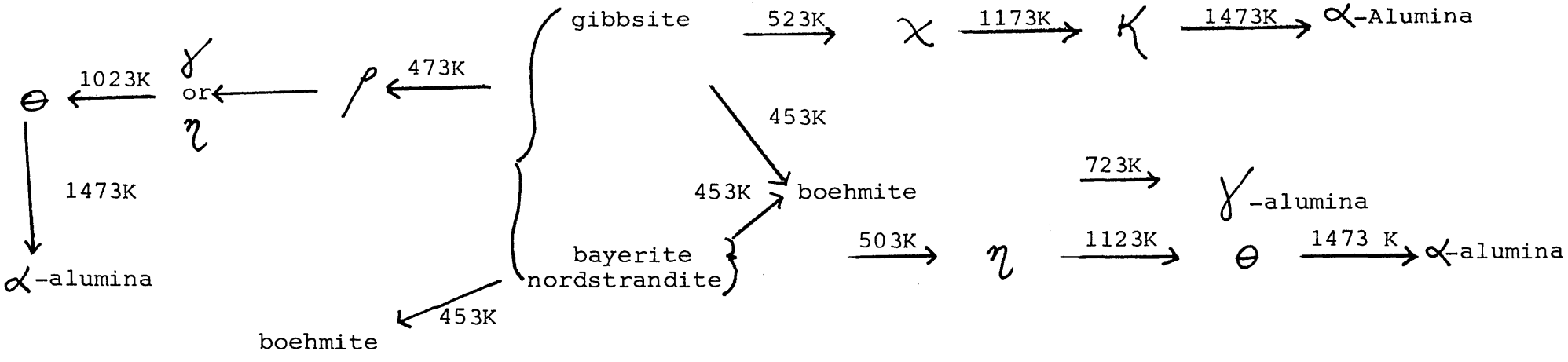

stability. One of their most important structural characteristics is the cubic close packing of oxygen which forms a lattice that is closely related to Spinel ($MgAl_2O_4$) (54-55).

1.3 Structural Properties of γ-Alumina.

The unit cell of Spinel (AB_2O_4) is formed by a cubic close packing of 32 oxygen atoms with 16 trivalent atoms in half of the octahedral interstices and eight divalent atoms in tetrahedral holes (56). Powder X-ray diffraction has established that γ-alumina crystallizes with a Spinel-related structure (46) in which 32 oxygen atoms per unit cell are arranged exactly as in Spinel but with 21 1/3 aluminium atoms distributed over the 24 cation positions available (57). There are on average 2 2/3 vacant cation sites per unit cell. Electrical neutrality is partially achieved by the occurrence of these vacant sites. The crystallite surface contains hydroxyl groups in place of oxygen ions which further contribute to the electrical neutrality of the γ-alumina crystallite.

The cleavage plane of boehmite is parallel to any array of parallel rows of oxygen atoms. The [110] face of boehmite is the cleavage plane, since γ-alumina maintains the spinel form of a cubic close-packed oxygen lattice. Cleavage of the [100] and [111] faces would result in a hexagonal close-packed stacking of oxygen atoms as in η-alumina (58).

During dehydration the array of oxygen atoms

remains in the spinel form, hence these parallel rows stack exclusively to form a cubic close-packed lattice resulting in the fairly well ordered oxygen lattice of γ-alumina. Two repeating types of layers can be derived from the [110] face of the spinel unit of γ-alumina (Figure 1B), and represented schematically as CDCD... The C-layer has equal numbers of tetrahedral and octahedral sites (Figure 1C). The D-layer has only octahedral Al^{3+} ions (Figure 1D).

The occurrence of sharp and diffuse lines in the X-ray diagram of γ-alumina indicated that the lattices are strongly disordered (59). The disorder in the γ-alumina is caused by the aluminium atoms. The cation distribution of γ-alumina was determined by Fourier Synthesis of the electron diffraction patterns (60) and it was found that the octahedral aluminium sublattice is fully occupied and hence the necessary vacant sites are distributed randomly over the tetrahedral interstices.

It is the surface of γ-alumina which is important in catalysis and since γ-alumina occurs in the form of lamellae, it is most probable that one type of surface plane is predominant, and for the reasons discussed above the predominant surface plane is likely to be the [110]plane (46).

The stoichiometry of γ-alumina based on the unit cell can be obtained from figures 1C and 1D to give $Al_{2.5}\square_{0.5}O_4$. In its fully hydroxylated or precursor state a significant fraction of the anions are hydroxyl groups which occupy the surface of a particle. By including

Figure 1B

Spinel Unit Cell

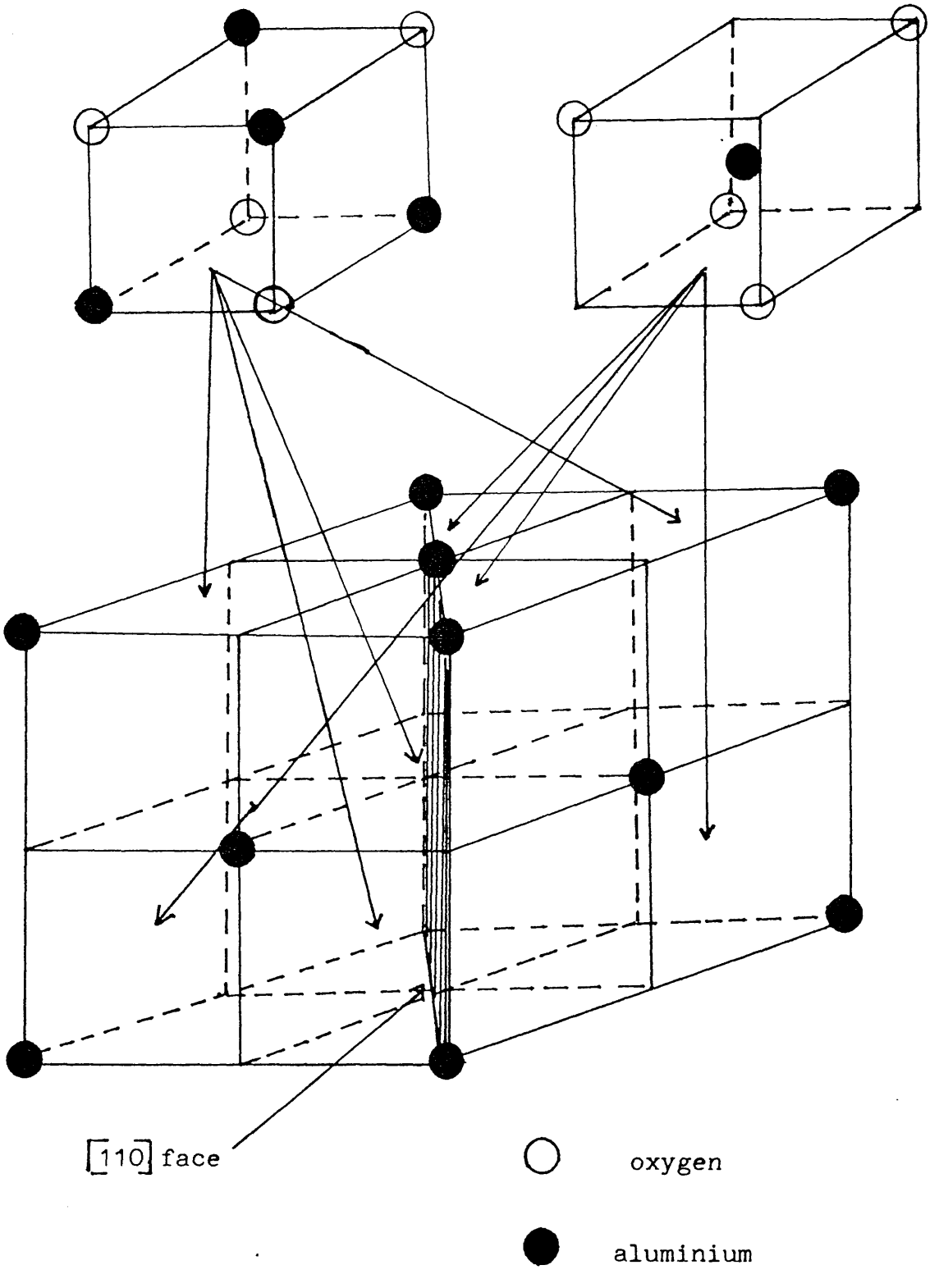

Figure 1C.

[110] Face of Gamma Alumina

C-layer

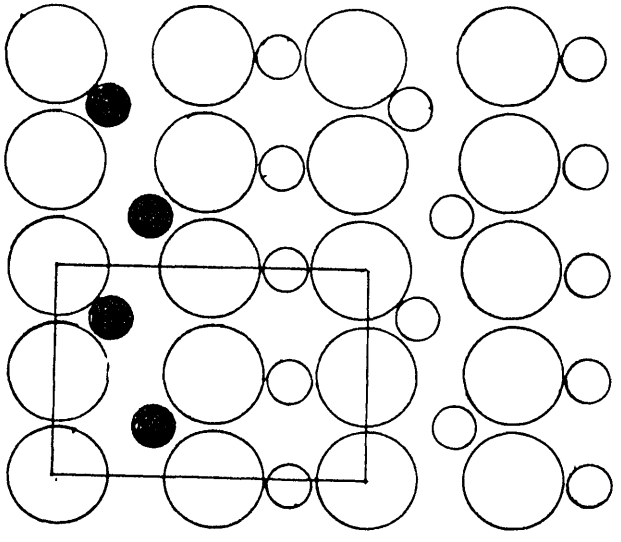

Contains both tetrahedral and octahedral aluminium atoms.

Figure 1D

[110] Face of Gamma Alumina

D-layer

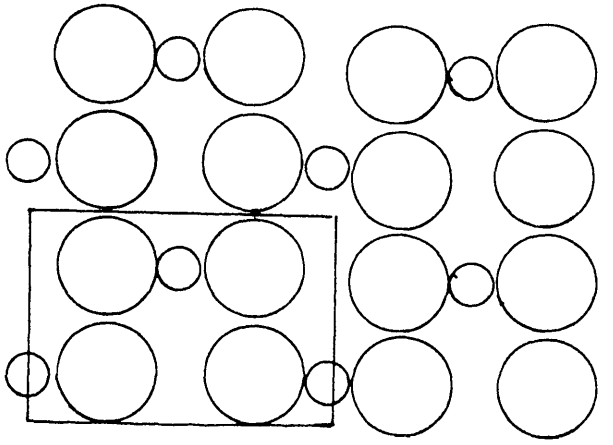

Contains exclusively octahedral aluminium atoms.

these hydroxyl groups we arrive at a precursor formulation of $Al_{2.5}H_{0.5}O_4$ or $Al_{2.5}\square_{0.5}O_{3.5}(OH)_{0.5}$. This formula of γ-alumina in its hydroxylated state was briefly discussed at a conference thirty five years ago (61) and has been confirmed recently (62).

A three dimensional representation of the surface of γ-alumina can be extrapolated from figures 1C and 1D. In this model there are six distinct aluminium environments that may occur for terminal hydroxyl groups (Figs. 1E, 1F) and this model illustrates the heterogeneity of the γ-alumina surface. In a separate model building study (63) five distinct aluminium environments were identified, however that model was based on the [100] face of γ-alumina.

1.4 Surface Hydroxyl Groups of γ-Alumina.

Active γ-alumina adsorbs water at the surface either as hydroxyl groups or as water molecules. When γ-alumina is exposed to water vapour at room temperature, the water is adsorbed as undissociated molecules bonded via strong hydrogen bonds to the underlying surface. At high water vapour pressures more water is bonded as a multilayer physical adsorption process (64). This water is easily removed when the sample is dried under vacuum at 393K (65). Infrared spectroscopy provides evidence for the occurrence of undissociated water molecules at low temperatures. With heating, the water molecules that are not desorbed and removed from the system, react to form surface hydroxyl groups (66). On heating to 1123K the surface hydroxyl groups are slowly

Figure 4.

SURFACE STRUCTURE OF [110] FACE OF γ-ALUMINA (IDEALISED DEFECT SPINEL)

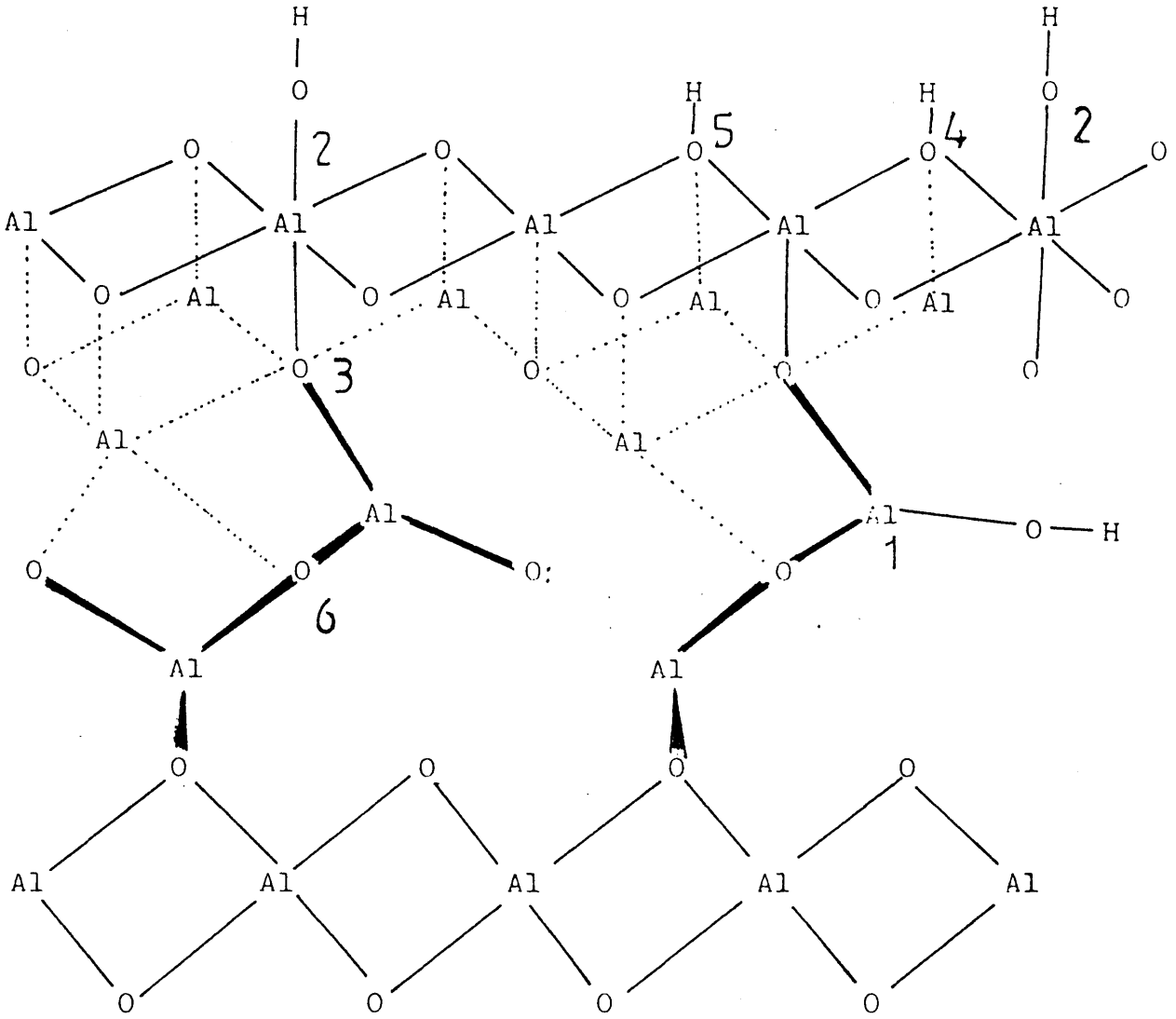

Sites:-

1) tetrahedral
2) octahedral
3) tet-O-oct
4) oct-O-oct
5) oct-O-oct
   |
   oct
6) tet-O-tet

Basic Cluster Models of Gamma Phase Alumina

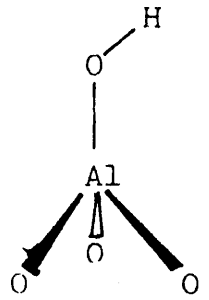

tetrahedral

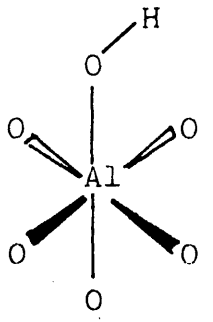

octahedral

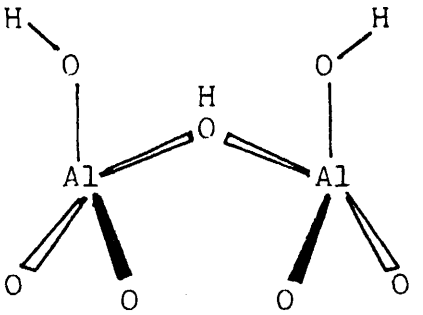

tetrahedral-O-tetrahedral

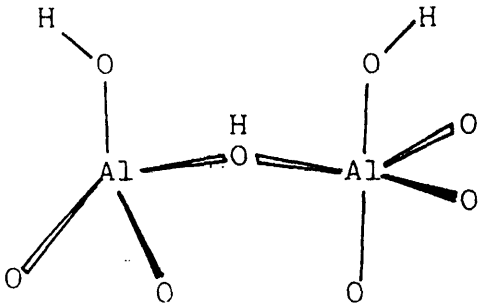

tetrahedral-O-octahedral

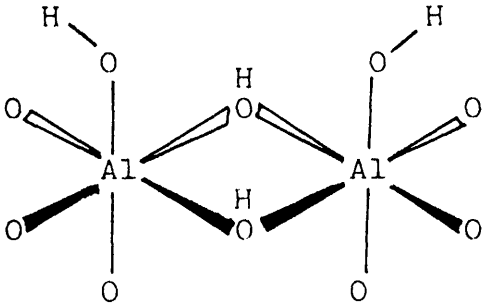

octahedral-O-octahedral

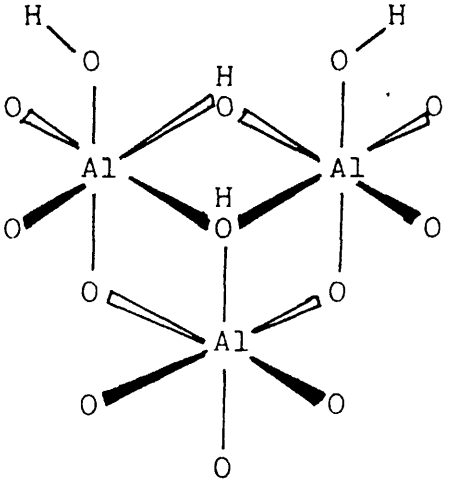

octahedral-O-octahedral
oct

removed as water, by a condensation process. The rate of removal of the surface hydroxyl groups is heterogeneous at these elevated temperatures. This independent behaviour of hydroxyl groups was also observed during the isotopic hydrogen-deuterium exchange of the surface hydroxyl groups (66). The surface hydroxyl group that gives rise to the lowest frequency hydroxyl vibration at 3698 cm^{-1} was able to undergo the ^{1}H - ^{2}H exchange faster than the hydroxyl groups which gave rise to the bands at the higher absorptions at 3737 cm^{-1} and 3795 cm^{-1}. Treatment of the surface with ^{2}H caused all three bands to disappear and be replaced by new bands at 2733, 2759 and 2803 cm^{-1}. All these bands are shifted by a constant factor of 0.738 which is close to the theoretical value for the ^{1}H - ^{2}H isotopic shift thus providing good evidence that the original absorptions were due to stretching vibrations of surface hydroxyl groups and not due to combination bands. By recording the infrared spectrum of all bands at 1073K the three bands broadened and moved to lower wavelengths, the displacement being about 30 cm^{-1}. These three bands remained distinct, together with the appearance of new surface hydroxyl vibrational frequencies that gave rise to absorptions at 3780 cm^{-1} and 3733 cm^{-1}. Since the original three bands remained distinct with only a small displacement and broadening of the absorptions observed at the elevated temperature, this is consistent with surface hydroxyl groups being localized on distinct surface sites, and not in random motion on the catalyst surface (69). The presence of the five types of hydroxyl groups at 1073K was attributed to variations in the number of nearest oxide

neighbours (70) owing to the calcination process. The experimental evidence for five types of hydroxyl groups owing to nearest oxide neighbours is in good agreement with a model building study (63) that also identified five distinct aluminium nearest neighbour environments for terminal hydroxyl groups.

The heat of adsorption of water on the surface of γ-alumina greatly depends upon the water content already retained by the γ-alumina surface. Residual surface water content can be determined by both physical and chemical methods (64,66,71-72) and the results can be expressed as fractional surface coverages. It is found that with an initial low surface coverage of water the enthalpy of adsorption for water is reported to exceed 410 kJ mol^{-1}, while at near complete hydroxyl coverage the enthalpy of adsorption for water is reduced to 82 kJ mol^{-1} (73). By calculating the fractional surface coverage of retained water as a function of calcination temperature it can be concluded that the free energy of activation for desorption of water from the surface will increase continuously as the surface concentration of hydroxyl groups is reduced (69). This feature will result in a finite number of hydroxyl groups being removed during the calcination process to a specific temperature.

1.5 The Brønsted-Lowry Definition of Acids and Bases.

There are similarities in the product distribution resulting from catalysis of many acidic solid surfaces which

contain protons, and by Brønsted acid solutions such as H_2SO_4. Carbonium ion reactions in strong acid solutions have been thoroughly studied and the structures and reactivities of these species are well understood. Isomerization of saturated hydrocarbons takes place through carbonium ion intermediates initiated by a hydride-ion abstraction (74) and isomerization of straight chain paraffins have been carried out in strong acid solutions. Similarly alkylation of isoparaffins by olefins require strong Brønsted acids (H_2SO_4 or HF) and propylation of benzene is catalysed by H_3PO_4 held in pores of kieselguhr.

These reactions are also catalysed by solid surfaces which possess strong Brønsted acid sites. Hence there are tenable similarities in the catalytic activity of homogeneous systems and heterogeneous systems in respect to Brønsted acidity definition.

In 1923, Brønsted and Lowry defined acids and bases in terms of the hydrogen ion or proton, in an attempt to broaden the scope of acid base systems to cover all protonic solvents. It should be emphasized that bases need not contain hydroxyl ions under the Brønsted-Lowry system, as was the requirement in the Arrhenius concept of acids and bases. Acids are defined as proton donors, and bases as proton acceptors. Every acid will have a conjugate base.

$$\text{Acid} \rightleftharpoons \text{Conjugate base}^- + H^+$$

eg:

$$HCl + H_2O \rightleftharpoons H_3O^+ + Cl^- \qquad \text{Equ.I.1}$$

(acid) (base) (conjugate acid) (conjugate base)

Hydrogen chloride is a Brønsted acid since it donates protons and Cl^- is its conjugate base. In aqueous medium H_2O accepts protons, therefore it is a base, and H_3O^+ is its conjugate acid. A strong acid has a weak conjugate base and vice versa. In a solid acid, the conjugate base is a site which accepts a proton and the protonated surface site is its conjugate acid. Hence a strong acid site has a weak conjugate base and a weak acid site will have a strong conjugate base.

In terms of the Brønsted-Lowry definition, it is reasonable to suppose that the catalytic activity of homogeneous and heterogeneous Brønsted acids in reactions that require the supply of protons, is dependent on the magnitude of the Brønsted acid to lose a proton. This ability to lose a proton should be related at least approximately to the dissociation constant of the acid. The dissociation constants of Brønsted acids are measured in aqueous medium and will apply to homogeneous systems in aqueous solution, and do not apply directly to heterogeneous systems. However, the dissociation constant is the equilibrium constant for the deprotonation of a conjugate acid into the conjugate base and a proton. This equilibrium constant is equal to the ratio of the specific rates of the direct and reverse reactions and this can be applied to heterogeneous systems.

Consider the dissociation of the solid acid AlO-OH; the equilibrium

$$\text{AlO-OH} \underset{k'}{\overset{k}{\rightleftharpoons}} H^+ + \text{AlO-O}^- \qquad \text{Equ.I.2}$$

is set up and the equilibrium constant of the system, which is the dissociation constant, is equal to:-

$$K_a = \frac{k}{k'} = \frac{\text{specific rate of reaction of AlO-OH}}{\text{specific rate of reaction } H^+ + \text{AlO-O}^-}$$

the quantity k is a measure of the tendency of the solid acid AlOOH to lose its proton and hence it might be expected to be related to the catalytic effect of the acid.

However it is not possible to separate the equilibrium constant into the component forward and reverse specific rates k and k^1. J.N. Brønsted (1924) (75) suggested the approximate relationships, as applied to homogeneous systems:-

$$k_{HA} = GK_a^x \qquad \text{Equ.I.3}$$

where G and x are constants for a given reaction and k_{HA} is the catalytic co-efficient of the Brønsted acid having the dissociation constant, Ka. According to Equation I.3 the stronger the acid the greater will be its catalytic activity. This has been found to be approximately true for a number of homogeneous catalytic reactions (76). The fact that the catalytic effect of acids in homogeneous systems, varying in strength, can be brought into one scheme lends support to the suggestion that it is a common property which determined the catalytic activity of these catalysts, i.e. the tendency to lose a proton. This property may be applied to solid acids which contain Brønsted acid sites.

It then follows that enhancement of the Brønsted acidity of a solid catalyst will enhance the catalytic activity, towards reactions that require a protonation step

in a catalytic process. Thus the use of promoters to enhance the Brønsted acidity of a solid catalyst will also promote the catalytic activity of the promoted catalyst.

1.6 Lewis Acid-Base Concept.

The role of the electron pair is the basis of the definition of acids and bases proposed by G.N. Lewis in 1923. G.N. Lewis defined an acid substance as one "which can employ a lone pair of electrons from another molecule in completing the stable group of its own atoms", and a basic substance as one "which has a lone pair of electrons which may be used to complete the stable group of another atom." Neutralisation thus corresponds to the formation of a co-ordinate bond. G. N. Lewis also proposed that the main functional criteria of an acid is that a stronger acid is able to displace a weaker acid from its acid base complex.

The forward acid base reaction step is shown in equilibrium I.4 where A represents the acid species and B the basic species:-

$$A + :B \rightleftharpoons A:B \qquad \text{Equ.I.4}$$

Equilibria I.5 to I.7 outline the related heterolytic processes, which follow from the above fundamental relationship outlined in equilibrium I.4. In the following equilibria the acidity of $A^1 > A^2$ and the basicity of $B^1 > B^2$.

$$A^1 + A^2:B \rightleftharpoons A^2 + A^1:B \qquad \text{Equ.I.5}$$

$$B^1 + A:B^2 \rightleftharpoons B^2 + A:B^1 \qquad \text{Equ.I.6}$$

$$A^1:B^1 + A^2:B^2 \rightleftharpoons A^1B^2 + A^2:B^1 \qquad \text{Equ.I.7}$$

A typical Brønsted-Lowry acid-base equilibrium is outlined in Equ.I.6 where the proton in Equ.I.8 represents the Lewis acid in Equ.I.6

$$B^1 + H^+:B^2 \rightleftharpoons B^2 + H^+:B^1 \qquad \text{Equ.I.8}$$

An advantage of the Lewis Acid-Base Concept is that it classifies as acids non-hydrogen containing molecules. A disadvantage however is that the approach is not applied on a quantitative basis since the Lewis Acid-Base approach is made variable by the dependence upon the reaction or method for their evaluation. In order to quantify Lewis acid-base reactions the hard/soft, acid/base formalism of R.G. Pearson (77) has been adopted.

1.6.1 The Application of the Lewis Acid-Base Concept to Heterogeneous Systems.

Although the original Lewis Acid-Base Concepts were based on homogeneous systems, they can be applied to gas solid reactions if the acid base definitions are restated as follows:-

A Lewis acid site on a solid surface is a site which has an unoccupied orbital with a high affinity for an electron pair. When such a site shares an electron pair donated by an adsorbed Lewis base molecule there is a decrease in the orbital energy of the system. Lewis base sites on the surface are those which have electron pairs available and a decrease in the orbital energy results if they share this electron pair with an adsorbed electron pair acceptor.

1.7 Relationship between Surface Properties and Catalytic Activity, and the Quantitative Determination of Site Density.

The presence of surface hydroxyl groups and exposed aluminium atoms created by the thermolytic dehydration of the surface, results in the formation of both Brønsted and Lewis acid sites on the surface of γ-alumina. Strong Brønsted acids are the seat of catalytic activity for skeletal transformations of hydrocarbons (79-86).

Lewis acidity appears as the result of dehydroxylation of the surface. This process occurs at elevated temperatures. A typical Lewis acid site will be a surface aluminium atom from which a hydroxyl group has been removed. The surface density of the Lewis acid centres is dependent on the calcination temperature (Section 1.4)(87,88). γ-Alumina which contains only Lewis acid sites has been shown to be very active in the catalytic cracking of hydrocarbons (89).

A quantitative measurement of the number of Brønsted and Lewis acid sites on the surface of γ-alumina, either as a function of weight of catalyst, or by the specific surface area of the catalyst, may be determined by means of titrating the surface with Lewis bases or by the infrared analysis of the absorbed base. Chemisorption of bases such as pyridine, piperidine, ammonia, quinoline and aliphatic amines is frequently used to characterize solid acid catalysts and to obtain a quantitative measurement of the density of Brønsted and Lewis acid sites on the surface.

In infrared analysis, pyridine has been the most widely used base for acid characterization purposes as it can interact with both Brønsted and Lewis sites giving specific infrared absorption bands for the pyridinium ion and co-ordinately bound pyridine to aluminium (66,87,90-92).

In titration work, it has been shown (93) that the chemisorption of sterically hindered dimethylpyridine and ditertiarybutylpyridine can be very useful probe molecules in specifically titrating Brønsted acid sites. These bulky groups at the 2,6 positions of the pyridine ring render the molecule sterically specific for the protonic centres since they hinder the formation of the Al-N bond at a Lewis acid site (92). These substituted groups increase the basicity of the ring, relative to pyridine, owing to the methyl groups having a positive inductive effect on the pyridine ring (96). This in turn leads to the formation of a stronger bond being formed between the pyridine ring and the surface proton in the substituted pyridines, relative to pyridine itself.

Therefore where an acid catalyst contains both Brønsted and Lewis acid sites titrating with pyridine will quantify the total number of acid sites on the catalyst surface. Titrating the surface with substituted pyridines will quantify the total number of Brønsted acid sites and hence the total number of Lewis acid sites are obtained by difference.

1.8 Chlorination of γ-Alumina.

Addition of chlorine to γ-alumina enhances the catalytic activity of the Lewis and Brønsted acid sites. At low chlorine levels (0.1 - 1% by weight) chlorine promoted γ-alumina is widely used as the acidic component of bifunctional reforming catalysts owing to its high selectivity for isomerization of alkene intermediates produced under reforming conditions (19-21). This high selectivity of chlorinated alumina at low loadings of chlorine towards isomerization of olefins is attributed to the small increase in the acidity of the surface relative to the acid strengths required at reforming conditions (97). The low loadings of chlorine on γ-alumina produce acid sites that are not strong enough to break the carbon-carbon bonds in hydrocarbons as would be the case required of strong acidic oxides at reforming conditions. Comparison of the promotional effects of chlorine and fluorine indicate that fluorine is indeed the stronger promoter towards catalytic activity in the cracking of hydrocarbons, and this is attributed to the greater electronegativity of fluorine. The acid sites produced by chlorine promotion are weaker than those created in the case of fluorine, and this has been confirmed by acidity measurements with arylcarbinol (98).

Although chlorine promoted γ-alumina is not strongly acidic at low chlorine levels infrared studies demonstrated that the chemisorption of hydrogen chloride on γ-alumina does form Brønsted acid sites as well as non-acidic hydroxyl groups (99). Infrared spectra of chemisorbed pyridine examined before and after the γ-alumina had been exposed to

anhydrous gaseous hydrogen chloride showed the formation of the absorption band due to the pyridinium ion at 1545 cm^{-1}. This is direct evidence for the creation of Brønsted acid sites in the chlorinated product (1.6% by weight chlorine).

Strongly acidic chlorinated γ-alumina, which contain up to 15% by weight chlorine content, have been prepared by the reaction of alumina with the chlorinating reagents in table 1.1

These strong acid chlorine promoted γ-aluminas can be prepared by passing carbon tetrachloride vapour in an inert carrier gas over predried γ-alumina at temperatures above 423K (22). The carbon tetrachloride reacts with oxide and hydroxyl groups on the γ-alumina surface to produce carbon dioxide, phosgene, hydrogen chloride and water in the exit gases. These 'high activity' surfaces prepared from the chlorination of γ-alumina by chlorocarbon reagents require an oxygen sink and a chlorine source, such as solid carbon and chlorine, carbon monoxide and chlorine, phosgene, or carbon tetrachloride. The rate of chlorination of the γ-alumina surface when using phosgene is greater than those obtained when carbon monoxide and chlorine, or carbon and chlorine are used at much higher temperatures (111,115-116). The kinetic advantage is thought to be related to the requirement that phosgene exists on the γ-alumina surface prior to the formation of the metal chloride. Phosgene has been detected 'in situ' as the predominant adsorbed species on the surface of γ-alumina chlorinated by carbon tetrachloride (117). The use of a solid carbon source (coke or coal) with chlorine

Table 1.1

Reagent	Reference
Aluminium Chloride	22, 100
Carbon Tetrachloride	22, 101-104
Phosgene	101-103, 105-109
Chloroform	102
Tetrachloroethylene	102
Sulphur Dichloride	102
A mixture of Carbon monoxide and dichlorine	107, 110-111
Carbon with dichlorine	112-113

has limitations. It has been shown that the carbon must be within 30 microns of the γ-alumina surface to obtain reasonable chlorination rates (112,118) and it is suggested that the close proximity is necessary for successful transfer of active chlorine species from carbon to the γ-alumina surface. Coking of the γ-alumina surface has been prepared by using hydrocarbons in a reducing atmosphere prior to the admission of chlorine to the system (110,113).

It appears that the basic reaction of the chlorocarbons with the γ-alumina surface involves the chlorination of oxygen containing groups on the surface of the catalyst with the simultaneous elimination of the oxygen atom from the γ-alumina surface. It is believed that this relationship defines the unique character of the chlorination reaction and the specific range of chlorine compounds necessary to bring the reaction about. Thus the chlorinating reagent must be one that can donate two chlorine atoms and receive one oxygen atom in such a manner that the resulting oxygenated product is easily removed from the reaction zone. Hence the chlorocarbon reagent must contain derivatives of methane possessing at least two chlorine atoms to satisfy this requirement.

When nitrogen or oxygen are used as the carrier gas for the carbon tetrachloride chlorinating reagent during the chlorination of γ-alumina, active low temperature isomerization catalysts are obtained. However, when hydrogen was used as the carrier gas an inactive catalyst towards low temperature isomerization reactions was produced with copious amounts of hydrogen chloride being formed (22). It

has been shown that direct chlorination of γ-alumina by hydrogen chloride gas does not lead to the formation of an active catalyst, and it appears that the hydrogen stream reduces the carbon tetrachloride to hydrogen chloride faster than the carbon tetrachloride can chlorinate the γ-alumina surface.

Examination of the stoichiometry of the chlorination reaction when carbon tetrachloride vapour is passed at a high gas flow over the γ-alumina has shown that approximately equal amounts of reactive chlorine are incorporated into the catalyst and appear in the effluent gas. Mass spectromeric analysis of the effluent has shown that the major chlorine reaction product under the above conditions is phosgene and at reduced gas flow, increasing amounts of carbon dioxide are detected, indicating that the primary reaction product phosgene is undergoing a similar secondary reaction (22).

These chlorocarbon chlorinating reagents produce acid sites on the surface of γ-alumina that are several orders of magnitude more active for skeletal isomerization and the cracking of hydrocarbons than γ-aluminas promoted by hydrogen chloride. The high acidity of these acid surfaces are catalytically active towards the low temperature isomerization of aliphatic hydrocarbons and it is suggested that these chlorine promoted materials have acid sites that approach those of Friedel-Crafts catalysts $HCl/AlCl_3$ (114).

1.9 The Dehydrochlorination of 1,1,1 trichloroethane over Strong Acid Aluminium Surfaces.

Aluminium is a very reactive metal and it can react with a number of chlorinated hydrocarbons. The reaction between aluminium and carbon tetrachloride has been studied (119-120) and it has been shown that the aluminium metal is oxidised to aluminium trichloride (121). The addition of water promotes corrosion at the solvent-water interface and this has been attributed to the formation of a hydroxylated surface and/or bonded water (122).

At elevated temperatures (473K) it is known that the dehydrochlorination of 1,1,1 trichloroethane occurs over aluminium oxide (125) with the formation of aluminium trichloride as the reaction product. The proposed reaction sequence involves the adsorption of 1,1,1 trichloroethane onto the aluminium oxide surface via an aluminium-chlorine bond, by the displacement of an adsorbed hydroxyl group or water molecule (125). Ionisation of the carbon-chlorine bond then occurs to give the dichloroethane carbonium ion which then loses a proton to give 1,1 dichloroethene, that is identified as a gas phase product. The aluminium chloride formed, which is a strong Lewis acid has been shown to polymerise the gaseous 1,1 dichloroethene product from the dehydrochlorination reaction on the surface of aluminium trichloride (23).

It has been demonstrated that refluxing uninhibited 1,1,1 trichloroethane with high surface area γ-alumina causes the dehydrochlorination of the solvent to give

1,1 dichloroethene and hydrogen chloride (24). This reaction has been confirmed in this work by the thermolytic cracking at 403K, of gaseous 1,1,1 trichloroethane over γ-alumina precalcined to 523K. The effect of a high calcination temperature on the γ-alumina favours the formation of 1,1 dichloroethene (126-127). The mechanism of elimination of hydrogen chloride from the 1,1,1 trichloroethane was assumed to vary continuously, depending on the acid-base nature of the catalyst and the reactants (127,128-129). The chlorine and proton being eliminated almost simultaneously by the acid and base sites of the γ-alumina surface. γ-Alumina is known to have basic as well as acidic sites due to the dehydrated structure of the surface (88,130-131). It has already been established that the selective dehydrochlorination of 1,1,1 trichloroethane can be base catalysed (132) or acid catalysed by strong Lewis acid sources (123).

In this work the acid catalysed reaction was studied by producing strong Lewis acid sites via the treatment of γ-alumina with carbon tetrachloride at 523K.

CHAPTER 2.

EXPERIMENTAL

In this work, it was important to ensure that all moisture and air were excluded from the reactions examined owing to the hygroscopic properties of calcined γ-alumina and chlorinated γ-alumina. All the work was, therefore, performed in vacuo (10^{-4} Torr) or in an inert atmosphere box ($H_2O \leqslant 10$ ppm) and every precaution was taken to exclude water.

2.1 Equipment

2.1.1 The Vacuum System.

The vacuum line (Figure 2.1) was an enclosed Pyrex glass structure which consisted of a manifold, a constant volume manometer and a Vacustat, all of which were individually isolable. The line was pumped by means of a mercury diffusion pump and an oil-sealed rotary pump to a pressure of 10^{-4} mm.Hg. The pumps were protected from any volatile material in the line, by a series of waste traps. These were situated directly before the pumps and were long glass tubes surrounded by liquid nitrogen which trapped any volatile substance. The pumps and waste traps could be isolated from the rest of the line using a glass tap. The vacustat was used to measure the pressure which the pumps achieved.

The constant volume manometer was used to measure pressures of gases in the line to an accuracy of ± 0.5 Torr. The main manifold had various B14 ground glass sockets which

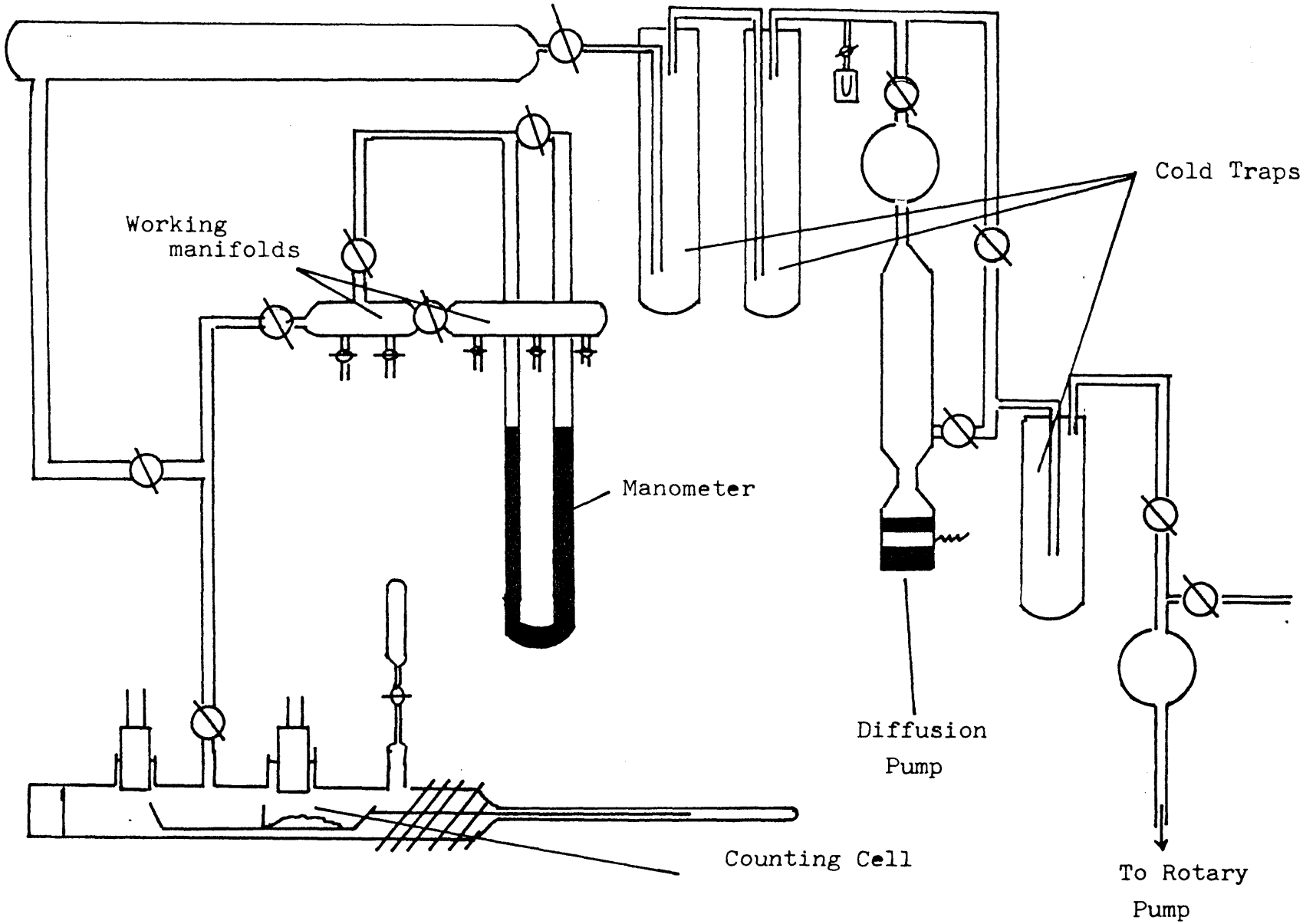
Working
manifolds
Manometer
Cold Traps
Diffusion
Pump
Counting Cell
To Rotary
Pump

Figure 2.1

could be isolated from the line using high vacuum stop-cocks (J. Young). Vacuum flasks (Figure 2.2) and ampoules (Figure 2.2), equipped with high vacuum stop-cocks (J.Young) and B14 cones, were attached to the sockets of the manifold using Kel-F grease. All vessels and the line itself were flamed out, while the system was pumping, using a gas/oxygen flame. This process results in a substantial reduction in the amount of absorbed moisture on a glass surface (141).

2.1.2 The Inert Atmosphere Box:

A nitrogen atmosphere glove box (Lintott) ($H_2O \leqslant 10$ ppm) was used when handling and storing all samples. Glass vessels used were previously evacuated and flamed out before being transferred to the box. The box contained a balance which allowed samples to be weighed.

2.2 Preparation and Purification of Reactants.

2.2.1 Preparation and Purification of [^{36}Cl]-Chlorine Labelled Dichlorine.

The main consideration in the preparation of [^{36}Cl]-chlorine labelled dichlorine was to produce anhydrous $^{36}Cl_2$ with a high specific activity. The uncertainty in a count N is $[N]^{\frac{1}{2}}$. If an active sample can produce 10^4 counts, this leads to an uncertainty of only 1%. In exchange reactions it is desirable to monitor the system at short intervals. The sample, therefore must be sufficiently active to produce a large number of counts in a short counting time. The preparation of $^{36}Cl_2$ was carried out

Figure 2,2

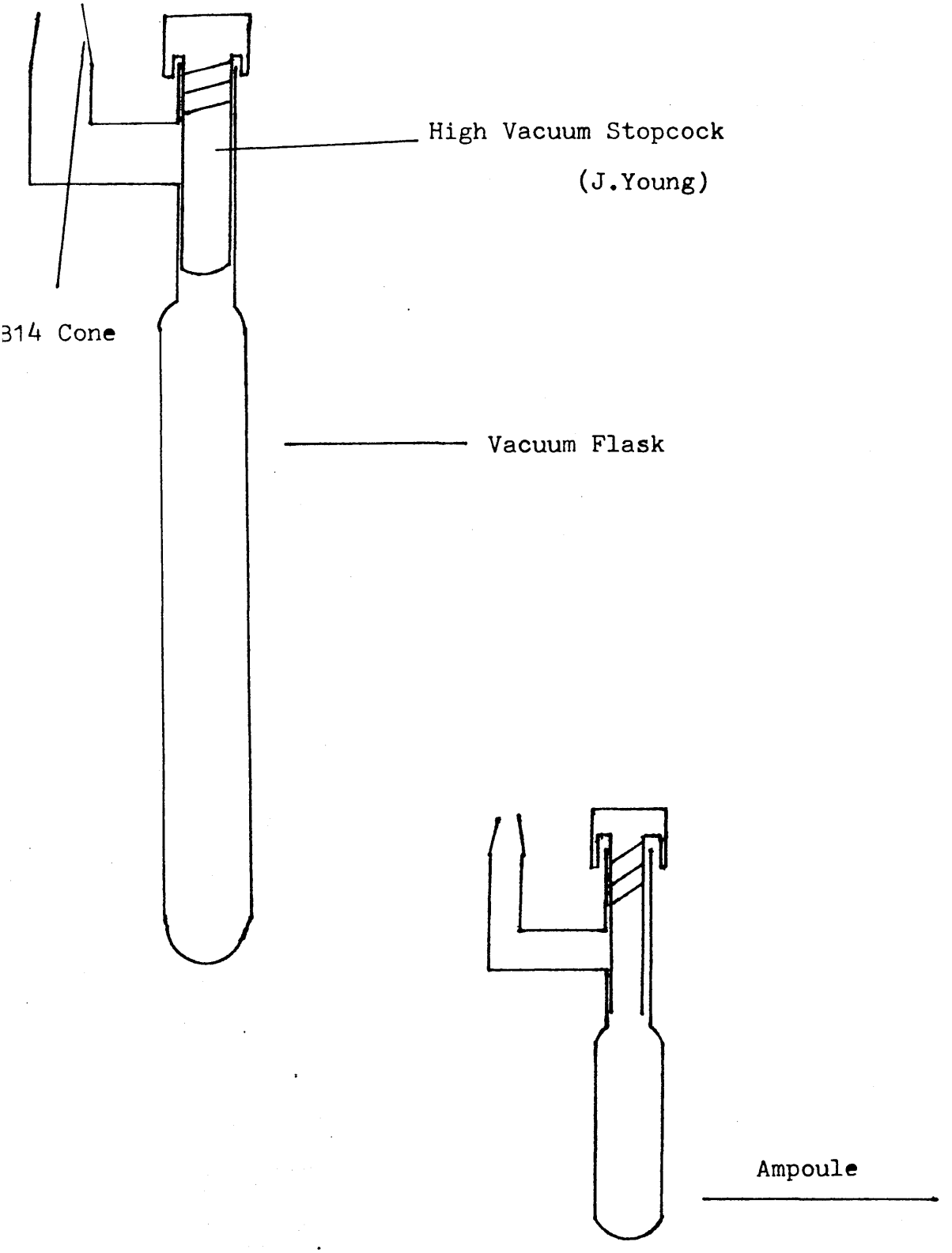

by the following procedure using the apparatus shown in figure 2.3.

[^{36}Cl]-chlorine labelled dichlorine was prepared by the reaction of [^{36}Cl]-chlorine labelled hydrochloric acid with potassium permanganate solution, according to Equation 2.1 (142)

$$4\ H^{36}Cl + KMnO_4 \longrightarrow [36Cl]\text{-}KCl + MnO_2 + 2H_2O + {}^{3}/_{2}\ [36Cl]\text{-}Cl_2$$

Equation 2.I.

[36Cl]-Chlorine labelled Cl_2 was generated in a round bottom flask reaction vessel (Figure 2.3, Vessel 1) to which a series of cooled traps were attached. Traps (ii) and (iii) contained solid $KMnO_4$ to remove HCl, and were cooled to 193K in dichloromethane/solid CO_2 baths. Traps (iv) and (v) contained solid phosphorus pentoxide to remove moisture, and were cooled to 193K in dichloromethane/solid CO_2 baths. The collection vessel (vi) was equipped with high vacuum stopcocks (J.Young) in order that it could be isolated from the rest of the apparatus. The ground-glass joints in the apparatus were sealed with Kel-F grease and the whole system, apart from the three necked flask, was evacuated before the reaction. The operations were carried out in dry air at reduced pressure.

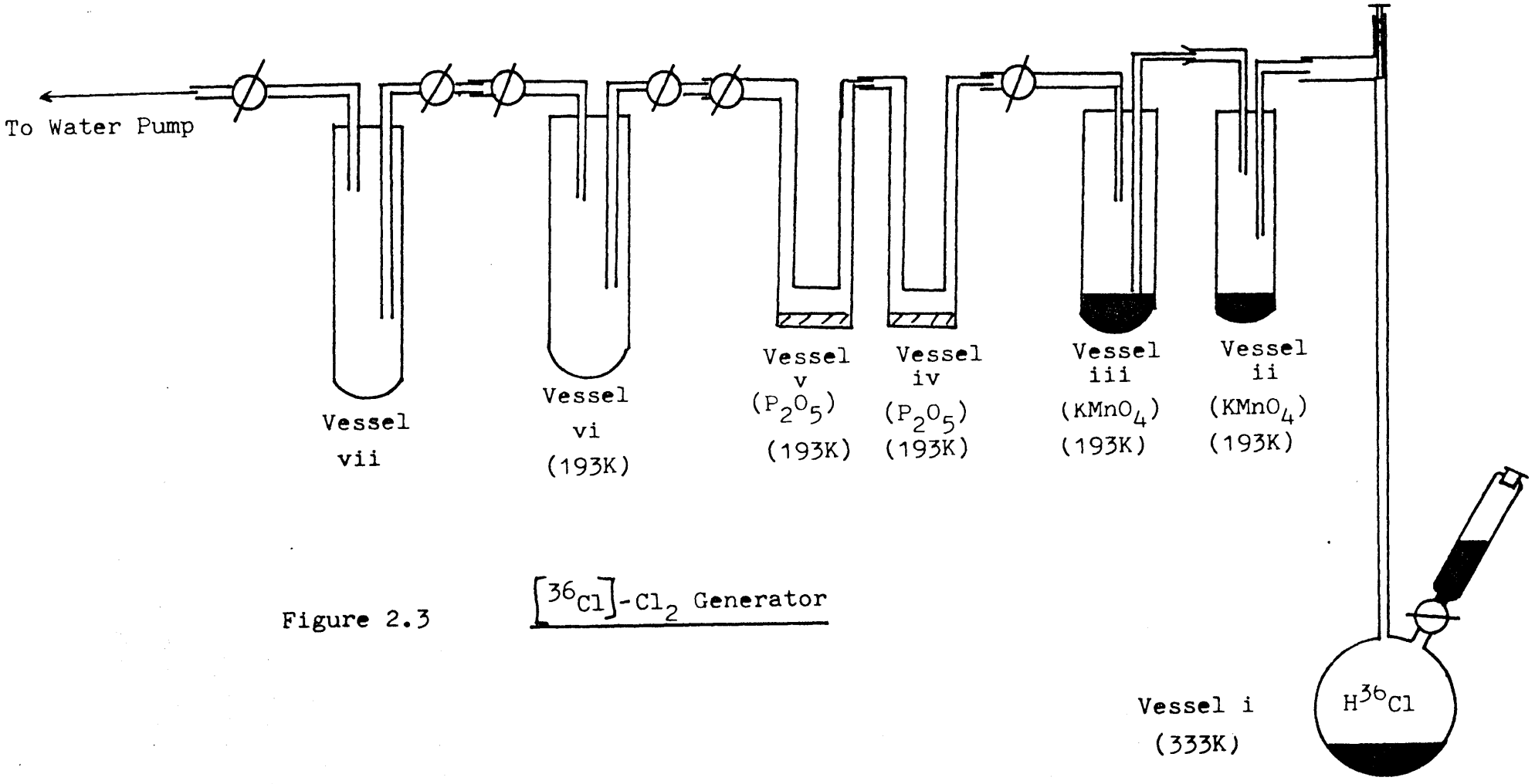

Figure 2.3 $[^{36}Cl]$-Cl_2 Generator

Aqueous [^{36}Cl]-NaCl (2.4 ml, 60 μCi, Amersham International) was added to 35.4% w/n hydrochloric acid (30 ml Hay's Chemicals) in (i) which was heated to 333K in a water bath. A saturated solution of $KMnO_4$ (16.0g $KMnO_4$/300ml H_2O) was added dropwise with stirring. The [36Cl]-Cl_2 liberated was distilled through traps (ii) to (v) and collected in (vi) at 193K. Trap (vi) was transferred to a vacuum line where the [36Cl]-Cl_2 was degassed and stored over phosphorus pentoxide in a Monel bomb.

2.2.2 Preparation and Purification of [36Cl]-Chlorine Labelled Hydrogen Chloride (143-144).

The main considerations were to produce anhydrous $H^{36}Cl$ with a high specific activity. The procedure was adopted from a literature method (143) to suit the radiochemical purpose.

$$H^{36}Cl\ (aq) + H_2SO_{4(aq)} \longrightarrow H^{36}Cl\ (g) + H_2SO_4\ (aq).$$

Equation 2.II

$H^{36}Cl$ was produced using the apparatus shown in figure 2.4.

[36Cl]-Chlorine labelled hydrogen chloride was generated in an apparatus consisting of a reaction vessel with a dropping funnel with a pressure equilibrating arm, to which a series of cooled traps were attached. Trap (i) contained phosphorus pentoxide and was cooled to 213K in dichloromethane/solid CO_2 bath. Trap (ii) contained phosphorus pentoxide and was cooled to 183K in a methanol/

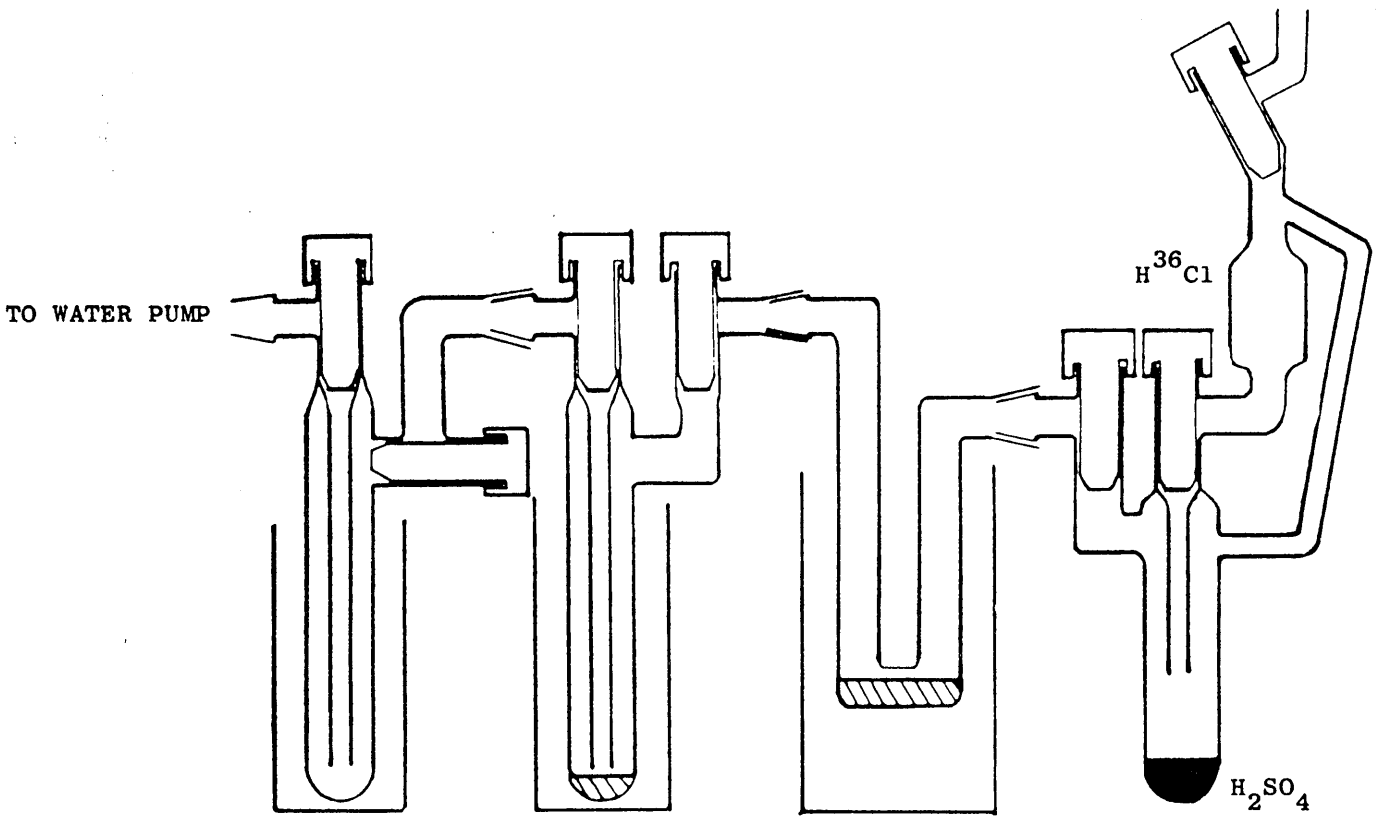

FIGURE 2.4 $H^{36}Cl$ GENERATOR

liquid nitrogen bath. The collection vessel (iii) was equipped with high vacuum stopcocks (J.Young) so that it could be isolated from the rest of the apparatus. The ground glass joints of the apparatus were sealed with Kel-F grease and the operations were carried out in dry air.

Aqueous [36Cl]-chlorine labelled sodium chloride (2.5 ml, 62.5 µCi Amersham International) was diluted with 35.4% hydrochloric acid (10ml, Hay's Chemicals) and this solution was added dropwise to concentrated sulphuric acid. The [36Cl]-HCl generated was distilled through traps (i) and (ii) and collected in trap (iii) at 153K. Trap (iii) was transferred to a vacuum line where the [36Cl]-HCl was degassed, vacuum distilled twice from 186K to 153K onto phosphorus pentoxide and stored over phosphorus pentoxide in a vacuum flask at 77K.

2.2.3 i Preparation and Purification of [14C]-Carbon Labelled Carbon Tetrachloride.

[14C]-Carbon labelled carbon tetrachloride (250 µCi Amersham International) was vacuum distilled from a breakseal vessel onto CCl_4 (20ml, ANALAR, May & Baker) which had been previously degassed.

The $[^{14}C]$-CCl_4 was stored over activated 3A molecular sieves and further degassed before use. The $[^{14}C]$-CCl_4 was stored under darkness to avoid photoxidation reactions that would degrade the sample.

2.2.3ii Preparation and Purification of [36 Cl]-Chlorine Labelled Carbon Tetrachloride.

[36 Cl]-Chlorine labelled carbon tetrachloride was prepared by thermal chlorination of chloroform with [36 Cl]-Cl_2 (145) according to equation 2.III

$$CHCl_3 + [36\ Cl]\text{-}Cl_2 \longrightarrow [36\ Cl]\text{-}CCl_4 + [36\ Cl]\text{-}HCl$$

Equation 2.III

A conditioned Monel metal bomb was loaded with $CHCl_3$ (10 mmol, ANALAR, May & Baker) and [36 Cl]-Cl_2 (20 mmol, on a vacuum line). The bomb was closed and held at 623K for 23 hours at the end of which the contents of the bomb were distilled into a vacuum vessel containing mercury. The contents of the vacuum vessel were allowed to react with the mercury for 2 hours at room temperature to remove any Cl_2 still present, by the direct reaction with mercury to produce involatile $HgCl_2$.

The flask containing the product mixture was held at 195K in a dichloromethane/solid CO_2 bath. The vapour in the manifold above the product mixture was isolated and condensed into a second flask held at 77K. This procedure was repeated three times to remove [^{36}Cl]-HCl and [^{36}Cl]-$COCl_2$ the latter being identified in the gaseous product mixture using infra-red spectroscopy. The presence of $COCl_2$ in the product mixture was attributed to the reaction of $CHCl_3$

with metal oxides or water on the walls of the Monel bomb. This was supported by a decrease in the amount of phosgene detected, using infra-red spectroscopy after successive preparations of $[^{36}Cl]$-CCl_4 using this technique.

The residual $[^{36}Cl]$-CCl_4 was identified using infra-red spectroscopy, vacuum distilled from 195K to 77K into a vessel containing activated 3A molecular sieves and degassed before use.

2.2.4 Preparation and Purification of $[^{36}Cl]$-Chlorine Labelled 1,1,1-trichloroethane.

$[^{36}Cl]$-Chlorine labelled 1,1,1-trichloroethane was prepared by iron(III) chloride catalysed hydrochlorination of 1,1-dichloroethene (Equation 2.IV) (25).

$$CH_2 = CCl_2 + [^{36}Cl]\text{-}HCl \xrightarrow[FeCl_3]{293K} [^{36}Cl]\text{-}CH_3CCl_3$$

Equation 2.IV.

A conditioned Monel metal bomb was loaded with $FeCl_3$ ('Anhydrous', 99.0% pure Fluka AG) in an inert atmosphere box and closed. The bomb was subsequently attached to the vacuum line and loaded with $CH_2 = CCl_2$ (34 mmol, 99% Aldrich Chemical Co) and $[^{36}Cl]$-HCl (35mmol). The bomb was closed and held at room temperature for 48h after which it was held at 195K and opened to the manifold.

The vapour in the manifold above the product mixture was isolated and condensed into a vacuum vessel held at 77K. This procedure was repeated three times to remove $[^{36}Cl]$-HCl.

The residual $[^{36}Cl]$-CH_3CCl_3 was identified using infrared spectroscopy and vacuum distilled from 193K to 77K into a vessel containing activated 3A molecular sieves.

2.2.5 Purification of 1,1 Dichloroethene.

1,1 Dichloroethene (99.0% Aldrich Chemical Co) was stored over activated 3A molecular sieves in a vacuum flask, under subdued light to inhibit photopolymerisation. This material contained small amounts of hydroquinone monomethyl ether, a stabilizer to inhibit oxidation and polymerisation. It was vacuum distilled, to remove the stabilizer and degassed prior to use.

2.2.6 Catalyst Modification by Thermolysis.

The types of γ-alumina used in this work were high purity commercial aluminas (Spence type A, Condea and Degussa 'C'). The standard catalyst pretreatment involved loading the catalyst to be calcined (generally 5g of catalyst) into a Monel bomb and fitting to the vacuum line. An electrical heater fitted with a vertical thermo-couple pocket was fixed around the Monel bomb.

Five samples of alumina were pretreated by calcining in vacuo at 300K, 373K, 423K, 473K and 523K respectively for 6 hours. After the catalyst pretreatment had been

completed the calcined samples were transferred, in a dry box, to dry labelled vacuum vessels, fitted with 4mm Rotaflow stoppers. The calcined alumina samples were stored under nitrogen in a dry box.

X-Ray examination of the calcined sample showed that the aluminas retained the γ-form. (Section 8.2.1).

2.3 Infrared Spectroscopy.

Infrared spectroscopic analysis of the vapour phase in gas/solid systems were carried out using a Perkin Elmer 983 grating infrared spectrometer with Data Station and a Nicolet 5DXC Fourier Transform infrared spectrometer. Kinetic infrared spectroscopic analysis of the vapour phase in gas/solid systems were carried out using the Perkin Elmer 983 grating infrared spectrometer.

2.3.1 Perkin Elmer 983 Grating Infrared Spectrometer and Fourier Transform Infrared System.

The gas cell had a purpose built holder to ensure reproducible positioning in the spectrometer beam. The gas cell (Figure 2.5) was of 10cm path length with AgCl windows. A B14 cone and trap arrangement facilitated attachment to the vacuum line. The cell also had a B14 socket for attachment of an ampoule loaded with solid, and a depression along the bottom to ensure that none of the solid impinged on the spectrometer beam. The cell had a volume of 54.44 ± 0.06 ml.

Figure 2.5

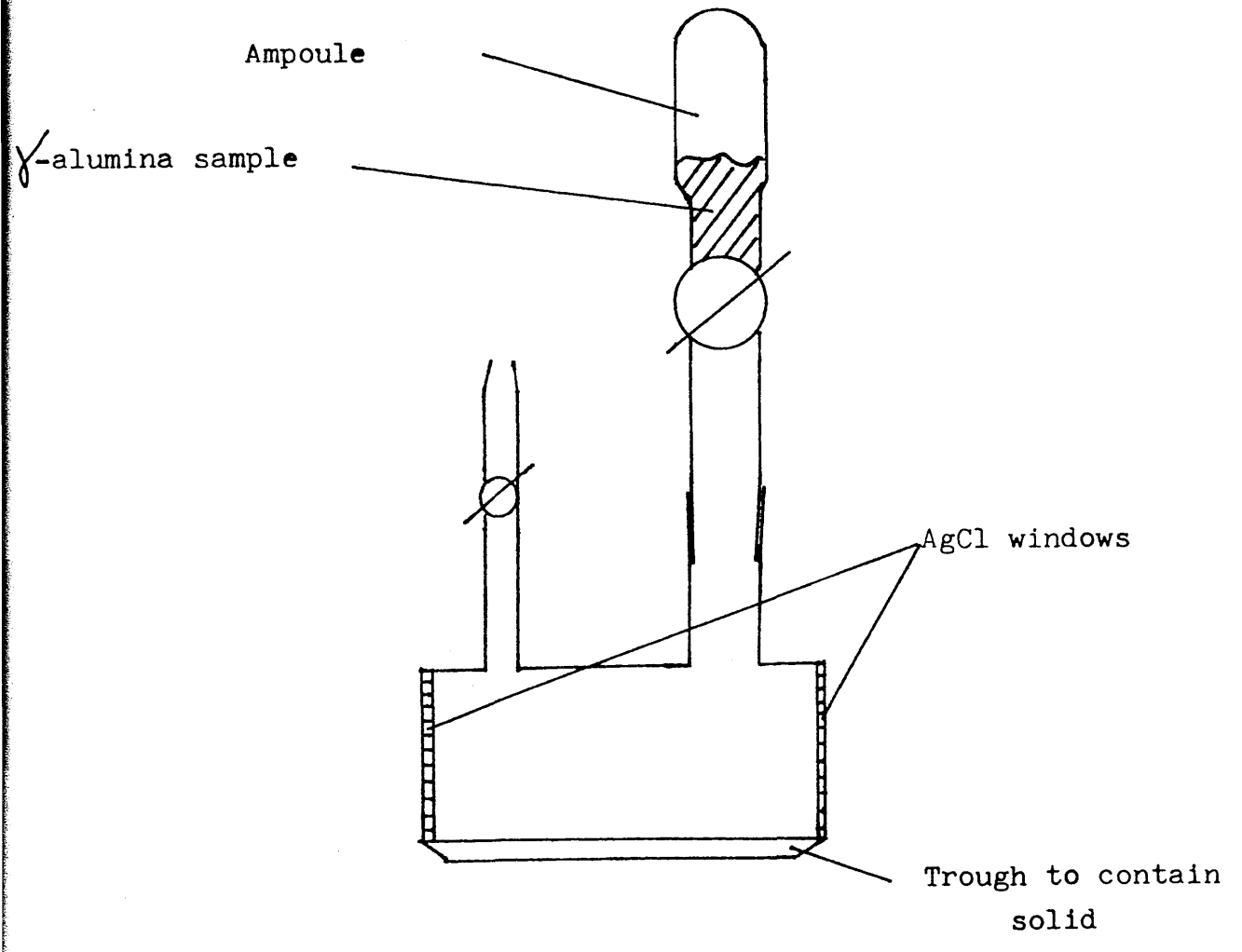

Gas Cell

2.3.2 Identification of Gaseous Compounds.

In all infrared spectroscopic analysis of the vapour phase in gas/solid systems, species were assigned by comparison with standard vapour phase spectra, obtained from the Aldrich Library of Infrared Spectra, or vapour phase spectra obtained from pure standard samples.

2.3.3 Calibration Spectra.

Analytically useful infrared peak positions of gaseous species are tabulated in table 2A. The 794 cm^{-1} peak of carbon tetrachloride is the only peak in the range 4000 - 600 cm^{-1} for this compound and the close proximity of a peak at 790 cm^{-1} for 1,1-dichloroethene reduces its analytical utility in systems where both gases are present. For this reason the peak at 1139 cm^{-1} was used to calibrate 1,1 dichloroethene. Spectra were obtained for various pressures of gaseous 1,1,1-trichloroethane and 1,1-dichloroethene.

Plots of absorbances and peak area vs pressure were constructed. Linear relationships with correlation co-efficients > 0.99 were obtained for the peaks in table 2A, and were considered acceptable calibrations. Examples are shown in figures 2.6 and 2.7.

Table 2A.

Infrared Peak Positions

	Absorption cm^{-1}	Assignment	Functional Group.
1,1,1-trichloroethane:	3010(m)	C-H str.	$-CH_3$
	2950		
	1440(m)	C-Cl 2v	$-CCl_3$
	1380(m)	C-H rock.	$-CH_3$
	1085(s)	C-C str	-C-C-
	1010(w)	C-C str	
	720(s)	C-Cl str	$-C\ Cl_3$
	520(m)	C-H rock	$-CH_3$
1,1 dichloroethene:	1730(w)	C=C str (cong)	-C=C-
	1620(s)	C=C str	-C=C-
	1570(m)	C-Cl 2v	$-CCl_2$
	1139(m)	C=C (cong) str	-C=C-
	1090(s)	C=C str	-C=C-
	865(s)	C-Cl str	$-CCl_2$
	790(s)	C-Cl str	$-CCl_2$
	595(m)	C-H rock.	$-CH_2$
Carbon tetrachloride	794(s)	C-Cl str.	CCl_4

Figure 2.6

Calibration of pressure of 1,1,1-trichloroethane versus Peak Intensity of absorbance band @ 720 cm^{-1}

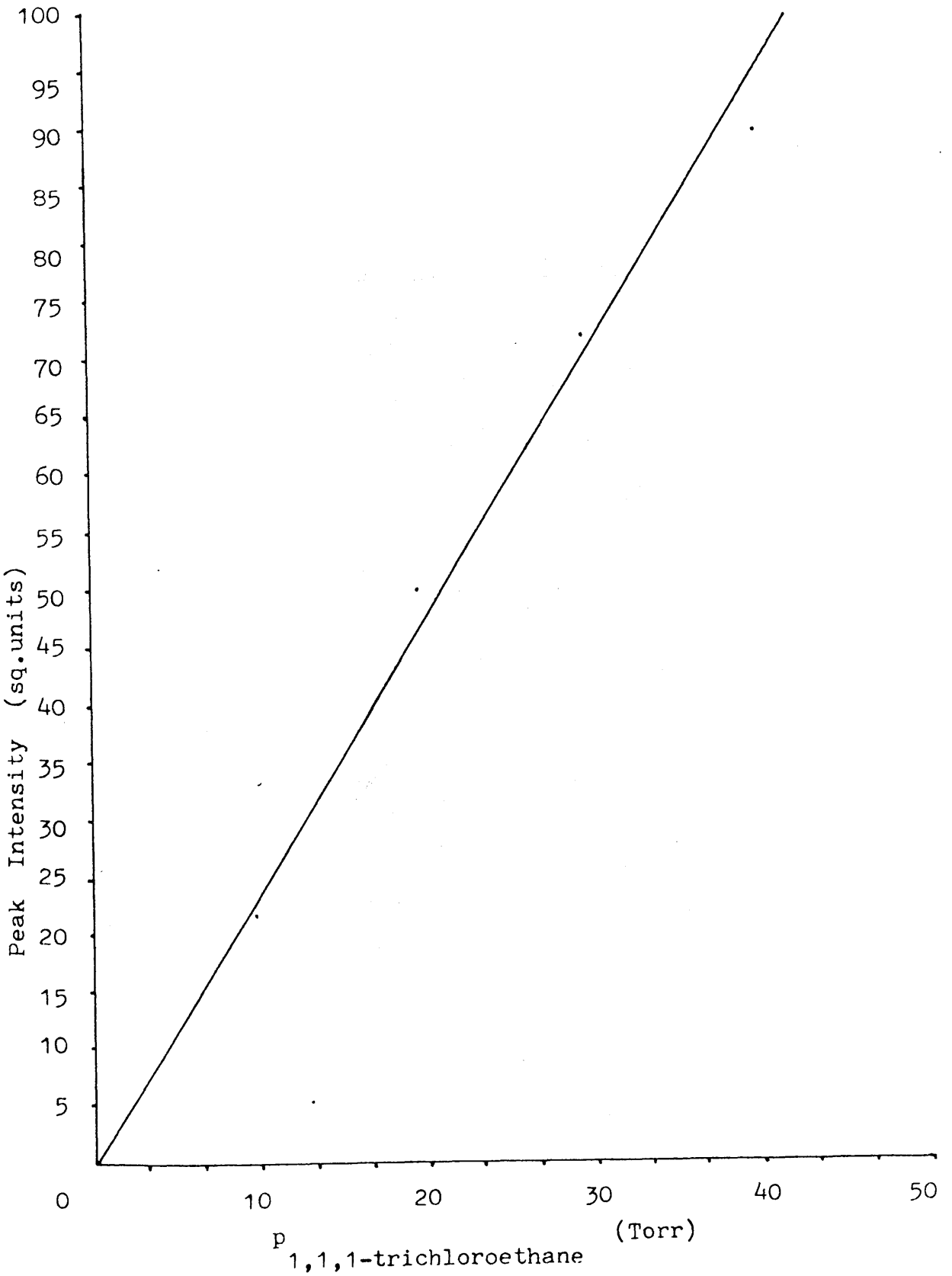

Figure 2.7

Calibration of pressure 1,1-dichloroethene versus peak intensity of band @ 1139 cm^{-1}

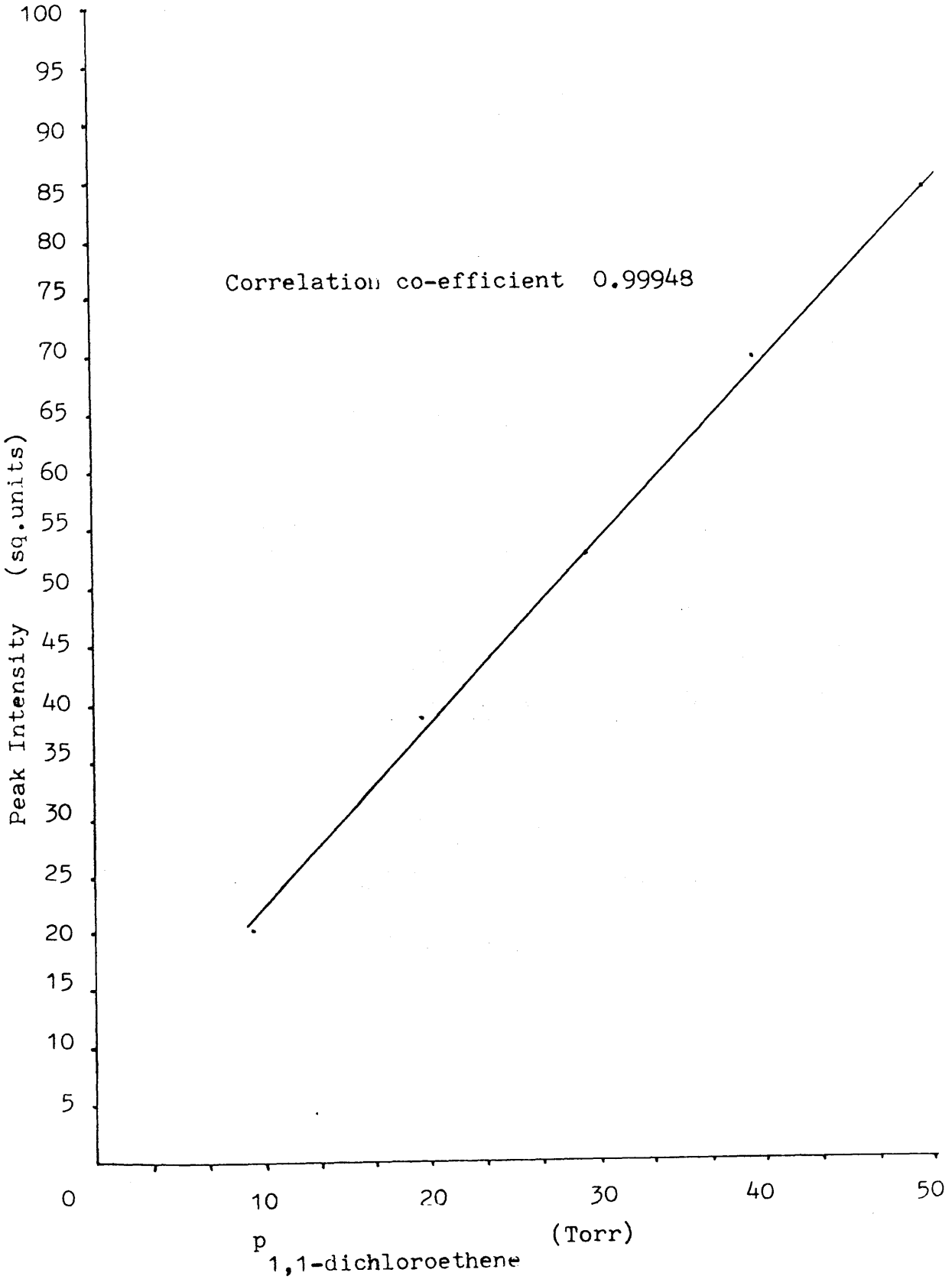

2.3.4 Vapour Phase Infrared Analysis in Gas/Solid Systems.

In infrared studies on the interaction of gases with solids, an ampoule containing a weighed sample of degassed solid was attached to the cell. The cell was evacuated and a desired pressure of gas was isolated in the cell. The cell was placed in the spectrometer beam and the stopcock of the ampoule was opened. Spectra were collected as required.

2.3.5 Kinetic Analysis of Vapour Phase Infrared Data.

The procedure was identical to that described above. The reaction was initiated when the stopcock on the ampoule was opened, and spectra were collected and stored at one per minute for the first 25 minutes of the reaction and subsequently one per 15 minutes for the following 4 hours of the reaction. A Perkin Elmer program was used to treat these data and to construct, for desired peaks, plots of absorbance/peak area vs. time, together with first and second order kinetic plots.

2.4 Radiochemical Counting Using Geiger-Müller Counters.

A Geiger-Müller counter is an earthed metal tube with a thin, gas tight, mica window at one end and a gas tight insulated support for a thin central wire at the other. The inside wall of the tube forms an enclosed cylindrical cathode and the central wire is an anode. The tube is filled with a gas mixture such as 90% argon/10% methane, and is connected to a scaler.

Ionising radiation (alpha, beta or gamma radiation) entering the tube causes partial ionisation of the gas, producing positive ions and free electrons. The central wire is held at a high positive potential with respect to the wall cathode, hence the electrons formed move rapidly towards the wire and the positive ions formed drift relatively slowly towards the wall.

At high applied voltages, the electrons gain sufficient energy to cause further ionisation as they collide with gas molecules, and the number of electrons collected on the wire becomes greater than the number created by the passage of radiation through the detector gas. This phenomenon is known as ion multiplication and its effect is often called an 'electron avalanche'.

The Geiger region is reached when the number of electrons produced by ion multiplication per primary electron/produced by radiation becomes so great that a given 'avalanche' spreads along the entire tube. At this stage the number of electrons collected on the wire, and hence the magnitude of the resultant voltage pulse, is independent of the number of electrons created by the passage of radiation through the detector (146).

Methane, alcohol or other vapour is present in the tube to act as a quench gas. When the positive ions formed by ion multiplication reach the cathode they can cause secondary electron emission from the surface of the wall which can in turn lead to a spurious discharge from the counter. This undesirable effect can be suppressed by

the presence of the quench gas which reacts by electron transfer with the positive ions to yield ultimately stable products.

[^{36}Cl]-Chlorine decays by beta-emission according to Equation 2.V and has a half-life of 3 x 10^5 years.

$$^{36}_{17}Cl \longrightarrow {}^{36}_{18}Ar + {}^{0}_{-1}\beta$$

Equation 2.V.

[^{14}C]-Carbon decays by beta-emission according to Equation 2.VI and has a half-life of 5370 years.

$$^{14}_{6}C \longrightarrow {}^{14}_{7}N + {}^{0}_{-1}\beta$$

Equation 2.VI

As the half-lives of these isotopes are large, no decay correction was required. The maximum energies of beta particles (electrons) for these isotopes are 0.714 MeV and 0.155 MeV respectively, (147).

The efficiency of the counter is typically < 5% for low energy beta emitters, owing to the absorption of much of the incident radiation by the mica window.

2.4.1 Plateau Curve.

In a Geiger-Müller counter no counts are recorded until the applied potential is large enough to attract

the free electrons to the anode. When this point known as the Geiger threshold is reached (Vo) the count rate begins to rise rapidly until a plateau is reached where the count rate increases only very slowly with voltage.

The plateau is never completely flat owing to the generation inside the counter of spurious discharges caused by secondary electron emission. As the potential increases the quench gas cannot cope with the large number of spurious discharges and the count rate begins to rise rapidly until the counter starts to discharge. It is desirable to work at a voltage which is in the middle of the plateau region.

The plateau region was determined for each Geiger-Müller counter used by constructing a plot of counts obtained from a solid ^{60}Co source *vs* applied voltage. Figure 2.8 shows a plot of a plateau curve. As the applied voltage was increased above the minimum voltage required to produce ion multiplication, V(o), the count rate increased until the plateau region was reached. As the applied voltage was increased towards the end of the plateau region the count rate began to increase and then increased very steeply. The working voltage was set in the middle of the plateau region.

2.4.2 Dead Time.

Immediately after the collection of electrons in a Geiger-Müller discharge, positive ions are still left in the counter and most of them are very near the central wire. These positive ions form a space charge which limits the

Figure 2.8

Plateau Curve obtained from G.M. Tube using ^{60}Co Source.

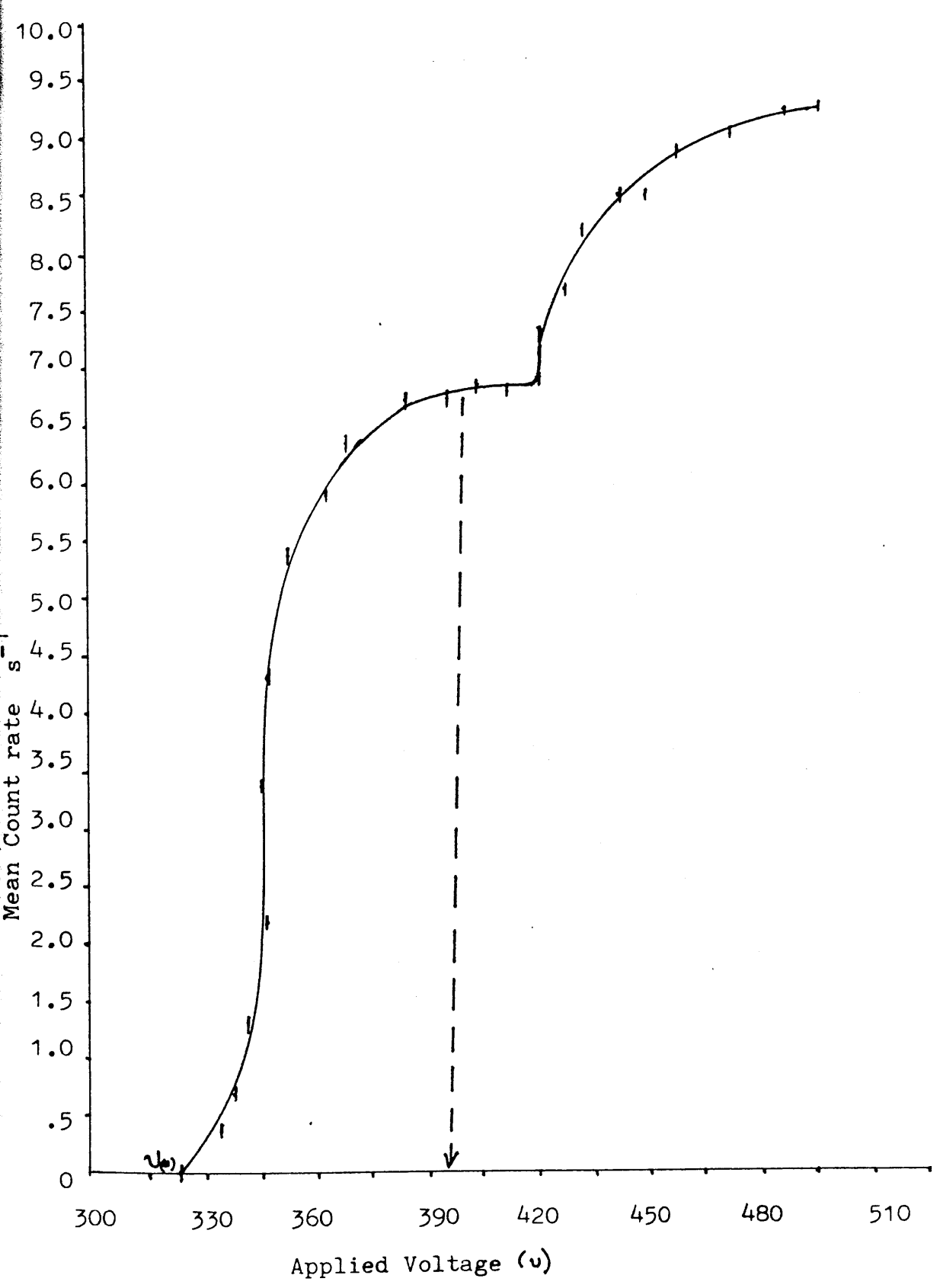

electric field near the centre wire.

If a second particle passes through the counter whilst the positive ions are in this region, an electron avalanche is unable to form, owing to the reduced field near the centre wire. The pulse size which a counter is able to deliver is reduced whilst there are positive ions in the counter. Each pulse from the Geiger-Müller tube is thus followed by a period which no particles can be detected. This lasts until the positive ions have moved far enough from the centre wire to allow an output pulse large enough to operate the recording equipment.

This insensitive period is known as the dead time of the counter, and in accurate counting experiments a correction is necessary for counts lost in such periods, especially if the counting rate is high.

The dead times of Geiger-Müller tubes were determined by counting samples of [^{18}F]-CsF for 330 minutes ($t_{\frac{1}{2}}[^{18}F]$ = 110 mins). Equation 2.VII is general for radioisotopes.

$$A(t) = A(o)e^{-\lambda t}$$

Equation 2.VII

λ = decay constant in seconds

A(t) = activity of sample at time t

A(o) = activity of sample at time zero

Thus a plot of ln A(t) vs time should be linear with the gradient $-\lambda$ and intercept lnA(o). When a plot

of ln A(t) versus time was drawn a linear relationship was obtained for t >200 minutes. At times t <200 minutes a curve was obtained because at these times the count rate was high enough for the dead time to have a considerable effect.

A linear portion of the plot was extrapolated to time t = 0 using the known half life of [^{18}F]-fluorine (109.72 ± 0.06 minutes). This line gave N(t) the true count rate which is related to N(o) the observed count rate N(o) by the relation

$$N(t) = \frac{N(o)}{(1-N(o)\tau)}$$

Equation 2.VIII

where τ is the dead time.

This calculation was performed using the first twenty points on the graph and the mean of these results was taken to be the dead time of the counting system. Figure 2.9 shows both the experimentally observed line and the calculated true line.

2.4.3 Background.

A Geiger-Müller counter will register some counts in the absence of a radioactive source. In laboratory environments these counts are due primarily to cosmic radiation and radiation from materials used in the construction of the laboratory. An average background count must be subtracted from all counts in radiochemical counting

Figure 2.9

Determination of the Dead Time for G.M. Tube by Decay of $[^{18}F]$- Fluorine.

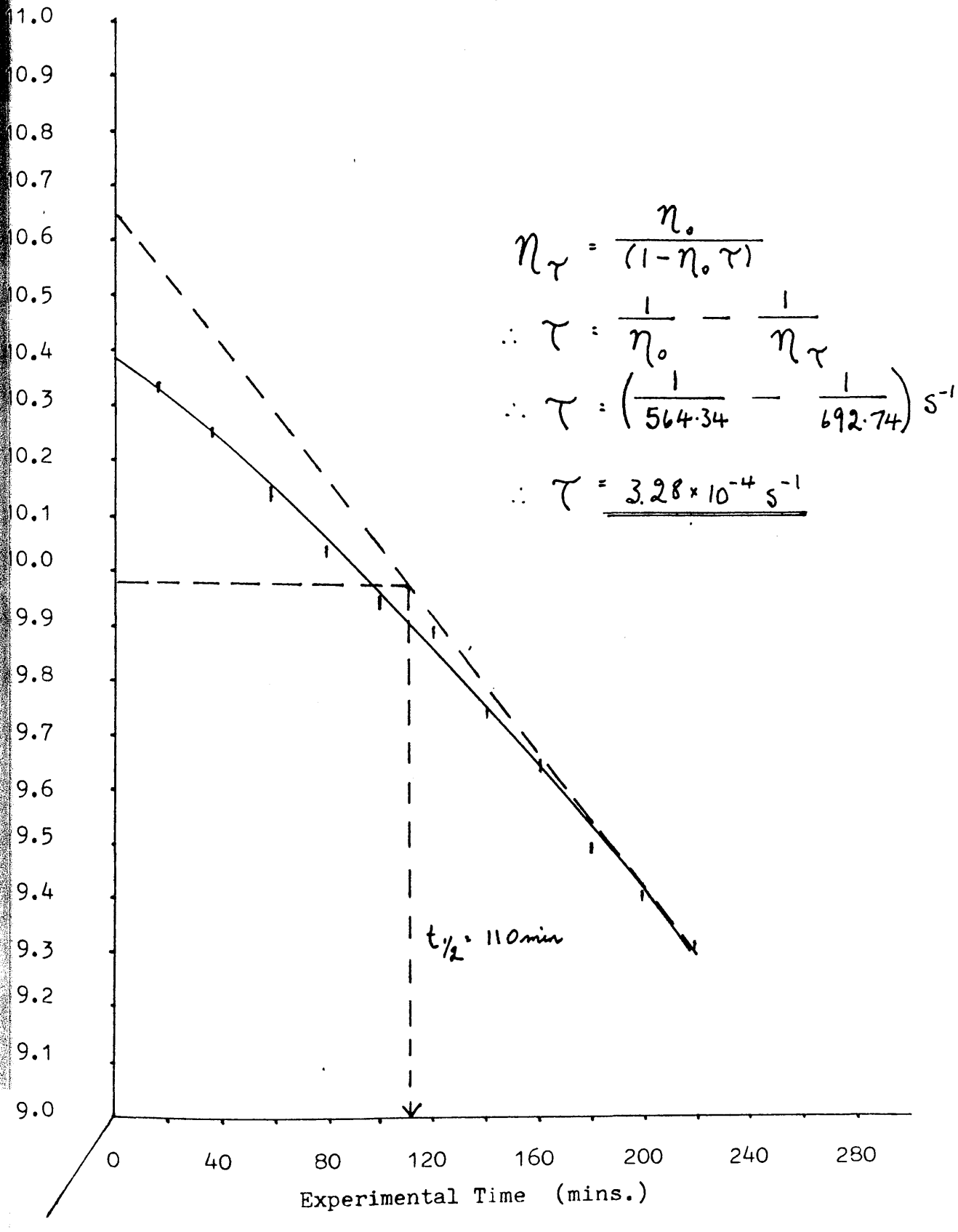

$$\eta_\tau = \frac{\eta_0}{(1-\eta_0\tau)}$$

$$\therefore \tau = \frac{1}{\eta_0} - \frac{1}{\eta_\tau}$$

$$\therefore \tau = \left(\frac{1}{564.34} - \frac{1}{692.74}\right) s^{-1}$$

$$\therefore \tau = \underline{3.28 \times 10^{-4}\ s^{-1}}$$

experiments to correct for this effect.

The background registered by a Geiger-Müller counter can be minimised by enclosing the tube and the sample to be counted in a lead walled container, often called a lead castle. The walls are several centimetres thick and the lead shields the tube from a significant fraction of the background radiation. Lead castles are used to count solid radioactive samples.

An important feature of lead castles is the use of a sampleholder or tray.

The sample to the tube distance is fixed, as is the relative geometry of sample and tube. These factors are important in the counting of solid β-emitters, where effects such as self-absorption (see following section) and self-scattering of beta-particles depend not only on beta-particle energy but also on the geometrical arrangement of sample and detector.

2.4.4 Self-Absorption.

As [^{36}Cl]-chlorine is a β-emitter care was taken to ensure that the Geiger-Müller counters were always the same distance from the sample because of the absorption of β-radiation.

When counting solid Ag^{36}Cl, a correction for the absorption of β-particles within the solid itself must be made unless the same weight of material is used in all comparative measurements. This correction is

achieved by measuring apparent β-activity obtained from different thicknesses of samples of identical specific activity. These measurements were obtained for $Ag^{36}Cl$ and a self-absorption curve constructed by plotting the count rate per mg (count s^{-1} mg^{-1}) against the weight of $Ag^{36}Cl$. The curve obtained is shown in figure 2.10. The absorption correction necessary to relate observations at one thickness to observations at any other thickness within the experimentally determined range is equal to the quotient of the values of log of activity mg^{-1} at the two weights. In all calculations, the activity was related to a weight of 15mg.

In all counts involving $Ag^{36}Cl$, corrections were made for background, dead time and self-absorption.

2.4.5 Statistical Errors.

The decay of a radioisotope is a completely random process and is therefore subject to fluctuations due to the statistical nature of the process. This means that if a source of activity is measured in such a way as to exclude all other errors in measurement, the number of disintegrations observed in successive periods of fixed duration will not be constant. The probability W(m) of obtaining just m disintegrations in time t from N_o original radioactive atoms is given by the binomial expression:

$$Wm = \frac{No!}{(No-m)!m!} \; p^m (1-p)^{No-m}$$

Equation 2.IX

Figure 2.10

Self Adsorption Curve for $Ag^{36}Cl$.

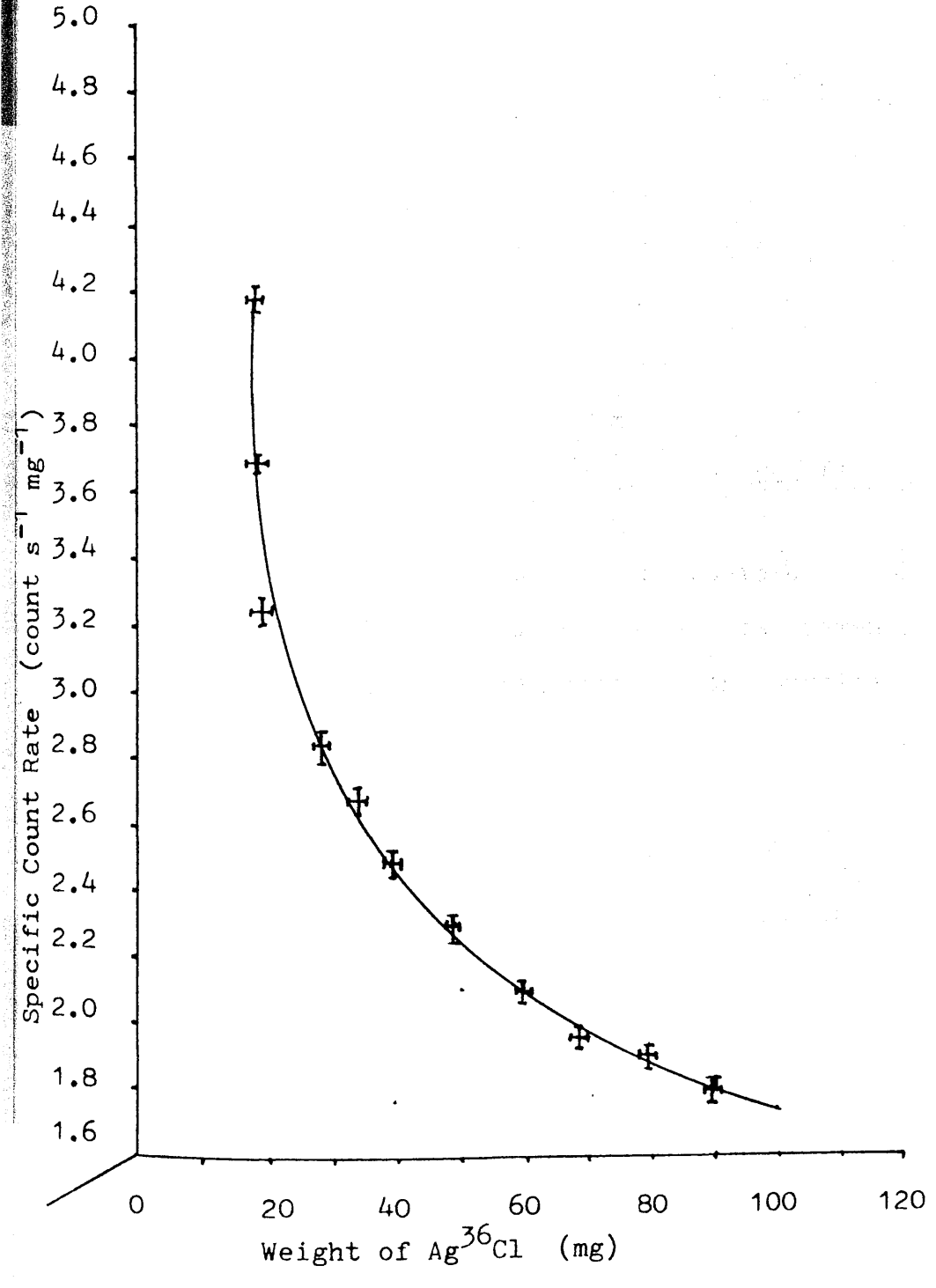

where p is the probability of a disintegration occurring within the time of observation (148). From this expression it can be shown (149-151) that the expected standard deviation for radioactive disintegration θ is given by:

$$\theta = me^{-\lambda t}$$

Equation 2.X

In practice the observation time t is short compared to the half-life so that λt is small, reducing equation 2.X to:

$$\theta = m$$

Equation 2.XI

where m is the number of counts obtained. In this work all errors quoted on radiochemical measurements are the combination of the uncertainty in the physical measurements such as weight of sample and pressure of gas, and the uncertainty in the count obtained.

2.5 The Direct Monitoring Geiger-Müller Radiochemical Counting Technique.

The direct monitoring Geiger-Müller radiochemical counting technique was developed by Thomson and modified by Al-Ammar and Webb (152) to determine surface radioactivity on solids exposed to radiolabelled gases. The technique

has been successfully used to detect both weakly and strongly absorbed species in a variety of situations (153) and has proved to be a powerful tool in the elucidation of mechanism in heterogeneous catalysis.

2.5.1 Equipment.

The Pyrex reaction vessel (Figure 2.11) contained two Geiger-Müller tubes, and was connected via a manifold to a constant volume manometer and gas handling facilities. The vessel had a B14 socket for the attachment of an ampoule containing the solid to be studied. Inside the vessel was a Pyrex boat which had two sections, each capable of being loaded with a solid, and which could be moved along the length of the vessel by means of a magnet. The whole apparatus was calibrated before use. The Geiger-Müller tubes were intercalibrated regularly by taking counts using varying pressures of radioactive gas ($H^{36}Cl$, $[^{14}C]$-CCl_4, $[^{36}Cl]$-CCl_4). A graph of pressure vs counts should give a straight line which passes through the origin. A typical set of results is tabulated in Table 2.B and the graph shown in figure 2.12a. When the counts from both tubes were plotted (Figure 2.12b), a straight line was obtained, whose gradient was equal to the counting ratio between the two tubes. This counting ratio should remain constant and was usually in the region of 1.04.

2.5.2 Application of the Technique to Gas/Solid Systems.

The procedure for application of the technique

Counting Cell

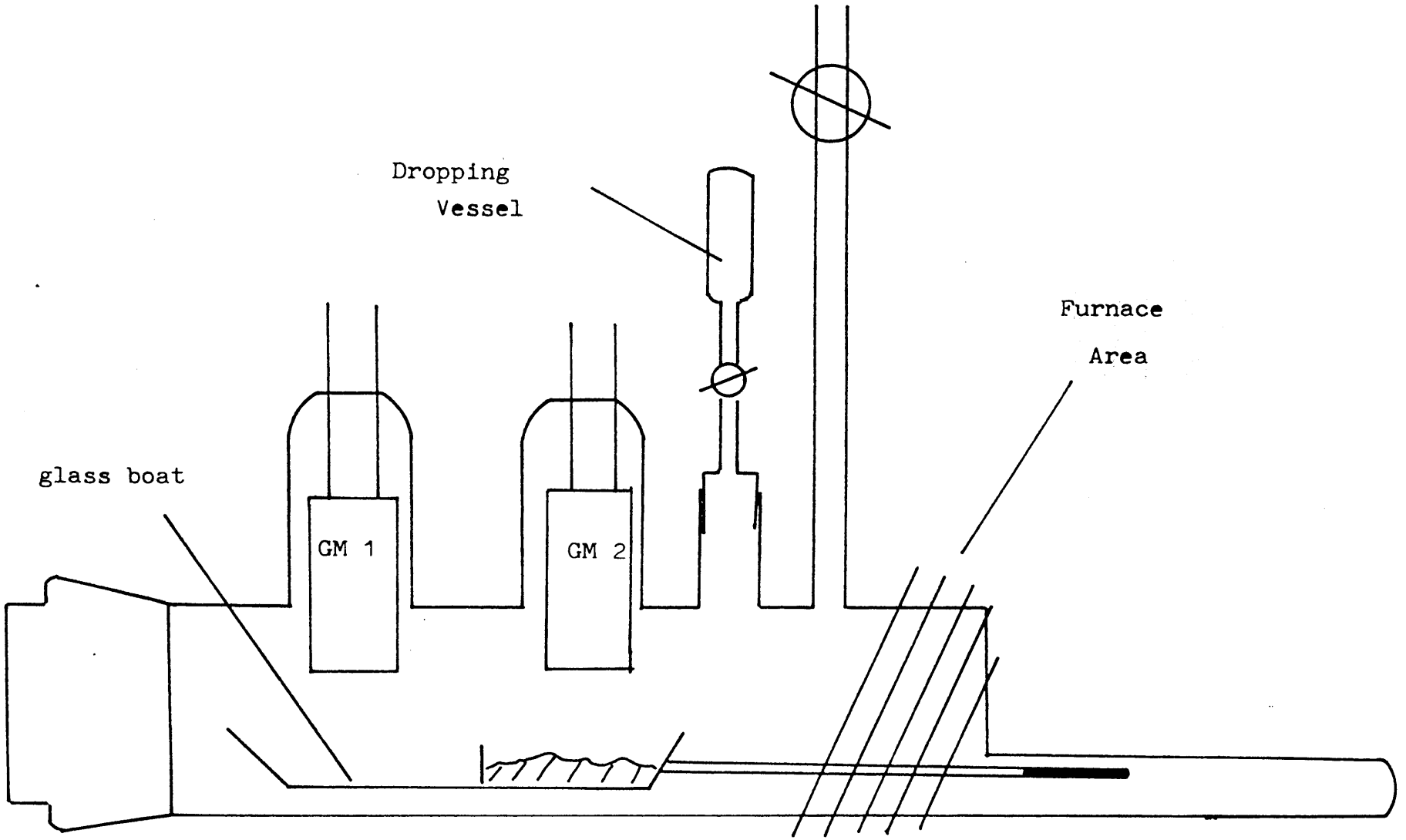

Table 2B.

Pressure of $H^{36}Cl$ Torr.

P1. Torr	P2. Torr	ΔP. Torr	Count s^{-1}
230.97 ±.07	181.37±.07	49.60 ±.10	43.12± 0.38
231.07 ±.07	183.37±.07	47.70 ±.10	39.76± 0.36
231.07 ±.06	186.47±.06	44.60 ±.09	36.52± 0.35
230.66 ±.06	187.42±.06	43.24 ±.09	35.24± 0.34
230.49 ±.06	191.43±.06	39.06 ±.08	32.28± 0.33
230.38 ±.05	193.73±.05	36.65 ±.07	30.19± 0.34
230.39 ±.05	200.01±.05	30.38 ±.06	25.03± 0.31
230.24 ±.04	203.55±.04	26.69 ±.05	21.47± 0.35
230.24 ±.04	204.73±.04	25.51 ±.05	20.42± 0.34
230.28 ±.04	206.27±.04	24.01 ±.05	18.55± 0.32
230.28 ±.02	210.01±.03	20.27 ±.04	16.07± 0.33
230.41 ±.02	213.47±.02	16.94 ±.03	12.96± 0.34
229.12 ±.02	213.56±.02	15.56 ±.03	11.96± 0.33
228.61 ±.02	215.55±.02	13.06 ±.03	9.32± 0.31
228.59 ±.01	218.69±.01	9.90 ±.02	7.73± 0.31
228.72 ±.01	219.81±.01	8.91 ±.02	6.74± 0.31
229.22 ±.01	222.50±.01	6.72 ±.02	5.02± 0.31
229.43 ±.01	223.24±.01	6.19 ±.01	4.17± 0.31

Figure 2.12a

Calibration of Pressure $H^{36}Cl$ versus Gas Phase Count Rate

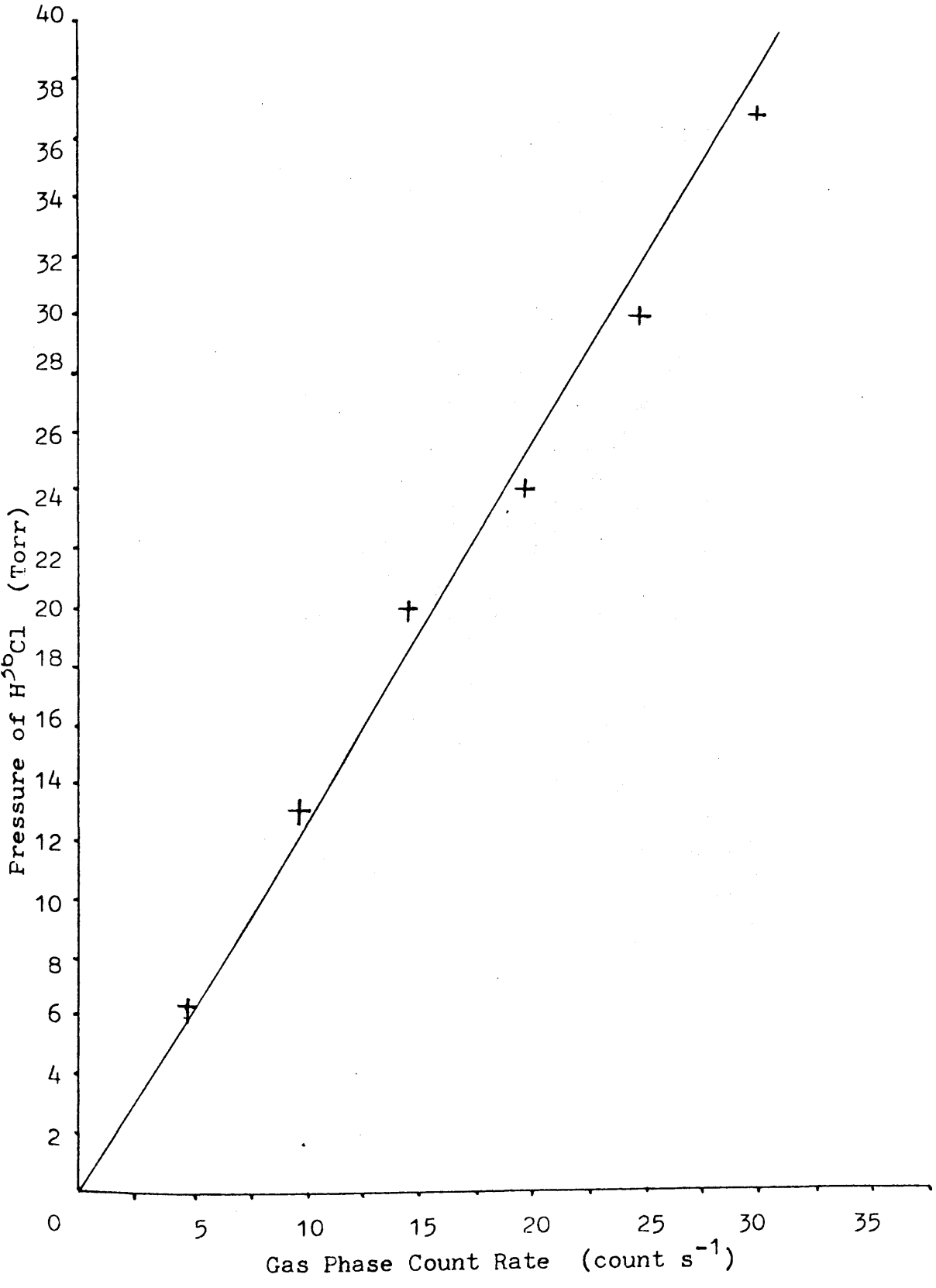

Figure 2.12b

Intercalibration of G.M. Tubes using various Pressures of $H^{36}Cl$

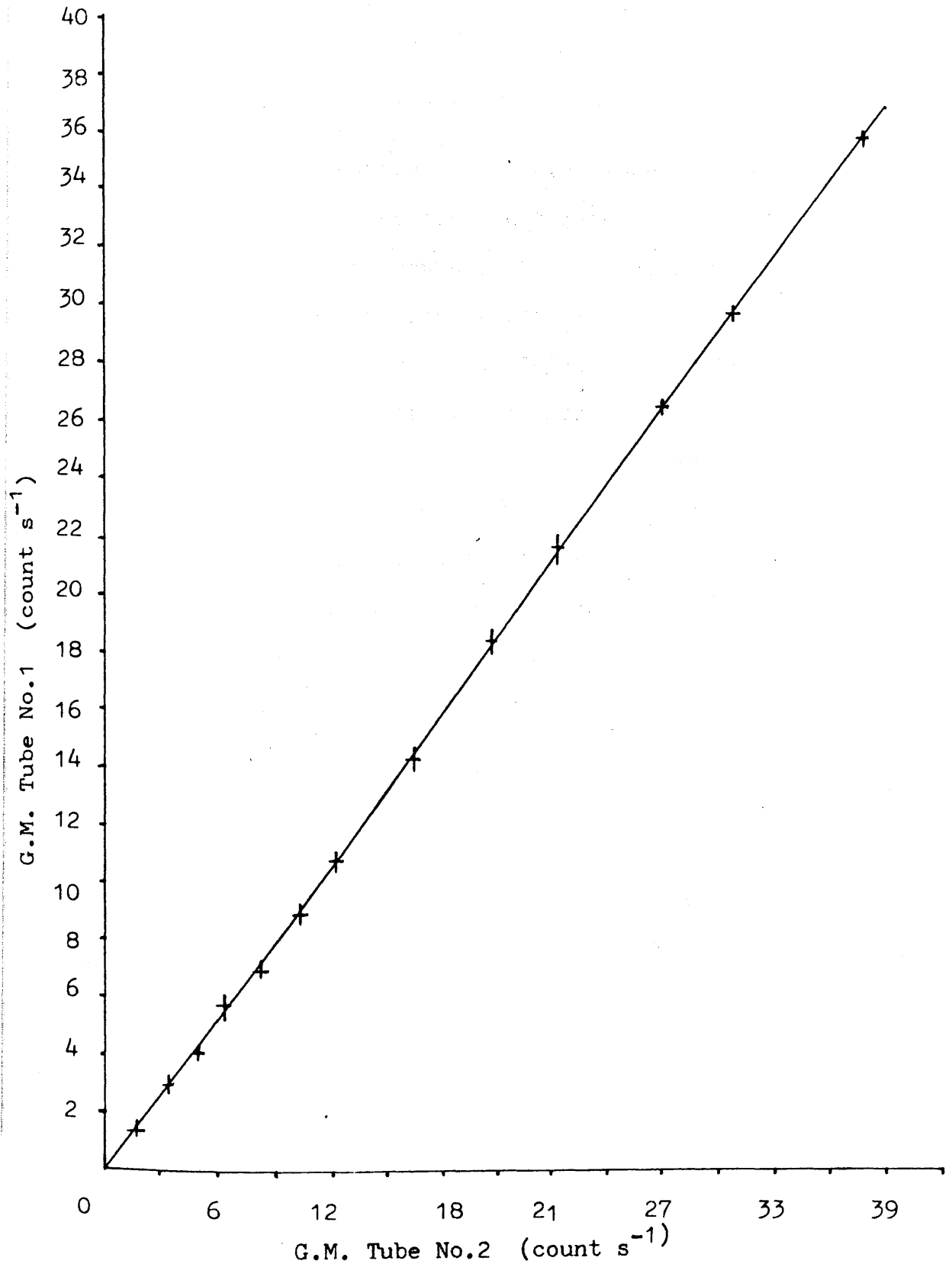

to gas/solid systems was as follows. The reaction vessel was evacuated, flamed out, and a weighed sample of solid was dropped into the right hand portion of the boat. The boat was moved so that the left-hand portion was directly under Geiger-Müller 1, and the right hand portion was directly under Geiger-Müller 2.

An accurately measured amount of radioactive gas of measured specific count rate was admitted at a desired initial pressure to the reaction vessel, and the reaction vessel was isolated from the rest of the system. Counts were taken from both Geiger-Müller tubes with time, so that the left hand side counts, from Geiger-Müller 1 were from the gas alone, whereas the right hand side counts from Geiger-Müller 2 were from the gas+solid. The counts from Geiger-Müller 1, corrected for the dead time background and intercalibration, were subtracted from the counts from Geiger-Müller 2, corrected for dead time and background to give values for surface counts, and plotted against time.

2.5.3 Determination of Specific Count Rates of [^{36}Cl]-Chlorine Labelled Hydrogen Chloride (154).

[^{36}Cl]-HCl was vacuum distilled onto an excess of a frozen aqueous solution of sodium hydroxide (98% pure, Hopkin & Williams), and both were allowed to warm up and react in a closed vessel at room temperature for at least 3 hours. The resultant solution was decanted into a beaker. The vessel was washed out with distilled water and the washings added to the solution in the beaker. The solution was acidified with ten drops of concentrated nitric acid.

Under subdued light a solution of silver nitrate (0.22 mol l^{-1} 98% pure, Johnson Matthey Chemicals) was added with stirring until precipitation of AgCl was judged to be complete. The precipitate was allowed to settle and a few more drops of silver nitrate solution were added. The suspension was heated nearly to boiling on a hotplate, with occasional stirring and digested until the precipitate coagulated. The beaker was removed from the hotplate and the precipitate allowed to settle. The beaker was set aside in the dark for at least one hour.

A sintered glass crucible (porosity 4) was dried to constant weight at 423K. The precipitate was filtered with very dilute nitric acid (approximately one part concentrated nitric acid to one thousand parts distilled water) and washed in the crucible with very dilute nitric acid until 3ml of the washings gave no turbidity with dilute hydrochloric acid.

The crucible and precipitate were dried to constant weight at 423K. The [^{36}Cl]-HCl was converted to [^{36}Cl]-AgCl with an efficiency >96%.

Accurately weighed portions of [^{36}Cl]-AgCl obtained were counted using a Geiger-Müller tube in a lead castle for periods of time sufficient to accumulate significant ($1x10^4$) counts.

2.6 Radioisotopes

2.6.1 The Radioisotope [^{18}F]-Fluorine.

The [^{18}F]-fluorine is a positron emitter, and annihilation of positron particles with negative electrons releases energy in the form of gamma-radiation. The maximum gamma-emission energy is 0.51 MeV and the half-life of [^{18}F]-fluorine is 109.72 ± 0.06 min (155). Since the half-life of the isotope is relatively short, experimental work must be completed in one working day. After six half-lives (11 hours) only 1.6% of the original activity remains.

2.6.2 The Radioisotope [^{36}Cl]-Chlorine.

The [^{36}Cl]-chlorine isotope decays by beta emission with a half-life of $3x10^5$ years (155). The isotope was supplied as an aqueous solution of [^{36}Cl]-NaCl (Amersham International p.l.c) and was diluted with concentrated hydrochloric acid to give a solution with a specific [^{36}Cl]-chlorine activity of circa 25 μCi cm^{-3}.

2.6.3 Preparation of [^{18}F]-CsF.

[^{18}F]-fluorine was prepared by irradiating lithium carbonate (ca. 2g) in the central core of the Scottish Universities Research Reactor at East Kilbride using the sequence:-

$$6Li(n,\alpha)^{3}H, \quad ^{16}O(^{3}H,n)^{18}F \qquad (156)$$

Typical irradiation conditions were 30 minutes at a flux of 3.6×10^{12} neutron $cm^{-2}s^{-1}$. The sample of Li_2CO_3 was contained within an aluminium screw-top can (height, 8cm: diameter, 3cm). A graphite rod (length, 7cm; diameter, 1.5cm) inside the aluminium can acted as a neutron moderator, slowing down the neutrons to improve the probability of collision with lithium nuclei. The [^{18}F]-LiF produced in the irradiation was converted to [^{18}F]-HF by reaction with sulphuric acid, (conc. H_2SO_4: H_2O 1:1 by volume). The [^{18}F]-HF was then distilled into a solution of caesium hydroxide at 273K. Neutralisation of the solution by addition of aqueous hydrogen fluoride was followed by evaporation to dryness to give [^{18}F]-CsF as a finely divided white powder.

2.7 Determination of Chlorine Uptake on γ-Alumina using Neutron Activation Analysis.

2.7.1 Calibration of Coaxial Ge(Li) detectors and the Determination of the Efficiency of the Ge(Li) Detector.

High resolution Ge(Li) detectors facilitate

multi-trace-element analysis by neutron activation. High capacity multi-channel analysers are required to resolve the many photopeaks in γ-ray spectra, and in modern instruments such analysis is carried out by micro-processors.

Calibration of Ge(Li) detectors with known gamma emitters is necessary to identify the activities produced in activated samples. A knowledge of detector resolution is required to confirm that the photopeaks are adequately resolved from other induced activities. Detection efficiency is therefore required in order to calculate the limits of detection for a specified system.

Calibration of Ge(Li) detectors was achieved by selecting standard sources and accumulating gamma-ray spectra over a period of 100 seconds for a number of sources. The spectrum of the relevant isotope was located in "Applied Gamma-Ray Spectrometry (Adams and Dams)". Using pattern recognition the relevant photopeaks in the spectrum were identified. The channel equivalent to the peak maximum was identified together with the resolution (peak width at half maximum). The observed disintegrations per second were obtained over the selected peak. This procedure was carried out using ^{60}Co, ^{133}Ba, ^{137}Cs, and ^{22}Na sources.

The energy calibration of the detector was obtained by constructing a plot of the channel number as a function of energy. The resolution in terms of channel number was then converted to KeV and a plot of resolution as a function of energy was obtained. The efficiency of the

detector was determined by obtaining the quotient of the observed disintegrations per second and the activities (in KBq) of the standard sources at the time of supply by the application of decay factors and the absolute intensity.

The calibration data of a Ge(Li) coaxial detector are tabulated in table 2C and the energy calibration calculated (Figure 2.13).

Table 2 C.

Source	Activity kBq	Energy KeV	Absolute Intensity %	Specified d-p-s $x10^3$	Observed c-p-s	Peak Centroid	Resolution KeV	Efficiency %
^{60}Co	65.115	1173	99.86	65.02	132.45	2196	2192-2159	0.20
	$t_{\frac{1}{2}}$ = 5.26 y	1333	99.98	65.10	116.91	2493	2488-2498	0.18
^{133}Ba	100.127	81	33.8	33.84	896.27	152	148-154	2.65
		276	7.1	7.11	85.17	518	514-520	1.20
		303	18.7	18.72	204.80	567	563-570	1.09
	$t_{\frac{1}{2}}$ = 7.2 y	356	61.9	61.98	589.00	667	662-670	0.95
		384	8.9	8.91	84.22	719	714-722	0.95
^{137}Cs	296.51	662	85.1	252.3	391.29	1239	961-952	0.16
	$t_{\frac{1}{2}}$ = 30.1 y							
^{22}Na	9.48	511	181	17.16	62.28	957	1242-1233	0.36
	$t_{\frac{1}{2}}$ = 2.58 y	1275	99.95	9.48	16.35	2385	2389-2379	0.17

Figure 2.13

Calibration of Coaxial Ge(Li) detector

Channel No. versus Energy

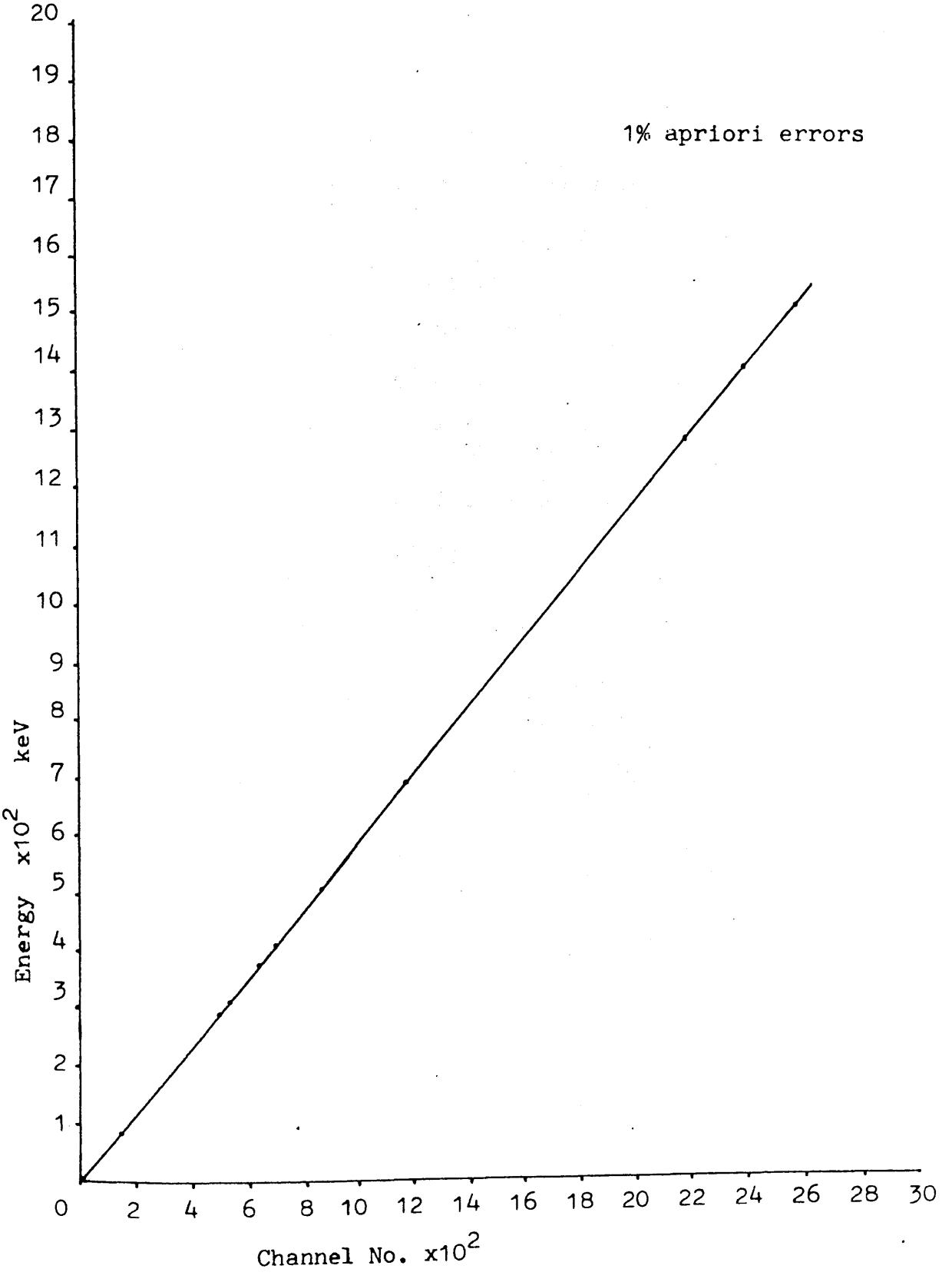

2.7.2 Neutron Activation Analysis.

Chlorine uptakes on γ-alumina were determined using neutron activation analysis, (N.A.A). N.A.A is a non-destructive analytical technique based on activation of stable isotopes to radioactive isotopes in a beam of neutrons. The identities of isotopes are deduced from the energy of gamma-rays emitted from the sample. By observing the intensity of the gamma-emissions with time, a count is obtained for the isotope of interest. Since the gamma-emission spectrum was observed self-absorption was not a problem and uptakes of chlorine on γ-alumina were obtained directly from the count rate data.

The formation of a radioisotope is governed by the first order rate laws:-

rate of formation = $n.\ \sigma.\ \phi$

where n = number of nuclei of stable isotope

σ = neutron capture cross section (barn)

ϕ = irradiation flux (neutrons $cm^{-2}\ s^{-1}$)

rate of decay = $N.\lambda$

where N = number of nuclei formed

λ = decay constant of product

$= \ln 2/t_{\frac{1}{2}}$

$t_{\frac{1}{2}}$ = half-life of isotope formed (s)

$\therefore$ overall

$$\frac{\delta N}{\delta t} = n.\sigma.\ \phi - N\lambda$$

$$\therefore \quad N = \frac{n.\sigma.\phi}{(1-e^{-\lambda.t})}$$

similarly $A = n.\sigma.\phi\ (1-e^{-\lambda.t})$

where A = activity at the end of irradiation. (Bq)

Equation 2.XII

If unknown samples are irradiated with samples of known chlorine content using an identical flux, the quantity of chlorine in an unknown sample is obtained by proportion:-

$$\frac{\text{Cl in sample}}{\text{Cl in standard}} = \frac{\text{Counts from Cl in sample}}{\text{Counts from Cl in standard}}$$

Equation 2.XIII

Samples were irradiated in the Scottish Universities Research Reactor, East Kilbride using the 'rabbit loop'. Weighed samples were contained in sealed plastic vials (Figure 2.14) which were placed in the rabbit. The rabbit (Figure 2.14) consists of a cylindrical plastic container which may be transferred between the laboratory and the reactor by means of an evacuated loop. Care was taken to ensure that all samples were placed in a similar position in the rabbit to ensure that each were subject to an identical flux. Typical irradiation conditions were 25s at 300 kW power (approximate flux 3.6×10^{12} neutrons cm^{-2} s^{-1}). During irradiation ^{38}Cl

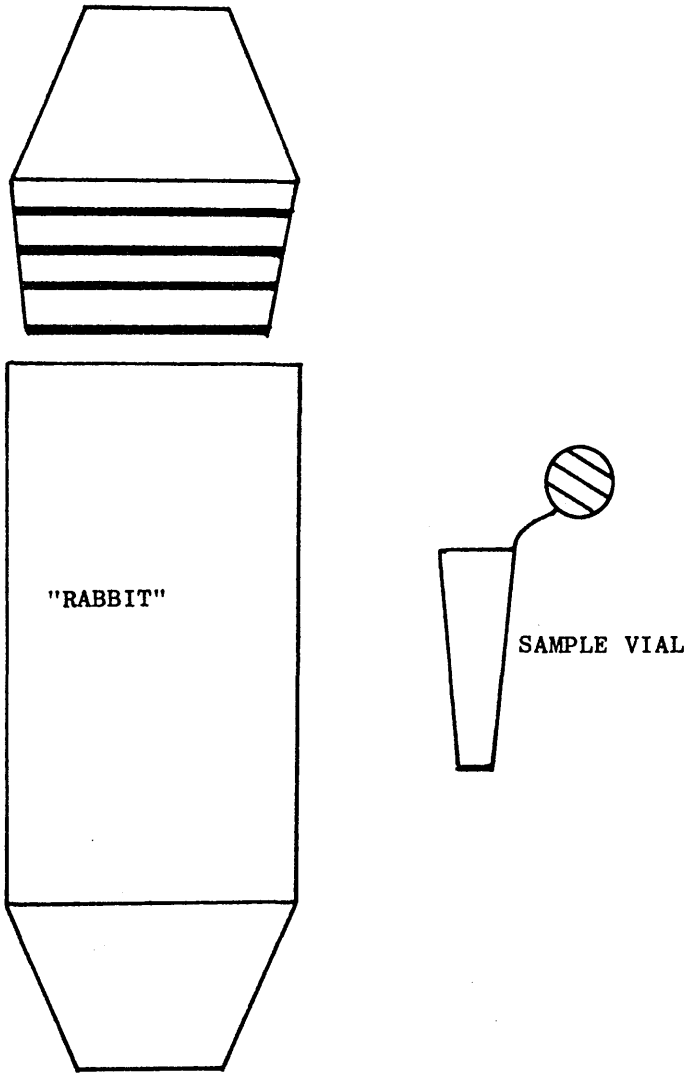

FIGURE 2.14 "RABBIT" AND SAMPLE VIAL USED IN NEUTRON ACTIVATION ANALYSIS.

($t_{\frac{1}{2}}$ = 37.3 min) was produced by the process $^{37}Cl(n,\gamma)^{38}Cl$. The ^{38}Cl gamma-emission peak (1642 ± 0.7 keV ref. 155) of irradiated samples was counted on a germanium-lithium counting system (Ortec 7030) and compared to a known quantity of $MgCl_2.6H_2O$ (typically 0.5 mmol) as a standard at the same time. This standard was selected to obtain an approximate quantity of chloride content, that would compare with the estimated chloride content of the sample.

2.8 Surface Area Determinations.

When a gas is allowed to come into contact with the surface of a solid, the gas may adsorb on the surface depending upon the experimental conditions. This adsorption may be either chemical (chemisorption) or physical in nature depending upon the type of bond formed between the gas molecules (the adsorbate) and the solid surface (the adsorbent). Chemisorption involves the formation of chemical bonds between the adsorbate and the adsorbent. In consequence, chemisorption is limited to the formation of a monomolecular layer at the surface and is limited to certain 'activated' solids and gases. In contrast, physical adsorption can, in principle occur between all gases and all solids provided the temperature is not considerably in excess of the boiling point of the adsorbate. Unlike chemisorption, physical adsorption forms no chemical bonds between the adsorbate and the adsorbent; forces similar to those responsible for the cohesive properties of liquids, i.e. van der Waal's forces,

are involved. Because of this, physical adsorption is not restricted to a mono-molecular layer, multi-layers may be built up on the surface.

The extent of coverage of the surface by the adsorbate will be related to the pressure of the adsorbate gas.

If a method of determining when the adsorbed monolayer is complete can be found, and the cross-sectional area of the gas molecule in the adsorbed state is known, the total surface area of the adsorbent presented to the gas phase can be calculated. Since chemisorption is limited to monolayer coverage it offers the best opportunity of determining surface areas. However, because of the restrictions on the type of solids which will partake in chemisorption, such methods are not generally applicable and physical adsorption methods must be employed.

The adsorption isotherm is obtained by plotting the relative pressure $^{P}/Po$ against the volume of the gas adsorbed. From the isotherm the adsorbed volume corresponding to a monolayer of gas on the surface may be determined using the B.E.T equation.

Brunauer, Emmett and Teller (157-158) postulated that layers of adsorbate molecules are adsorbed on those already on the surface of the adsorbent. They made two simplifying assumptions:-

(i) The molecules or atoms in successive layers are in dynamic equilibrium, and the amount adsorbed in each layer

when full is the same.

(ii) the heats of adsorption for all but the first layer are equal to each other and to E_L, the heat of liquefaction of the adsorbate. This is equivalent to say that the evaporation/condensation properties of the second and higher adsorbed layers are the same as those of the liquid state.

Using these postulates, Brunauer Emmett and Teller were able to derive an equation, now called the BET equation which fits the data for types II and III adsorption:

$$v = \frac{VmC}{(1-f)} \cdot \frac{f}{(1+(C-1)f)}$$

Equation 2.XIV

where

v = volume reduced to standard conditions of gas adsorbed per unit mass of adsorbent at a given pressure, P, and constant temperature T.

$f = P/Po$ where Po is the saturated vapour pressure at the experimental temperature.

Vm = volume, reduced to standard conditions of gas adsorbed per unit mass of adsorbent when the surface is covered by a unimolecular layer of adsorbate.

$C = e^{(E_1 - E_L)/RT}$ where E_1 is the heat of adsorption in the first layer and E_L is the heat of liquefaction of adsorbate.

Type II isotherms are given by equation 2.XIV when $E_1 > E_L$ i.e. $C > 1$.

Type III isotherms are given by equation 2.XIV when $E_1 < E_L$ i.e. $C < 1$.

$E_1 > E_L$ when the attractive forces between the adsorbent and adsorbate are greater than those between the adsorbate molecules in the liquefied state.

$E_1 < E_L$ when the attractive forces between the adsorbent and adsorbate are small in comparison with those between the adsorbate molecules in the liquid state.

In the surface area determinations helium gas was used to determine the dead space of the apparatus (Figure 2.15) and dinitrogen was used as the adsorbate in the surface area determinations.

The BET equation can be rearranged

$$\frac{f}{v(1-f)} = \frac{1}{VmC} + \frac{(C-1)}{VmC} \cdot f$$

Equation 2.XV

and a plot of $\frac{f}{v(1-f)}$ against f should be linear.

From the slope of this plot the value of $(C-1)/VmC$ can be obtained, and from the intercept on the ordinate a value

FIGURE 2.15

SURFACE AREA DETERMINATION

B.E.T. APPARATUS

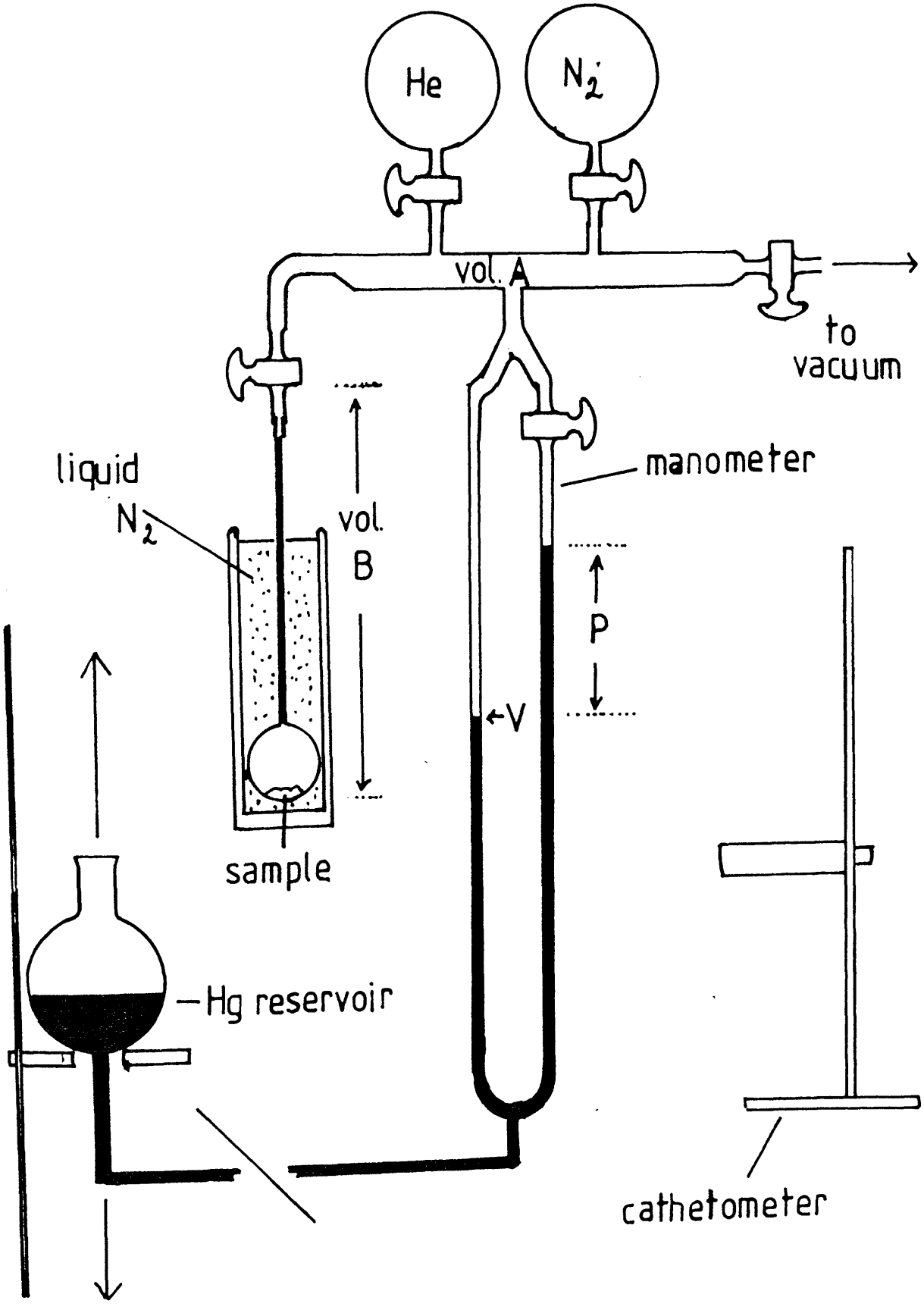

for $^{1}/VmC$ is obtained. From these two quantities the value Vm can be obtained.

The quantity of dinitrogen adsorbed may be determined by taking the difference between the measured volume of gas in the manometer and the volume expected on the basis of the gas laws if there has been no adsorption. For this reason the 'dead volumes', sections A and B in figure 2.15 were determined using helium, since it is not adsorbed to any appreciable extent, even at 77K.

Volume A was determined with volume B evacuated and helium in A. The height of mercury in the U-tube was varied by adjusting the height of the mercury reservoir and a set of readings of V and P obtained by the gas laws.

$$(V + A) = {}^{kT}/P$$

where k is a constant whose value depends on the size of the helium sample taken (cm^3 torr k^{-1}).

A is the dead volume above the zero mark on the burette (cm^3).

T is the temperature (K).

P is the pressure (Torr)

Equation 2.XVI

A plot of V against $^{T}/P$ has a slope K and intercept -A.

Volume B was determined using the same sample of helium but with the sample cooled to 77K and volume B open

to the apparatus hence:

$$(V+A+B) = kT/P$$

Equation 2.XVII

A plot of V against $^{T}/_{P}$ has slope k and intercept -(A+B).

This procedure was repeated for dinitrogen at room temperature and at 77K to give two further plots of V against $^{T}/_{P}$ with differing slopes but identical intercepts to the corresponding helium determinations. On the basis of the helium adsorption at 77K the corresponding data for dinitrogen should fit a line parallel to the room temperature isotherm for dinitrogen with an intercept -(A+B). At any pressure, the difference between the volume co-ordinate on this line and that on the experimental line is the volume adsorbed measured at the appropriate pressure. The number of molecules adsorbed, v, is given by

$$v = P.\ \delta v/_{T} \times \frac{N}{R}$$

where P is in Torr

δv is in cm^3

T is in Kelvin

N is the Avogardo Number

R is the gas constant in cm^3 torr K^{-1} mol^{-1}

Equation 2.XVIII

From the BET equation (Equation 2.XV) a plot of $P/Vm(po-p)$ versus p/Po is a straight line of slope $^{1}/Vm$. From this value the surface areas were calculated by

assuming that each nitrogen molecule occupied 16.2 $\mathring{A}^2$ of surface.

A surface area determination of γ-alumina is presented in Table 2D. Plots of V versus $^T/P$ under various conditions used and p/V(po-p) are shown in figures 2.16 and 2.17 respectively. From figure the gradient $= 1.3515 \times 10^{-21}$ (Figure 2.17).

$= 7.3990 \times 10^{20}$ molecules

for a sample mass of 0.5091g, this is equivalent to a surface area of $235.48 \pm 7.06\ m^2g^{-1}$.

Table 2D.

Surface Area Determination of calcined γ-alumina/523K. Sample weight 0.5091g.

Run.	Temp.(K)	Volume cm^3	P_1(Torr)	P_2(Torr)	ΔP(Torr)	$T/\Delta P$ (K $Torr^{-1}$)
He @ RT	295.9	88.2	525.91	384.88	141.03	2.098
	295.9	68.6	657.22	499.33	157.89	1.874
	295.9	54.1	756.72	583.22	173.40	1.707
	295.9	30.5	926.46	721.67	204.79	1.445
He @ 77K	295.9	83.8	526.80	410.57	116.23	2.545
	295.8	58.5	689.36	558.07	131.29	2.253
	295.8	39.8	812.21	667.30	144.91	2.041
	295.9	23.6	921.22	762.02	159.20	1.858
N_2 @ RT	295.8	95.4	525.59	343.11	182.48	1.621
	295.9	78.8	640.08	440.08	200.00	1.480
	295.9	53.4	821.25	587.89	233.36	1.268
	295.9	38.8	931.83	673.21	258.62	1.144
N_2 @ 77K	296.0	73.5	525.53	470.68	54.85	5.397
	295.8	53.4	647.76	588.82	58.94	5.019
	295.9	32.0	778.32	713.37	64.95	4.556
	295.7	6.2	936.82	863.69	73.13	4.043

Figure 2.16

Plot of He @ RT, He @ 77 K, N_2 @ RT and N_2 @ 77 K adsorption on 0.5094 g of Alumina calcined to 523 K

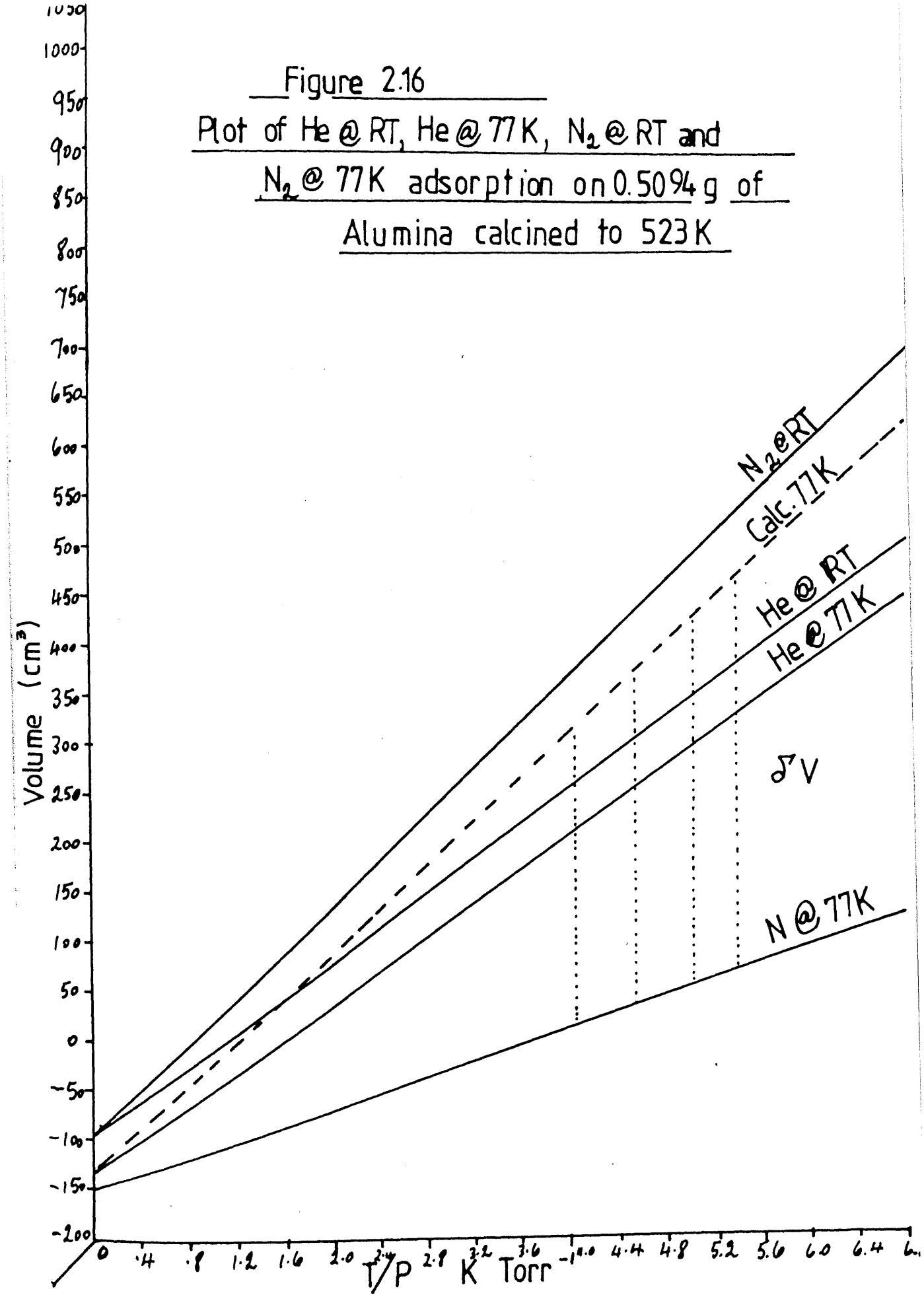

Figure 2.17

Determination of Surface Area of Sample A5 Calcined at 523K

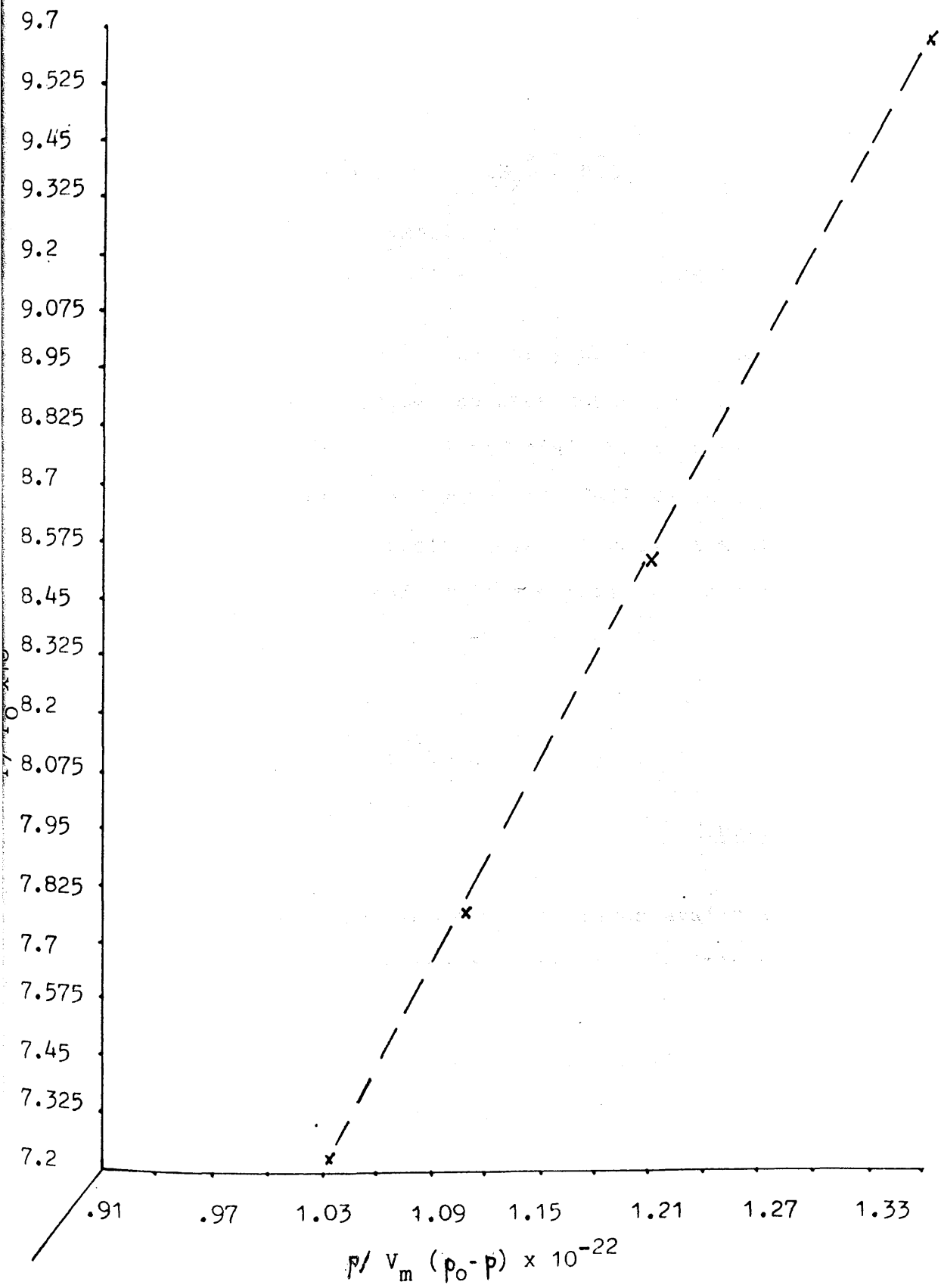

2.9 Exchange Reactions.

An exchange reaction occurs when atoms of a given element interchange between two different chemical states. Exchange can be observed by labelling one of the elements with a radioisotope and following the position of the isotope (159).

$$AB_x^* + BC_y \qquad AB_x^* + B^*C_y$$

($m_1$mol) ($m_2$mmol)

Equation 2.XIX

At first only the heavy elements with naturally occurring radioactivity isotopes could be used to follow exchange reactions. Artificial radioactivity was discovered in 1934 when aluminium foil which had been bombarded with α-particles gave off radiation after the bombardment had ceased (158) and this led to the availability of radioisotopes of the lighter elements (160).

$$^{27}_{13}Al + {}^{4}_{2}He \qquad {}^{30}_{15}P + {}^{1}_{0}N$$

Equation 2.XX

Due to the low neutron fluxes available at this time only short-lived isotopes of low specific activity were produced. After 1945, the development of nuclear reactors and particle accelerators enabled the production of both short and long-lived radioisotopes of nearly all elements. This removed most of the restrictions on the systems which could be examined and exchange reactions

have provided much information on a wide variety of topics, for example molecular structure, bond types and reaction kinetics (161-162).

They are also very useful in investigating catalytic reactions. Sensitivity in the detection of radioactivity renders it of considerable value in the study of surface processes (163).

The rate of disappearance of the isotopic species from an initially unlabelled reactant is described by a first order rate law regardless of the number of atomic species which participate, since there can be no change in the concentration of the reactants (164). It is possible therefore to perform quantitative investigations of exchange reactions. Results can be expressed in terms of the fraction of activity exchanged (f) where (f) is defined by Equation 2.XXI.

$$f = \frac{\text{fraction of activity in the initially unlabelled compound}}{\text{fraction of chlorine (mg-atom) in the initially unlabelled compound}}$$

Equation 2.XXI

The fraction exchanged (f) can be determined experimentally using equations 2.XXII, 2.XXIII, or 2.XXIV.

$$f = \frac{A_1}{A_1+A_2} \left(\frac{xm_1}{xm_1+ym_2} \right)^{-1}$$

Equation 2.XXII

or

$$f = \frac{(Ao-A_2)(xm_1+ym_2)}{A_o xm_1}$$

Equation 2.XXIII

where A_1 and A_2 are the counts corrected for decay after exchange between m_1 and m_2 mmol of reactants (m_1 being inactive initially) containing respectively x and y chlorine atoms. Ao is the corrected counts of reagent 2 prior to exchange.

Also derived from equation 2.XIX is the fundamental definition of the fraction exchanged, where the initial count rate of AB_x^* at time = 0 is Ao count s^{-1}, and the final count rate of AB_x^* at time = t is A_t count s^{-1}.

The initial specific count rate of AB_x^* (So) is defined by $\frac{Ao}{xm_1}$ count s^{-1} (mg atom Cl)$^{-1}$. For 100% exchange the specific count rate of AB_x^* (S∞) becomes:-

$$\frac{Ao}{xm_1 + ym_2} \quad \text{count } s^{-1} \text{ (mg atom Cl)}^{-1}$$

Should zero exchange (0%) occur the specific count rate of AB_x^* remains $\frac{Ao}{xm_1}$ count s^{-1} (mg atom Cl)$^{-1}$.

Therefore at exchange equilibrium (x%) the specific count rate of AB_x^* (St) will be $\frac{A_t}{xm_1}$ count s^{-1} (mg atom Cl)$^{-1}$.

Therefore the fraction exchanged can be

calculated from:

Fraction exchanged (f) =

$$\frac{\text{specific count rate(0\%)-specific count rate (x\%)}}{\text{specific count rate(0\%)-specific count rate (100\%)}}$$

$$\therefore f = \frac{So - Sf}{So - S\infty}$$

Equation 2.XXIV

Equations 2.XXII, 2.XXIII, 2.XXIV should in theory give the same answer providing the radiochemical balance is >95%, i.e. $Ao = A_1+A_2$. In practice this is not always the case since three possible events can arise from the chlorinated exchange reagents.

1. Chlorine exchange with no retention of the gas by the solid. In this situation any of the fraction exchanged equations may be used and the value of f obtained indicates the degree to which exchanged has occurred. For f = 0 then no exchange has occurred and for f = 1 corresponds to complete exchange, that is a random distribution of activity.

2. Retention of the gas by the solid with no chlorine exchange. In this situation equation 2.XXII would give a value of f>1 and equation 2.XXIII would give a value of f = 0. Therefore as soon as uptake of gas occurs equation 2.XXII becomes invalid and equation 2.XXIII must be used.

3. Chlorine exchange and retention of gas by the solid. In this case equation 2.XXII will give a value of f>1. Since equation 2.XXIII depends on the counts of the gas before and after reaction, a true measure of the fraction exchanged will be obtained if this equation is used.

Equation 2.XXIII will give a true measure of the fraction exchanged whereas equation 2.XXII will only give a true result if there is no uptake of gas. Verification of the fraction exchanged can be obtained by using equation 2.XXIV which is dependent on the specific count rates prior and after reaction. The specific count rates prior and after reaction are obtained via the procedure described in section 3.3.6.

2.10 ^{27}Al - MAS - NMR

2.10.1 Instrumentation

The ^{27}Al magic angle spinning nuclear magnetic resonance spectroscopy investigation was carried out at the Industrial Research Laboratories of the University of Durham, using a Varian UXR-300/89 NMR spectrometer. This instrument is dedicated to solid-state NMR work and is equipped with a 7.0 Tesla superconducting magnet with 89mm vertical bore. It operates at 300 MHz for ^{1}H and at 78.152 MHz for ^{27}Al nuclei. The MAS-NMR spectrum was obtained by way of a pulse of width 15 degrees and decoupling the protons. Typically 40 μs pulses were

used to excite the $(\frac{1}{2}, -\frac{1}{2})$ transitions and 1000 free induction decays were accumulated with a repetition time of 0.5 seconds. The spectra were obtained using a probe which was aluminium free and gave no background signal. Chemical shifts were recorded, with an aqueous solution of $Al(H_2O)_6Cl_3$ serving as an external standard contained in a 300 microlitre (μl) zirconia tube. The response of the samples under a single-pulse excitation combined with magic-angle spinning at 3kHz and 4 kHz were used to obtain time domain data which were Fourier transformed for frequency domain information.

CHAPTER 3.

Reactions of Anhydrous Hydrogen Chloride with γ-Alumina

It has been demonstrated that the chemisorption of anhydrous gaseous hydrogen chloride on γ-alumina (1.6% by wt. of chlorine) leads to the formation of Brønsted acid sites as well as non-acidic hydroxyl groups (99) on the surface of γ-alumina. γ-Alumina samples with varying chlorine content show increased ^{1}H-^{2}H exchange rates as the chlorine content of the γ-alumina is increased. However the acid sites produced by the chlorination of γ-alumina with anhydrous gaseous hydrogen chloride does not lead to the formation of an active catalyst towards low temperature isomerization of olefins (22).

In the present work the uptake of anhydrous hydrogen chloride by γ-alumina was studied as a function of the calcination temperature of the γ-alumina using [^{36}Cl]-chlorine labelled hydrogen chloride. The chlorine content of the hydrogen chloride treated γ-aluminas was determined by a gas phase count *vs* pressure calibration procedure (Section 2.5.2). The lability of the chemisorbed chlorine species on the precalcined γ-alumina was studied as a function of the calcination temperature, by exchanging anhydrous gaseous [^{36}Cl]-chlorine labelled hydrogen chloride with precalcined γ-alumina treated with anhydrous hydrogen chloride, subsequently determining the specific count rate of the exchanged gas phase. The B.E.T. area of the calcined γ-alumina and the B.E.T. areas of the anhydrous hydrogen chloride treated precalcined γ-aluminas were determined as a function of the calcination

temperature using nitrogen as the adsorbate gas (Section 2.8).

3.2.1 The B.E.T Area Determination of Calcined Spence γ-Alumina and Calcined Condea γ-Alumina.

The results of the B.E.T area determinations for the calcined γ-alumina samples are presented together with the surface areas of the calcined γ-alumina samples treated with anhydrous gaseous hydrogen chloride at 293K (Table 3.1). The B.E.T areas are presented from three B.E.T area determinations for each calcined sample. The results for the calcined Spence γ-alumina samples and the hydrogen chloride treated materials are shown schematically in figure 3.1. Calcination of the γ-alumina samples up to 523K resulted in an increase in the surface area of the material as the calcination temperature was increased. Different behaviour was observed between 293K and 373K and between 373K and 523K respectively. The smaller increase in the surface area for the region from 293K to 373K relative to the region from 373K to 523K was consistent with the desorption of water molecules which are present on the surface up to 373K (66). The region from 373K to 523K showed an initial rapid increase in the surface area between 373K and 423K which is attributed to the loss of chemisorbed water from the surface of the γ-alumina together with the loss of water by the condensation of hydroxyl groups from the surface of the γ-alumina. The smaller rate of increase in the surface area as a function of the calcination temperature in the region from 423K to 523K relative to the

Table 3.1

Sample	Calcination Temp. (K)	Calcined Surface area m^2g^{-1}	Chlorinated Surface area m^2g^{-1}	Ratio chlorinated Surf. area/calcined surface area	Reduction in the B.E.T area due to the chlorination process m^2g^{-1}	Surface density of chlorine atoms
A1	293	129.28 ± 10.26	47.12 ± 4.13	.36	82.16	13.27 ± 0.75
A2	373	143.39 ± 21.34	53.30 ± 2.52	.37	90.09	8.82 ± 1.15
A3	423	202.15 ± 2.56	123.82 ± 5.97	.61	78.33	6.10 ± 0.08
A4	473	232.32 ± 21.11	147.62 ± 9.14	.64	84.70	5.05 ± 0.30
A5	523	252.08 ± 23.86	167.20 ± 22.96	.66	84.88	4.89 ± 0.42
C1	293	161.96 ± 2.56	141.95 ± 2.37	.88	20.01	8.9 ± 0.05
C3	423	174.29 ± 2.98	153.03 ± 3.47	.88	21.26	4.8 ± 0.12
C5	523	191.20 ± 3.25	172.78 ± 1.88	.90	18.42	4.4 ± 0.08

Figure 3.1

B.E.T. Areas of Calcined Spence γ-Alumina and Hydrogen Chloride Treated γ-Alumina Samples.

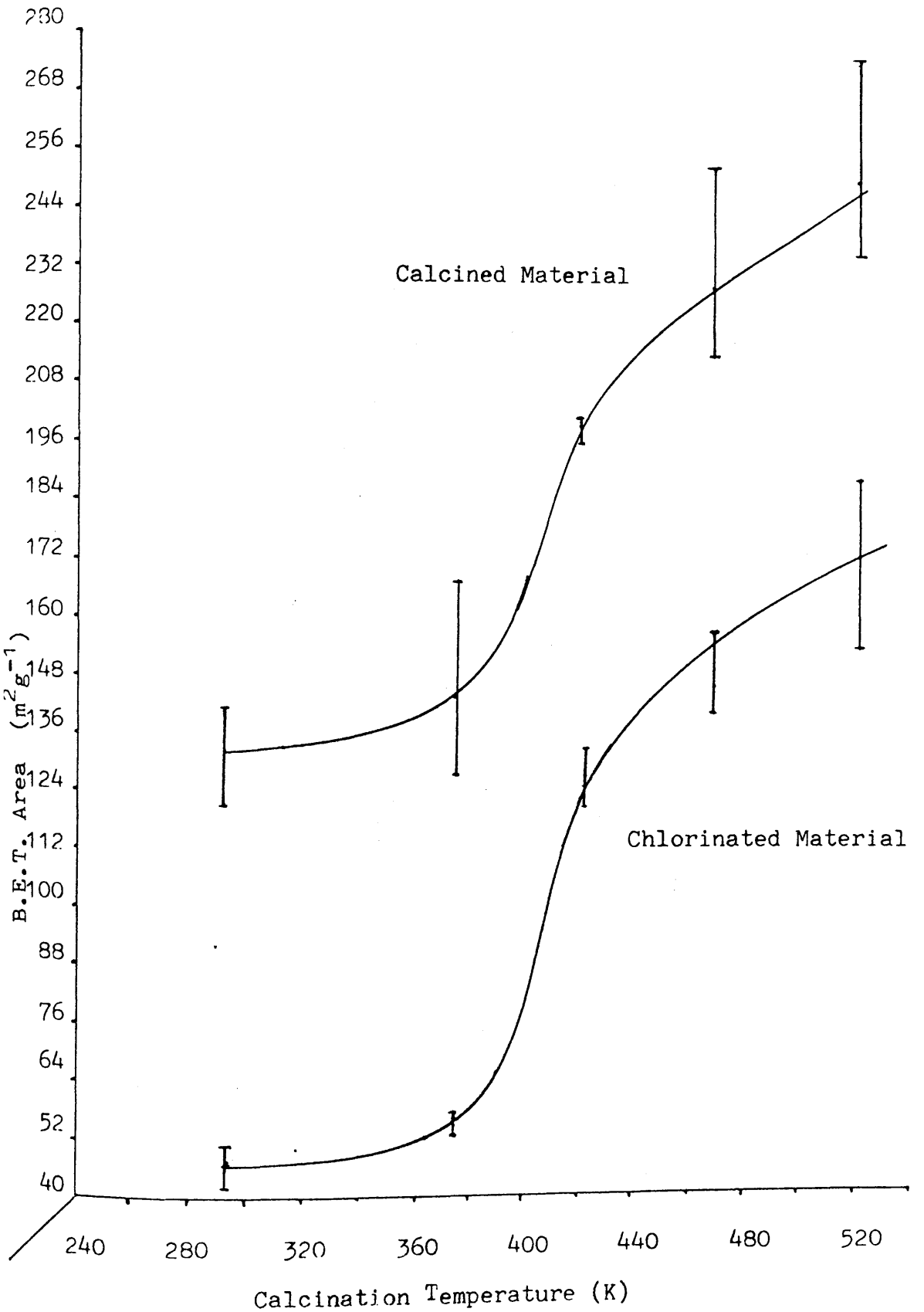

region from 373K to 423K is consistent with the loss of water owing to the condensation of hydroxyl groups from the surface of γ-alumina.

The calcined Condea γ-alumina exhibited the same characteristics described above in that an increase in the calcination temperature resulted in an increase in the B.E.T area of the material (Figure 3.1b). It was not possible to identify any region due to the desorption of water by the condensation of hydroxyl groups owing to the small number of data points as a result of a limited sample supply.

3.2.2 The Interaction of Gaseous [^{36}Cl]-Chlorine-labelled Hydrogen Chloride with the Pyrex Counting Cell.

When anhydrous gaseous [^{36}Cl]-chlorine-labelled hydrogen chloride was admitted into the counting cell (Figure 2.11) at room temperature, the count rates monitored by both Geiger-Müller tubes remained constant over 4h. The initial and final background count rates were identical. This result was reproducible and indicated that the adsorption of [^{36}Cl]-chlorine labelled hydrogen chloride on the Pyrex glass of the counting cell at 293K was not significant.

3.2.3 The Interaction of Gaseous [^{36}Cl]-Chlorine Labelled Hydrogen Chloride with Calcined Spence γ-Alumina

In the experiments where anhydrous gaseous [^{36}Cl]-chlorine labelled hydrogen chloride was admitted into the counting cell (Figure 2.11)a substantial detectable surface count rate was observed from the solid which increased

Figure 3.1b

B.E.T. Areas of Calcined Condea γ-Alumina and Hydrogen Chloride Treated γ-Alumina

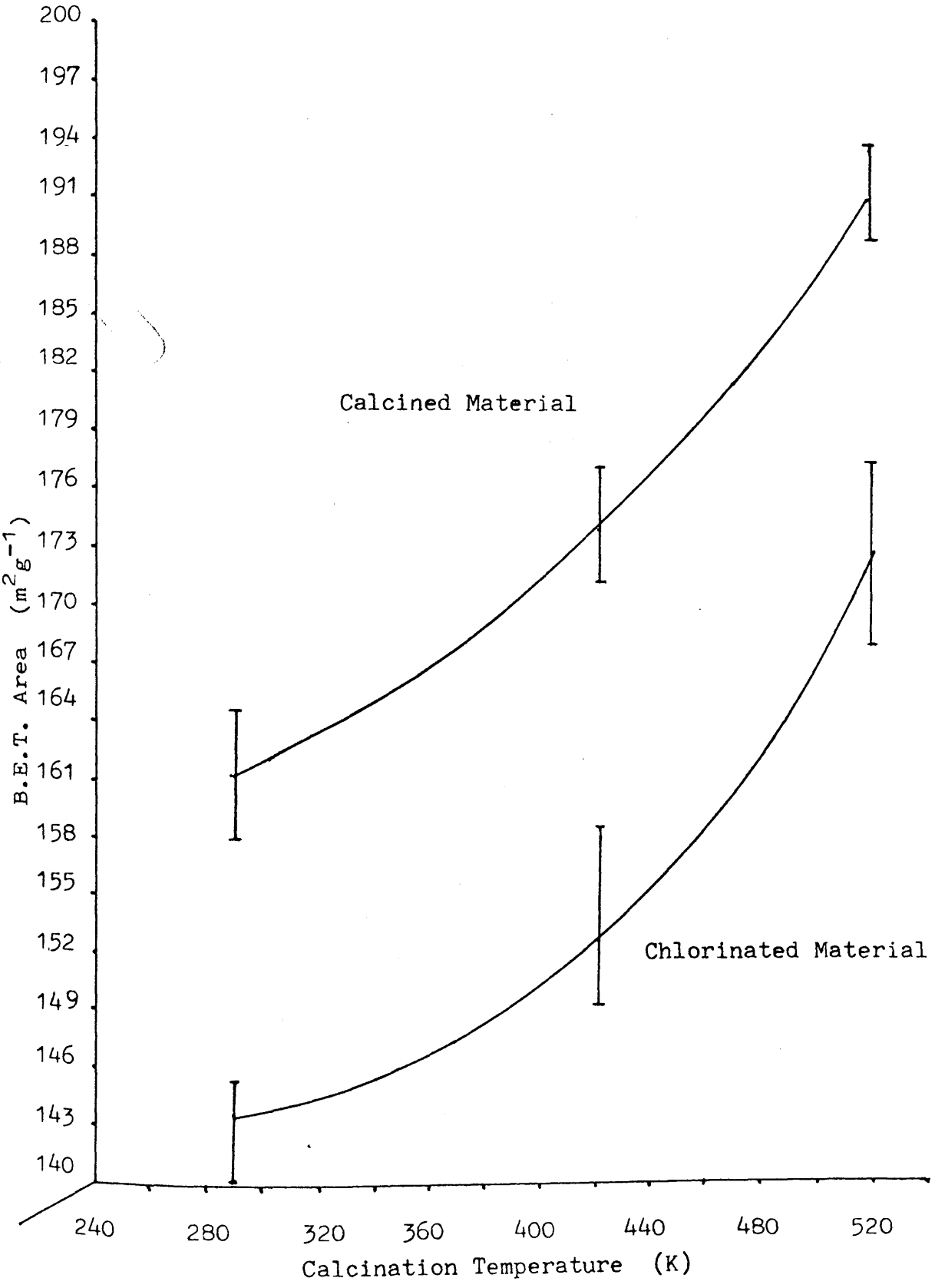

significantly over a period of 4 min. before reaching a constant value (Figure 3.2). The surface count rates were monitored for γ-alumina samples calcined to 293K, 373K, 423K, 473K and 523K as a function of time to determine the effect of the calcination temperature of the solid on the uptake of [^{36}Cl]-chlorine labelled hydrogen chloride. The results of the equilibrium surface count rate for the calcined γ-alumina samples are shown schematically in figure 3.2. The surface count rate in these experiments is dependent on the calcination temperature in that an increase in the calcination temperature lowers the equilibrium surface count rate of the oxide material. Pumping the solid for up to 5 days after removal of volatile material did not lead to a significant decrease in the surface count rate.

The uptake of [^{36}Cl]-chlorine labelled hydrogen chloride was determined by measuring the decrease in the gas phase count rate of the anhydrous [^{36}Cl]-chlorine labelled hydrogen chloride which is directly proportional to the pressure of the [^{36}Cl]-chlorine labelled hydrogen chloride adsorbed by the solid during the experimental period. Using the gas phase counts versus pressure of [^{36}Cl]-chlorine labelled hydrogen chloride calibration graph (Section 2.5.2) the number of millimoles of anhydrous gaseous [^{36}Cl]-chlorine labelled hydrogen chloride adsorbed by the calcined γ-alumina was determined as a function of the calcination temperature of the γ-alumina. To illustrate the method of determining the [^{36}Cl]-chlorine labelled hydrogen chloride uptake by a sample of γ-alumina, a specimen calculation of the uptake of [^{36}Cl]-chlorine labelled hydrogen chloride by Spence γ-alumina calcined to

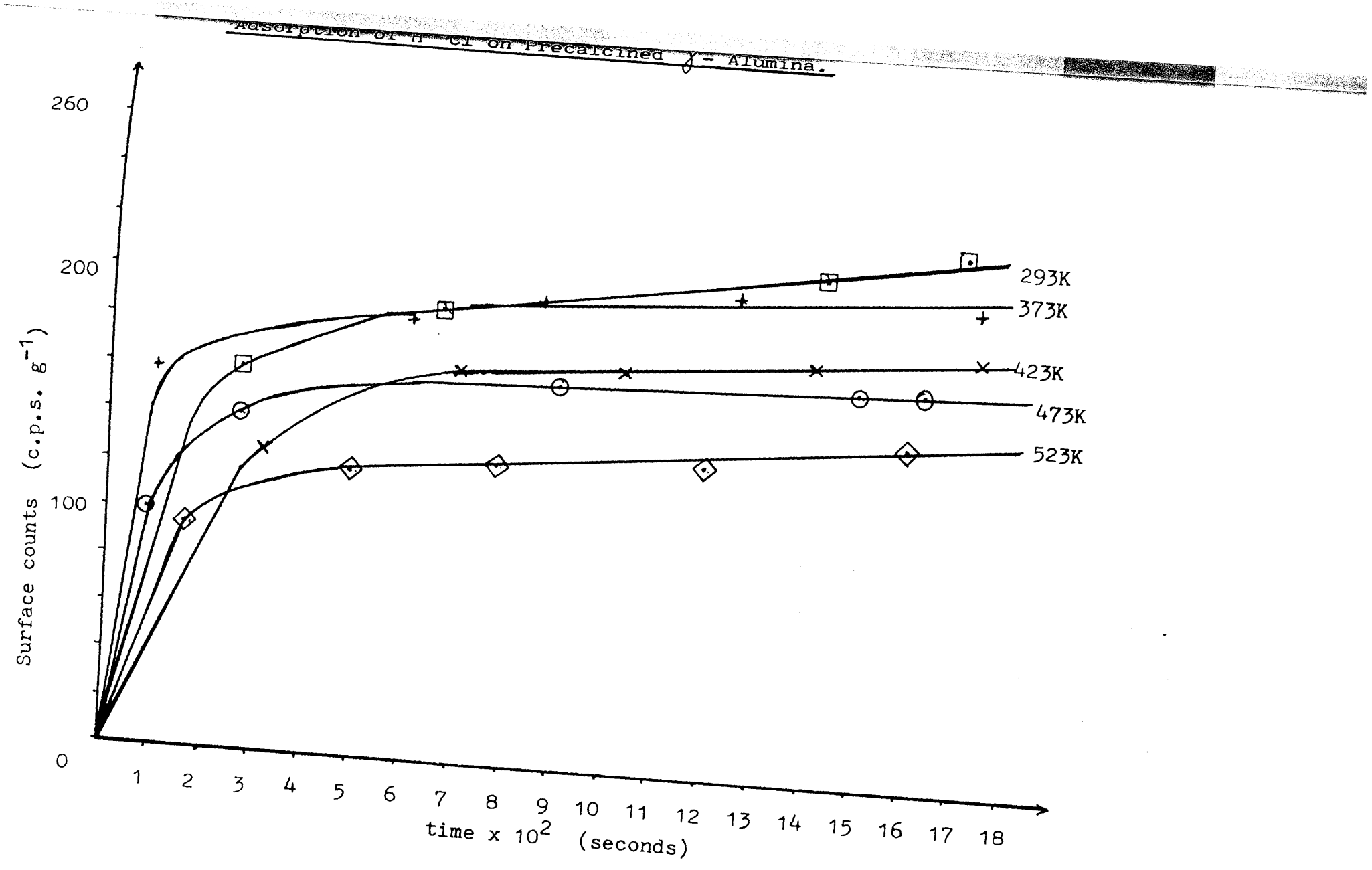
Adsorption of H Cl on Precalcined γ - Alumina.
260
200
100
0
Surface counts (c.p.s. g⁻¹)
293K
373K
423K
473K
523K
1 2 3 4 5 6 7 8 9 10 11 12 13 14 15 16 17 18
time x 10² (seconds)

473K is presented.

The volume of the manifold including the constant volume manometer and the counting cell (Figure 2.1) was 1356.72cm^3. The pressure of gaseous [^{36}Cl]-chlorine labelled hydrogen chloride at 300K required to deliver 1 mmol to the system is 13.80 Torr. From the gas phase count rate of H^{36}Cl versus pressure of anhydrous hydrogen chloride calibration graph (Figure 2.12a) the equivalent gas phase count rate from a pressure of 13.80 Torr would be 10.81 count s^{-1}. Hence expansion of [^{36}Cl]-chlorine labelled hydrogen chloride (2mmol;27.6Torr) into the counting cell was equivalent to 21.62 count s^{-1} in the system. The residual gas phase count rate at equilibrium was 9.04 count s^{-1}. Therefore the total adsorption of gas phase [^{36}Cl]-chlorine labelled hydrogen chloride by the calcined γ-alumina was equivalent to a pressure which gave a count rate of 12.58 count s^{-1}. From the gas phase count rate versus pressure of anhydrous [^{36}Cl]-chlorine labelled hydrogen chloride calibration graph (Figure 2.12a), 12.58 count s^{-1} is equivalent to 15.8 Torr of [^{36}Cl]-chlorine labelled hydrogen chloride. The number of moles of [^{36}Cl]-chlorine labelled hydrogen chloride taken up by the γ-alumina sample can be calculated using the gas laws to be 1.14mmoles. If the sample weight is known (0.5593g) the specific uptake of the sample can be calculated and is found to be 2.05 mmol g^{-1}. This method of calculating the uptake of [^{36}Cl]-chlorine labelled hydrogen chloride was carried out for the samples of γ-alumina calcined to 293K, 373K, 423K and 523K respectively. The uptake of

[^{36}Cl]-chlorine labelled hydrogen chloride as a function of the calcination temperature for Spence and Condea γ-aluminas is shown schematically in figure 3.3 and is tabulated in table 3.3. From the results of the specific uptakes of [^{36}Cl]-chlorine labelled hydrogen chloride by the calcined γ-alumina samples together with the B.E.T. area determinations, the density of the chlorine species on the surface of the γ-alumina can be calculated (Table 3.3) given the assumption that the chlorination process is a surface phenomena. Experimental evidence that this is the case is presented in section 3.2.5. For the γ-alumina calcined at 293K the surface density was determined as 13.27±0.75 chlorine atoms per nm^2 and this value is in good agreement with the evaluation of a surface density of 12-16 hydroxyl groups per nm^2 for the complete mono-layered hydroxyl surface coverage on γ-alumina reported by J.J. Kipling and D.B. Peakall (37). The uptake of anhydrous [^{36}Cl]-chlorine labelled hydrogen chloride by γ-alumina calcined to 373K resulted in a surface density of 1 chlorine atom per 11 $Å^2$ and this value is in exact agreement with the surface concentration of hydroxyl groups at 373K reported by J.B. Peri (69).

3.2.4 The Interaction of Anhydrous Gaseous [^{36}Cl]-Chlorine Labelled Hydrogen Chloride with Condea γ-Alumina.

The method to determine the uptake of anhydrous gaseous [^{36}Cl]-chlorine labelled hydrogen chloride is described in section 3.2.3, and the results are tabulated in table 3.3. The uptake of the [^{36}Cl]-chlorine labelled hydrogen chloride on the Condea γ-alumina samples as a

Figure 3.3

Uptake of $H^{36}Cl$ as a function of the Calcination Temperature

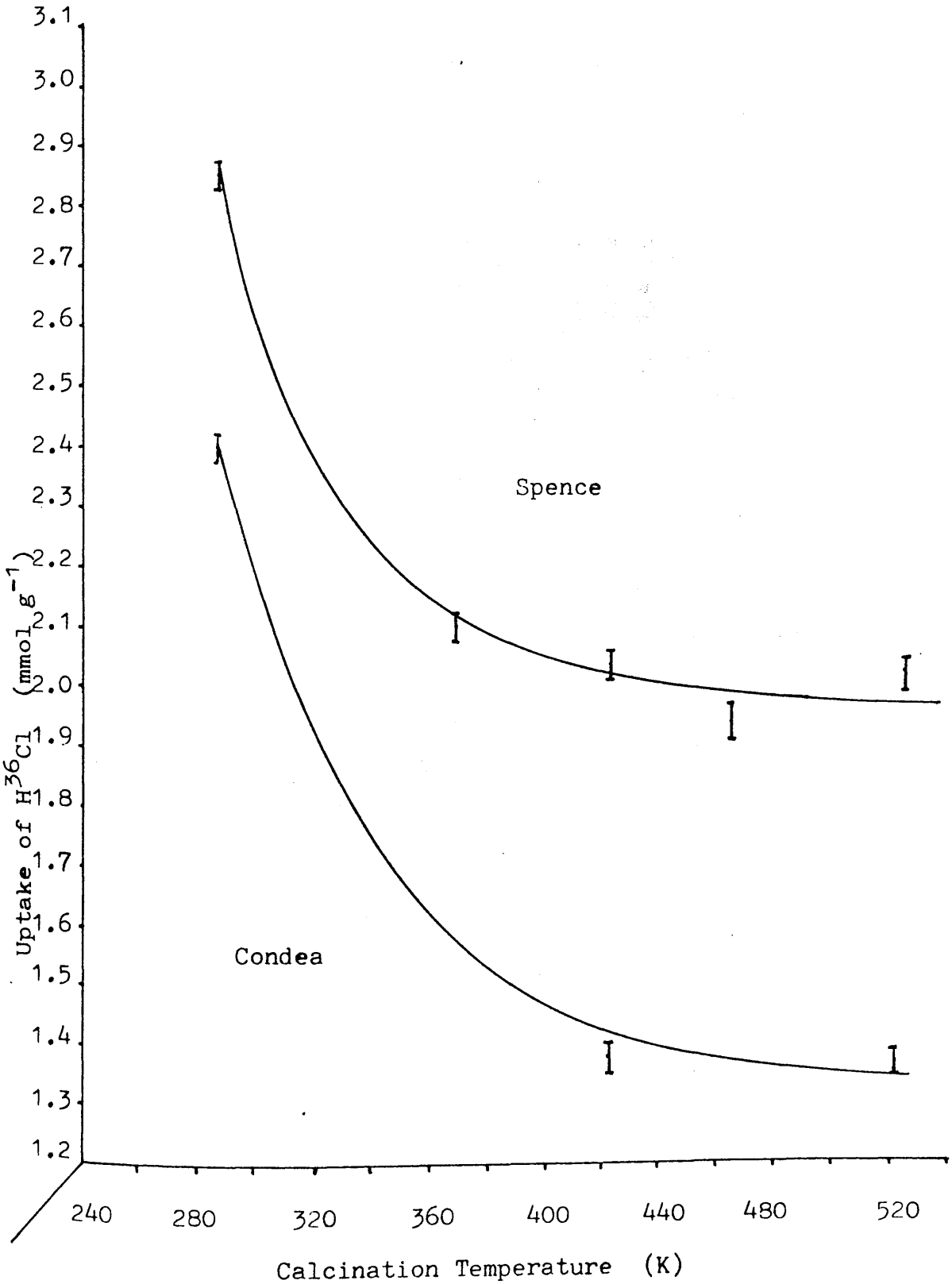

Table 3.3 Uptake of [^{36}Cl]-chlorine labelled hydrogen chloride by γ-alumina as a function of the calcination temperature.

Spence type:

Calcination Temp. (K)	B.E.T Surface Area ($m^2 g^{-1}$)	Uptake of $H^{36}Cl$ (mmol g^{-1})	Density of Chlorine (atoms nm^2)
293	129.28 ± 10.26	2.85 ± 0.30	13.27 ± 0.75
373	143.39 ± 21.34	2.10 ± 0.20	8.82 ± 1.15
423	202.15 ± 2.56	2.05 ± 0.20	6.10 ± 0.08
473	232.32 ± 21.11	1.95 ± 0.20	5.05 ± 0.30
523	252.08 ± 23.86	2.05 ± 0.20	4.89 ± 0.42
Condea γ-alumina			
293	161.96 ± 15.31	2.4 ± 0.20	8.9 ± 0.05
423	174.29 ± 13.95	1.4 ± 0.15	4.8 ± 0.12
523	191.20 ± 18.71	1.4 ± 0.15	4.4 ± 0.08

function of the calcination temperature are shown in figure 3.3. The uptake of 2.4 ± 0.20 mmol g^{-1} by Condea γ-alumina calcined at 293K of anhydrous gaseous [^{36}Cl]-chlorine labelled hydrogen chloride is attributed to the solubility of anhydrous gaseous [^{36}Cl]-chlorine labelled hydrogen chloride in water which is present on the surface of γ-alumina at this calcination temperature. This is the same as the result obtained for the Spence γ-alumina calcined to 293K (Section 3.2.3). The calcination of the Condea γ-alumina resulted in chlorine surface densities on the γ-alumina comparable to the results obtained for the Spence γ-alumina samples (Table 3.3). As the calcination temperature increases the chlorine surface density of the Condea γ-alumina also decreases, as is the case for the Spence γ-alumina samples (Figure 3.3a). The results showed that the surface densities of the chlorine species on the Spence and Condea γ-alumina samples were becoming equal as the calcination temperature was increased.

3.2.5 The B.E.T Area Determinations of Calcined Spence γ-Alumina Treated with Anhydrous Hydrogen Chloride at 293K.

The procedure to determine the B.E.T area of chlorinated calcined γ-alumina samples is described in section 3.3.4. The results are presented in table 3.1 and figures 3.1a and 3.1b The treatment of calcined γ-alumina with anhydrous hydrogen chloride at 293K resulted in a uniform reduction in the surface area of the γ-alumina samples across the calcination range from 293K to 523K from the initial surface area of the untreated calcined material. There is a relationship between

Figure 3.3a

Surface Density of Chlorine for Spence and Condea Calcined γ-Alumina Samples.

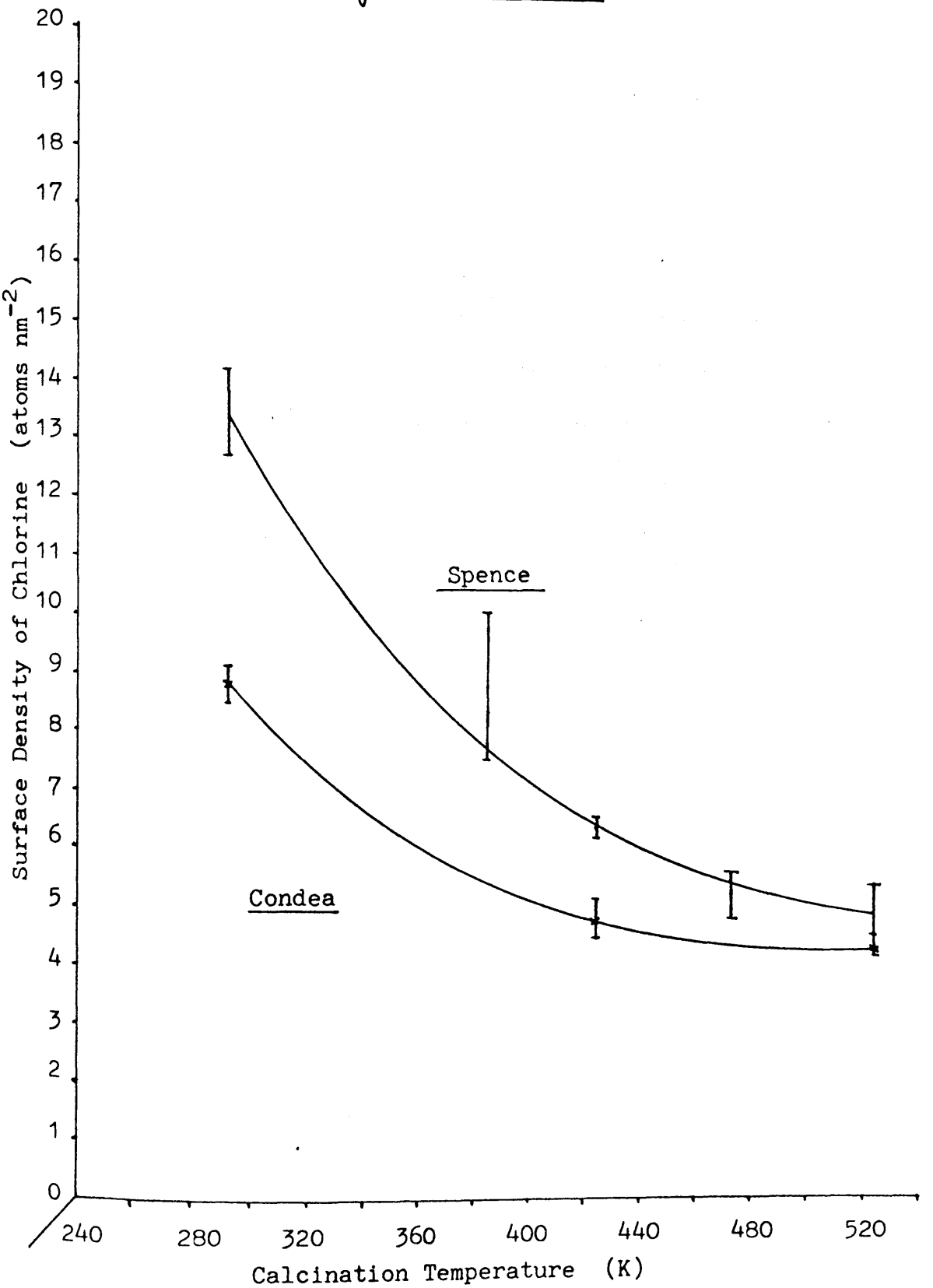

the calcined γ-alumina surface area and the surface area of the hydrogen chloride treated γ-alumina. The ratio of the surface area of the chlorinated γ-alumina to the surface area of the calcined material will show up the extent of the reduction in the surface area of the calcined material owing to the chlorination process. This ratio of the B.E.T area of the chlorinated calcined γ-alumina sample to the B.E.T area of the calcined γ-alumina sample as a function of the calcination temperature is shown in figure 3.4. The surface area ratios of the chlorinated to the calcined γ-alumina (Figure 3.4) as a function of the calcination temperature parallels the relationship between the surface area of either the chlorinated material as a function of the calcination temperature or that of the surface area of the calcined material as a function of the calcination temperature (Figure 3.1). The reduction in the B.E.T area of the calcined solid due to the chlorination process as a function of the calcination temperature is tabulated (Table 3.1). The mean and standard deviation of this reduction in the surface area of the solid due to the chlorination process at 293K for the samples calcined between 293K and 523K is $84.032 \pm 4.29\ m^2g^{-1}$ and the small variance in the deviation is a measure of the uniformity of the reduction in the surface of the solid across the calcination range from 293K to 523K. Figure 3.5 represents the ratio of the chlorinated surface area to the calcined surface area as a function of the surface density of chlorine (Table 3.1). The final point at 13.27 ± 0.75 chlorine atoms nm^{-2} deflects from linearity owing to the solvation of chlorine in surface bound water, which is not consistent with the system where the treatment of calcined

Figure 3.4

Surface Area of Chlorinated γ-Alumina / Surface Area calcined γ-Alumina as a function of Calcination Temperature.

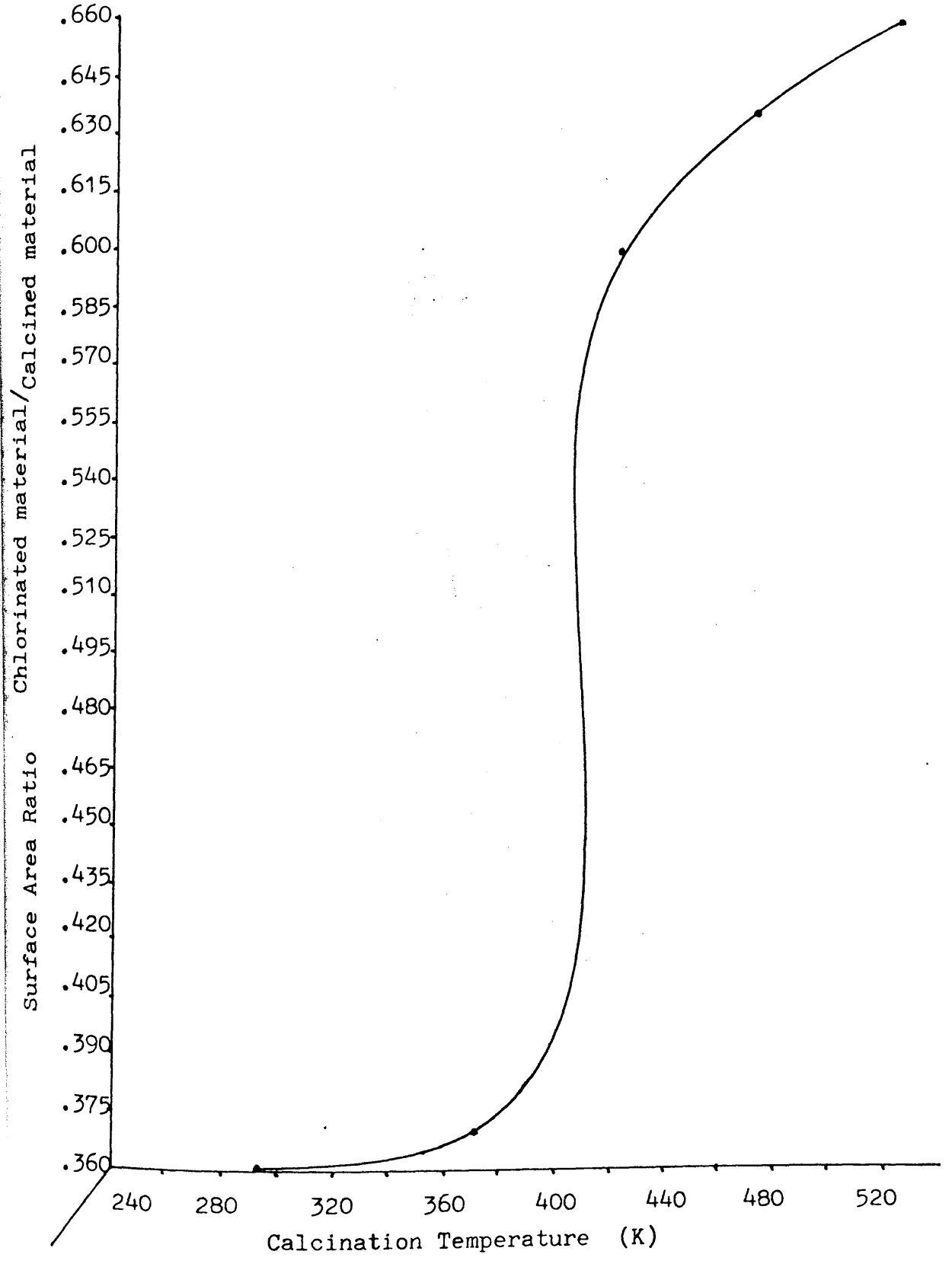

Figure 3.5

Ratio of B.E.T. Area of Chlorinated γ-Alumina / B.E.T Area of Calcined γ-Alumina versus Chlorine Surface Density.

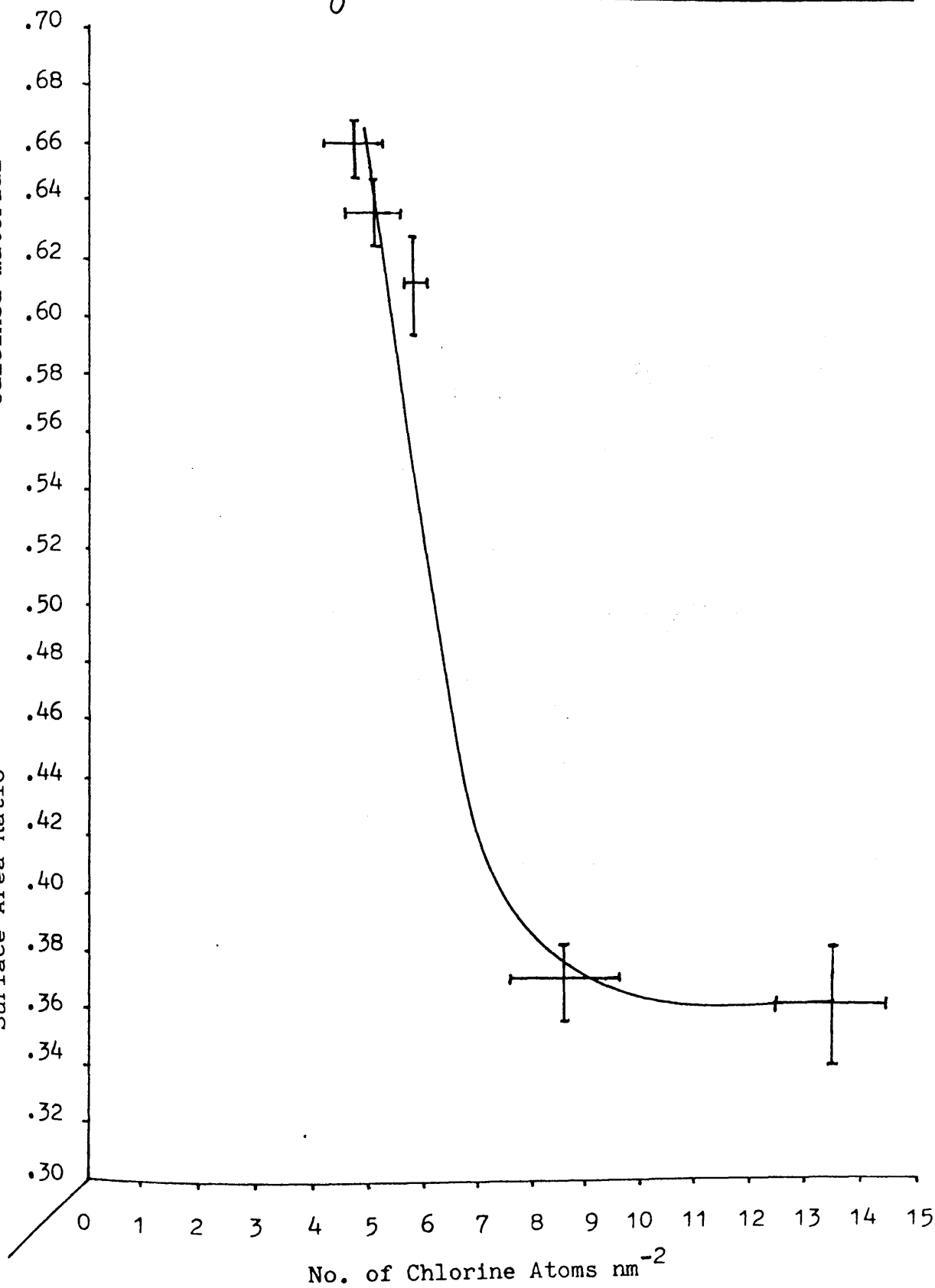

γ-alumina with anhydrous hydrogen chloride is a true surface process. This uniform decrease in the surface areas of the chlorinated materials across the calcination range, together with the consistency in the observed relationships between:-

i) The B.E.T areas of the calcined γ-alumina

ii) The B.E.T areas of the calcined γ-alumina treated with anhydrous gaseous hydrogen chloride at 293K.

iii) The ratio of the B.E.T area of the chlorinated material to the B.E.T area of the calcined material as functions of the calcination temperature.

The general pattern of the results are consistent with the chlorination process of γ-alumina at 293K with anhydrous hydrogen chloride being a surface phenomena.

3.2.6 Exchange at 293K between Anhydrous [^{36}Cl]-Chlorine -labelled Hydrogen Chloride and Anhydrous Hydrogen Chloride treated Calcined Spence γ-Alumina.

When [^{36}Cl]-chlorine labelled hydrogen chloride was admitted into the counting cell containing calcined Spence γ-alumina a rapid increase in the surface activity of the solid calcined hydrogen chloride treated γ-alumina sample resulted over the first 15 min (Figure 3.6). This increase in the surface activity of the calcined γ-alumina was followed by a period in which the increase in the surface activity with time was slower and after 48 min a constant value was obtained. At this point equilibrium for the exchange reaction was established. The increase in the surface activity indicated that the chlorine on the surface of the catalyst had exchanged with the anhydrous [^{36}Cl]-chlorine labelled

Figure 3.6

Surface Activity of Anhydrous Hydrogen Chloride treated γ-Alumina @ 293K Calcined at 423K on exchange with 1mmol $H^{36}Cl$ @ 293K.

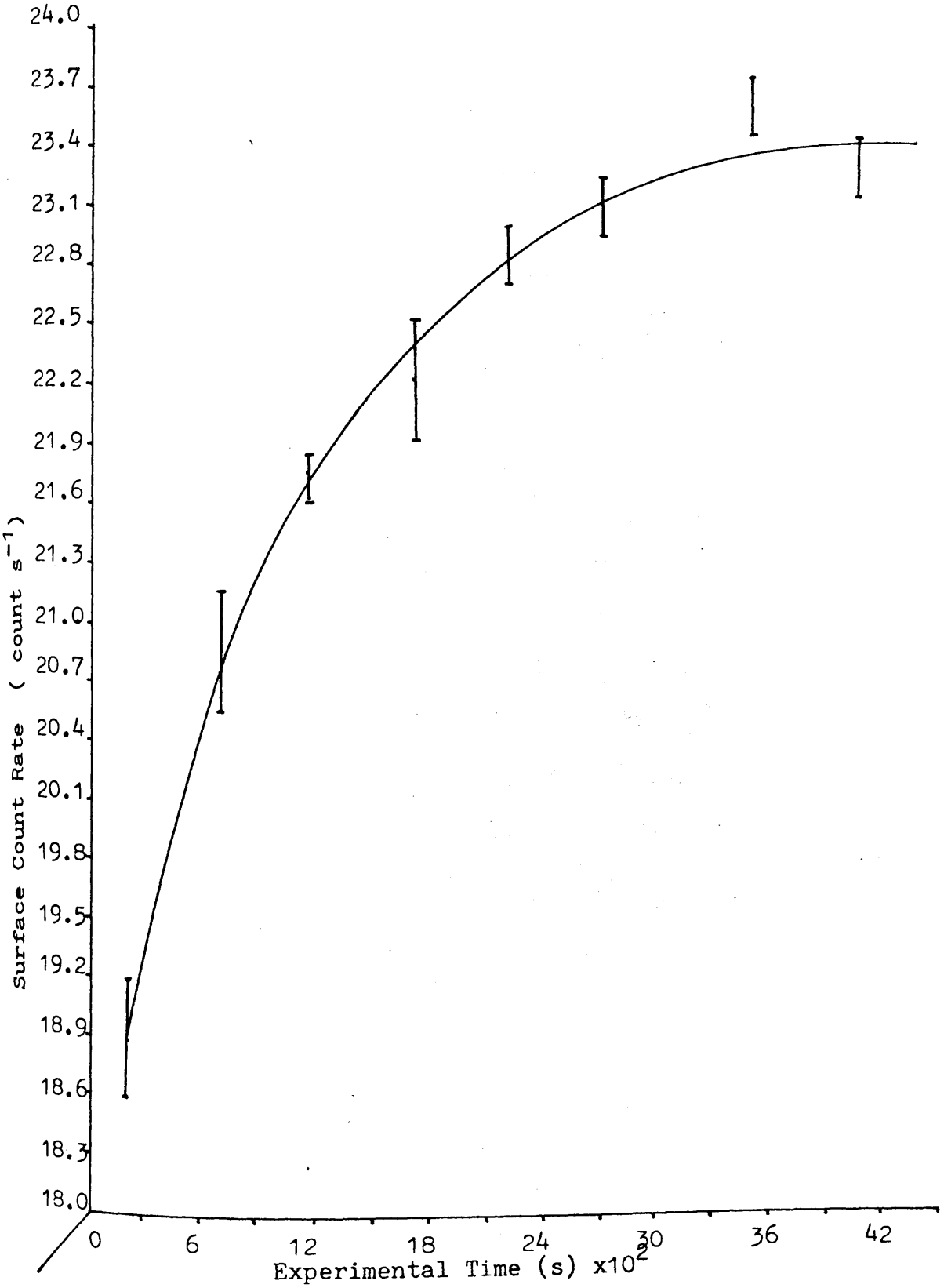

hydrogen chloride in the gas phase. The specific count rate of the anhydrous [^{36}Cl]-chlorine labelled hydrogen chloride was determined prior to the exchange by the procedure described in section 2.5.3 and was found to be 0.52 count s^{-1} mg^{-1} $Ag^{36}Cl$. The specific count rate was obtained from the equilibrium gas phase for the exchange reaction and determined by the procedure described in section 3.3.6. The reduction in the specific count rate obtained from the equilibrium gas phase after the exchange of the aliquot of [^{36}Cl]-chlorine labelled hydrogen chloride (Table 3.4) with the chlorinated calcined γ-alumina sample from the specific count rate of the [^{36}Cl]-chlorine labelled hydrogen chloride before the exchange reaction was obtained (Table 3.4). The results are shown in figure 3.7. As the surface area of the chlorinated γ-alumina increases (Figure 3.7) and the surface density of the chlorine falls (Figure 3.7a) the change in the specific count rate of the equilibrium gas phase from the starting value of 0.52 count s^{-1} $mg^{-1}Ag^{36}Cl$ is increased.

The fraction of the surface chlorine exchanged which was calculated using equation 2.xxiv (Section 2.9)

$$f = \frac{S_o - S_t}{S_0 - S_{100}} \qquad \text{(Equation 2.xxiv)}$$

where f = fraction exchanged

S_o = Specific count rate of the [^{36}Cl]-chlorine labelled hydrogen chloride before exchange.

S_t = Specific count rate of the exchanged gas phase at equilibrium.

Table 3.4 : Exchange of Hydrogen Chloride treated Spence Type and Condea precalcined γ-alumina with equimolar aliquots of [^{36}Cl]-chlorine labelled hydrogen chloride.

Sample	Calcination Temp. (K)	Uptake HCl (mmol g^{-1})	Sample weight of exchange precalcined γ-alumina (g)	mmol $H^{36}Cl$ expanded into cell	specific count rate gas phase at equilibrium (count s^{-1} mg^{-1} $Ag^{36}Cl$)	change in specific count rate from starting specific count rate of $H^{36}Cl$ of 0.52 count s^{-1} mg^{-1}AgCl. (count $s^{-1}mg^{-1}$AgCl)
Spence Type						
A1	293	2.85 ±.30	0.4618	1.32	0.29 ± .003	0.23 ±.006
A2	373	2.10 ±.20	0.3854	0.89	0.27 ± .003	0.25 ±.006
A3	423	2.05 ±.20	0.5274	1.08	0.25 ± .003	0.27 ±.006
A4	473	1.95 ±.20	0.6469	1.26	0.24 ± .002	0.28 ±.006
A5	523	2.05 ±.20	0.5136	1.05	0.24 ± .002	0.28 ±.006
Condea						
C1	293	2.40 ±.20	0.4811	1.15	0.29 ± .003	0.23 ±.005
C3	423	1.40 ±.15	0.4050	0.56	0.24 ± .003	0.28 ±.006
C5	523	1.40 ±.15	0.5090	0.71	0.23 ± .002	0.29 ±.005

Figure 3.7

Change in the Specific Count Rate of Gaseous $H^{36}Cl$ from an initial value of 0.52 count s^{-1} mg^{-1} $Ag^{36}Cl$ on exchange with HCl treated Spence γ-Alumina and Condea γ-Alumina @ 293K

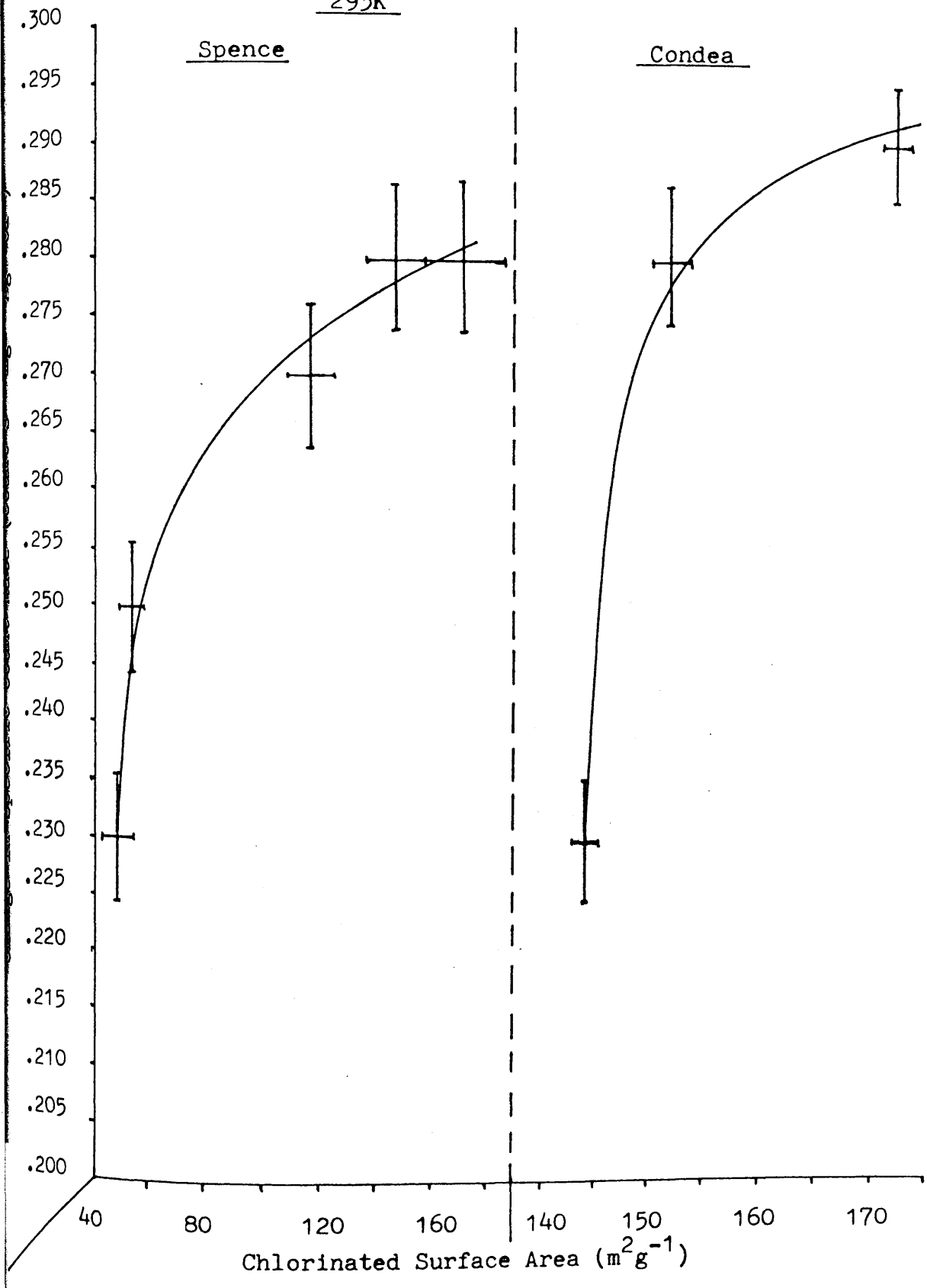

Figure 3.7a

Change in Specific Count Rate of Gaseous $H^{36}Cl$ versus Chlorine Surface Densities for HCl treated Spence and Condea γ-Alumina Samples

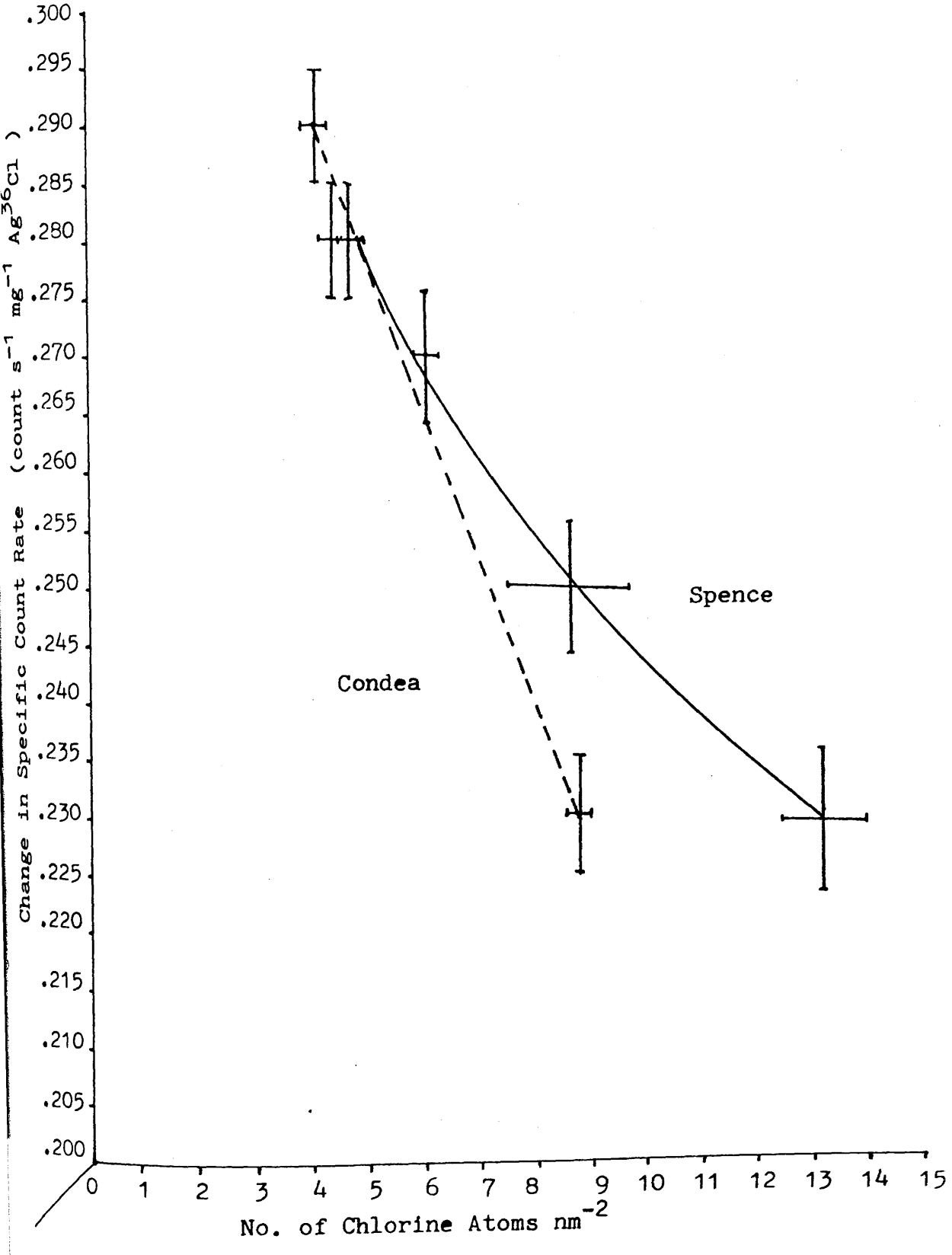

S_{100} = Theoretical specific count rate of the exchanged gas phase at equilibrium based on the number of exchangeable chlorine atoms in the exchanging reagents.

are presented in table 3.5. The results have indicated that total exchange has occurred for all the precalcined Spence and Condea γ-alumina samples treated with anhydrous hydrogen chloride at 293K. No uptake by the γ-alumina samples of anhydrous [^{36}Cl]-chlorine labelled hydrogen chloride from the gas phase was observed.

3.2.7 The Exchange at 293K of Anhydrous Gaseous [^{36}Cl]-Chlorine labelled Hydrogen Chloride with Anhydrous Hydrogen Chloride treated Calcined γ-Alumina.

When [^{36}Cl]-chlorine labelled hydrogen chloride was expanded into the counting cell that contained a sample of calcined Condea γ-alumina (0.5314g; 4.02mmol) treated with anhydrous hydrogen chloride at 293K, a rapid increase in the surface activity of the solid occurred in the first 10 min. of the exchange reaction followed by a period of a slow detectable increase in the surface activity which extended to 40 min into the reaction. Thereafter no further change in the surface count rate of the solid was observed indicating that the exchange reaction had reached a state of equilibrium. The specific count rate of the equilibrium gas phase was obtained and has shown similar surface trends to that observed by the Spence γ-alumina in that the fraction exchanged by the chlorine that was retained on the surface of γ-alumina by the treatment with anhydrous hydrogen chloride at 293K was complete (Table 3.5).

Also consistent with the Spence γ-alumina results was that the smaller the surface density of the chlorine species on the surface of γ-alumina the greater is the change in the specific count rate obtained from the exchange gas phase at equilibrium (Figure 3.7a).

3.2.8 The Exchange at 293K of Anhydrous Hydrogen Chloride with Anhydrous [^{36}Cl]-Chlorine labelled Hydrogen Chloride treated Spence γ-Alumina.

When anhydrous gaseous hydrogen chloride (1mmol ; 13.80 Torr) was admitted into the counting cell which contained a calcined sample of Spence γ-alumina treated with anhydrous gaseous [^{36}Cl]-chlorine labelled hydrogen chloride, a significant drop in the surface activity was observed (Figure 3.8). When the exchange reaction between the gas phase hydrogen chloride and the surface chlorine retained by the calcined γ-alumina was complete the sample was pumped out and the residual surface activity was determined. The surface activity of the saturated surface with [^{36}Cl]-chlorine labelled hydrogen chloride (count s^{-1}) was compared with that attained by the surface after exchange with 1 mmol aliquot of anhydrous gaseous hydrogen chloride and the percentage drop in the surface activity due to the exchange of 1 mmol of hydrogen chloride was determined. The results are presented in table 3.6 and a drop in the surface activity of 26.26 ± 1.17% was observed when the exchange reaction had reached equilibrium for the Spence γ-alumina samples calcined between 293K and 523K;

Exchange @ 293K of Anhydrous HCl (1mmol) with Spence γ-Alumina calcined at 373K and Treated with Anhydrous $H^{36}Cl$.

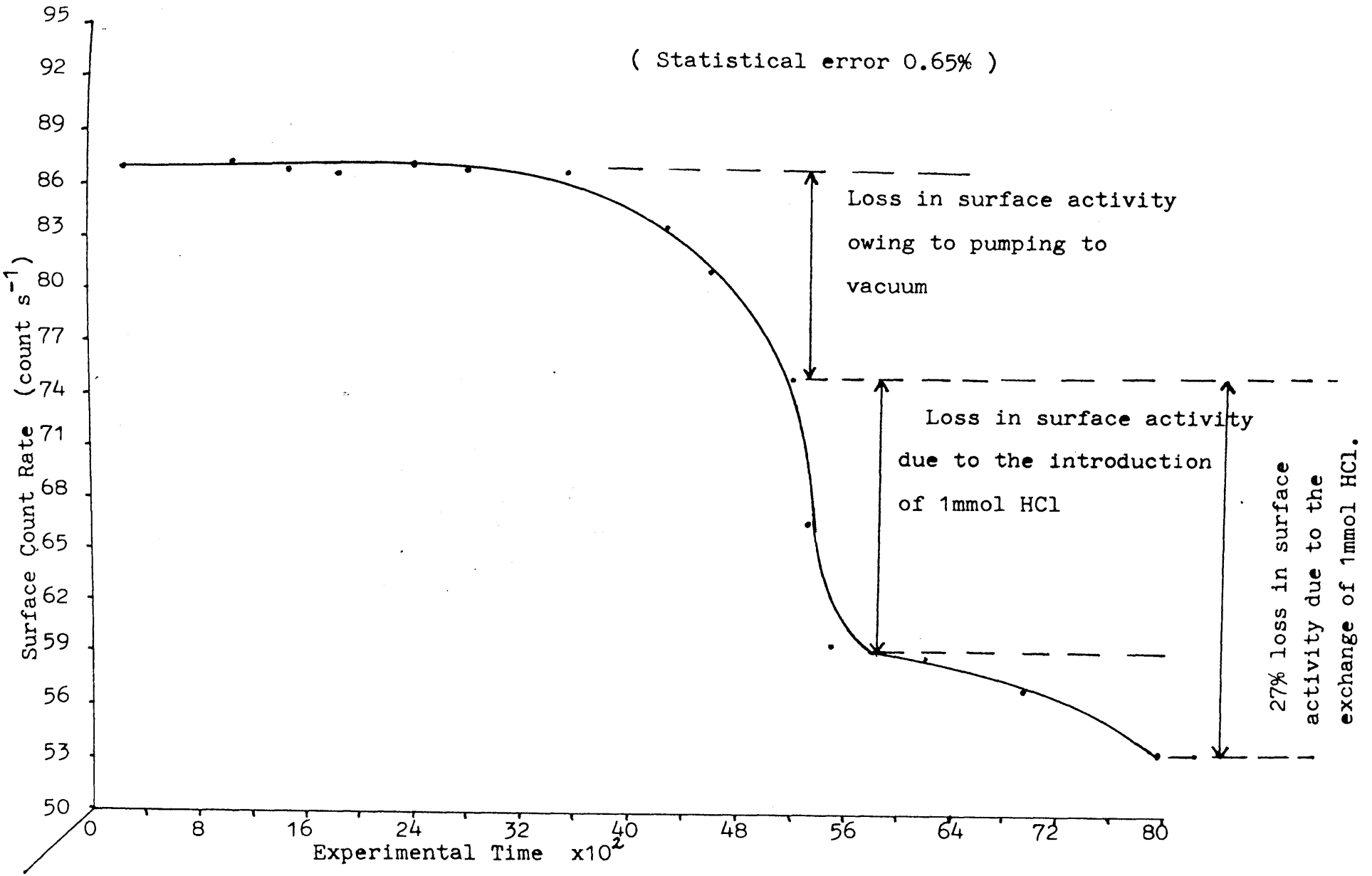

Table 3.6 : *Change in Surface Activity of Spence Type γ-Alumina treated with $H^{36}Cl$ after exchange with Anhydrous Hydrogen Chloride.*

Sample	Calcination Temp. (K)	Sat. Surface activity with $H^{36}Cl$ (count s^{-1})	Surface activity after exchange with HCl, (count s^{-1})	% drop in surface activity
A1	293	90.85	62.30	26.44
A2	373	74.34	54.16	27.00
A3	423	93.30	70.60	24.32
A4	473	64.36	47.86	25.64
A5	523	55.02	39.77	27.71

3.2.9 The Infrared Analysis of the Exchange at 293K of Calcined Spence γ-Alumina treated with Anhydrous Gaseous Deuterium Chloride with Anhydrous Gaseous Hydrogen Chloride.

The experimental procedure for the above investigation is described in section 3.3.9. The infrared spectrum shows the characteristic peak of hydrogen chloride at 2850 cm^{-1} and also a much smaller but distinctive peak at 2050 cm^{-1} of deuterium chloride (Figure 3.9). The appearance of this band due to deuterium chloride indicates that the protons on the surface of the catalyst are labile to exchange.

3.2.10 The Exchange at 293K of Calcined Spence γ-Alumina treated with Anhydrous Gaseous Hydrogen Chloride at 523K with Anhydrous Gaseous [^{36}Cl]-Chlorine labelled Hydrogen Chloride.

The experimental procedure for the above investigation is described in section 3.3.10. In the investigation of the lability at 293K of anhydrous hydrogen chloride, from the treatment at 523K of Spence γ-Alumina calcined to 523K, it was observed that a rapid increase in the surface activity resulted when the [^{36}Cl]-chlorine labelled hydrogen chloride was admitted into the counting cell. The increase in the surface activity indicated that the [^{36}Cl]-chlorine labelled hydrogen chloride had exchanged with the chlorine that was retained by the surface during the chlorination process. At the exchange equilibrium the specific count rate of the equilibrium gas phase was obtained (Section 2.5.3), and was

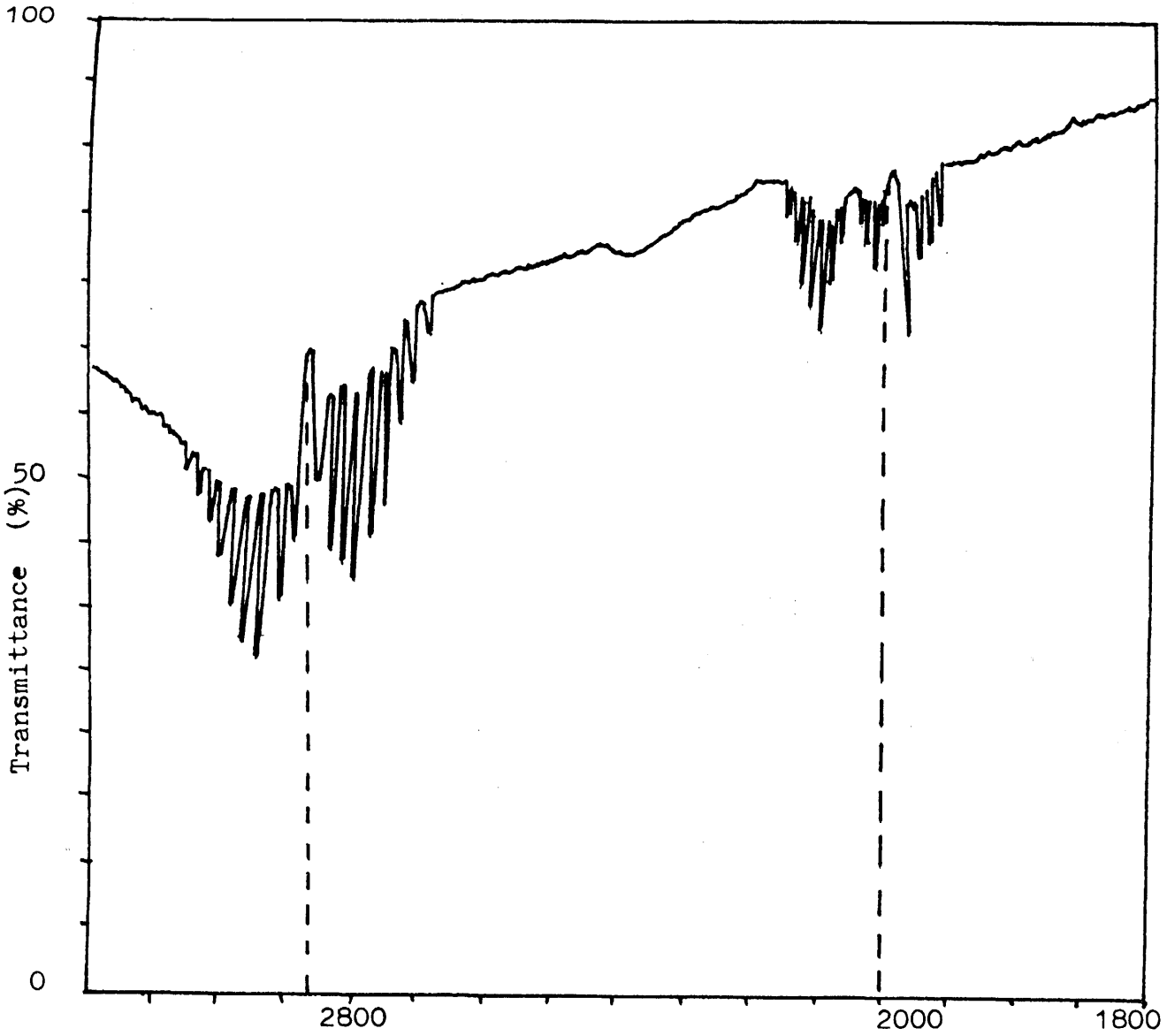

Equilibrium gas phase components from the exchange reaction between anhydrous gaseous HCl and γ-alumina treated with DCl

found to be 0.24 count $s^{-1}mg^{-1}Ag^{36}Cl$. The fraction exchanged at 293K (Equation 2.xxiii) was 1.00 ± 0.03. This result was the same as the fraction exchanged that resulted from the exchange work at 293K (Section 3.2.6), table 3.5, sample A5. It can be concluded that the chlorine retained by the surface from the hydrogen chloride treatment at 293K was indistinguishable from chlorine retained by the surface from the hydrogen chloride treatment at 523K.

3.2.11 The Exchange at 293K of Calcined Spence γ-Alumina Treated with Anhydrous Gaseous [^{36}Cl]-Chlorine labelled Hydrogen Chloride at 523K with Anhydrous Gaseous Hydrogen Chloride.

In this study, it was observed that a significant decrease in the surface activity of the Spence γ-alumina calcined to 523K and treated with [^{36}Cl]-chlorine labelled hydrogen chloride when anhydrous hydrogen chloride (1 mmol) was admitted into the counting cell (Figure 3.10). This resulted in a drop of 20.79% in the surface activity from the solid. The drop in the surface count rate was the same as the amount of surface activity removed by a 1 mmol aliquot of anhydrous gaseous hydrogen chloride at 293K by the anhydrous hydrogen chloride treatment at 293K of Spence γ-alumina (Section 3.2.7, Table 3.6). This information supports the results that were observed in a quantitative determination of the specific count rate obtained from the exchange gas phase at equilibrium, (Section 3.2.10) and the fraction of chlorine exchanged. The chlorine retained by the surface produced by the treatment with anhydrous hydrogen

Figure 3.10

Loss in Surface Activity of $H^{36}Cl$ treated γ-Alumina @ 523K when exchanged with 1mmol of HCl @ 293K.

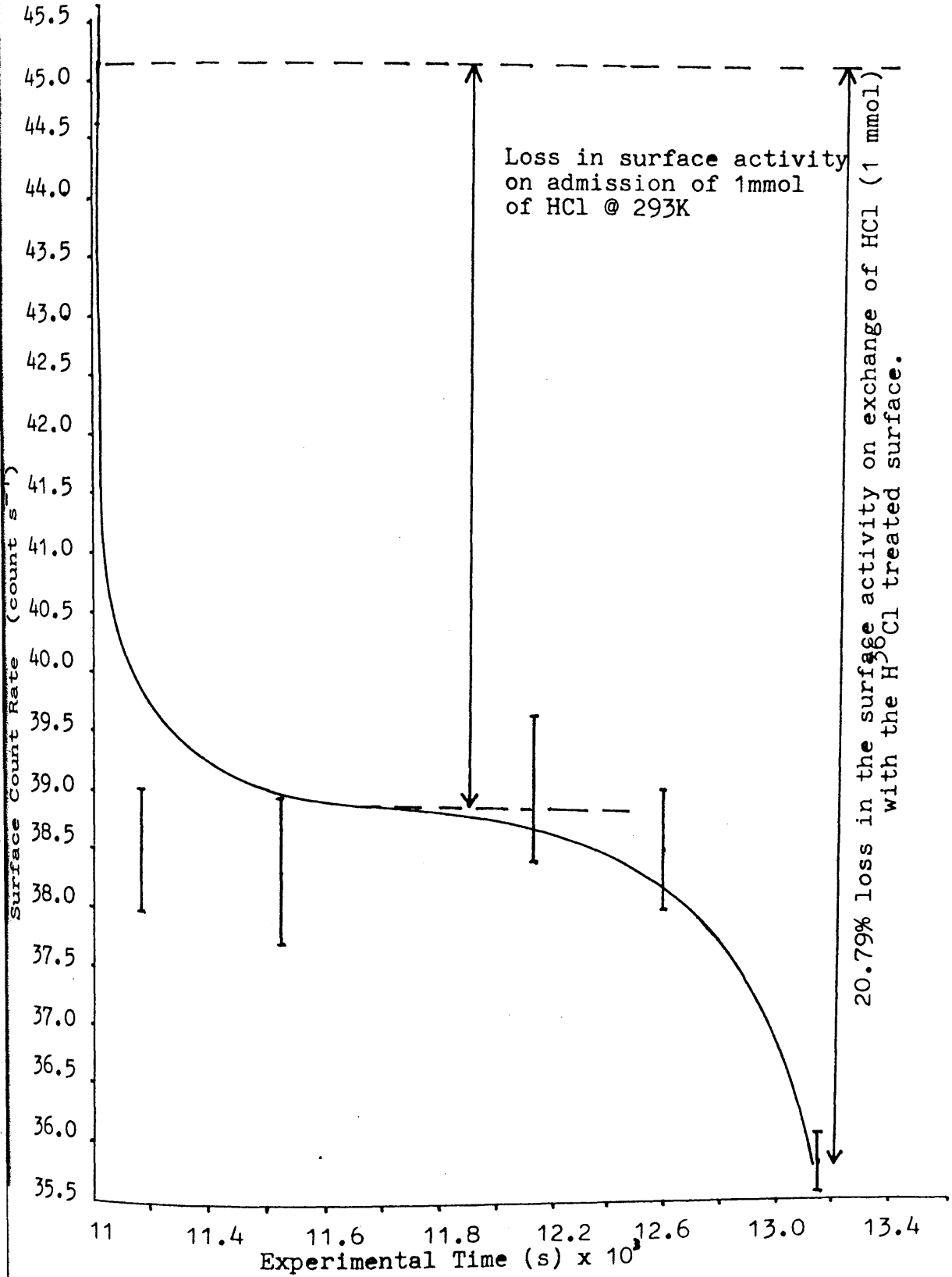

chloride at 523K was indistinguishable from the chlorine retained by the surface from the treatment at 293K of anhydrous hydrogen chloride.

3.2.12 Removal of the Surface Activity at 293K from Calcined Condea γ-Alumina treated with [^{36}Cl]-Chlorine labelled Hydrogen Chloride at 523K.

The surface activity from a Condea γ-alumina sample (0.5734g; 0.55 mmol) calcined to 523K and treated with anhydrous gaseous [^{36}Cl]-chlorine labelled hydrogen chloride (1 mmol) at 523K was recorded after degassing the sample at 293K for 1h (Figure 3.11). After the exchange with anhydrous hydrogen chloride (13.8 Torr; 1mmol) to equilibrium at 293K and degassing the solid for 1h, the count rate for the solid sample fell to 19.98 count s^{-1} recording a drop in the surface activity of 26.35% which was consistent with the results of the experimental findings in section 3.2.8 (Table 3.6). The addition of further aliquots of anhydrous hydrogen chloride was able to exchange out the [^{36}Cl]-chlorine label retained by the surface (Figure 3.11). After the addition of fifteen aliquots of anhydrous hydrogen chloride (13.8 Torr; 1 mmol), 88% of the initial surface activity had been removed. This experiment shows that the chlorine retained by the surface of γ-alumina by the hydrogen chloride treatment at temperatures < 523K is labile.

Figure 3.11

Removal of Surface Activity @ 293K from $H^{36}Cl$ Treated γ-Alumina by the sequential addition of Anhydrous HCl.

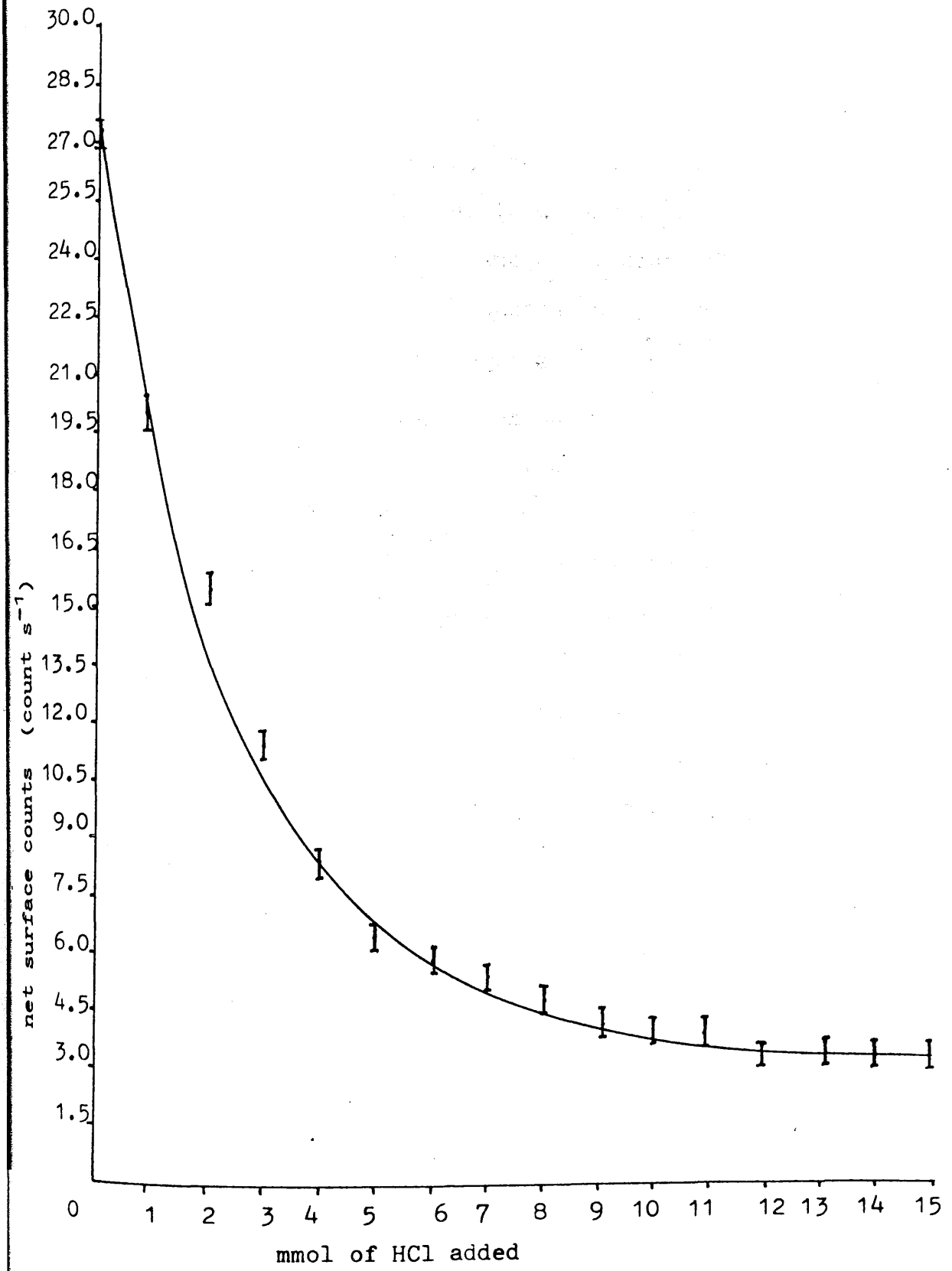

3.3 EXPERIMENTAL

3.3.1 The B.E.T Area Determination of Calcined Spence γ-Alumina and Calcined Condea γ-Alumina with the B.E.T Area Determinations of the Calcined γ-Alumina Samples treated with Hydrogen Chloride at 293K.

The B.E.T apparatus used in the determination of the surface areas of the calcined γ-alumina and hydrogen chloride treated γ-alumina samples is described in section 2.8 and figure 2.15. The apparatus was used in conjunction with nitrogen as the adsorbate gas.

The calcined γ-alumina samples (typically 0.5000g; 4.76mmol) were loaded in the dry box into a preweighed dry capillary sample holder by means of a side arm on the sample bulb. The weight of the calcined γ-alumina sample was accurately determined prior to the removal of the side arm, sealing the sample bulb under vacuum. The calcined γ-alumina samples were degassed for 30 min. prior to the calibration procedures being carried out which determined the dead space of the apparatus. The B.E.T area determination is described in Section 2.8. This process was repeated for all the calcined Spence γ-alumina samples, calcined Condea γ-alumina samples and the samples of γ-alumina treated with anhydrous gaseous hydrogen chloride at 293K.

3.3.2 The Interaction at 293K of Calcined Spence γ-Alumina with Anhydrous Gaseous [^{36}Cl]-Chlorine labelled Hydrogen Chloride.

An accurately weighed sample of the calcined γ-

alumina (0.5000g; 4.76 mmol) was transferred to a dry dropping vessel in the dry box. The sample was degassed for 30 min before being transferred to a dry counting cell. The calcined γ-alumina was then dropped into the boat contained in the counting cell (Figure 2.11) and manouvered under Geiger-Müller tube No.2. Anhydrous gaseous [^{36}Cl]-chlorine labelled hydrogen chloride (2.0 mmol; 27.6 Torr) was expanded into the counting cell. The gas phase counts (Geiger-Müller tube No.1) and the solid phase plus gas phase counts (Geiger-Müller tube No.2) were recorded at intervals of 300s collecting counts $>10^4$ where the statistical error was <1% (Section 2.4.5). When no change in the counts were detected by either Geiger-Müller tube, the gas phase contained in the counting cell was condensed into a vacuum vessel held at 77K. The surface count rate from the solid was recorded prior to pumping out the solid at periods of 2h, 4h, 8h and daily intervals up to 5 days. At this stage a final surface count rate was obtained.

This procedure was repeated for all the calcined samples of γ-alumina where the uptake of anhydrous [^{36}Cl]-chlorine labelled hydrogen chloride was determined as a function of the calcination temperature.

3.3.3 The Interaction at 293K of Calcined Condea γ-Alumina with Anhydrous Gaseous [^{36}Cl]-Chlorine labelled Hydrogen Chloride.

The procedure to investigate the interaction at 293K of anhydrous gaseous [^{36}Cl]-chlorine labelled hydrogen chloride with Condea γ-alumina was the same as the procedure for the

interaction of [^{36}Cl]-chlorine labelled hydrogen chloride with Spence γ-alumina and is described in section 3.3.2.

3.3.4 The B.E.T Area Determinations of Calcined Spence γ-Alumina and Calcined Condea γ-Alumina treated with Anhydrous Gaseous Hydrogen Chloride at 293K.

The procedure used to investigate the B.E.T areas of calcined γ-alumina samples treated with anhydrous gaseous hydrogen chloride at 293K was the same as the procedure reported for the B.E.T area determinations for the calcined γ-aluminas (Section 3.3.1).

3.3.5 The Determination of the Specific Count Rate of Anhydrous [^{36}Cl]-Chlorine labelled Hydrogen Chloride.

It was required that the specific count rate of the anhydrous gaseous [^{36}Cl]-chlorine labelled hydrogen chloride was known prior to the exchange experiments involving the hydrogen chloride treated calcined γ-alumina and the [^{36}Cl]-chlorine labelled hydrogen chloride gas phase at 293K. The procedure involved the precipitation of [^{36}Cl]-chlorine labelled Ag^{36}Cl from an acidified aqueous solution of silver nitrate. The procedure to obtain the precipitate and the specific count rate of the Ag^{36}Cl precipitate is described in section 2.5.3.

3.3.6 The Exchange at 293K of Calcined Spence γ-Alumina treated with Anhydrous Gaseous Hydrogen Chloride at 293K with Anhydrous Gaseous [^{36}Cl]-Chlorine labelled Hydrogen Chloride.

An accurately weighed sample of the calcined Spence γ-alumina (0.5000g ; 4.76 mmol) was transferred to a dry vacuum vessel as described in section 3.3.2 and fitted to the vacuum line. A second vacuum vessel containing ~2g of dampened Analar sodium hydroxide pellets was also fitted to the vacuum line. The damp sodium hydroxide pellets were frozen down to 77K and this vessel was pumped out. The apparatus was then flamed out under vacuum to remove any moisture that may have been retained by the Pyrex glass of the vacuum line. The vacuum vessel containing the calcined γ-alumina was degassed before being transferred to the counting cell. The γ-alumina sample was dropped into the boat (Figure 2.11) and anhydrous hydrogen chloride (2.0mmol, 27.6 Torr) was expanded into the counting cell. The anhydrous hydrogen chloride gas was reacted with the γ-alumina sample for 1h. The hydrogen chloride treated γ-alumina sample was degassed by pumping to remove any volatile species that may be present. The apparatus was flamed out prior to the expansion of anhydrous [^{36}Cl]-chlorine labelled hydrogen chloride into the counting cell based on a 1:1 ratio of labelled chlorine to unlabelled chlorine in the system (Table 3.4). The gas phase count rate and the solid phase count rate (from Geiger-Müller tube 1 and Geiger-Müller tube 2 respectively) were monitored during the course of the exchange reaction. When no change in the count rate by either Geiger-Müller tube was

detected the equilibrium gas phase was condensed into the vacuum vessel containing the damp sodium hydroxide pellets at 77K. A [^{36}Cl]-chlorine labelled Ag^{36}Cl precipitate was prepared and the specific count rate of the [^{36}Cl]-chlorine labelled Ag^{36}Cl was obtained as described in section 2.5.3. The specific count rate of the [^{36}Cl]-chlorine labelled Ag^{36}Cl sample was standardized to a weight of 15mg as described in section 2.4.4. This procedure was carried out for all the hydrogen chloride treated γ-alumina samples.

3.3.7 The Exchange at 293K of Calcined Condea γ-Alumina treated with Anhydrous Hydrogen Chloride at 293K with Anhydrous Gaseous [^{36}Cl]-Chlorine labelled Hydrogen Chloride.

The procedure to investigate the exchange at 293K of anhydrous gaseous [^{36}Cl]-chlorine labelled hydrogen chloride with calcined Condea γ-alumina treated with anhydrous gaseous hydrogen chloride at 293K was the same as the procedure used for the Spence γ-alumina samples treated with anhydrous gaseous hydrogen chloride at 293K and is described in section 3.3.6.

3.3.8 The Exchange at 293K of Calcined Spence γ-Alumina treated with Anhydrous Gaseous [^{36}Cl]-Chlorine labelled Hydrogen Chloride at 293K with Anhydrous Hydrogen Chloride.

The transfer of the calcined Spence γ-alumina and the treatment of the calcined γ-alumina at 293K with anhydrous [^{36}Cl]-chlorine labelled hydrogen chloride is described in section 3.3.2. The exchange of anhydrous gaseous hydrogen

chloride with the [^{36}Cl]-chlorine labelled hydrogen chloride treated calcined Spence γ-alumina is described in section 3.3.6. The exchange reaction in this investigation was between anhydrous gaseous hydrogen chloride in the gas phase and [^{36}Cl]-chlorine labelled hydrogen chloride retained by the surface of the calcined Spence γ-alumina at 293K. The surface count rate and the gas phase count rate was monitored with time. When no change in the gas phase or the surface phase count rate was observed the equilibrium gas phase from the exchange reaction was pumped out and the solid was degassed by pumping. The final solid phase count rate was then obtained.

3.3.9 The Infrared Analysis of the Exchange at 293K of Calcined Spence γ-Alumina treated with Deuterium Chloride at 293K with Anhydrous Gaseous Hydrogen Chloride.

A sample of Spence γ-alumina (0.5423g ; 4.79 mmol) which was calcined at 523K and transferred to a dry vacuum vessel in the dry box was reacted with anhydrous gaseous deuterium chloride (100 Torr ; 2.23 mmol) for 1h prior to degassing the solid to remove any volatiles from the system. Anhydrous gaseous hydrogen chloride was condensed into the vacuum vessel and allowed to react for 1h. The equilibrium gas phase mixture was expanded into an infrared gas cell to a pressure of 40 Torr. The infrared analysis of the gas phase mixture was carried out using a Perkin-Elmer 983 Grating Infrared Spectrometer.

3.3.10 The Exchange at 293K of Calcined Spence γ-Alumina treated with Anhydrous Gaseous Hydrogen Chloride at 523K with Anhydrous Gaseous [^{36}Cl]-Chlorine labelled Hydrogen Chloride.

An accurately weighed sample of Spence γ-alumina (0.5684g ; 4.30 mmol) was calcined to 523K and transferred to the counting cell (Section 3.3.2). The Spence γ-alumina sample was dropped into the boat contained in the counting cell (Figure 2.11). The γ-alumina sample was pulled into the furnace section of the counting cell where the temperature was increased to 523K. Anhydrous gaseous hydrogen chloride (27.2 Torr ; 2 mmol) was expanded into the counting cell and reacted with the γ-alumina sample at 523K for 4h. The sample was cooled to 293K and the treated solid was degassed by pumping. The treated solid sample was placed under Geiger-Müller tube No 2 (Figure 2.11) and a sample of [^{36}Cl]-chlorine labelled hydrogen chloride (13.8 Torr, 1 mmol) was expanded into the counting cell and allowed to exchange with the treated γ-alumina sample until the exchange equilibrium was established.

The equilibrium gas phase was condensed over dampened sodium hydroxide pellets contained in a vacuum vessel at 77K. A [^{36}Cl]-chlorine labelled silver chloride precipitate was prepared (Section 2.5.3) and the specific count rate of the exchanged gas phase was obtained.

3.3.11 The Exchange at 293K of Calcined Condea γ-Alumina treated with [^{36}Cl]-Chlorine labelled Hydrogen Chloride at 523K with Anhydrous Gaseous Hydrogen Chloride.

The procedure carried out in the above investigation of the exchange at 293K of [^{36}Cl]-chlorine labelled hydrogen chloride treated Condea γ-alumina calcined to 523K was the same as the procedure described for the calcined Spence γ-alumina in section 3.3.10.

3.3.12 The Removal of the Surface Activity at 293K from Calcined γ-Alumina treated with [^{36}Cl]-Chlorine labelled Hydrogen Chloride at 523K.

A sample of Condea γ-alumina (0.5734g ; 4.35 mmol) was calcined to 523K and transferred into a dry vacuum vessel in the dry box. The sample was degassed before being transferred to the counting cell (Section 3.3.2). Anhydrous gaseous [^{36}Cl]-chlorine labelled hydrogen chloride (27.8 Torr, 2.01 mmol) was reacted with the γ-alumina sample at 523K in the furnace section of the counting cell for 4h after which the sample was cooled to 293K and degassed by pumping. The treated sample was placed under Geiger-Müller Tube No.2 (Figure 2.11) and the initial activity of the solid was recorded. Anhydrous gaseous hydrogen chloride (13.8 Torr, 1 mmol) was expanded into the counting cell and allowed to exchange with the surface [^{36}Cl]-chlorine labelled hydrogen chloride until equilibrium was established. The solid was degassed by pumping and the surface activity of the sample was again

recorded. This procedure was repeated for the addition of aliquots of anhydrous gaseous hydrogen chloride (13.8 Torr; 1 mmol) until the observed surface activity from the solid had been removed.

CHAPTER 4.

INTRODUCTION:

Reactions of Carbon Tetrachloride with γ-Alumina

Strongly acidic chlorinated γ-aluminas that contain unusually high chlorine content (up to 15% by weight chlorine) have been prepared using chlorocarbon compounds (100-111). In order to obtain a highly acidic surface from the calcined γ-alumina it is a requirement that the chlorocarbon reagent contains at least two chlorine atoms per methane derivative (Section 1.8). The high acid activities of these surfaces suggest that treating the γ-alumina with a chlorocarbon reagent produces a surface with acid strengths approaching those of Friedel-Crafts catalysts $HCl/AlCl_3$ (114).

This work was undertaken to investigate the distinctive process of the chlorination of γ-alumina by carbon tetrachloride.

Carbon tetrachloride was selected as a definitive reagent which is able to produce strong acid sites when reacted with γ-alumina. The reaction conditions required to chlorinate the γ-alumina were determined to establish the minimum temperature and the minimum reaction time required to produce the known by-products of the chlorination process namely carbon dioxide and 1,1 dichloromethanone (phosgene) and hydrogen chloride as gaseous products (22). The uptake of chlorine by the γ-alumina from the carbon tetrachloride treatment was studied as a function of the calcination temperature of the solid. The chlorine content of the calcined γ-alumina samples were determined using Neutron Activation Analysis (Section 2.7.2).

The lability of the chemisorbed chlorine produced by the treatment of the calcined γ-alumina with carbon tetrachloride was studied as a function of the calcination temperature of the γ-alumina by exchanging anhydrous gaseous [^{36}Cl]-chlorine labelled hydrogen chloride with the carbon tetrachloride treated γ-alumina samples and subsequently obtaining the specific count rate of the exchanged gas phase. The B.E.T areas of the calcined γ-alumina samples that were treated with carbon tetrachloride were determined as a function of the calcination temperature of the γ-alumina using nitrogen as the adsorbate gas (Section 2.8).

4.2.1 The Interaction of Gaseous [^{36}Cl]-Chlorine labelled Carbon Tetrachloride and [^{14}C]-Carbon Tetrachloride with the Pyrex Counting Cell at 293K.

When gaseous [^{36}Cl]-chlorine labelled carbon tetrachloride (13.8 Torr; 1mmol) was expanded into the counting cell (Figure 2.11) at room temperature, the gas phase count rates monitored by both Geiger-Müller tubes decreased over a period of 1h (Figure 4.1). The initial and final background count rates were not identical. This result was reproducible indicating that the adsorption of [^{36}Cl]-chlorine labelled carbon tetrachloride onto the Pyrex glass counting cell at 293K was significant. Calibration for the loss in the gas phase count rate of [^{36}Cl]-chlorine labelled carbon tetrachloride with time was obtained (Figure 4.1) to correct the gas phase count rate as a function of time in studies where the [^{36}Cl]-chlorine labelled carbon tetrachloride gas phase count rate was monitored. The slopes and intercepts to the linear fit

Figure 4.1

Interaction of Gaseous $[^{36}Cl]$-Chlorine labelled CCl_4 with the Pyrex Counting Cell @ 293K as a function of Time

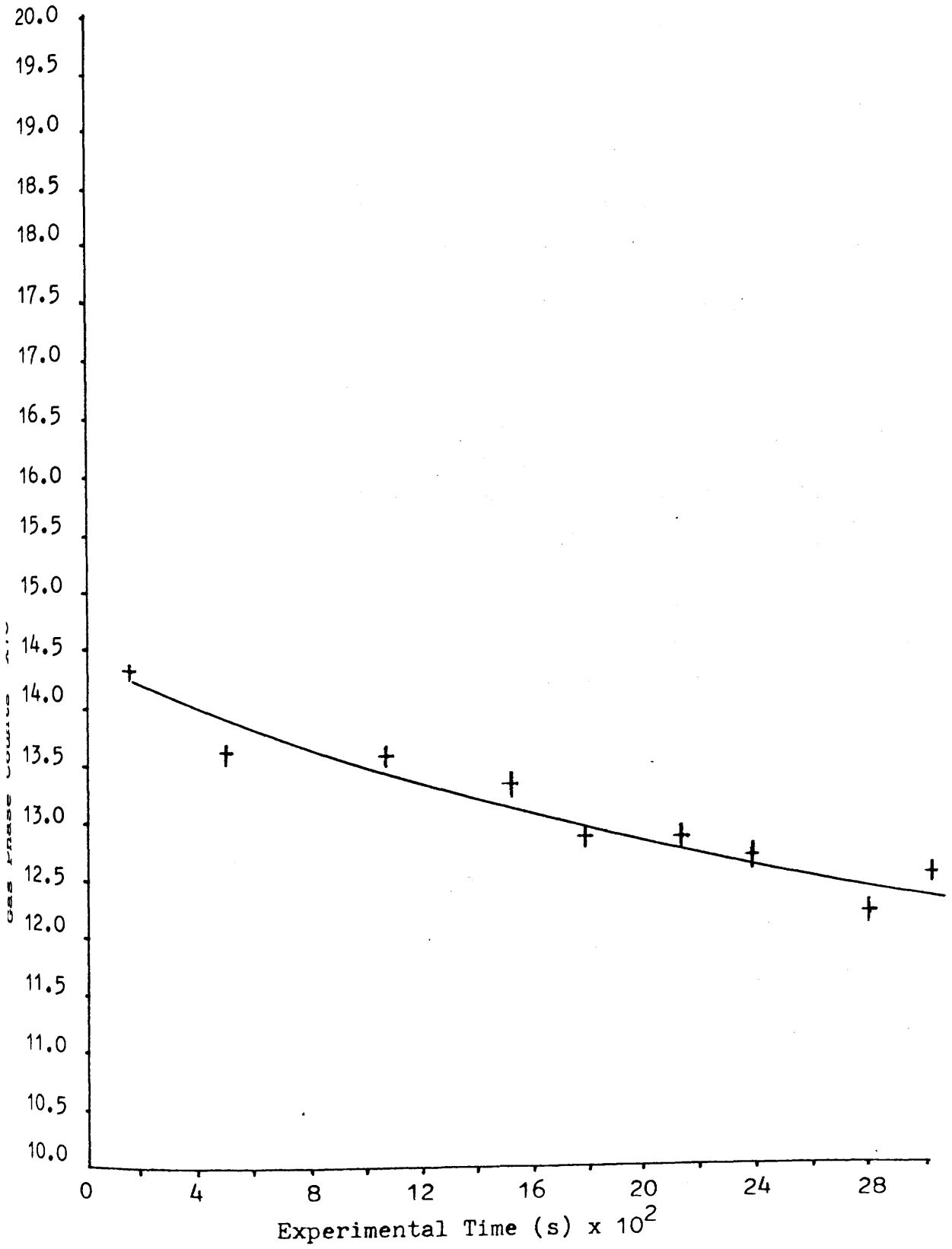

of the Napierian logarithm of the gas phase count rate recorded from the sample of [^{36}Cl]-chlorine labelled carbon tetrachloride as a function of time was obtained for both Geiger-Müller tubes. These slopes and intercepts were obtained to facilitate the gas phase count rate correction in the [^{36}Cl]-chlorine labelled carbon tetrachloride or the [^{14}C]-carbon labelled carbon tetrachloride adsorption studies. A computer program was written to incorporate the slope and intercept values for the adsorption of the [^{36}Cl]-chlorine labelled carbon tetrachloride or the [^{14}C]-carbon labelled carbon tetrachloride onto the walls of the Pyrex counting cell.

The slopes and the intercepts values obtained from a specific batch of [^{36}Cl]-chlorine labelled carbon tetrachloride that produced the results shown in figure 4.1 were evaluated to a slope of -4.675×10^{-5} and an intercept on the y-axis of 1.5798 for the data produced from Geiger Müller tube number 1. The correction to the gas phase count rate of time x (s) into the reaction is ln (gas phase count rate) = 4.675×10^{-5} times (x + 1.5798). Therefore 1000s into the adsorption study the correction to the gas phase count rate monitored by Geiger-Müller tube No.1 will be 0.95 count s^{-1}. The slope and intercept values for Geiger-Müller tube No.2 were -3.046×10^{-5} and 1.5358 respectively. A correction to the gas phase count rate as a function of time was applied to all results which used the gas phase count rate from [^{36}Cl]-chlorine labelled carbon tetrachloride. The same procedure was used in studies where the gas phase count rate from [^{14}C]-carbon labelled carbon tetrachloride was monitored.

4.2.2 The Determination of the Minimum Temperature Required to React Anhydrous Gaseous Carbon Tetrachloride with Calcined Spence γ-Alumina.

The procedure for the above investigation is described in the experimental section of this chapter (Section 4.3.2). The infrared analysis of the gas phase contents of the Monel bomb for the reaction temperature at 423K showed only carbon tetrachloride in the gas phase with a single absorbance at 794 cm^{-1} as did the gas phase contents from the Monel bomb for the reaction temperature at 443K. At the reaction temperature of 453K the gas phase contents from the Monel bomb showed weak absorbances at 2365 cm^{-1} and 680 cm^{-1} which was attributed to the presence of a small quantity of carbon dioxide in the gas phase. A strong peak at 794 cm^{-1} from the same gas sample was also observed indicating that much of the gaseous carbon tetrachloride was still unreacted. A sample of the gas phase contents of the Monel bomb for the reaction temperature of 473K showed strong absorbances at 2365 cm^{-1} and 680 cm^{-1} attributed to the presence of carbon dioxide together with the characteristic absorbance due to hydrogen chloride at 2895 cm^{-1}. The presence of 1,1 dichloromethanone (phosgene) was also observed in the infrared spectrum from weak broad absorbances at 1825 cm^{-1} (Table 4A). The absorbances attributed to the presence of phosgene and carbon dioxide were confirmed by obtaining the infrared spectra from a small pressure of the respective gases from lecture bottles. The absorbances from the known gas samples confirmed the infrared analysis of the gas contents from the reaction bomb. It was concluded that the threshold to the reaction between carbon tetrachloride and

Table 4A

Gas Phase Products from the Reaction of Anhydrous Carbon Tetrachloride with calcined γ-Alumina @ 473K.

Gas Product	Absorption (cm^{-1})
Hydrogen chloride	2895
Carbon dioxide	2365, 680
1,1-Dichloromethanone	1825, 850
Carbon Tetrachloride	794

calcined γ-alumina was at 473K.

4.2.3 The Determination of the Minimum Time required to React Carbon Tetrachloride with Calcined Spence γ-Alumina.

The procedure for the above investigation is described in section 4.3.3. The infrared analysis of 50 Torr of the gas phase contents of the Monel bomb held at 473K for 30 min showed weak absorbances at 2365 cm^{-1} and 680 cm^{-1} due to the presence of carbon dioxide in the gas phase together with a strong absorbance at 794 cm^{-1} due to the presence of the chlorinating reagent carbon tetrachloride. The absorbances due to the presence of carbon dioxide indicates that the chlorination of the γ-alumina surface had began. When the experiment had reached 60 min into the reaction the absorbances at 2365 cm^{-1} and at 680 cm^{-1} had grown stronger to medium strength and at 120 min into the reaction the development of a new small peak at 850 cm^{-1} indicated the presence of phosgene in the gas phase. It was not until 180 min into the reaction that the presence of hydrogen chloride with the characteristic absorbance at 2895 cm^{-1} was observed and the absorbance at 4160 cm^{-1} indicated the presence of a small quantity of water vapour. The absorbances at 2365 cm^{-1} and 680 cm^{-1} due to the presence of carbon dioxide had grown very strong which indicated a large partial pressure of carbon dioxide in the gas phase sample. Finally at 240 min into the reaction the clear presence of all the identified gaseous products, hydrogen chloride, carbon dioxide and phosgene were observed from the strong intensity of their characteristic absorbances. It was concluded

that the reaction conditions required to adequately chlorinate the γ-alumina sample with carbon tetrachloride was 4h or greater at a minimum reaction temperature of 473K.

4.2.4 The Interaction of Anhydrous Gaseous [^{36}Cl]-Chlorine labelled Hydrogen Chloride with Anhydrous Gaseous Carbon Tetrachloride in a Glass Reaction Vessel held at 523K.

The experimental procedure for the above investigation is described in section 4.3.4. The specific count rate obtained from the gas phase [^{36}Cl]-chlorine labelled hydrogen chloride after the reaction with gaseous carbon tetrachloride at 523K in a glass system was found to be 0.48 ± 0.02 count s^{-1} mg^{-1} $Ag^{36}Cl$. This compares with 0.52 ± 0.03 count s^{-1} mg^{-1} $Ag^{36}Cl$ for the specific count rate of the [^{36}Cl]-chlorine labelled hydrogen chloride (Section 3.3.5) before any exchange had taken place. In the system there are a total of 5 chlorine atoms available for exchange. If complete exchange had taken place the final specific count rate obtained from the exchanged gas phase would have been 0.06 count s^{-1} mg^{-1} $Ag^{36}Cl$ (Equation 2.xxiv). The fraction exchanged in the gas phase at 523K under glass between [^{36}Cl]-chlorine labelled hydrogen chloride and gaseous carbon tetrachloride was 0.087 ± 0.006. Investigations by other workers where studies involving the exchange reaction at temperatures between 453K and 493K were inconclusive (165) in that the results from the exchange work were irreproducible. Studies between [^{36}Cl]-chlorine labelled hydrogen chloride and carbon tetrachloride at 293K concluded that a very slow exchange did occur between the reagents.

In this investigation between the exchange of [^{36}Cl]-chlorine labelled hydrogen chloride and carbon tetrachloride at 523K the fraction exchanged at 0.087 indicated that a very slow exchange had occurred over the 6h period of the reaction.

4.2.5 The Chlorination of Calcined Spence γ-Alumina and Calcined Condea γ-Alumina with Anhydrous Gaseous Carbon Tetrachloride.

The procedure for the above chlorination process is described in section 4.3.5. The infrared analysis had shown that hydrogen chloride, phosgene, carbon dioxide, carbon tetrachloride and water vapour was present in the gaseous products from the reaction between carbon tetrachloride and γ-alumina samples calcined at 293K, 373K, 423K, 473K and 523K. The infrared absorbances due to the presence of the gases are listed in table 4A. The presence of phosgene and carbon dioxide in the gas phase products were indicative that the chlorination of the γ-alumina sample had taken place (22), and this criteria was used during the chlorination of all the calcined γ-alumina samples by carbon tetrachloride at 500K.

4.2.6 The Determination of the B.E.T Area of Calcined Spence γ-Alumina and Calcined Condea γ-Alumina treated with Anhydrous Gaseous Carbon Tetrachloride.

The B.E.T areas of the Spence and Condea γ-alumina samples treated with anhydrous carbon tetrachloride at 500K for 6h are presented in table 4.2 and figure 4.2 together with the B.E.T areas of the calcined γ-alumina samples as a function of the calcination temperature to evaluate the relationship between the calcination temperature and B.E.T area of the calcined γ-alumina sample. The B.E.T areas of the calcined carbon tetrachloride Condea γ-alumina samples together with the B.E.T areas of the calcined Condea samples are shown in figure 4.2 Treatment of the γ-alumina by carbon tetrachloride at 500K reduced the surface area of the calcined material between the calcination temperatures 293K to 523K (Figures 4.2 and 4.2A.) This reduction in the surface area for a given sample caused by the chlorination of the γ-alumina had shown a uniform decrease in the surface area between the extremes of the calcination range studied. The extent of the reduction in the surface area of the calcined sample caused by the carbon tetrachloride treatment can be seen by obtaining the ratio of the B.E.T. area of the carbon tetrachloride treated calcined Spence γ-alumina samples to the B.E.T area of the untreated calcined material and the results are presented in table 4.2 and figure 4.3. The relationship in the extent of the reduction in the surface area due to the carbon tetrachloride treatment as a function of the calcination temperature of the sample (Figure 4.3) parallels with the B.E.T areas of both:-

Table 4.2 : B.E.T surface areas of precalcined Spence Type and Condea γ-alumina samples treated with Carbon Tetrachloride at 500K for 6h.

Sample.	Calcination. Temp. (K)	B.E.T chlorinated surface area m^2g^{-1}	B.E.T precalcined surface m^2g^{-1}	Ratio chlorinated surface area/ precalcined surface area.	Reduction in the surface area due to chlorination (m^2g^{-1})
A1	293	44.26 ±3.86	129.28 ±10.26	.34	85.02
A2	373	52.29 ±5.31	143.39 ±21.34	.36	91.11
A3	423	90.60 ±8.15	202.15 ±2.56	.45	111.55
A4	473	118.30 ±6.29	232.32 ±21.11	.50	114.02
A5	523	156.63 ±11.30	252.08 ±23.86	0.62	95.45
C1	293	137.47 ±4.35	161.96 ±2.56	0.85	24.49
C3	423	141.84 ±2.65	174.29 ±2.98	0.81	32.45
C5	523	160.23 ±3.23	191.20 ±3.25	0.84	30.97

Figure 4.2

B.E.T. Areas of Calcined Spence and CCl_4 / γ-Alumina Samples.

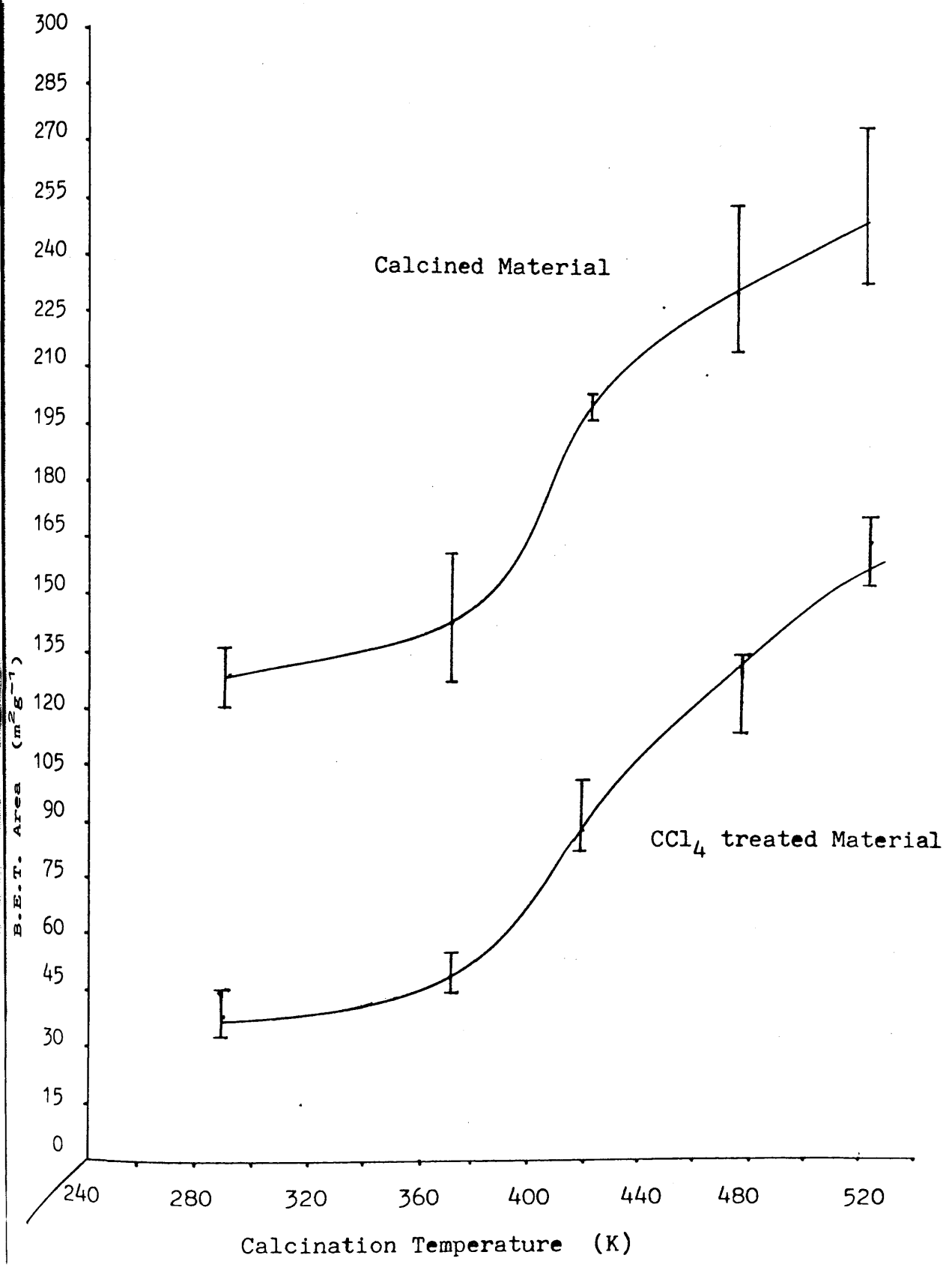

Figure 4.2A

B.E.T. Areas of Calcined Condea γ-Alumina and CCl_4 treated Samples.

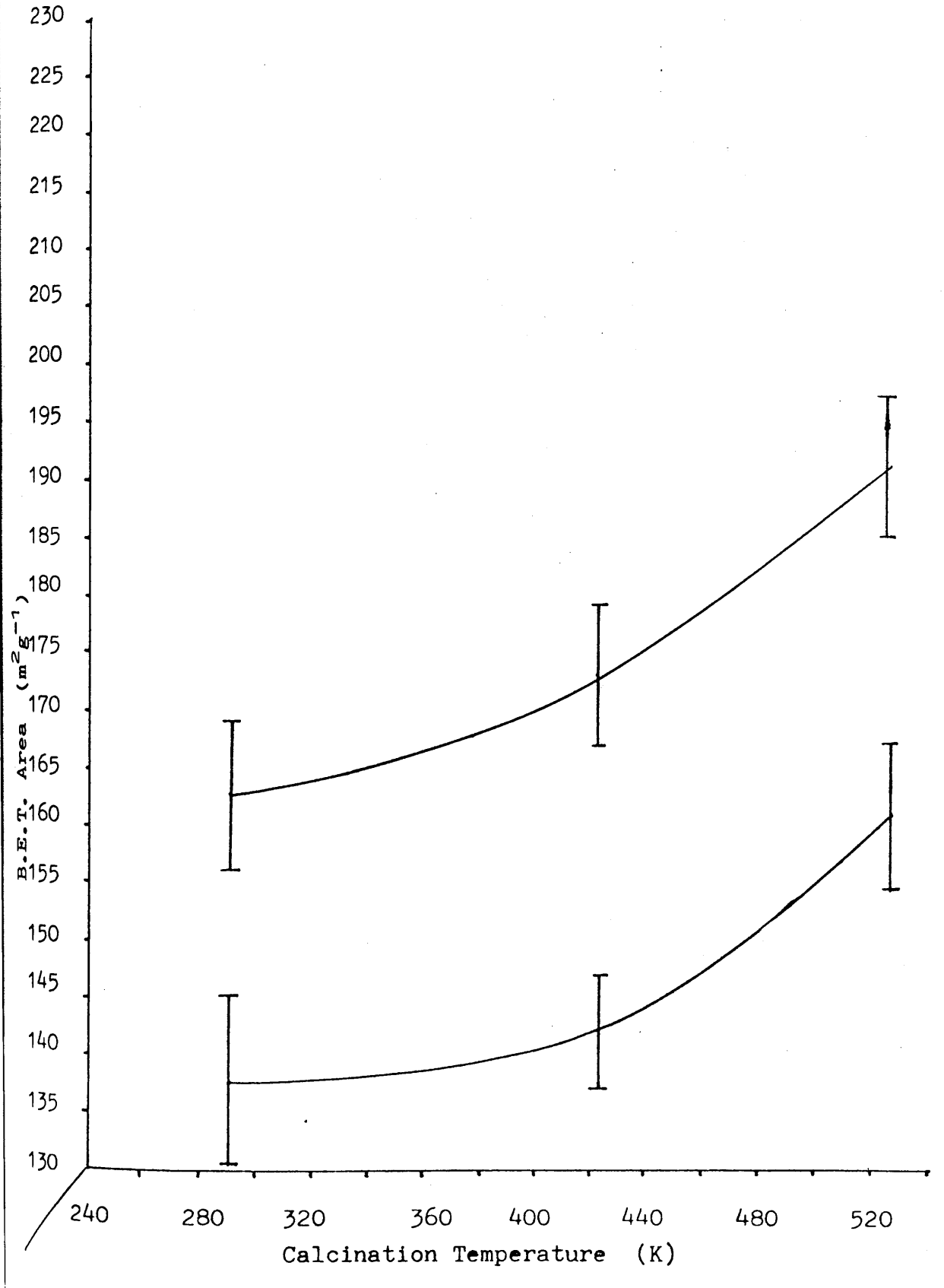

Figure 4.3

Ratio of B.E.T. Areas of Chlorinated γ-Alumina / Calcined Sperce γ-Alumina as a function of Calcination Temperature.

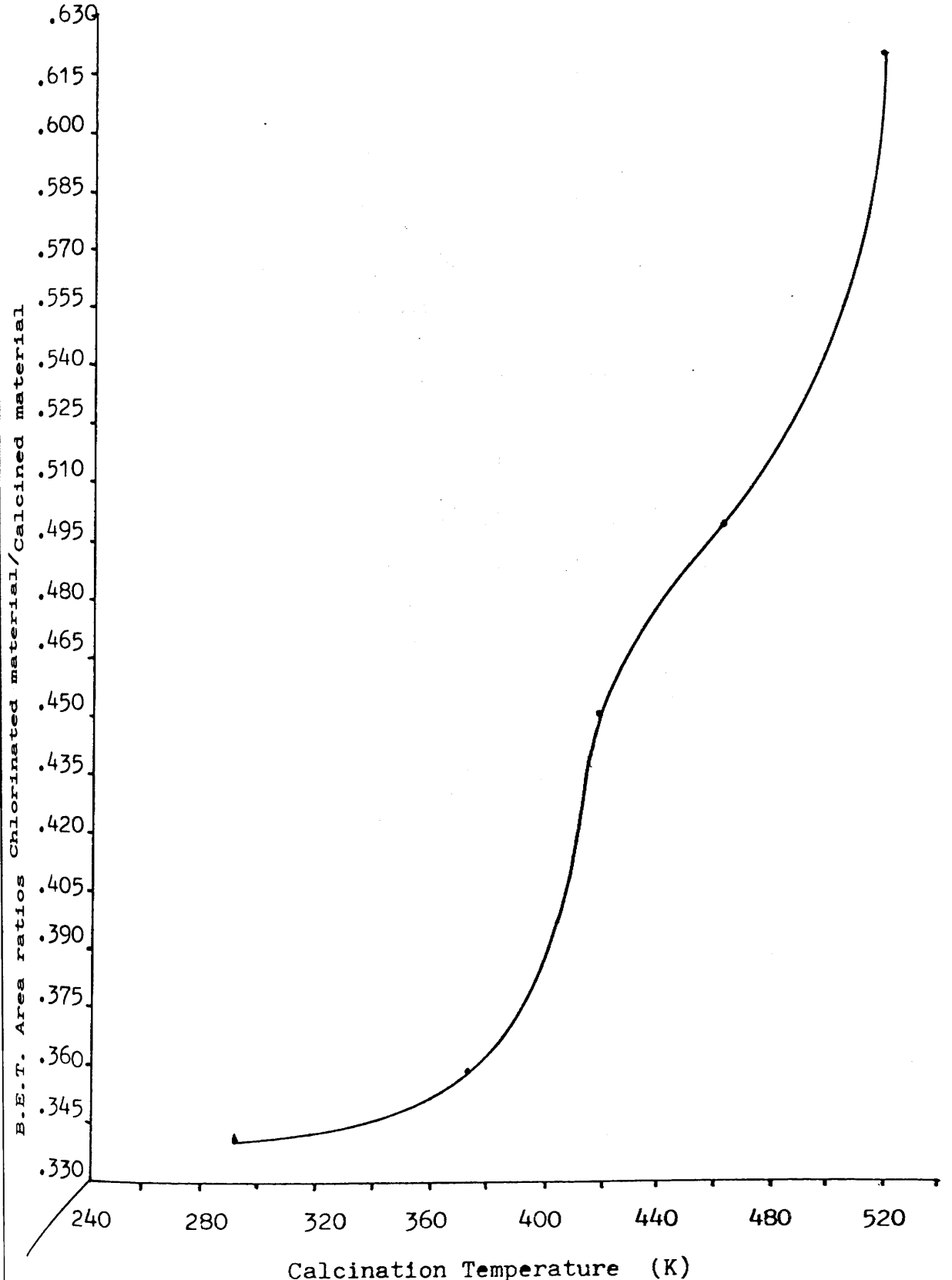

i) the calcined Spence γ-alumina samples and
ii) the carbon tetrachloride treated calcined Spence γ-alumina samples up to the calcination temperature of 473K. These results are consistent with the carbon tetrachloride treatment of the calcined Spence γ-alumina samples being a surface phenomena up to the calcination temperature of 473K. The deviation from this relationship observed by the material calcined to 523K (Figure 4.3) indicated that the carbon tetrachloride was effecting an attack on the bulk of this calcined γ-alumina sample.

This observation was previously recorded by Melchor et al (100) who showed that at 473K the reaction between γ-alumina and carbon tetrachloride lead to hydroxyl substitution by chlorine and the removal of the surface oxygen atoms. At 573K a more severe reaction was noted involving a bulk attack of the solid by the carbon tetrachloride with the formation of aluminium trichloride as a reaction product.

4.2.7 The Neutron Activation Analysis of the Chlorine Content of Carbon Tetrachloride treated calcined Spence γ-Alumina and Condea γ-Alumina.

The experimental procedure for the above investigation is described in section 4.3.7. The calcined γ-alumina samples were pretreated with anhydrous carbon tetrachloride at 500K for 6h and are presented in table 4.3 together with the neutron activation analysis results of the specific chlorine content of each calcined γ-alumina sample. The chlorine content of the calcined γ-alumina samples are shown schematically in figure 4.4.

Table 4.3 : Neutron Activation Analysis of Chlorine uptake on calcined Spence type and Condea γ-Alumina samples treated with Carbon Tetrachloride at 500K.

Sample.	Calcination Temp. (K)	Chlorine Content (ppm)	uptake Chlorine (mmol g^{-1})	Surface Density of chlorine atoms nm^{-2}
A1	293	$8.0278 \times 10^{4} \pm 1.092 \times 10^{3}$	2.26 ±0.003	10.52 ±0.77
A2	373	$9.7666 \times 10^{4} \pm 9.668 \times 10^{2}$	2.75 ±0.003	11.55 ±1.51
A3	423	$10.799 \times 10^{5} \pm 1.758 \times 10^{3}$	3.05 ±0.005	9.08 ±0.11
A4	473	$7.9692 \times 10^{4} \pm 9.728 \times 10^{2}$	2.24 ±0.003	5.80 ±0.48
A5	523	$7.6359 \times 10^{4} \pm 1.300 \times 10^{3}$	2.15 ±0.004	5.13 ±0.44
C1	293	$7.9352 \times 10^{4} \pm 5.081 \times 10^{2}$	2.20 ±0.001	8.17 ±0.12
C3	423	$8.7774 \times 10^{4} \pm 8.645 \times 10^{2}$	2.47 ±0.002	8.53 ±0.15
C5	523	$6.8459 \times 10^{4} \pm 4.937 \times 10^{2}$	1.93 ±0.001	6.08 ±0.11

Figure 4.4

Uptake of Chloride by calcined Spence and Condea γ-Alumina Samples treated with Carbon Tetrachloride @ 500K.

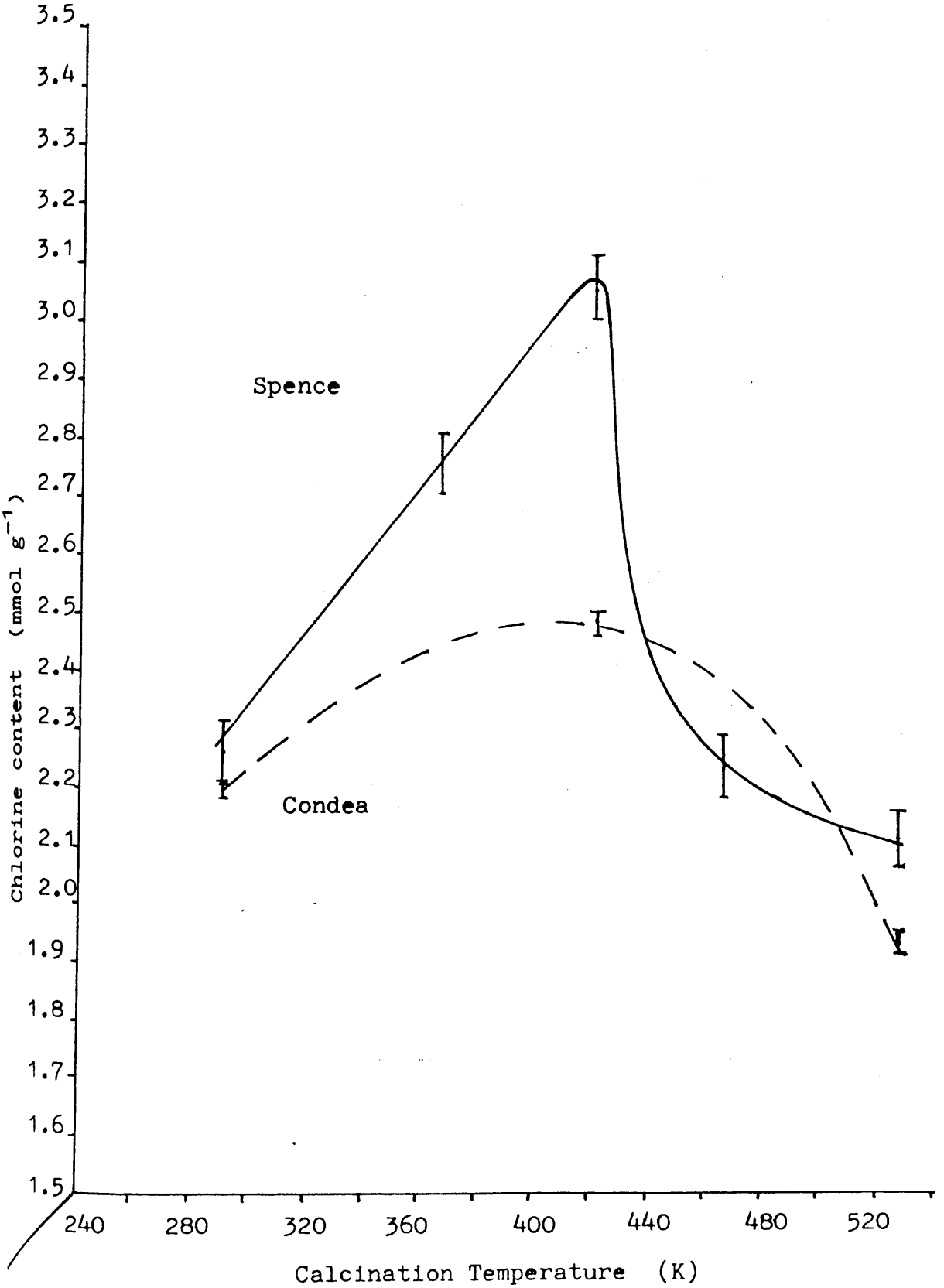

It was observed that the chlorine content of the calcined Spence γ-alumina samples (Figure 4.4) from 293K to 423K increased reaching a maximum at the calcination temperature of 423K where the chlorine content was 3.05 ± 0.005mmol g^{-1}. The chlorine content decreased thereafter until at the calcination temperature of 523K it had fallen to 2.15 ± 0.004 mmol g^{-1}. The uptake of chlorine by the calcined Condea γ-alumina samples (Figure 4.4) had the same relationship in that a maxima in the chlorine content occurs at the calcination temperature of 423K. At this calcination temperature the chlorine content of the calcined Condea γ-alumina sample was 2.47 ± 0.002 mmol g^{-1}, and fell to 1.93 ± 0.001 mmol g^{-1} at the calcination temperature of 523K.

This was a different relationship to the chlorine content of the calcined γ-alumina samples where the γ-alumina was treated with anhydrous gaseous hydrogen chloride at 293K (Section 3.2.3 and Section 3.2.11). With the exception of the material calcined to 293K the chlorine content of the carbon tetrachloride treated γ-alumina samples was greater than the chlorine content of the comparable calcined γ-alumina samples treated with anhydrous gaseous hydrogen chloride (Table 4.3; Table 3.3). The surface density of chlorine atoms was greater for the carbon tetrachloride treated calcined γ-alumina samples than the calcined γ-alumina samples treated with anhydrous gaseous hydrogen chloride at 293K. The relationship between the calcination temperature and the surface density of chlorine atoms are shown schematically in figure 4.5. In the case of the calcined Spence γ-alumina the maximum chlorine surface density of 11.55

Figure 4.5

Surface Density of Chlorine as a function of Calcination Temperature.

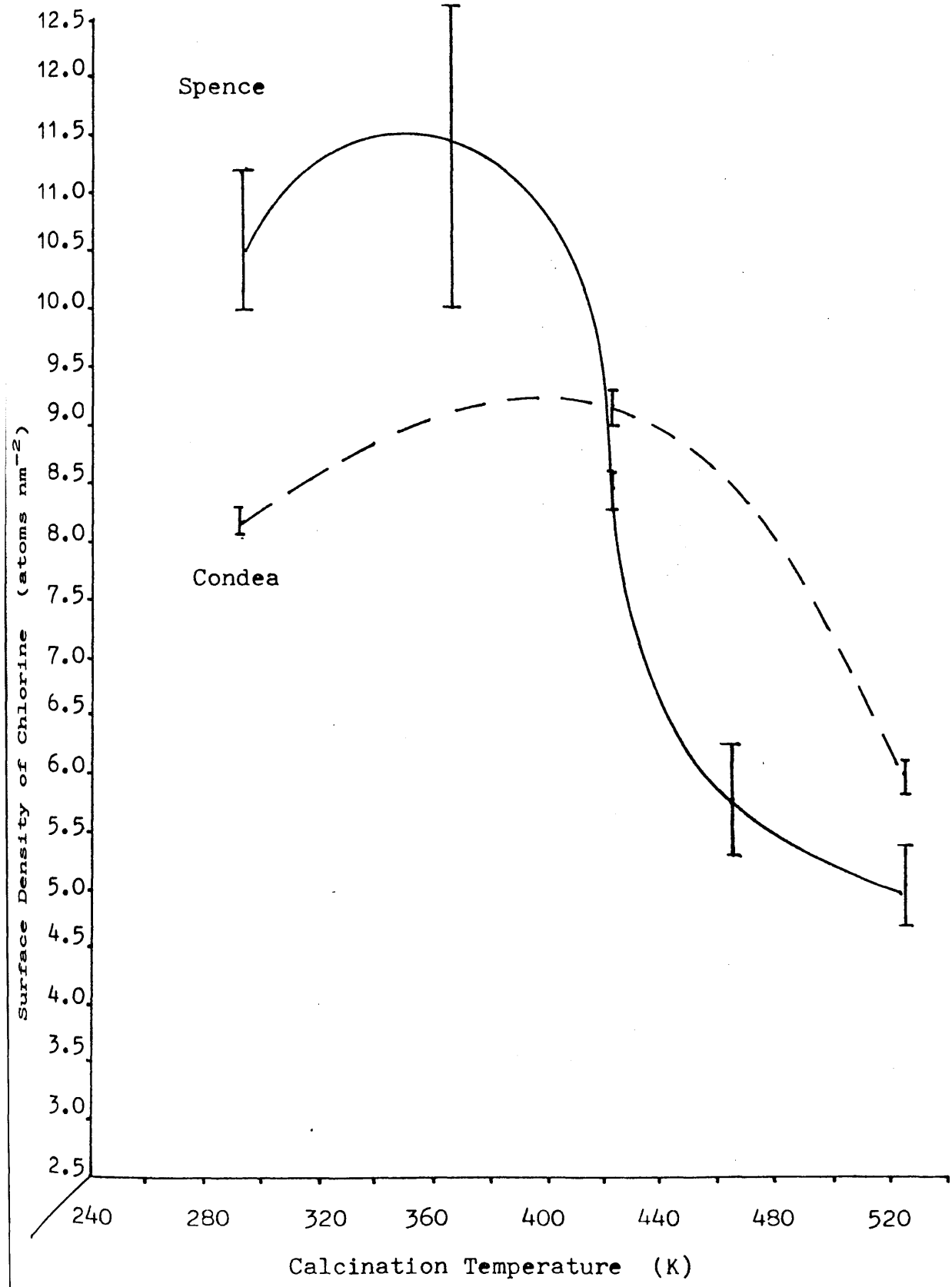

chlorine atoms nm^{-2} was obtained when the γ-alumina was calcined at 373K compared with 8.82 chlorine atoms nm^{-2} obtained for the treatment with anhydrous hydrogen chloride (Table 3.3). The carbon tetrachloride treatment of the calcined γ-alumina at 500K resulted in a chlorine content of 7.6 - 10.8% wt/wt of chlorine compared with 6.5 - 7% wt/wt of chlorine from the treatment of the calcined γ-alumina by anhydrous gaseous hydrogen chloride.

It has been shown in this investigation that up to 50% more chlorine was retained by the surface of γ-alumina with the carbon tetrachloride treatment than was the case for the treatment with hydrogen chloride.

4.2.8 The Exchange at 293K of Calcined Spence and Condea γ-Alumina Samples treated with Anhydrous Gaseous Carbon Tetrachloride with [^{36}Cl]-Chlorine labelled Anhydrous Hydrogen Chloride.

In the experiments that were designed to determine the lability of the chlorine retained by the surface of calcined Spence and Condea γ-alumina samples after the treatment with anhydrous carbon tetrachloride at 500K for 6h it was observed that when [^{36}Cl]-chlorine labelled anhydrous hydrogen chloride (13.8 Torr; 1mmol) was expanded into the counting cell a rapid increase in the surface activity of the carbon tetrachloride treated γ-alumina sample had occurred over the first 10 min (Figure 4.6). The rapid increase in the surface activity was followed by a period lasting 30 min when a small increase in the surface

Figure 4.6

Increase in the Surface Activity on exchange of $H^{36}Cl$ with CCl_4 treated with Spence γ-Alumina calcined at 523K

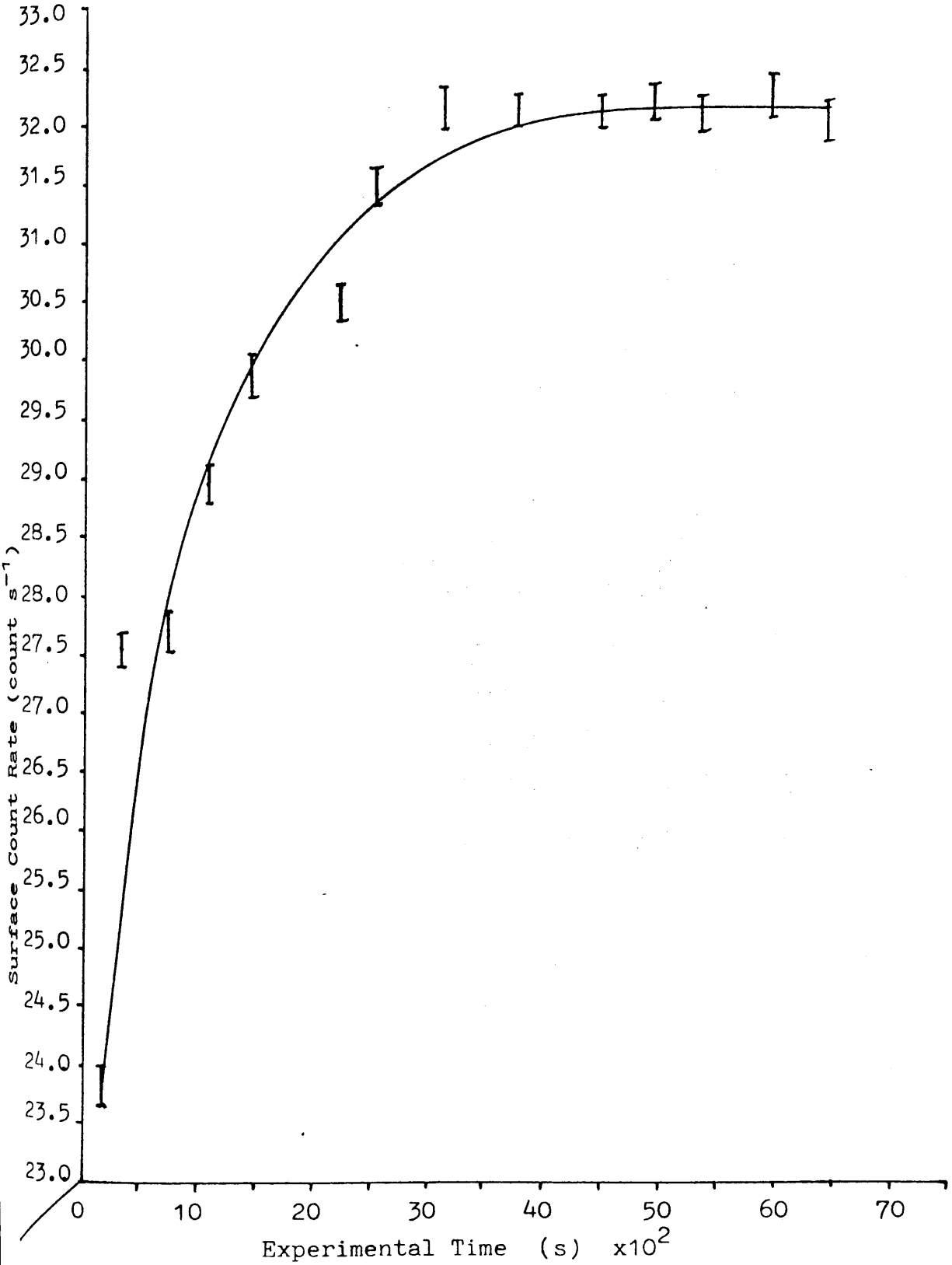

activity of the solid was observed. Finally, after 1h no change in the surface activity was observed. At this point equilibrium for the exchange reaction was established. The increase in the surface activity of the carbon tetrachloride treated γ-alumina solid indicated that exchange between the [^{36}Cl]-chlorine labelled anhydrous hydrogen chloride and the carbon tetrachloride treated surface had taken place. The specific count rate of the equilibrium gas phase for the exchange reaction was obtained (Section 3.3.6). The reduction in the specific count rate of the exchanged gas phase from the starting specific count rate of 0.52 count $s^{-1}mg^{-1}Ag^{36}Cl$ for the [^{36}Cl]-chlorine labelled hydrogen chloride was obtained (Table 4.4). The exchange results for the calcined Spence and calcined Condea γ-alumina samples are presented in figure 4.7. The change in the specific count rate of the equilibrium gas phase ranges from 0.16 count $s^{-1}mg^{-1}Ag^{36}Cl$ for the Spence and Condea γ-alumina samples calcined at 293K, to 0.20 count $s^{-1}mg^{-1}Ag^{36}Cl$ for the samples calcined to 523K. The fraction of chlorine exchanged from the chlorinated surface using Equation 2.xxiv (Section 2.9) was calculated and the results are presented in table 4.5. The results show that in the case of the calcined Spence and Condea γ-alumina samples treated with carbon tetrachloride, total exchange did not occur, and that between 60-80% of the chlorine retained by the surface was labile to exchange at 293K with anhydrous gaseous [^{36}Cl]-chlorine labelled hydrogen chloride.

This result contrasts with the calcined γ-alumina samples treated with anhydrous hydrogen chloride at 293K

Table 4.4 : Results from the Exchange of Carbon Tetrachloride treated precalcined Spence -type and Condea γ-aluminas with equimolar aliquots of [^{36}Cl]-chlorine labelled hydrogen chloride at 293K.

Sample	Calcination Temp. (K)	Chlorine content mmol g^{-1}	Sample weight of exchange chlorinated γ-alumina (g)	mmol $H^{36}Cl$ expanded into counting cell	Specific count rate gas phase at thermal equilibrium count $s^{-1}mg^{-1}$ $Ag^{36}Cl$	change in specific count rate from initial count rate of $H^{36}Cl$ of 0.52 count $s^{-1}mg^{-1}$ $Ag^{36}Cl$
A1	293	2.26 ±0.003	0.4141	0.94	.36± .004	0.16 ±0.007
A2	373	2.75 ±0.003	0.5593	1.54	.34± .003	0.18 ±0.006
A3	423	3.05 ±0.005	0.4466	1.36	.33± .003	0.19 ±0.006
A4	473	2.24 ±0.003	0.4609	1.03	.32± .003	0.20 ±0.006
A5	523	2.15 ±0.004	0.6364	1.36	.32± .003	0.20 ±0.006
C1	293	2.20 ±0.001	0.5342	1.17	.36± .004	0.16 ±0.008
C3	423	2.47 ±0.002	0.6175	1.52	.33± .003	0.19 ±0.006
C5	523	1.93 ±0.001	0.5187	1.00	.32± .-03	0.20 ±0.006

Figure 4.7

Decrease in the Specific Count Rate of Gaseous $H^{36}Cl$ from an initial value of 0.52 count s^{-1} mg^{-1} $Ag^{36}Cl$ on exchange with CCl_4 treated γ-Alumina.

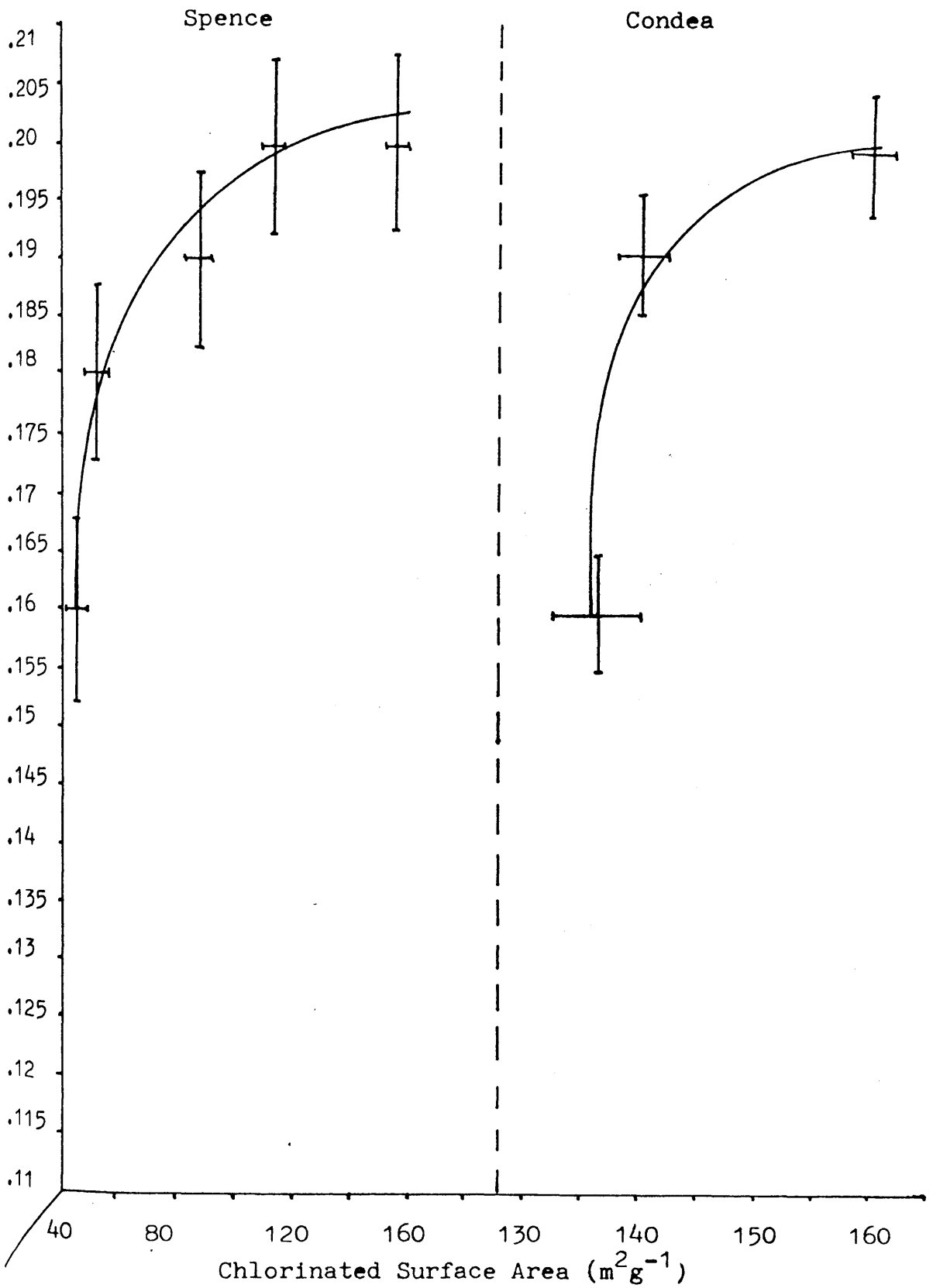

Table 4.5 : Fraction of chlorine exchanged at 293K from the surface of calcined γ-alumina samples treated with anhydrous gaseous carbon tetrachloride.

Sample.	Calcination Temperature (K)	Chlorinated Surface Area m^2g^{-1}	$\frac{\delta_o-\delta_t}{\delta_o-\delta_{100}}$
A1	293	44.26 ± 3.86	0.61 ±0.08
A2	373	52.29 ± 5.31	0.69 ±0.07
A3	423	90.60 ± 8.15	0.73 ±0.07
A4	473	118.30 ± 6.29	0.76 ±0.07
A5	523	156.63 ± 11.30	0.76 ±0.07
C1	293	137.47 ± 4.35	0.61 ±0.08
C3	423	141.84 ± 2.65	0.73 ±0.08
C5	523	160.23 ± 3.23	0.77 ±0.07

where total exchange was found for all the samples calcined between 293K and 523K (Table 3.5).

4.2.9 The Exchange at 293K of Calcined Spence γ-Alumina treated with [^{36}Cl]-Chlorine labelled Carbon Tetrachloride with Anhydrous Gaseous Hydrogen Chloride.

The experimental procedure is described in section 4.3.8. When anhydrous gaseous hydrogen chloride (13.80 Torr; 1mmol) was expanded into the counting cell containing a sample of Spence γ-alumina calcined to 523K (0.4826g; 3.65mmol) and treated with [^{36}Cl]-chlorine labelled hydrogen chloride (13.8 Torr; 1mmol) at 293K, a significant drop in the surface activity of the solid phase was observed (Table 4.6). When the exchange reaction between the gas phase hydrogen chloride and the surface chlorine retained from the treatment of the γ-alumina samples by [^{36}Cl]-chlorine labelled carbon tetrachloride had reached equilibrium after 1h, the solid phase was degassed by pumping. The residual surface activity was recorded. The residual surface activity retained by the solid after the exchange reaction with 1 mmol of anhydrous gaseous hydrogen chloride at 293K was taken as a ratio to the surface activity obtained from the [^{36}Cl]-chlorine labelled carbon tetrachloride treatment. A decrease in the surface activity of 12.61 ± 1.24% was observed at the exchange equilibrium for the exchanged γ-alumina samples calcined between 293K and 523K after exchange with 1 mmol of anhydrous gaseous hydrogen chloride at 293K (Table 4.6).

Table 4.6 : Change in the surface activity of Spence Type γ-alumina treated with [^{36}Cl]-chlorine treated labelled carbon tetrachloride at 500K for 6h with anhydrous gaseous hydrogen chloride.

Sample.	Calc.Temp. (K)	Surf. Activity with [^{36}Cl]-CCl_4 (counts)	Surf. Activity after exchange with HCl (counts)	% drop in surface activity.
A1	293	13639	11945	12.42
A2	373	11847	10242	13.57
A3	423	16284	14561	10.58
A4	473	12466	10857	12.91
A5	523	12064	10423	13.60

4.2.10 The Exchange at 293K of Calcined Spence γ-Alumina treated with Anhydrous Gaseous Carbon Tetrachloride with [^{36}Cl]-Chlorine labelled Carbon Tetrachloride.

When anhydrous gaseous [^{36}Cl]-chlorine labelled carbon tetrachloride (13.8 Torr, 1mmol) was expanded into the counting cell at 293K containing a sample of γ-alumina (0.5324g; 4.03mmol) treated with carbon tetrachloride, the count rates monitored by both Geiger-Müller tubes remained constant over a 2h period. The initial and final count rates, corrected for [^{36}Cl]-chlorine labelled carbon tetrachloride adsorption to the Pyrex glass walls of the counting cell (Section 4.2.1) were identical. This result was reproducible and indicated that there was no exchange between anhydrous [^{36}Cl]-chlorine labelled carbon tetrachloride at 293K and the chlorine retained by the surface of Spence γ-alumina calcined to 523K over a 2h period.

4.2.11 The Reaction of Anhydrous Gaseous [^{36}Cl]-Chlorine labelled Carbon Tetrachloride with Calcined Spence γ-Alumina and Calcined Condea γ-Alumina in the Temperature Range 293K to 523K.

In this investigation the surface count rate of [^{36}Cl]-chlorine from anhydrous gaseous [^{36}Cl]-chlorine labelled carbon tetrachloride was investigated as a function of the reaction temperature. The surface activity was recorded at reaction temperatures that were incremented at approximately 20K through the temperature range 293K to 523K. The results are shown in figure 4.8 and show that at 293K

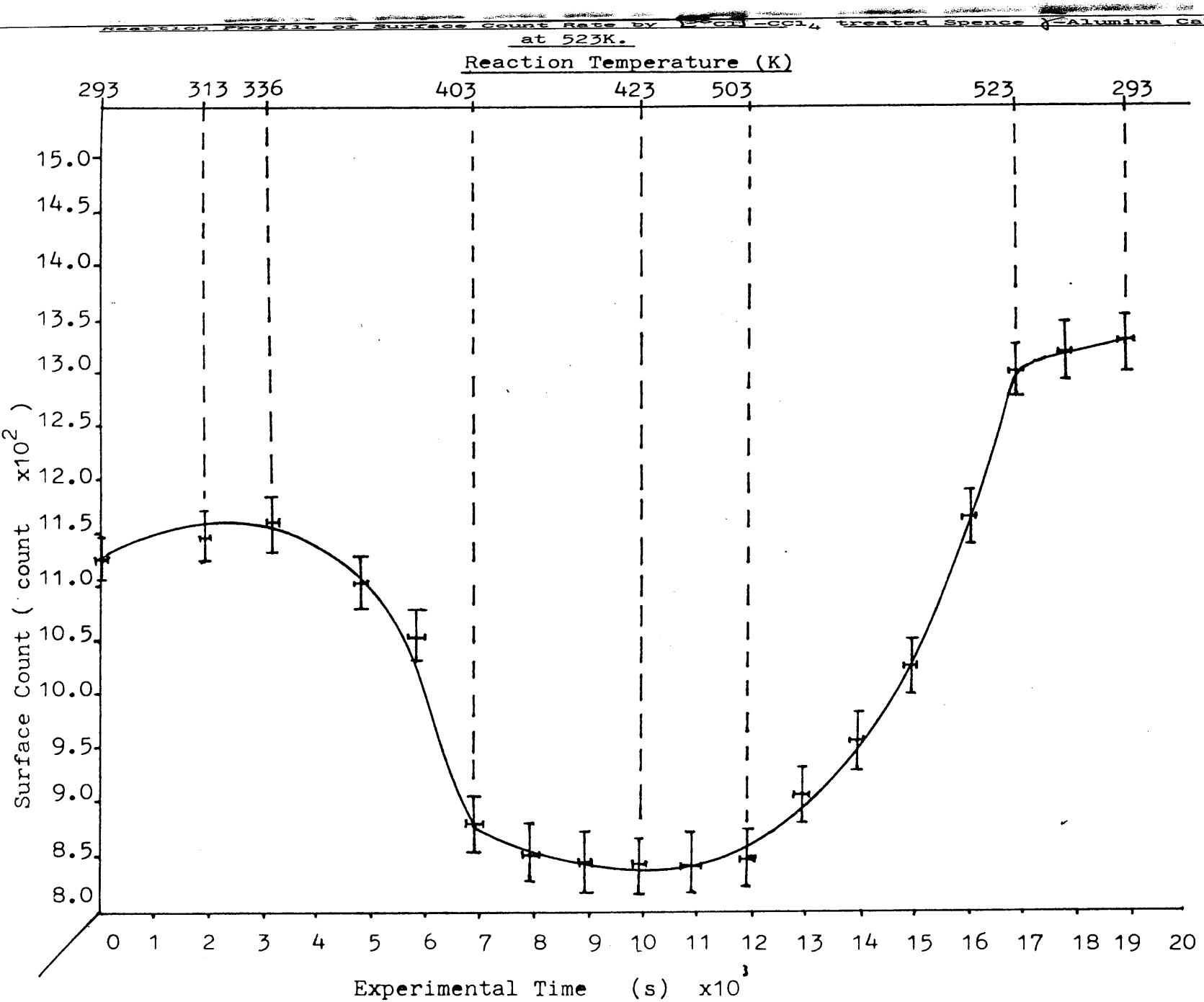
Reaction Profile of Surface Count Rate by ^{14}C-CCl_4 treated Spence γ-Alumina Calcined at 523K.
Reaction Temperature (K)
293
313
336
403
423
503
523
293
15.0
14.5
14.0
13.5
13.0
12.5
12.0
11.5
11.0
10.5
10.0
9.5
9.0
8.5
8.0
Surface Count (count x10^2)
0 1 2 3 4 5 6 7 8 9 10 11 12 13 14 15 16 17 18 19 20
Experimental Time (s) x10^3

[^{36}Cl]-chlorine labelled carbon tetrachloride was adsorbed onto the surface of the calcined γ-alumina. This surface activity was removed by pumping the sample. When the temperature of the sample was increased to 336K there was a small increase in the surface activity. Above 336K the [^{36}Cl]-chlorine labelled carbon tetrachloride was removed thermally from the surface of the calcined γ-alumina. Between 403K and 503K the surface activity from [^{36}Cl]-chlorine labelled carbon tetrachloride was at a minimum and at temperatures up to 403K the surface activity from the [^{36}Cl]-chlorine labelled carbon tetrachloride was removed by pumping which indicated that the [^{36}Cl]-chlorine labelled carbon tetrachloride was physisorbed onto the sample. Above 503K the surface activity from [^{36}Cl]-chlorine had increased and was attributed to chlorination of the surface by the [^{36}Cl]-chlorine labelled carbon tetrachloride. From 503K to 523K a rapid increase in the surface activity from [^{36}Cl]-chlorine was detected and this activity could not be removed by pumping the solid which indicated that chemisorption of the [^{36}Cl]-chlorine had taken place. The surface activity of [^{36}Cl]-chlorine labelled carbon tetrachloride as a function of the reaction temperature is shown schematically in figure 4.8. This relationship was reproducible for the calcined Spence γ-alumina samples calcined to 293K, 373K, 423K and 473K.

4.2.12 The Surface Activity of [^{14}C]-Carbon labelled Carbon Tetrachloride with Calcined Spence γ-Alumina in the Temperature Range 293K to 523K.

A sample of degassed Spence γ-alumina calcined to 523K (0.5214g; 3.95mmol) was transferred to the counting cell. An aliquot of anhydrous gaseous [^{14}C]-carbon labelled carbon tetrachloride (18.07 Torr; 1.34mmol) was expanded into the counting cell at 293K. The surface activity was recorded at temperature increases of approximately 30K and the results are shown schematically in figure 4.9.

The initial count rate recorded at 293K was liable to removal by pumping and was attributed to physisorbed [^{14}C]-carbon labelled carbon tetrachloride on the surface of the calcined γ-alumina. As the temperature was increased the surface activity fell sharply until the system reached a plateau region between the temperatures 413K to 473K. A further increase in the temperature removed the [^{14}C]-carbon labelled carbon tetrachloride surface activity which was not detected for the duration of the experiment.

At 400 min into the reaction the gas phase products were examined by infrared analysis using a Perkin-Elmer 983 Grating Infrared Spectrometer. The infrared analysis showed absorptions at 2895 cm^{-1} from hydrogen chloride, 2365 cm^{-1} and 680 cm^{-1} due to the presence of carbon dioxide in the gas phase and absorbances at 1825 cm^{-1} and 850 cm^{-1} due to the presence of phosgene in the gas phase. These compounds indicated that chlorination of the surface had occurred. Because no surface activity was detected from [^{14}C]-carbon

Figure 4.9

$[^{14}C]$-Carbon surface activity on γ-Alumina calcined to 523K as a function of Temperature.

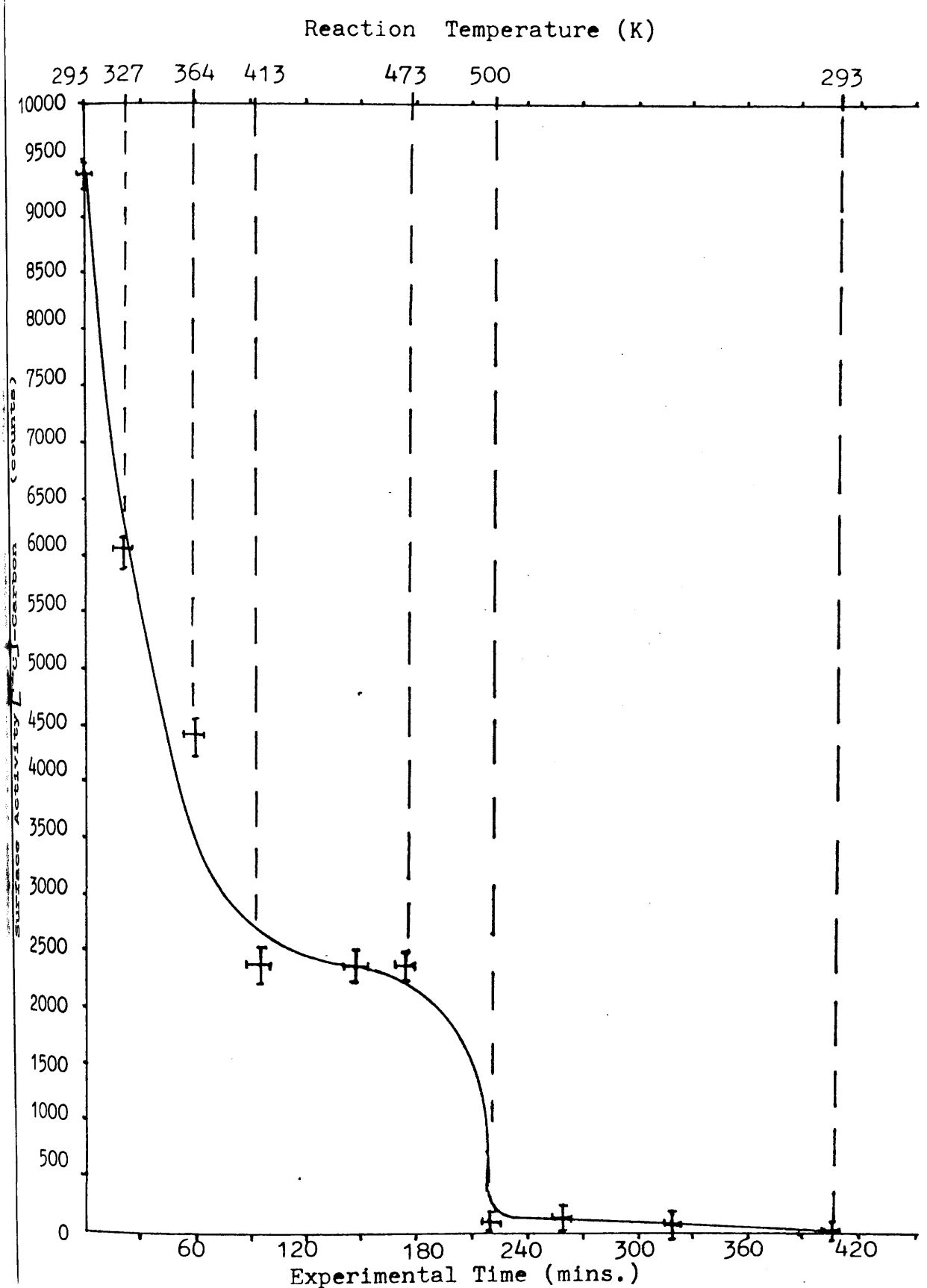

labelled carbon tetrachloride at the end of the experiment it was concluded that there was no carbon laydown during the chlorination process at the reaction temperature of 500K. This observation was in agreement with work carried out by Goble and Lawrance (22) who concluded that there was no carbon laydown in the treatment of γ-alumina with carbon tetrachloride by thermogravimetric methods.

The plateau region that was observed from the [^{14}C]-carbon labelled carbon tetrachloride reaction between the temperatures of 413K and 473K was also detected in the [^{36}Cl]-chlorine labelled carbon tetrachloride experiment (Figure 4.8) between the reaction temperatures of 403K and 473K.

4.2.13 The Adsorption Isotherm at 296K of Spence γ-Alumina Calcined to 523K with [^{14}C]-Carbon labelled Carbon Tetrachloride.

The adsorption isotherm of [^{14}C]-carbon labelled carbon tetrachloride with Spence γ-alumina calcined to 523K was carried out at 296K and the results are shown in figure 4.10. The amount of [^{14}C]-carbon labelled carbon tetrachloride adsorbed on the calcined Spence γ-alumina increased rapidly between the pressures 0-40 Torr and thereafter much more slowly as the pressure of anhydrous gaseous [^{14}C]-carbon labelled carbon tetrachloride was increased beyond a pressure of 40 Torr. The adsorption isotherm (Figure 4.10) is of the classical or Langmuir form (169). At a pressure of 85 Torr the gas phase [^{14}C]-carbon labelled carbon tetrachloride was approaching the saturation vapour pressure of 100 Torr at 293K

Figure 4.10

Adsorption isotherm @293K for Anhydrous Gaseous $[^{14}C]$-Carbon labelled CCl_4 on Spence γ-Alumina calcined @ 523K

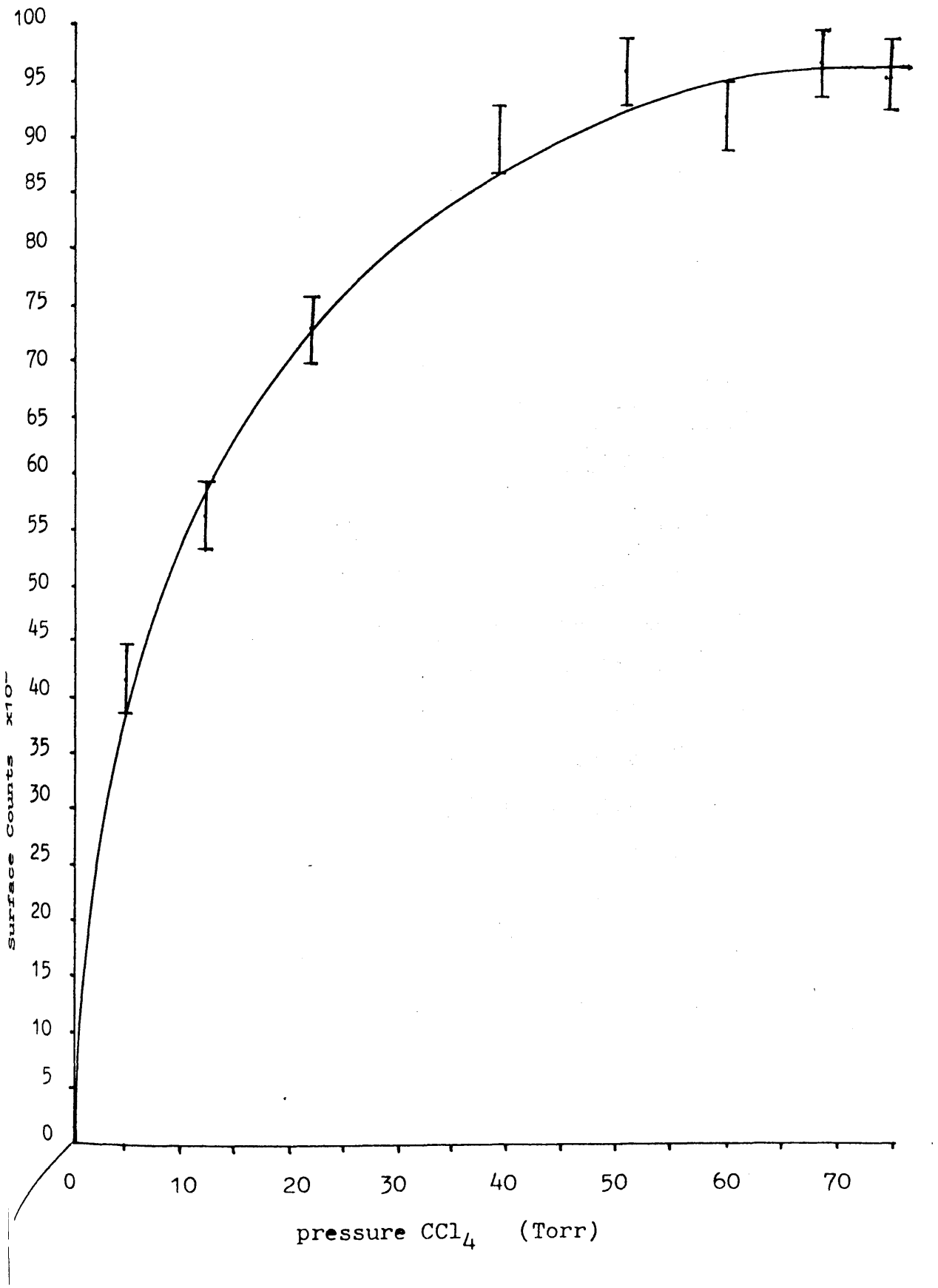

(168) and no deviation from the Langmuir adsorption isotherm was observed.

The results were consistent with the formation of a single unimolecular layer of [^{14}C]-carbon labelled carbon tetrachloride being formed on the surface of the calcined γ-alumina sample at 293K. The surface activity from the [^{14}C]-carbon labelled carbon tetrachloride was reversible at 293K, hence the adsorption of the gas phase on the solid was due to a physisorption process.

4.2.14 The Treatment of Spence γ-Alumina with Deuterium Oxide and the Reaction of the treated γ-Alumina with Anhydrous Gaseous Carbon Tetrachloride.

The preparative procedure is described in section 4.3.13. The infrared spectrum of the gas phase products from the reaction of anhydrous gaseous carbon tetrachloride with a sample of Spence γ-alumina (0.5031g; 3.80mmol) that was treated with deuterium oxide and subsequently calcined at 523K showed absorbances at 2895 cm^{-1} due to the presence of hydrogen chloride, 2365 cm^{-1} and 680 cm^{-1} due to the presence of carbon dioxide and at 2080 cm^{-1} from the characteristic signal obtained from deuterium chloride. The presence of phosgene was observed by the absorptions at 1825 cm^{-1} and at 850 cm^{-1}.

This experiment had shown that it was possible to label the surface of γ-alumina with ^{2}H to allow the study of ^{2}H-^{1}H exchange reactions by the carbon tetrachloride treated γ-alumina samples.

4.2.15 The Reaction of Spence γ-Alumina with Gaseous 1,1-Dichloromethanone at 293K.

The experimental procedure is described in section 4.3.14. The infrared analysis of the gas phase products after 2h exposure of phosgene at 296K to a sample of Spence γ-alumina calcined to 523K showed that a small hydrolysis of phosgene had occurred with surface hydroxyl groups or water retained by the surface of the calcined γ-alumina. Medium absorbances at 2895 cm^{-1} due to the presence of hydrogen chloride and at 2350 cm^{-1} and 680 cm^{-1} due to the presence of carbon dioxide with strong absorbances at 1825 cm^{-1}, 1675 cm^{-1} and 850 cm^{-1} due to the presence of phosgene in the gas phase were observed. The infrared analysis after an 18h exposure of the phosgene to the calcined γ-alumina sample had shown absorbances due to the presence of hydrogen chloride, carbon dioxide and phosgene in the gas phase. From the relative strengths of the absorbances due to the presence of the gas phase components, no further significant increase in the hydrolysis of the gas phase phosgene had occurred over the subsequent 18h period. A substantial drop in the total pressure in the manifold as measured by the constant volume manometer had indicated that adsorption of the gas phase by the calcined γ-alumina sample had occurred at 293K. All the gas phase components, hydrogen chloride, carbon dioxide and phosgene were shown to physically adsorb onto the surface of the calcined γ-alumina at 293K (Sections 4.2.12 and Section 3.2.3).

4.2.16 The Reaction of Calcined Spence γ-Alumina with Anhydrous Gaseous 1,1 Dichloromethanone at 523K.

The infrared analysis of the gas phase products from the chlorination of Spence γ-alumina calcined to 523K with phosgene at 500K for 6h showed strong absorbances at 2085 cm^{-1} due to the presence of hydrogen chloride at 2320 cm^{-1} and 675 cm^{-1} due to the presence of carbon dioxide together with absorbances at 1825 cm^{-1}, 1680 cm^{-1} and 850 cm^{-1} from the presence of phosgene (1,1 dichloromethanone). In all respects the gas phase products had shown the by-products of the reaction between calcined γ-alumina and anhydrous gaseous carbon tetrachloride at 500K after 6h of reaction (Section 4.2.2).

4.2.17 The Exchange at 293K of Calcined Spence γ-Alumina treated with 1,1 Dichloromethanone at 523K with Anhydrous Gaseous [^{36}Cl]-Chlorine labelled Hydrogen Chloride.

The procedure for the above investigation is as described in section 4.3.8 for the investigation of the lability of chlorine retained by the surface of calcined γ-alumina treated with anhydrous gaseous carbon tetrachloride at 500K over a 6h period.

The anhydrous gaseous [^{36}Cl]-chlorine labelled hydrogen chloride used in the exchange reactions had a specific count rate of 0.52 count $s^{-1}mg^{-1}Ag^{36}Cl$ (Section 3.2.6). An aliquot of the anhydrous gaseous [^{36}Cl]-chlorine labelled hydrogen chloride (18.7 Torr; 1.36mmol) based on the equimolar exchange of chlorine (Table 4.4), was allowed to exchange

with a sample of Spence γ-alumina (0.6416g) calcined to 523K which had been treated with 2mmol of phosgene at 500K over a 6h period. The specific count rate obtained from the gas phase at equilibrium from the exchange reaction gave a specific count rate of 0.33 ± 0.005 count $s^{-1}mg^{-1}Ag^{36}Cl$. The specific count rate from the equilibrium gas phase compared with the value of 0.32 ± 0.003 count $s^{-1}mg^{-1}Ag^{36}Cl$ obtained from the Spence γ-alumina sample calcined to 523K but treated with carbon tetrachloride for 6h. The labile chlorine produced by the carbon tetrachloride treatment of γ-alumina was indistinguishable from the labile chlorine produced by the phosgene treatment to the exchange of anhydrous gaseous hydrogen chloride at 293K.

4.2.18 The Removal of Labile Chlorine retained by the surface of Calcined Condea γ-Alumina treated with Anhydrous Gaseous [^{36}Cl]-Chlorine labelled Carbon Tetrachloride.

The experimental procedure for the above investigation is described in section 4.3.16 and the results are presented in figure 4.11. The surface activity produced from the reaction of 1mmol of [^{36}Cl]-chlorine labelled carbon tetrachloride after degassing the sample for 45 min was recorded as the initial count rate at 23.17 count s^{-1}. The addition of the first millimole aliquot of anhydrous gaseous hydrogen chloride brought about a decrease in the surface activity of 22.23% which was greater than anticipated considering the results from section 4.2.9 which concluded that a decrease in the surface activity from the 1st mmol aliquot should be in the region of 12.61%. The second 1mmol aliquot of anhydrous

Figure 4.11

Removal of Surface Activity from labile Chlorine retained by the Surface of γ-Alumina treated with $[^{36}Cl]$-Chlorine labelled CCl_4.

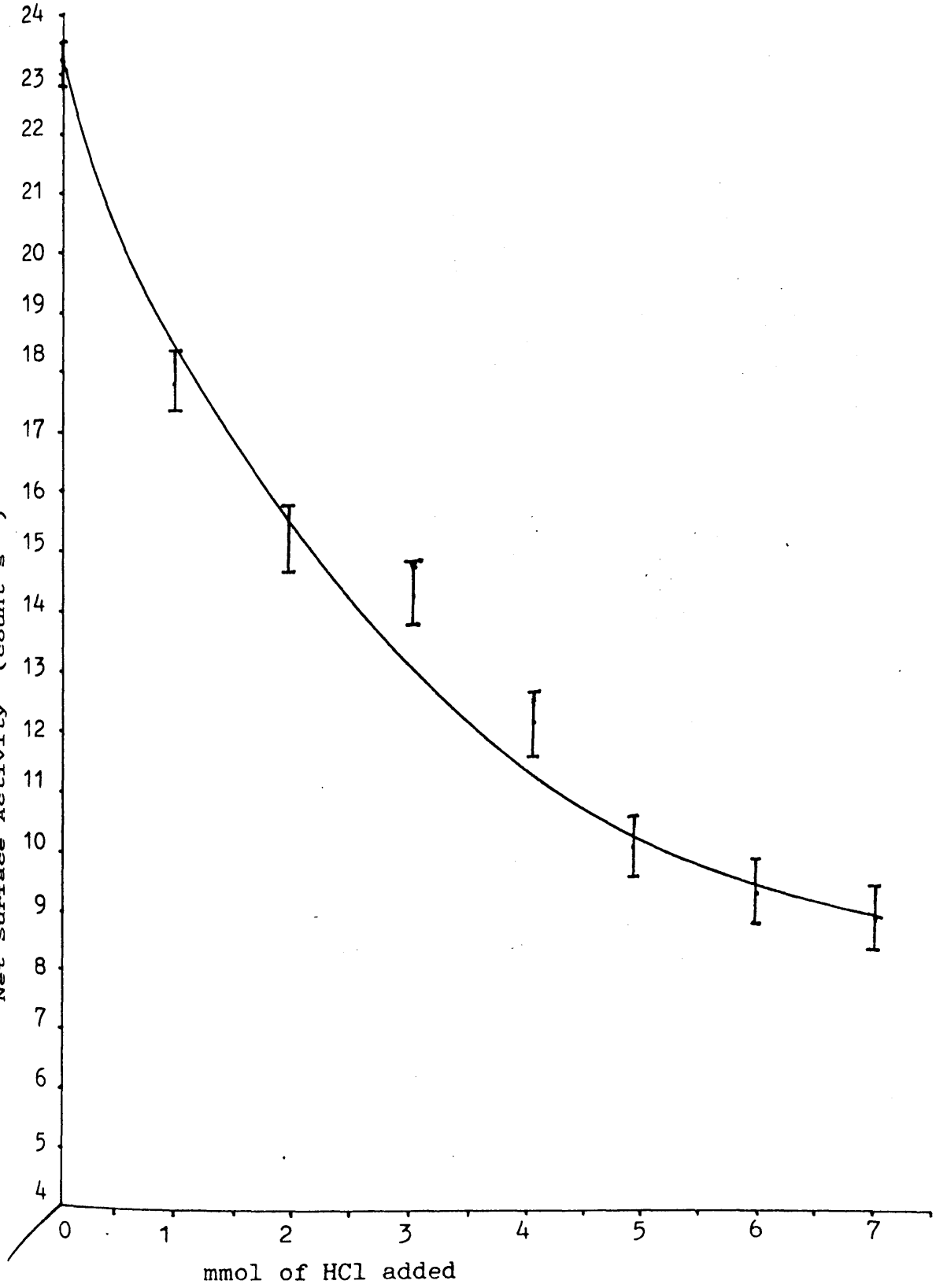

gaseous hydrogen chloride produced a decrease in the surface activity of 12.36%. After the eighth millimole aliquot was exchanged the total surface activity that had been removed from the sample was 60.98% leaving 39.02% of the initial surface activity as non-exchangeable with anhydrous hydrogen chloride at 293K.

This result was different to the comparative experiment where anhydrous gaseous [^{36}Cl]-chlorine labelled hydrogen chloride was the chlorinating reagent (Section 3.2.12). In that study the removal of the labile surface activity left 12% of the surface activity from the exchanges with anhydrous hydrogen chloride at 293K.

4.2.19 The Exchange at 293K between 1,1 Dichloromethanone with Calcined Degussa 'C' γ-Alumina treated with [^{36}Cl] Chlorine labelled Carbon Tetrachloride.

The experimental procedure for the above investigation is described in section 4.3.18 and the results are shown in figure 4.12.

The [^{36}Cl]-chlorine activity from the labile chlorine produced during the [^{36}Cl]-chlorine labelled carbon tetrachloride treatment was removed by the addition of sequential aliquots of 2mmol of anhydrous gaseous hydrogen chloride at 293K and allowed to reach exchange equilibrium. After the addition of 10mmol of anhydrous gaseous hydrogen chloride all the labile [^{36}Cl]-chlorine had been removed, leaving the activity on the surface due to non-exchangeable [^{36}Cl]-chlorine on the γ-alumina sample. The solid was degassed by pumping

Figure 4.12

Investigation of the Reaction of Phosgene @ 293K with residual $[^{36}Cl]$ -Chlorine activity after exchange of HCl with $[^{36}Cl]$-CCl_4 treated γ-Alumina.

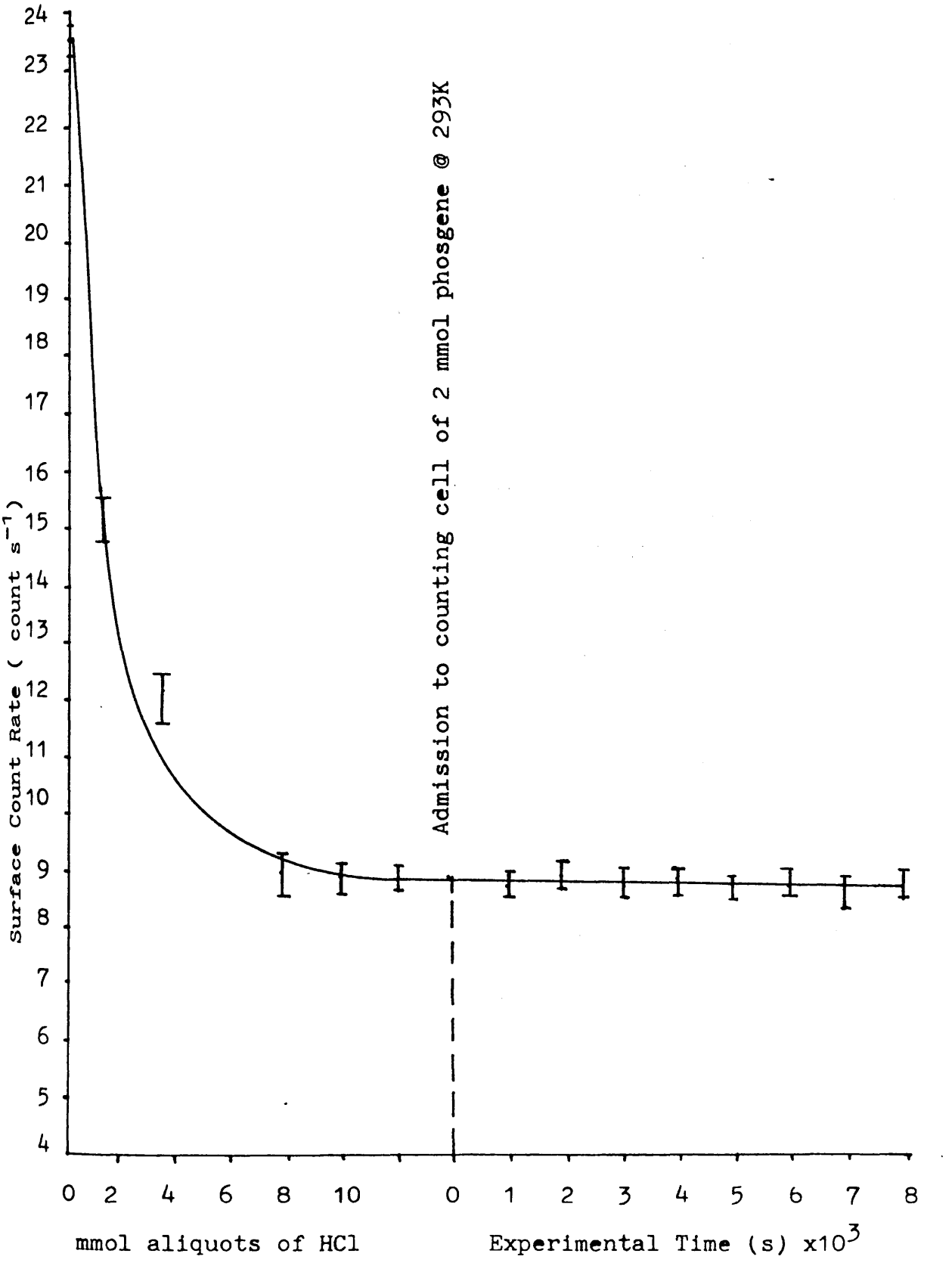

and 2mmol (27.6 Torr) of anhydrous gaseous phosgene was expanded into the counting cell. No change in the surface count rate over 100 min was observed, therefore no exchange was detected between the non-labile surface [^{36}Cl]-chlorine and the gaseous anhydrous phosgene at 293K. The non-exchangeable surface activity produced during the carbon tetrachloride treatment of calcined γ-alumina was shown to be non-exchangeable at 293K with hydrogen chloride (Section 4.2.8 and 4.2.18), carbon tetrachloride (Section 4.2.10) and phosgene (this section). These compounds are the chlorine containing species from the reaction of calcined γ-alumina with carbon tetrachloride.

4.3 EXPERIMENTAL.

4.3.1 The Interaction of Anhydrous Gaseous [^{36}Cl]-Chlorine labelled Carbon Tetrachloride and [^{14}C]-Carbon labelled Carbon Tetrachloride with the Pyrex Counting Cell at 293K.

Owing to the adsorption of carbon tetrachloride on the Pyrex glass walls of the counting cell at 293K it was necessary to calibrate the loss in the gas phase count rate from the [^{36}Cl]-chlorine labelled carbon tetrachloride and the [^{14}C]-carbon labelled carbon tetrachloride as a function of time.

An aliquot of anhydrous gaseous [^{36}Cl]-chlorine labelled carbon tetrachloride (13.8 Torr; 1mmol) was expanded into the counting cell and manifold (Figure 2.1). The gas phase count rates were recorded by the Geiger-Müller tubes as a function of time. The process was repeated using [^{14}C]-carbon labelled carbon tetrachloride (13.8 Torr; 1mmol).

4.3.2 The Determination of the Minimum Temperature required to react Carbon Tetrachloride with Calcined Spence γ-Alumina.

An accurately weighed sample of Spence γ-alumina (0.5054g; 3.8mmol) was calcined to 523K and transferred in the dry box to a dry Monel bomb. The sample was degassed by pumping and an aliquot of dry gaseous carbon tetrachloride (44.8 Torr; 1mmol) was condensed into the bomb at 77K. The bomb and its contents were warmed up to 423K and held at this temperature for 6h. The bomb was allowed to cool to 293K before being transferred to a vacuum line, which was fitted with an infrared gas cell. The gas contents of the bomb were expanded into the manifold and the infrared gas cell to a pressure of 30 Torr. The gas cell was transferred to a Perkin-Elmer 983 Grating Infrared Spectrometer and the gas contents of the cell were analysed by infrared.

This procedure was repeated for the reaction temperatures 423K, 443K, 453K, 473K and 523K.

4.3.3 The Determination of the Minimum Reaction Time to react Carbon Tetrachloride at 473K with Calcined Spence γ-Alumina.

The procedure for the above experiment was the same as the investigation described in section 4.3.2. The contents of the bomb were warmed up to 473K for 30min. The bomb was allowed to cool to 293K before being transferred to a vacuum line which was fitted with an infrared gas cell. The gas contents of the bomb were expanded into the gas cell to a

pressure of 30 Torr. The gas cell was transferred to a Perkin-Elmer 983 Grating Infrared Spectrometer where the gas contents of the infrared gas cell were analysed by infrared. This procedure was carried out at the reaction temperature of 473K for the periods of 30 min, 60 min, 120 min, 180 min, and 240 min respectively.

4.3.4 The Interaction of Anhydrous Gaseous [^{36}Cl]-Chlorine labelled Hydrogen Chloride with Anhydrous Gaseous Carbon Tetrachloride under Glass at 523K.

An aliquot of anhydrous gaseous carbon tetrachloride (44.7 Torr; 1mmol) was condensed into a strong walled vacuum vessel held at 77K followed by an aliquot of anhydrous gaseous [^{36}Cl]-chlorine labelled hydrogen chloride (44.7 Torr; 1mmol). The vacuum vessel was warmed up to 523K, by means of an electrical furnace fitted with a Comark electronic thermometer and a thermocouple, and the reaction mixture was held at 523K for 6h. The gas phase mixture was then cooled to 293K and condensed into a vacuum vessel held at 77K. A slush bath at 193K was placed around the reagents to freeze down the carbon tetrachloride. The gas phase [^{36}Cl]-chlorine labelled hydrogen chloride was then condensed over dampened Analar sodium hydroxide pellets (~2g) from which a silver chloride precipitate was prepared (Section 2.5.3). The specific count rate of the silver chloride precipitate was obtained.

4.3.5 The Chlorination of Calcined Spence γ-Alumina and Calcined Condea γ-Alumina Samples with Anhydrous Gaseous Carbon Tetrachloride.

An accurately weighed sample of calcined γ-alumina (typically 0.5000g; 3.78mmol) was transferred to a dry Monel bomb in a dry box. The bomb and its contents were transferred to a vacuum line where the sample was degassed and an aliquot of anhydrous gaseous carbon tetrachloride (89.4 Torr; 2mmol) was condensed into the bomb which was held at 77K. The contents of the bomb were warmed up to 500K and reacted for 6h. The system was allowed to cool to 293K before being transferred to a vacuum line which was fitted with an infrared gas cell. The gas phase contents of the bomb were expanded into the vacuum line and the infrared gas cell to a pressure of 80 Torr. The gas cell was then transferred to a Perkin-Elmer 983 Grating Infrared Spectrometer where the infrared spectrum of the gas contents of the gas cell was obtained.

4.3.6 The Determination of the B.E.T. Areas of Calcined Spence γ-Alumina and Calcined Condea γ-Alumina Samples treated with Carbon Tetrachloride.

The procedure to determine the B.E.T. areas of the calcined γ-alumina samples treated with carbon tetrachloride at 500K for 6h was the same as the procedure to determine the B.E.T surface areas of the calcined γ-alumina samples treated with anhydrous gaseous hydrogen chloride and is described in section 3.2.5.

4.3.7 Neutron Activation Analysis of the Chlorine Content of Carbon Tetrachloride treated Calcined Spence γ-Alumina and Calcined Condea γ-Alumina Samples.

Owing to the production of [^{36}Cl]-chlorine labelled hydrogen chloride and [^{36}Cl]-chlorine labelled 1,1 dichloromethanone in the gas phase from the reaction of [^{36}Cl]-chlorine labelled carbon tetrachloride with calcined γ-alumina samples at 500K, it was not possible to determine quantitatively the uptake of chlorine by the γ-alumina samples using the gas phase count rate versus pressure calibration procedure that was applied in the determination of the uptake of [^{36}Cl]-chlorine labelled hydrogen chloride by the calcined γ-alumina samples (Section 3.2.3). The neutron activation analysis of [^{38}Cl]-chlorine was used to obtain an accurate determination of the chlorine content of the calcined γ-alumina samples. The procedure for the quantitative determination of [^{38}Cl]-chlorine by neutron activation analysis is described in section 2.7.2,

Spence γ-alumina samples calcined to 293K, 373K, 423K, 473K, 523K and Condea γ-alumina samples calcined to 293K, 423K and 523K were treated with anhydrous gaseous carbon tetrachloride (89.7 Torr; 2mmol) as described in section 4.3.5. The samples were degassed by pumping before being transferred to the sample vials (Figure 2.14) in the dry box. The net weights of the chlorinated γ-alumina samples were accurately determined together with the weight of the standard sample of $MgCl_2.6H_2O$. The samples were irradiated for 25s through the 'rabbit loop' when the reactor power was up to 300 kW. The

irradiated samples were counted consecutively for 1800s on a Ge(Li) scintillation counter fitted to an ORTEC 7030 multi-channel analyser which was set to analyse [^{38}Cl]-chlorine from the characteristic energy peaks at 1642 keV and at 1145 keV.

4.3.8 The Exchange of Calcined Spence γ-Alumina and Calcined Condea γ-Alumina Samples treated with Anhydrous Gaseous Carbon Tetrachloride with [^{36}Cl]-Chlorine labelled Anhydrous Hydrogen Chloride.

The procedure for the above investigation was the same as the procedure described in sections 3.3.6 and 3.3.7 for the exchange of [^{36}Cl]-chlorine labelled hydrogen chloride with calcined γ-alumina samples treated with anhydrous hydrogen chloride at 293K. The determination of the specific count rate of the [^{36}Cl]-chlorine labelled anhydrous hydrogen chloride at the beginning of the exchange work is described in section 3.3.5.

The carbon tetrachloride treated calcined Spence and Condea γ-alumina samples were degassed by pumping. An accurately weighed chlorinated sample (0.5000g; 3.80mmol) was transferred to the counting cell (Figure 2.11) and exchanged with an equimolar amount of [^{36}Cl]-chlorine labelled anhydrous hydrogen chloride (Table 4.4). The specific count rate of the exchanged gas phase was obtained.

4.3.9 The Exchange at 293K of Calcined Spence γ-Alumina treated with Anhydrous Gaseous Carbon Tetrachloride with [^{36}Cl]-Chlorine labelled Carbon Tetrachloride.

A sample of Spence γ-alumina (0.5324g;4.03mmol) was loaded into a dry dropping vessel in the dry box, transferred to a vacuum line and degassed. The sample was chlorinated with anhydrous gaseous [^{36}Cl]-chlorine labelled carbon tetrachloride (13.8 Torr;1mmol) at 500K for 6h in the counting cell (Figure 2.11). The gas phase products from the reaction were expanded into the manifold of the vacuum line, which was fitted with a dry infrared gas cell, to a pressure of 40 Torr. The gas cell was fitted to a Perkin Elmer 983 Grating Infrared Spectrometer where the gaseous products were analysed by infrared.

The [^{36}Cl]-chlorine labelled carbon tetrachloride treated γ-alumina sample was degassed by pumping and an aliquot of anhydrous carbon tetrachloride (13.8 Torr; 1mmol) was expanded into the counting cell where the surface activity of the solid sample was monitored with time.

4.3.10 The Surface Activity from [^{36}Cl]-Chlorine labelled Anhydrous Gaseous Carbon Tetrachloride with Spence γ-Alumina in the Temperature Range 293K to 523K.

A sample of Spence γ-alumina (0.5841g;4.42mmol) was calcined at 523K and transferred into a dropping vessel in the dry box. The sample was degassed before being transferred to the counting cell (Figure 2.11). The glassware of the vacuum line was flamed out under vacuum to remove

any moisture. The Spence γ-alumina sample was dropped into the boat and placed under Geiger-Müller tube No.2. An aliquot of [^{36}Cl]-chlorine labelled anhydrous gaseous carbon tetrachloride (13.8 Torr;1mmol) was expanded into the counting cell where the gas phase and the solid phase count rates were monitored.

The sample was drawn into the furnace and held at 336K for 1h, after which the sample was allowed to stand for 15 min until cool enough to place under Geiger-Müller tube No.2. The gas phase and the solid phase count rate was again recorded. This procedure was repeated through the temperature range 293K to 523K with increments of approximately 20K. At 523K the sample was allowed to react for a further 4h period. The solid was cooled to 293K and degassed by pumping. A final surface count rate at 293K was obtained.

4.3.11 The Surface Ac tivity from [^{14}C]-Carbon labelled Carbon Tetrachloride with Calcined Spence γ-Alumina in the Temperature Range 293K to 523K.

The procedure used in this investigation was the same as the procedure used in section 4.3.10. In this work an aliquot of [^{14}C]-carbon labelled carbon tetrachloride (13.8 Torr;1mmol) was expanded into the counting cell containing the calcined Spence γ-alumina sample (0.4971g; 3.76mmol) at 293K. The surface activity of the solid was monitored as a function of the reaction temperature through the temperature range 293K to 523K.

4.3.12 The Adsorption Isotherm of Calcined Spence γ-Alumina with [^{14}C]-Carbon labelled Carbon Tetrachloride at 296K.

A calcined sample of Spence γ-alumina (0.4879g;3.69 mmol) was calcined to 523K and loaded into a dry dropping vessel in the dry box. The sample was degassed and transferred to the counting cell where it was dropped into the boat (Figure 2.11) and placed under Geiger-Müller tube No.2. Dry anhydrous [^{14}C]-carbon labelled carbon tetrachloride was expanded into the counting cell to pressures of 6, 12, 23, 41, 51, 61, 72, 81 and 85 Torr respectively. After the [^{14}C]-carbon labelled carbon tetrachloride was admitted into the counting cell, the system was allowed to equilibriate at ambient temperatures for 90 min. The gas phase and the solid phase count rates were recorded. After each reading the sample was degassed by pumping. The next incremental pressure of [^{14}C]-carbon labelled carbon tetrachloride was expanded into the counting cell. The vapour pressure of carbon tetrachloride at 300K is 100 Torr (168) and this was the limiting vapour pressure that could be used in this study.

4.3.13 The Treatment of Spence γ-Alumina with Deuterium Oxide and the Reaction of the Treated γ-Alumina Sample with Anhydrous Gaseous Carbon Tetrachloride.

A sample of Spence γ-alumina (0.5g) was loaded into a stainless steel bomb together with an aliquot of Analar deuterium oxide (2ml; 0.11mol), and fitted to a vacuum line. The bomb was frozen down to 77K and its contents were evacuated prior to heating the bomb up to 500K for 4h. The bomb was then opened and the sample was calcined at 523K for 4h. After the calcination an aliquot of anhydrous gaseous carbon tetrachloride (44.7 Torr; 1mmol) was condensed into the bomb at 77K. The contents of the bomb were reacted at 500K for 6h. After the reaction the gas phase contents were expanded into the manifold of the vacuum line which was fitted with an infrared gas cell to a pressure of 80 Torr. The gaseous products of the reaction were analysed by infrared using a Perkin-Elmer 983 Grating Infrared Spectrometer.

4.3.14 The Reaction of Calcined Spence γ-Alumina with Anhydrous Gaseous 1,1 Dichloromethanone at 296K.

A sample of Spence γ-alumina (0.4887g;3.7mmol) was calcined to 523K and loaded into a dry vacuum vessel in the dry box. The vacuum vessel was fitted to a dry vacuum line which had been flamed out. An aliquot of anhydrous gaseous 1,1 dichloromethanone (phosgene:89.4 Torr;2 mmol) was condensed into the vacuum vessel at 77K. The contents of the vacuum vessel were allowed to interact at 296K for 2h. The gas phase contents of the vacuum vessel were expanded into the manifold fitted with an infrared gas cell to a pressure of

50 Torr. The gas phase products were analysed by infrared. The phosgene and the calcined γ-alumina were allowed to interact for a further 18h after which the gas phase products (50 Torr) were again analysed by infrared using a Perkin-Elmer 983 Grating Infrared Spectrometer.

4.3.15 The Reaction of Calcined Spence γ-Alumina with Anhydrous Gaseous 1,1 Dichloromethanone at 523K.

The experimental procedure to chlorinate a sample of Spence γ-alumina (0.5000g; 3.78mmol) calcined to 523K with phosgene (179 Torr; 4mmol) was the same as the procedure described in section 4.3.5 to treat calcined γ-alumina with anhydrous gaseous carbon tetrachloride.

4.3.16 The Removal of the Surface Activity from Calcined Condea γ-Alumina treated with Anhydrous Gaseous [^{36}Cl]-Chlorine labelled Carbon Tetrachloride.

A sample of Condea γ-alumina (0.5429g;4.11mmol) was calcined to 523K and loaded into a dry vacuum vessel in the dry box. The sample was degassed by pumping before being transferred to the counting cell (Figure 2.11). The sample was reacted in the counting cell furnace at 500K for 6h with [^{36}Cl]-chlorine labelled carbon tetrachloride (13.8 Torr; 1mmol). After the chlorination process the sample was degassed by pumping. The surface activity produced by the chlorination process was removed by the addition of sequential aliquots (13.8 Torr; 1mmol) of anhydrous gaseous hydrogen chloride to the counting cell.

Each aliquot of anhydrous gaseous hydrogen chloride was allowed to exchange for 1h with the [^{36}Cl]-chlorine labelled surface of the γ-alumina. When the exchange reaction had reached equilibrium the solid was degassed by pumping. This procedure was repeated until no further reduction in the surface activity was detected.

4.3.17 The Reaction at 293K between Phosgene and Calcined Degussa 'C' γ-Alumina treated with [^{36}Cl]-Chlorine labelled Carbon Tetrachloride after the Labile [^{36}Cl]-Chlorine had been removed.

A sample of Degussa 'C' γ-alumina (0.5349g;4.05mmol) was calcined to 523K and transferred in the dry box to a dry vacuum vessel. The sample was transferred to a vacuum line and degassed by pumping and transferred to the counting cell. The sample was chlorinated with an aliquot of anhydrous gaseous [^{36}Cl]-chlorine labelled carbon tetrachloride (27.6 Torr; 2mmol) at 500K for 6h. After the chlorination process the sample was degassed by pumping. The [^{36}Cl]-chlorine activity from labile chlorine on the surface of the calcined γ-alumina was removed by the sequential addition of aliquots of anhydrous hydrogen chloride (27.6 Torr; 2mmol) at 293K until no change was recorded from the surface activity by the residual [^{36}Cl]-chlorine on the surface of the calcined γ-alumina at 293K. The solid was again degassed by pumping. Anhydrous gaseous phosgene was admitted into the counting cell (100 Torr; 2.13mmol). The surface count rate was monitored with time during the exposure of the phosgene to the active non-labile [^{36}Cl]-chlorine that was retained by the surface.

CHAPTER 5.

The Reactions of 1,1,1-Trichloroethane with Chlorine Promoted Calcined γ-Alumina.

5.1 Introduction

The dehydrochlorination of 1,1,1 trichloroethane to give the gaseous products hydrogen chloride and 1,1 dichloroethene can occur from a base catalysed reaction (132) or from an acid catalysed reaction (23-24). In the base catalysed reaction, the initial step in the degradation of the 1,1,1-trichloroethane involves the abstraction of a proton from the chlorocarbon, whereas in the acid catalysed dehydrochlorination reaction the initial step involves the abstraction of a chlorine anion from the chlorocarbon reagent.

It has been shown that refluxing γ-alumina with uninhibited 1,1,1 trichloroethane can cause the dehydrochlorination of the chlorocarbon producing 1,1 dichloroethene and hydrogen chloride (24). It is also known that the acid sites produced by the γ-alumina with carbon tetrachloride are known to possess strong Lewis acid centres approaching those of Friedel Crafts solids $HCl/AlCl_3$ (Section 1.8).

The purpose of this investigation is to examine the interaction of 1,1,1 trichloroethane with carbon tetrachloride promoted γ-alumina calcined at 523K. This was achieved by using [^{36}Cl]-chlorine labelled reagents. These reagents included [^{36}Cl]-chlorine labelled 1,1,1-trichloroethane and [^{36}Cl]-chlorine labelled hydrogen chloride as radiolabelled gas phase probes. The γ-alumina surface was labelled by the [^{36}Cl]-chlorine labelled carbon tetrachloride treatment

(Section 4.3.10). The radiolabelling techniques were used in conjunction with infrared analysis of the gas phase components produced during a reaction.

The treatment of calcined γ-alumina with carbon tetrachloride produced two types of surface chlorine, exchangeable and non-exchangeable (Section 4.2.9) compared with the treatment of γ-alumina with anhydrous gaseous hydrogen chloride at 523K which produced only exchangeable surface chlorine (Section 3.2.6, Section 3.2.7). It was therefore of interest to examine the behaviour of both types of chlorinated γ-alumina in order to detect what, if any, differences in behaviour could be observed.

The acid catalysed dehydrochlorination of 1,1,1-trichloroethane with aluminium trichloride has been studied extensively (23). The dehydrochlorination of 1,1,1 trichloroethane is thought to proceed via a carbonium intermediate and the product from the dehydrochlorination process, 1,1-dichloroethene is known to polymerize over strong Lewis acid sites (23). This investigation has therefore limited the area of interest with respect to the reactions of 1,1-dichloroethene, to the rate of depletion from the gas phase by the carbon tetrachloride promoted γ-alumina, to identify reactions that involve 1,1-dichloroethene as a surface or gas substrate, and not to include an investigation of the polymer products.

5.2.1 Determination of the Reaction Conditions Required to Dehydrochlorinate 1,1,1-Trichloroethane with Calcined Spence γ-Alumina.

The infrared spectrum of the gaseous products from the reaction of 293K of 1,1,1-trichloroethane with Spence γ-alumina calcined to 523K showed only the presence of 1,1,1 trichloroethane in the gas phase. No dehydrochlorination of 1,1,1 trichloroethane with calcined γ-alumina was observed until the system had reached 373K. At this temperature the infrared spectrum (Table 2A) showed the presence of 1,1 dichloroethene in the gas phase. The presence of hydrogen chloride or 1,1,1 trichloroethane was not observed. The presence of 1,1 dichloroethene in the gas phase indicated that the dehydrochlorination reaction had taken place. Since no hydrogen chloride was observed the calcined γ-alumina appeared to function as a sink for the hydrogen chloride.

5.2.2 Reaction of 1,1,1 Trichloroethane over Calcined Condea γ-Alumina treated with Anhydrous Hydrogen Chloride at 293K.

The infrared spectrum showed only 1,1,1 trichloroethane in the gas phase (Table 2A) and showed that no dehydrochlorination reaction had occurred.

5.2.3 Reaction of 1,1,1 Trichloroethane over Calcined Degussa 'C' γ-Alumina treated with Anhydrous Gaseous [^{36}Cl]-Chlorine labelled Hydrogen Chloride at 293K.

The experimental procedure for the above investigation is described in section 5.3.3. Over the period of 2h in which the gas phase and solid phase counts were recorded, it was observed that no change in the surface activity from the [^{36}Cl]-chlorine labelled hydrogen chloride treated Degussa 'C' γ-alumina had occurred. This indicated that there was no exchange of [^{36}Cl]-chlorine from the surface to the gas phase. This information together with the results from section 5.2.2 showed that there was no interaction between 1,1,1 trichloroethane and γ-alumina calcined to 523K treated with anhydrous gaseous hydrogen chloride.

5.2.4 Reactions of 1,1,1 Trichloroethane at 293K with Calcined γ-alumina treated with Anhydrous Gaseous Carbon Tetrachloride.

The infrared analysis showed strong absorbance bands due to the presence of 1,1,1 trichloroethane(Table 2A). Also present was the strong absorbance at 2895 cm^{-1} due to hydrogen chloride and absorbance bands due to 1,1 dichloroethene (Table 2A). Therefore dehydrochlorination of 1,1,1 trichloroethane had occurred at 293K over γ-alumina which had been treated with carbon tetrachloride to form the gaseous products hydrogen chloride and 1,1 dichloroethene.

5.2.5 Reaction of 1,1,1 Trichloroethane with Calcined Degussa 'C' γ-Alumina treated with 1,1 Dichloromethanone at 293K.

The infrared analysis of the gas phase compounds showed the presence of 1,1,1 trichloroethane in the gas phase. There was no infrared evidence for the presence of 1,1 dichloroethene or hydrogen chloride in the gas phase. Therefore the dehydrochlorination reaction was not observed over calcined γ-alumina that was treated with 1,1 dichloromethanone at 293K.

5.2.6 Reaction of 1,1,1 Trichloroethane with Calcined Degussa 'C' γ-Alumina treated with 1,1 Dichloromethanone at 500K.

The infrared spectrum showed a band at 2895 cm^{-1} due to the presence of hydrogen chloride in the gas phase together with bands due to the presence of 1,1 dichloroethene (Table 2A). The infrared spectrum also showed bands due to the presence of 1,1,1 trichloroethane in the gas phase sample. Hence a calcined sample of Degussa 'C' γ-alumina treated with 1,1 dichloromethanone at 500K was able to dehydrochlorinate 1,1,1 trichloroethane at 293K. This result was the same as the findings from the dehydrochlorination of 1,1,1 trichloroethane at 293K with γ-alumina treated with carbon tetrachloride at 500K (Section 5.2.4).

5.2.7 Reaction of 1,1 Dichloroethene and Anhydrous Gaseous Hydrogen Chloride at 293K.

The infrared spectrum showed bands due to the presence of hydrogen chloride and 1,1 dichloroethene in the gas phase. There were no infrared bands observed due to the presence of 1,1,1 trichloroethane. It was concluded that there was no homogeneous reaction under glass in darkened conditions at room temperature between 1,1 dichloroethene and hydrogen chloride.

5.2.8 Reaction of 1,1 Dichloroethene with Calcined Condea γ-Alumina treated with Anhydrous Gaseous Hydrogen Chloride at 296K.

The infrared spectrum of the gas phase components showed the presence of 1,1 dichloroethene (Table 2A). It was concluded that there is no reaction between 1,1 dichloroethene and the surface of Condea γ-alumina treated with anhydrous gaseous hydrogen chloride at 296K.

5.2.9 Reaction of 1,1 Dichloroethene with Calcined Degussa 'C' γ-Alumina treated with [^{36}Cl]-Chlorine labelled Hydrogen Chloride at 293K.

The experimental procedure for the above investigation is described in section 5.3.9. The initial surface activity of the solid prior to the expansion of 1 mmol of uninhibited 1,1 dichloroethene into the counting cell was 30.51 ± 0.34 count s^{-1}. After the exposure of the 1 mmol aliquot of uninhibited 1,1 dichloroethene to the solid for

104 min the recorded surface activity was 30.98 ± 0.34 count s^{-1} which indicated that no observed exchange reaction had taken place at 293K. This information together with the results from section 5.2.8 indicated that 1,1 dichloroethene did not react with the surface of calcined γ-alumina treated with anhydrous gaseous hydrogen chloride at 293K.

5.2.10 Reactions of 1,1 Dichloroethene with Calcined Condea γ-Alumina treated with Anhydrous Gaseous Carbon Tetrachloride at 500K.

The experimental procedure for the above investigation is described in section 5.3.10. It was observed that the carbon tetrachloride treated calcined γ-alumina sample had changed colour from an 'off white' to a deep blue/black which indicated that a reaction had occurred between the 1,1 dichloroethene and the chlorinated surface. The darkening of the solid was attributed to the polymerization products of 1,1 dichloroethene. This darkening of the catalyst surface had been reported in the study of the dehydrochlorination of 1,1,1 trichloroethane with aluminium trichloride (23).

It was not possible to obtain an infrared analysis of the gas phase products from the reaction. The pressure of the gas contents of the vacuum vessel was so small that it was not possible to obtain an infrared analysis of any gas that may have been present.

5.2.11 The Reaction of 1,1 Dichloroethene with Calcined Spence γ-Alumina treated with Anhydrous Gaseous Carbon Tetrachloride previously used in the Dehydrochlorination of 1,1,1 Trichloroethane at 296K.

Uninhibited 1,1 dichloroethene (100 Torr; 2.24 mmol) was condensed into a thick walled vacuum vessel containing a degassed, discoloured blue/black carbon tetrachloride treated Spence γ-alumina which had been used previously in the dehydrochlorination of 1,1,1 trichloroethane. The vacuum vessel and its contents were allowed to warm up to room temperature and allowed to react for 4h. The infrared analysis of the gas contents of the vacuum vessel showed 1,1 dichloroethene in the gas phase (Table 2A).

There was no evidence for the hydrochlorination reaction to the reformation of 1,1,1 trichloroethane by 1,1 dichloroethene reacting with chlorine containing species on the surface of the promoted catalyst.

5.2.12 Reaction of 1,1 Dichloroethene and Anhydrous Gaseous Hydrogen Chloride with Calcined Degussa 'C' γ-Alumina previously treated with Anhydrous Gaseous Carbon Tetrachloride.

The infrared spectrum of the gas phase products showed bands due to the presence of 1,1,1 trichloroethane and 1,1 dichloroethene (Table 2A), together with the absorbance at 2895 cm^{-1} due to the presence of hydrogen chloride. This result showed that the reformation at

296K of 1,1,1 trichloroethane over calcined γ-alumina treated with carbon tetrachloride had occurred.

5.2.13 Infrared Analysis of the Decomposition of 1,1,1-Trichloroethane over Calcined γ-Alumina treated with Anhydrous Gaseous Carbon Tetrachloride.

The results of the decomposition of 1,1,1 trichloroethane, initial vapour pressure 10.1 Torr, over 4h are presented in table 5.1. The partial pressure of 1,1,1-trichloroethane in the reaction as a function of time is shown in figure 5.1. A first order plot of the data is shown in figure 5.2. The plot of the data was not of the first order. A second order plot of the data is shown in figure 5.3. A linear fit was obtained for t>30min for the reaction. The correlation coefficient was 0.9953 and the derived second order rate constant was 5.81×10^{-4} $l\ mol^{-1} min^{-1}$.

The non-linear behaviour in the first 30 min. was probably the result of the initial pressure of the 1,1,1 trichloroethane at 10.1 Torr resulting in a strong absorbance of the 720 cm^{-1} band. This band did not reduce in intensity sufficiently to give an accurate correlation with the partial pressure of 1,1,1 trichloroethane in the stages of the reaction where t<30 min. A fresh sample of carbon tetrachloride treated γ-alumina was prepared and the absorbance for the 720 cm^{-1} band was monitored using a smaller pressure of 1,1,1 trichloroethane (6.9 Torr). The results from this investigation are presented in table 5.2 and shown schematically in figure 5.4.

Table 5.1

Time (min)	Area under 720 cm^{-1} peak sq. units	P. 1,1,1-trichloroethane (Torr)	1st order $\log \frac{p_o}{p}$	2nd order $\frac{p_o - p}{p_o p}$
0	23.88	10.1	1.004	0.099
3	21.05	9.4	0.973	0.106
5	18.94	8.6	0.934	0.116
8	18.20	8.2	0.914	0.122
10	17.65	8.0	0.903	0.125
13	17.42	7.9	0.895	0.127
16	16.77	7.6	0.880	0.132
18	16.48	7.5	0.875	0.133
21	16.12	7.4	0.869	0.135
31	15.01	6.9	0.839	0.145
44	13.93	6.5	0.813	0.154
57	13.02	6.1	0.785	0.164
81	11.69	5.5	0.740	0.182
105	10.73	5.2	0.716	0.192
137	9.75	4.7	0.672	0.212
165	8.95	4.5	0.653	0.222
188	8.66	4.3	0.633	0.233
217	8.03	4.1	0.613	0.244
246	6.96	3.7	0.568	0.270

p_o = the initial pressure

p = the pressure of 1,1,1 trichloroethane at time = t

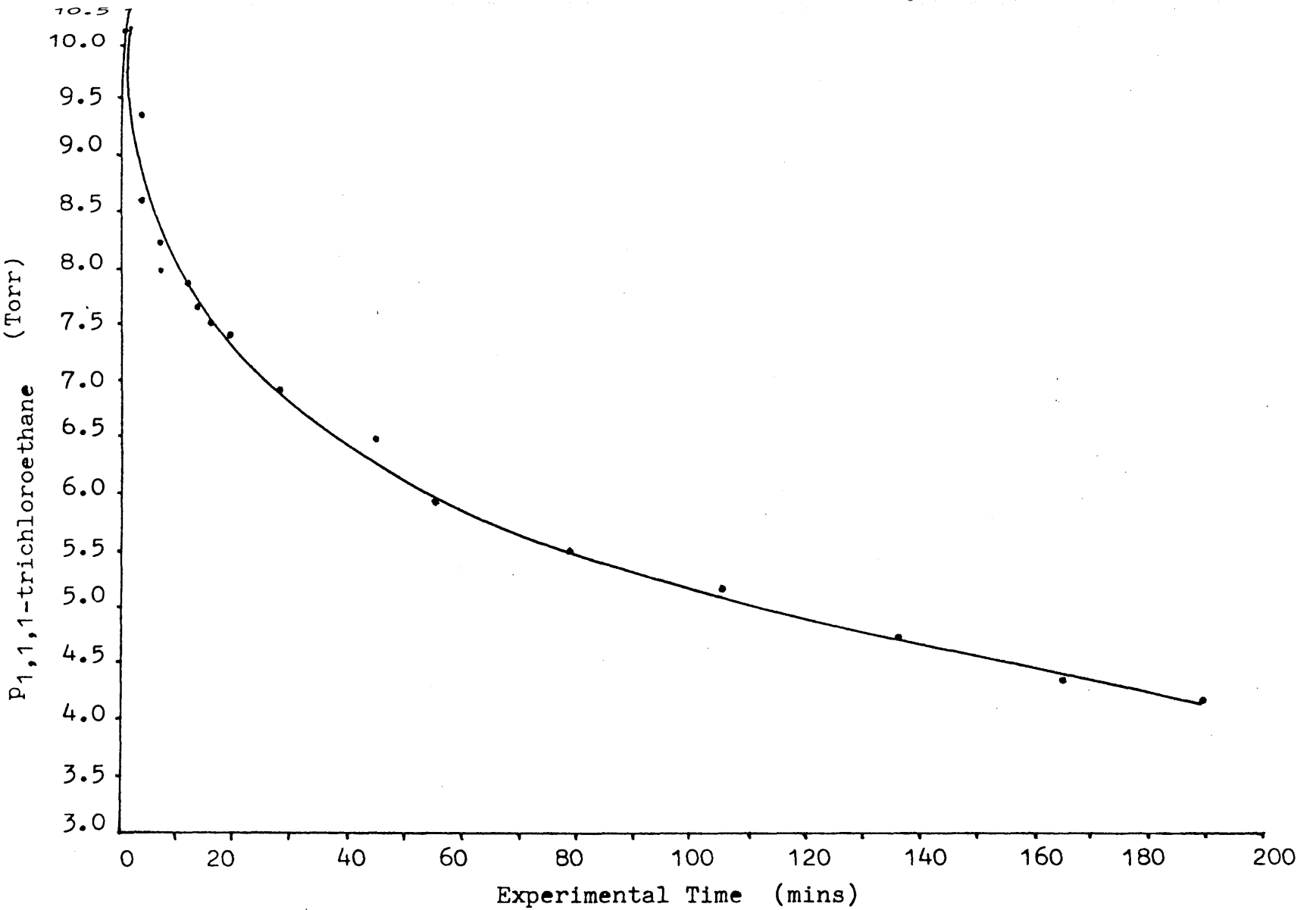
10.5
10.0
9.5
9.0
8.5
8.0
7.5
7.0
6.5
6.0
5.5
5.0
4.5
4.0
3.5
3.0
$p_{1,1,1\text{-trichloroethane}}$ (Torr)
0
20
40
60
80
100
120
140
160
180
200
Experimental Time (mins)

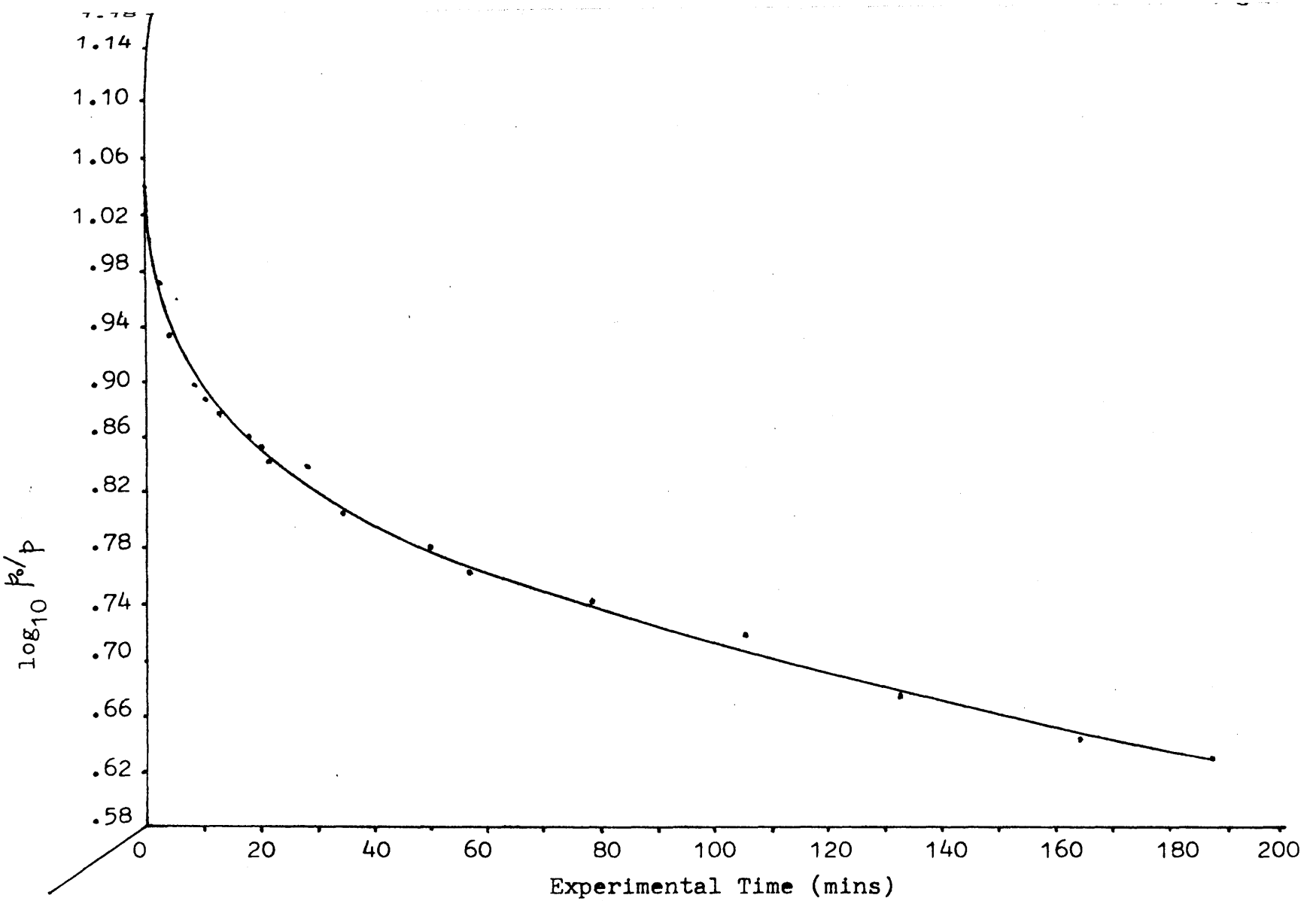
1.14
1.10
1.06
1.02
.98
.94
.90
.86
.82
.78
.74
.70
.66
.62
.58
$\log_{10} p^{\circ}/p$
0
20
40
60
80
100
120
140
160
180
200
Experimental Time (mins)

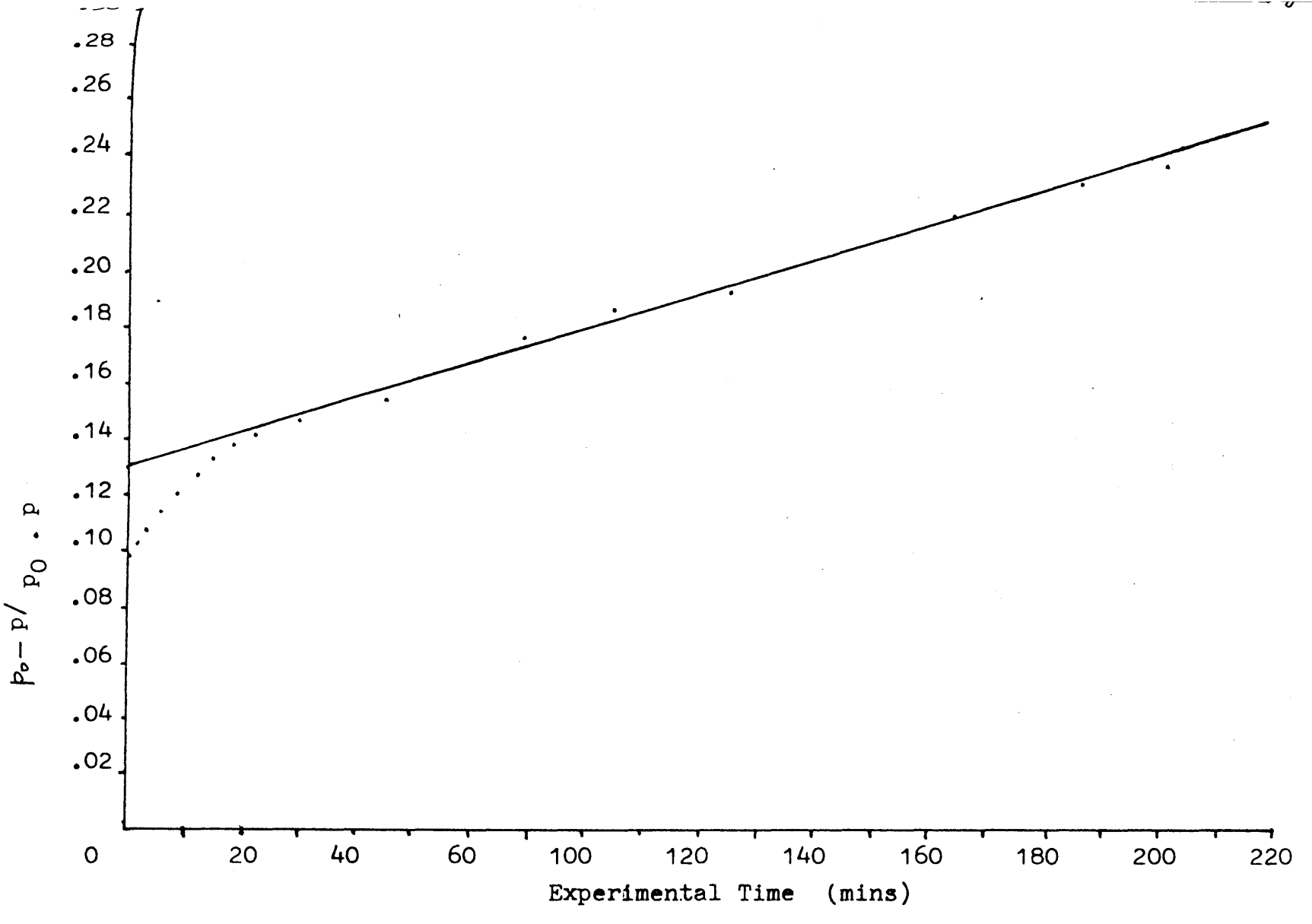
.28
.26
.24
.22
.20
.18
.16
.14
.12
.10
.08
.06
.04
.02
$p_o - p / p_o \cdot p$
0
20
40
60
100
120
140
160
180
200
220
Experimental Time (mins)

Table 5.2

Experimental Time. (min)	Area under 720 cm^{-1} peak (sq.units)	p 1,1,1 trichloro -ethane (Torr)	1st Order $\log \frac{po}{p}$	2nd Order $\frac{po-p}{po.p}$
0	16.7391	7.547	0.878	0.133
2	14.0692	6.439	0.809	0.155
3	13.1024	6.038	0.780	0.166
4	11.1227	5.216	0.717	0.192
5	9.1763	4.408	0.644	0.227
6	9.0887	4.372	0.641	0.228
7	7.3861	3.665	0.564	0.273
9	6.7928	3.419	0.534	0.292
10	6.2899	3.210	0.507	0.312
11	6.2452	3.192	0.504	0.313
12	5.9411	3.066	0.487	0.333
13	5.3377	2.815	0.450	0.355
14	5.0091	2.679	0.428	0.373
15	4.9054	2.636	0.421	0.379
16	4.9027	2.635	0.421	0.380
17	4.8546	2.615	0.417	0.382
18	4.4726	2.456	0.390	0.407
20	4.4098	2.430	0.386	0.416
22	4.1875	2.338	0.369	0.428
23	4.1995	2.343	0.370	0.427
25	4.0582	2.284	0.359	0.438

po = pressure at t = 0

p = pressure at t = t

Figure 5.4

Consumption of 1,1,1-Trichloroethane @ 296K over Condea γ-Alumina treated with CCl_4

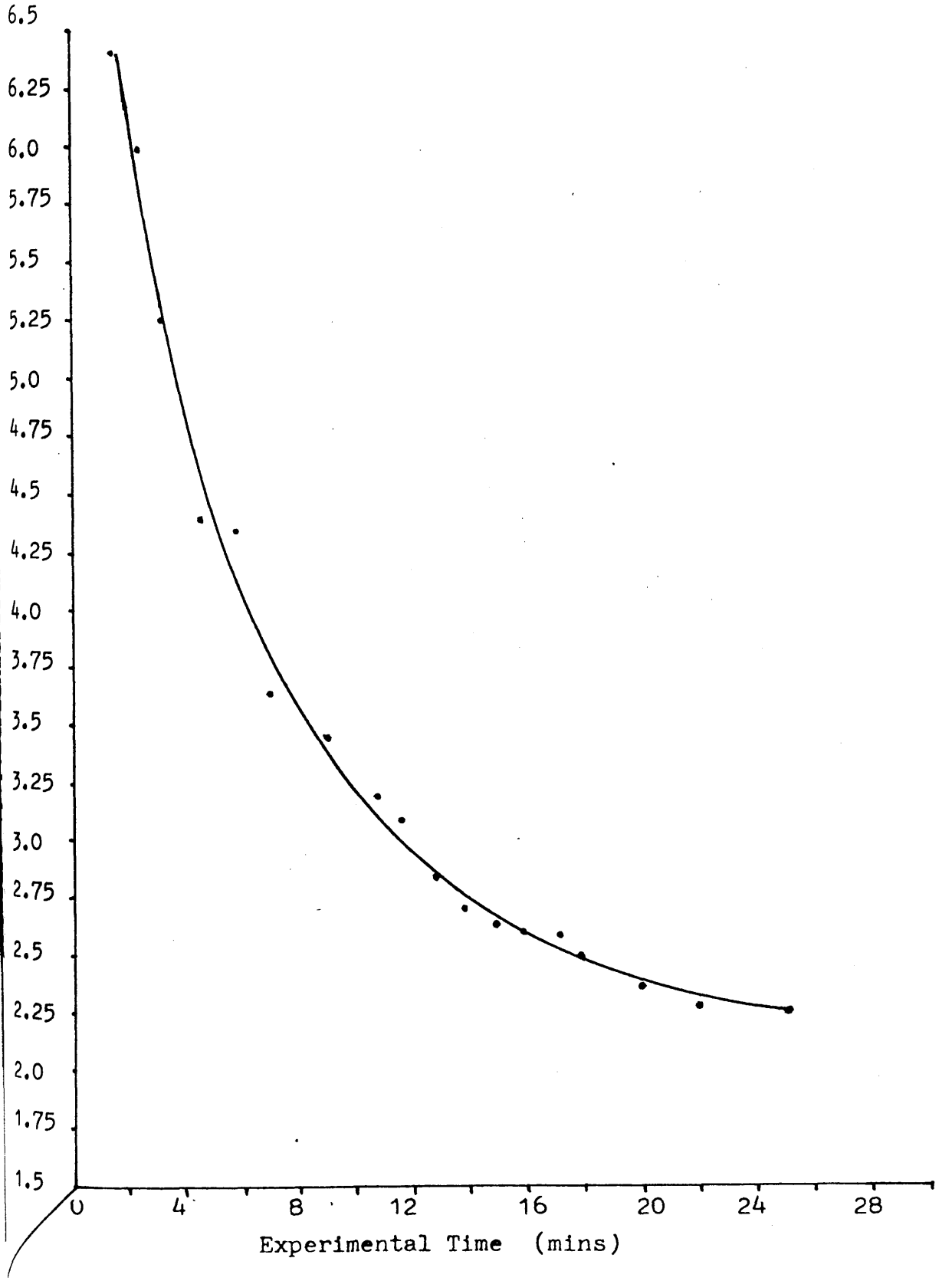

Figure 5.5

1st Order Plot of the Consumption of 1,1,1-Trichloroethane over Condea CCl_4/γ-Alumina during first 25 mins. of Reaction

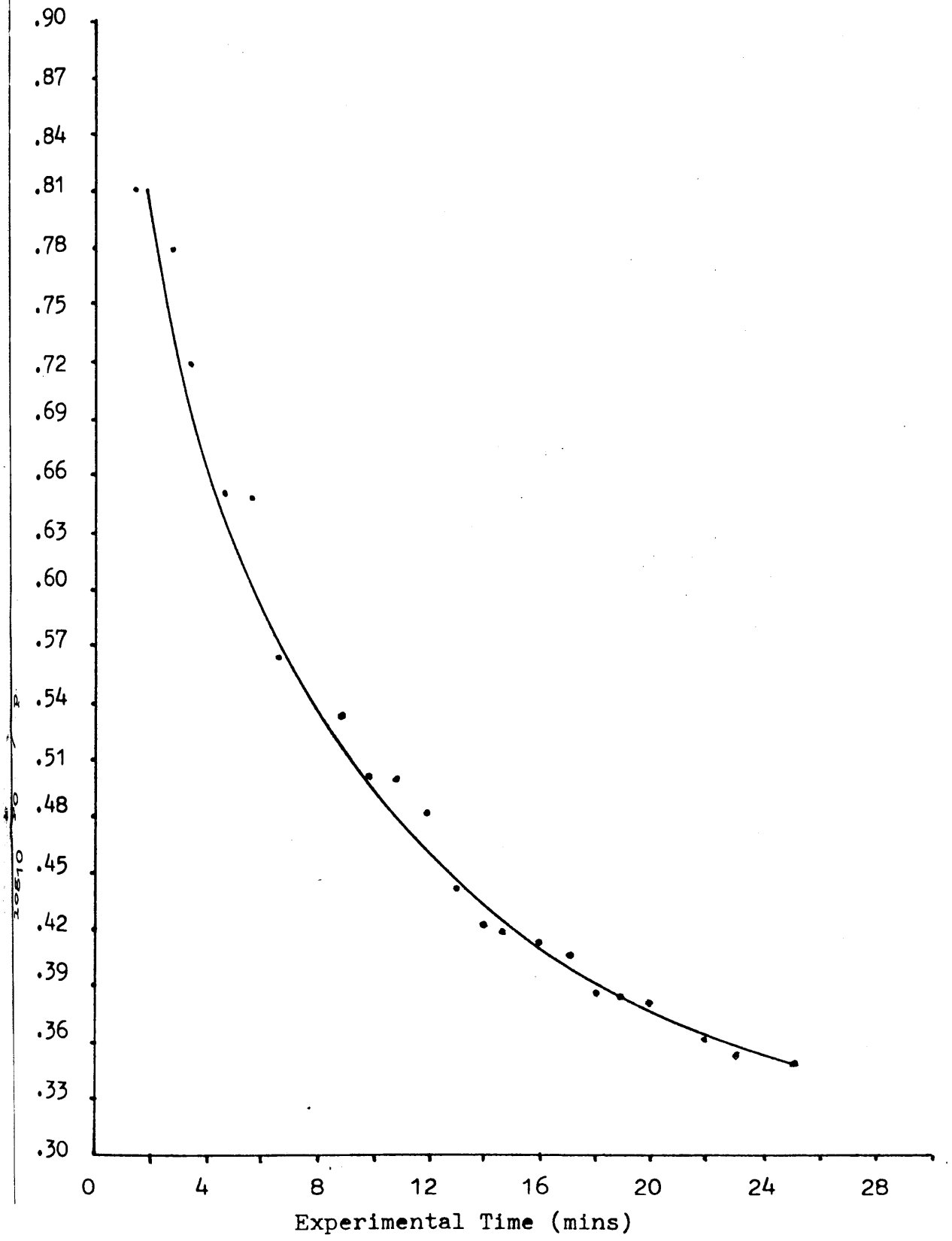

Figure 5.6

2nd Order Plot of the Consumption of 1,1,1-Trichloroethane over Condea CCl_4/γ-Alumina in the 20 mins. of the reaction.

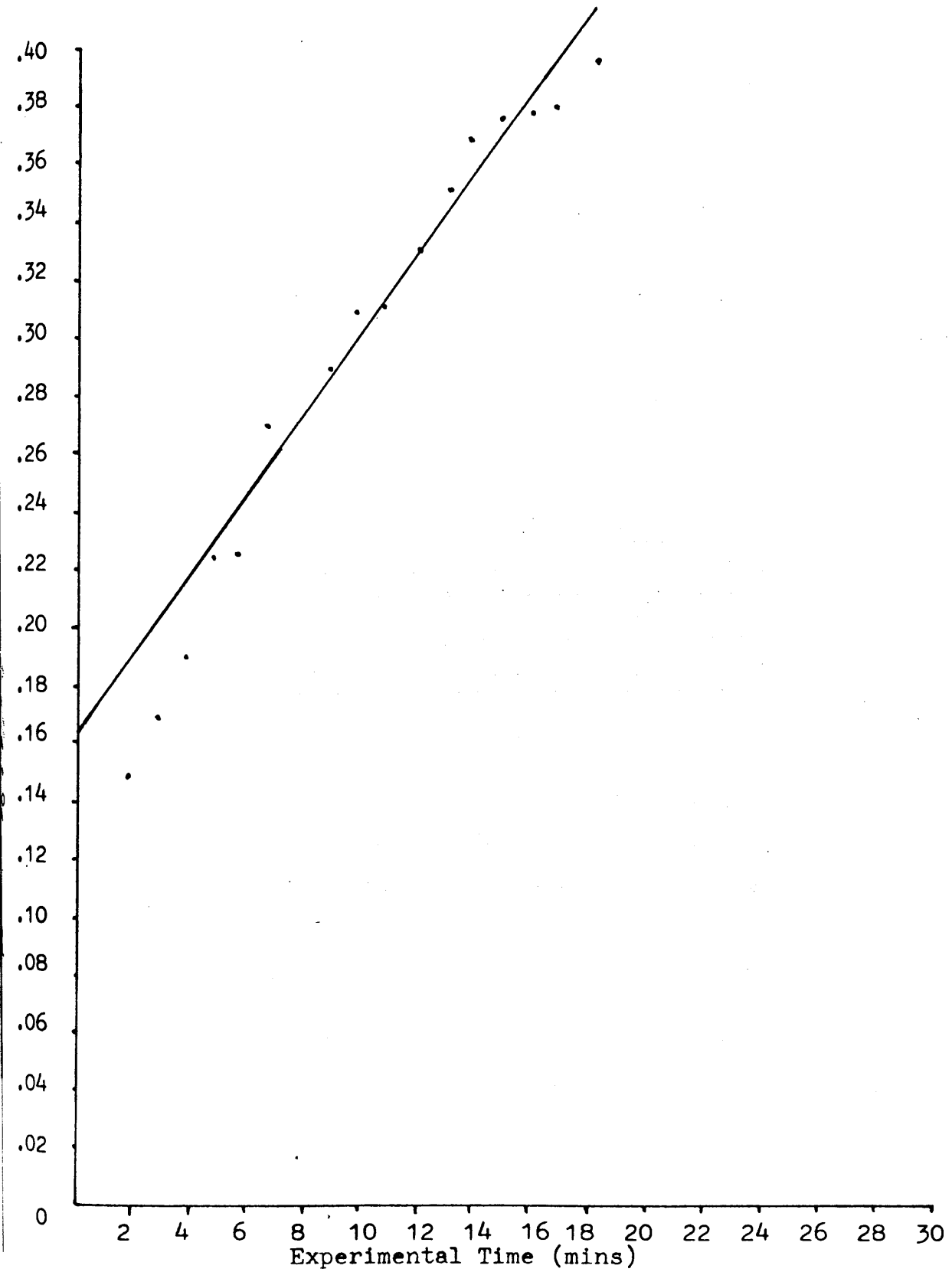

The first order plot from the results do not give a linear fit (Figure 5.5). A second order plot of the data (Figure 5.6, Table 5.2) gave a straight line with a correlation co-efficient of 0.9846, the deviation from the linefit for the results where t>18 min was due to the very small partial pressure of 1,1,1 trichloroethane in the system. From this study it was concluded that the decomposition of 1,1,1 trichloroethane with Condea γ-alumina calcined to 523K and treated with carbon tetrachloride was second order overall.

5.2.14 The Infrared Analysis of the Concentration with time of 1,1 Dichloroethene at 296K by the Dehydrochlorination of 1,1,1 Trichloroethane with Calcined Condea γ-Alumina treated with Carbon Tetrachloride.

The results from the above investigation are presented in table 5.3. The area under the absorbance at 1139 cm^{-1} was directly proportional to the partial pressure of the 1,1 dichloroethene in the system which was obtained from the appropriate correlation graph (Figure 2.7). The results are presented in table 5.3 for the partial pressure of 1,1 dichloroethene produced from the dehydrochlorination of 1,1,1 trichloroethane at time = t mins. Figure 5.7 shows schematically the relative pressures of 1,1,1 trichloroethane and 1,1 dichloroethene in the gas phase as a function of time. The production and depletion of 1,1 dichloroethene is shown in figure 5.8 with time during the dehydrochlorination

Table 5.3

Experimental Time (min)	Area under 1139 cm^{-1} peak (sq. units)	P. 1,1 Dichloro-ethene. (Torr)	1st Order $\log \frac{p_o}{p}$	2nd Order $\frac{p_o - p}{p_o \cdot p}$
3	12.9	4.428	0.646	0.226
5	12.19	3.972	0.599	0.252
8	11.86	3.761	0.575	0.266
10	11.58	3.581	0.554	0.279
13	11.29	3.395	0.531	0.294
16	11.11	3.279	0.516	0.305
18	10.92	3.157	0.499	0.317
21	10.70	3.016	0.479	0.332
31	10.09	2.625	0.419	0.381
44	9.39	2.143	0.331	0.467
57	8.89	1.855	0.268	0.539
81	8.07	1.328	0.123	0.753
105	7.50	0.962	0.016	1.040
137	7.02	0.655	0.183	1.527
165	6.63	0.404	0.394	2.475
188	6.38	0.244	0.613	4.098
217	6.14	0.090	1.045	11.111

p_o = the initial pressure

p = the pressure of 1,1 Dichloroethene @ time = t

Figure 5.7

Decomposition of 1,1,1-Trichloroethane and the Consumption of 1,1-Dichloroethene @ 296K over Condea CCl_4/γ-Alumina.

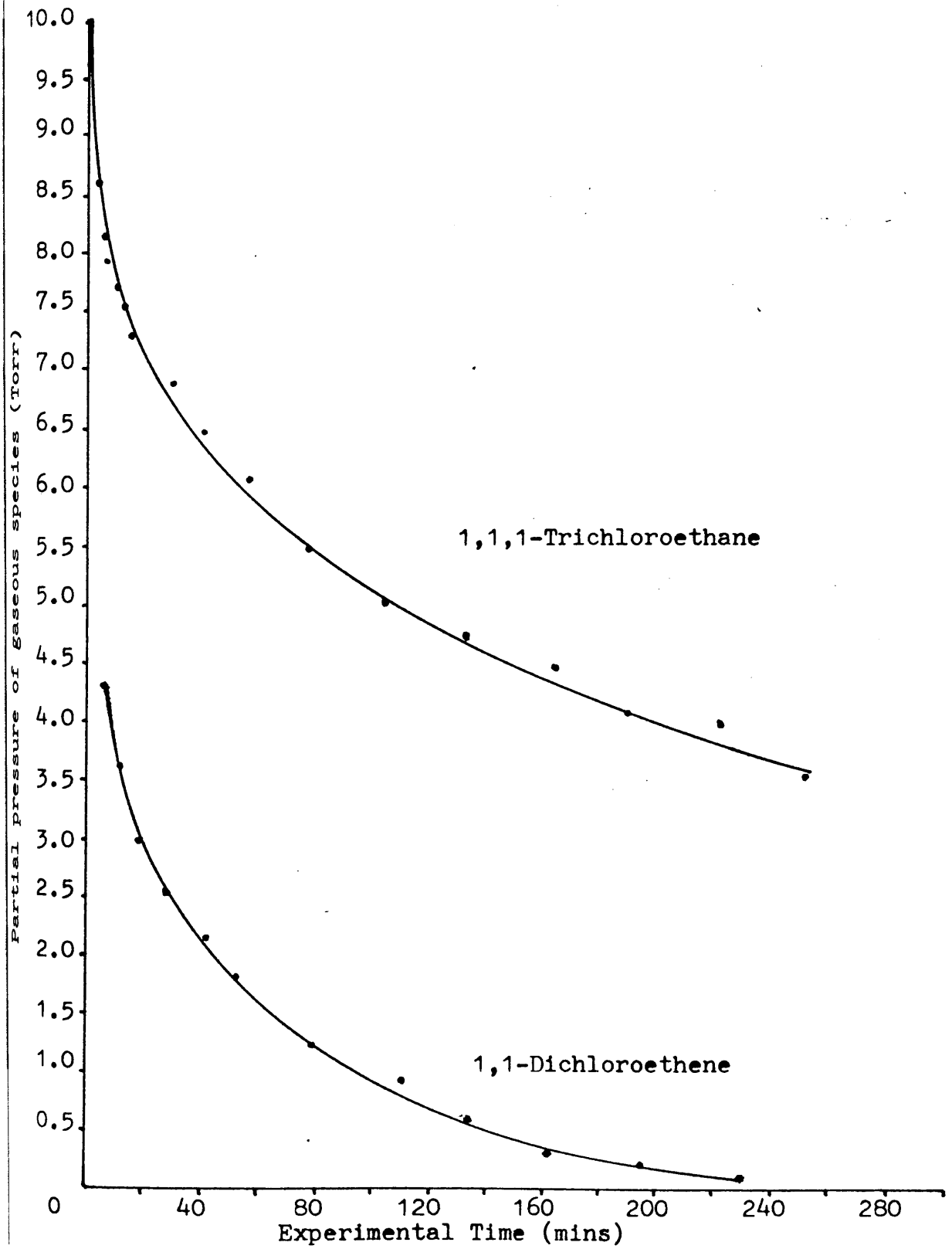

Figure 5. 8

Pressure of 1,1-Dichloroethene from the Dehydrochlorination of 1,1,1-Trichloroethane over Condea CCl_4/γ-Alumina as a function of time.

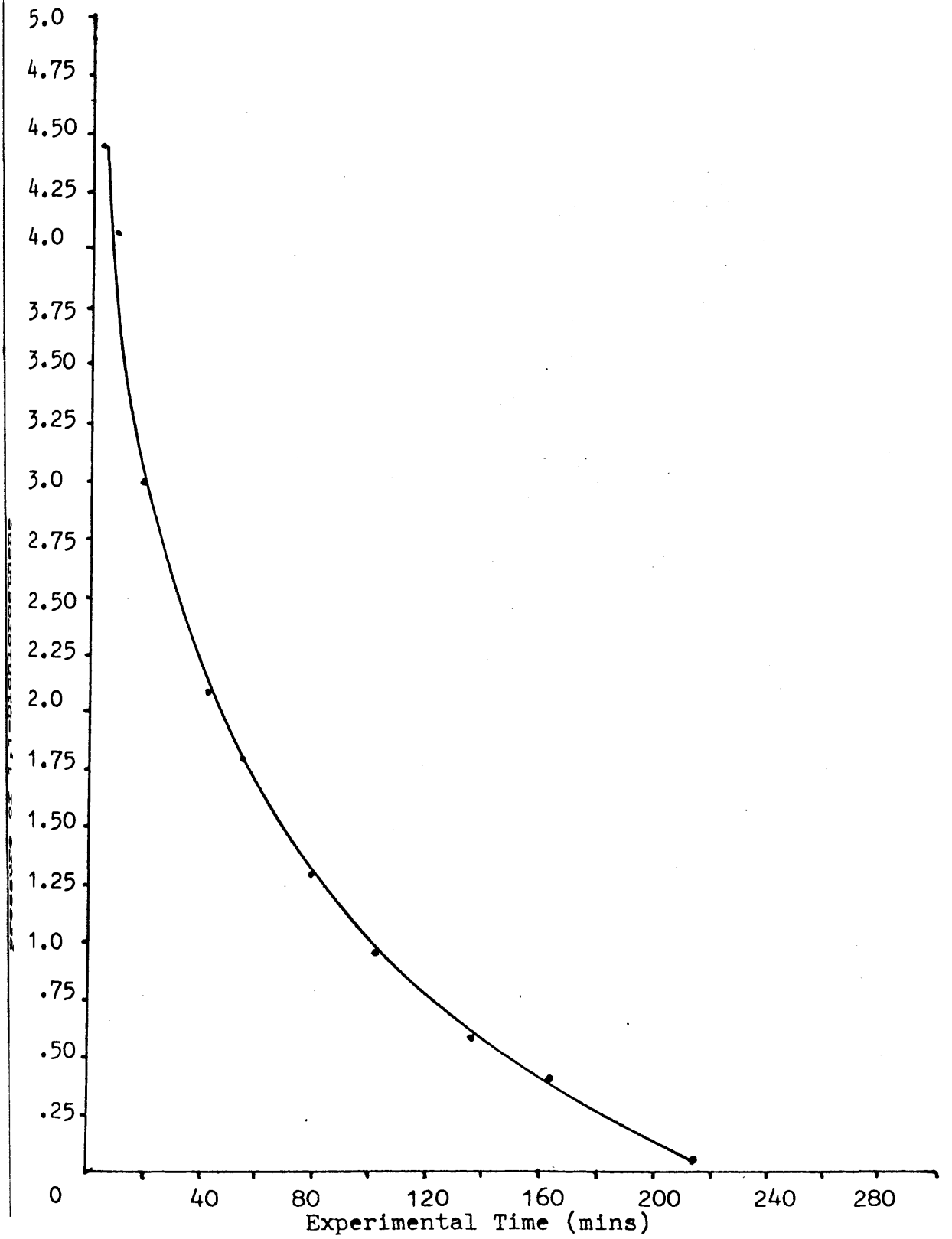

reaction.

A second order plot of the results presented in table 5.3 is shown schematically in figure 5.8a for the partial pressure of 1,1 dichloroethene at time = t min during the production and depletion of the 1,1 dichloroethene.

The second order plot was not linear and hence the rate of depletion of 1,1 dichloroethene was not considered to be second order. At pressures between 3.0 Torr and 0.70 Torr the depletion of 1,1 dichloroethene showed 1st order kinetics (Figure 5.9). However, at these low pressures the fraction of the surface covered would be proportional to the pressure of 1,1 dichloroethene and the rate of depletion would have first order dependence on the 1,1 dichloroethene pressure.

The second order plot of pressures of 1,1 dichloroethene > 3 Torr is shown in figure 5.10. The depletion of 1,1 dichloroethene at pressures > 3 Torr showed second order kinetics. The linefit for the data points gave a correlation coefficient of 0.9965 and a rate constant of 4.939×10^{-3} l $mol^{-1} min^{-1}$. The rate constant for the dehydrochlorination of 1,1,1 trichloroethane in the same study was 0.581×10^{-3} l $mol^{-1} min^{-1}$ (Section 5.2.14) which showed that the rate of depletion of 1,1 dichloroethene from the gas phase was greater than the rate of its formation from the dehydrochlorination reaction after the initial production of 1,1 dichloroethene in the first 3 mins of the exposure of 1,1,1 trichloroethane to the activated γ-alumina surface.

Absorbance bands due to the presence of hydrogen chloride at 2895 cm^{-1} in the gas phase were not observed

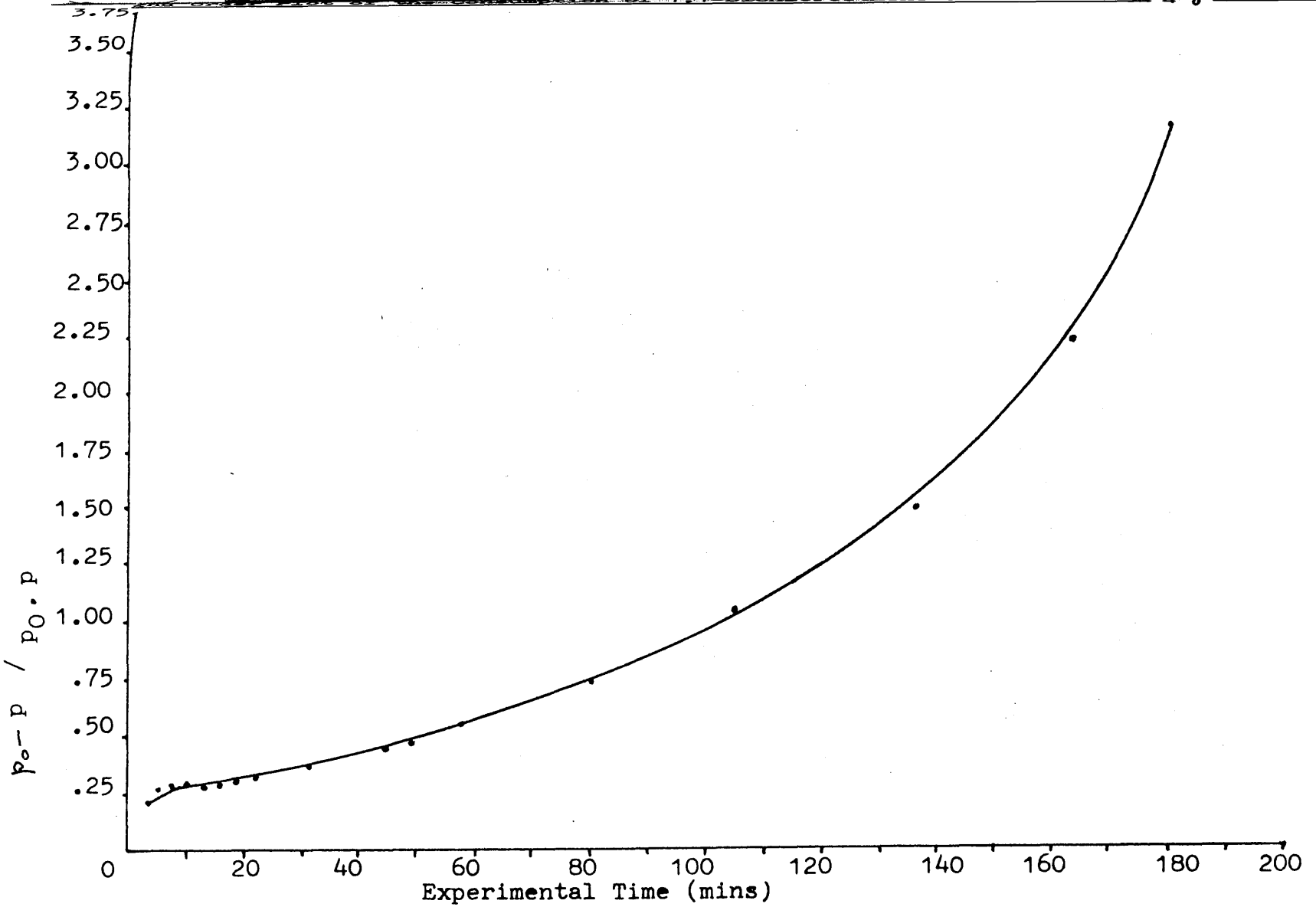
3.75
3.50
3.25
3.00
2.75
2.50
2.25
2.00
1.75
1.50
1.25
1.00
.75
.50
.25
0
20
40
60
80
100
120
140
160
180
200
$p_o - p \;/\; p_o \cdot p$
Experimental Time (mins)

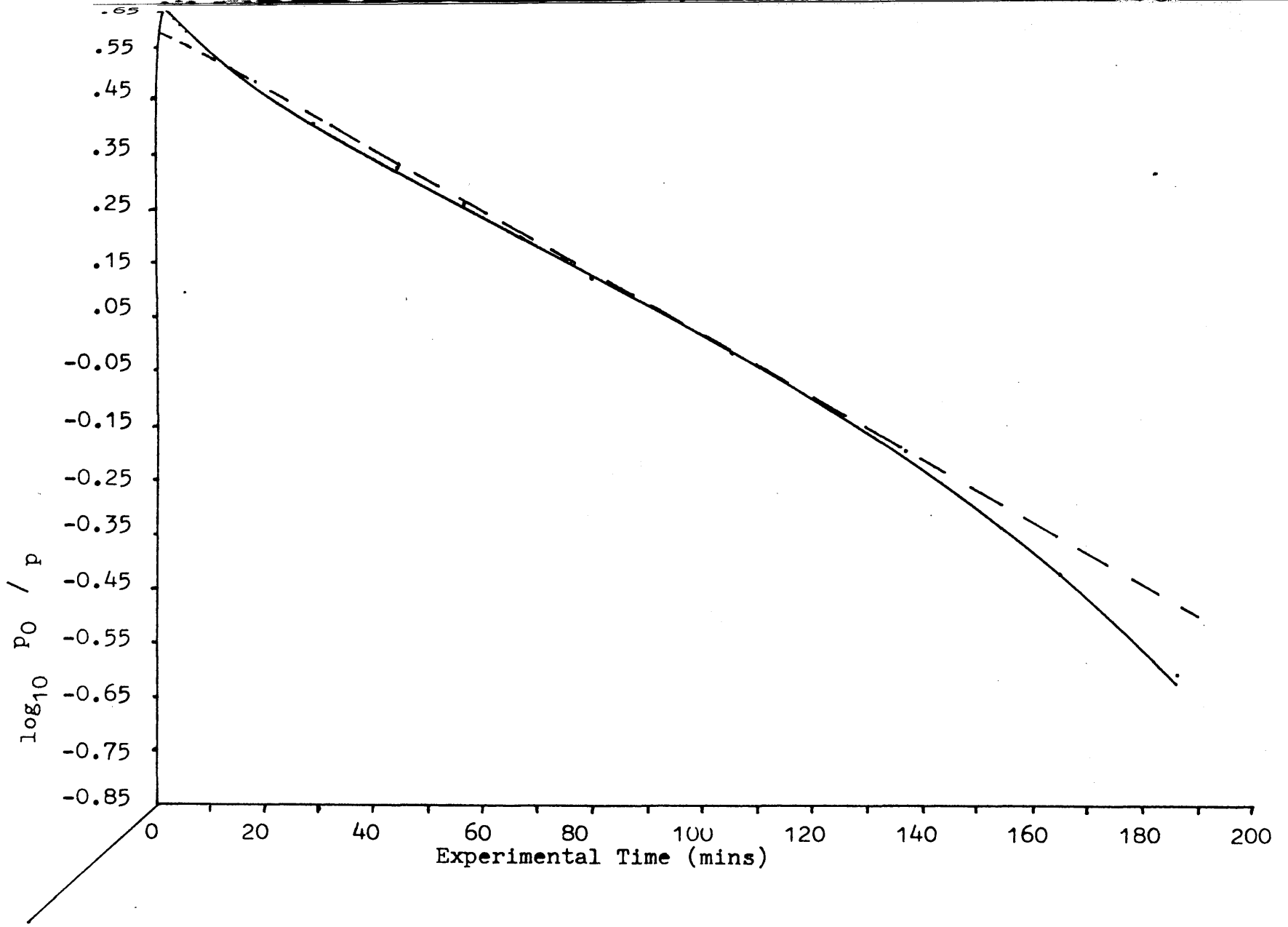
.65
.55
.45
.35
.25
.15
.05
-0.05
-0.15
-0.25
-0.35
-0.45
-0.55
-0.65
-0.75
-0.85
log10 p0 / p
0
20
40
60
80
100
120
140
160
180
200
Experimental Time (mins)

Figure 5.10

2nd Order Plot for pressure of 1,1-Dichloroethene less than 3 Torr over Condea CCl_4/γ-Alumina.

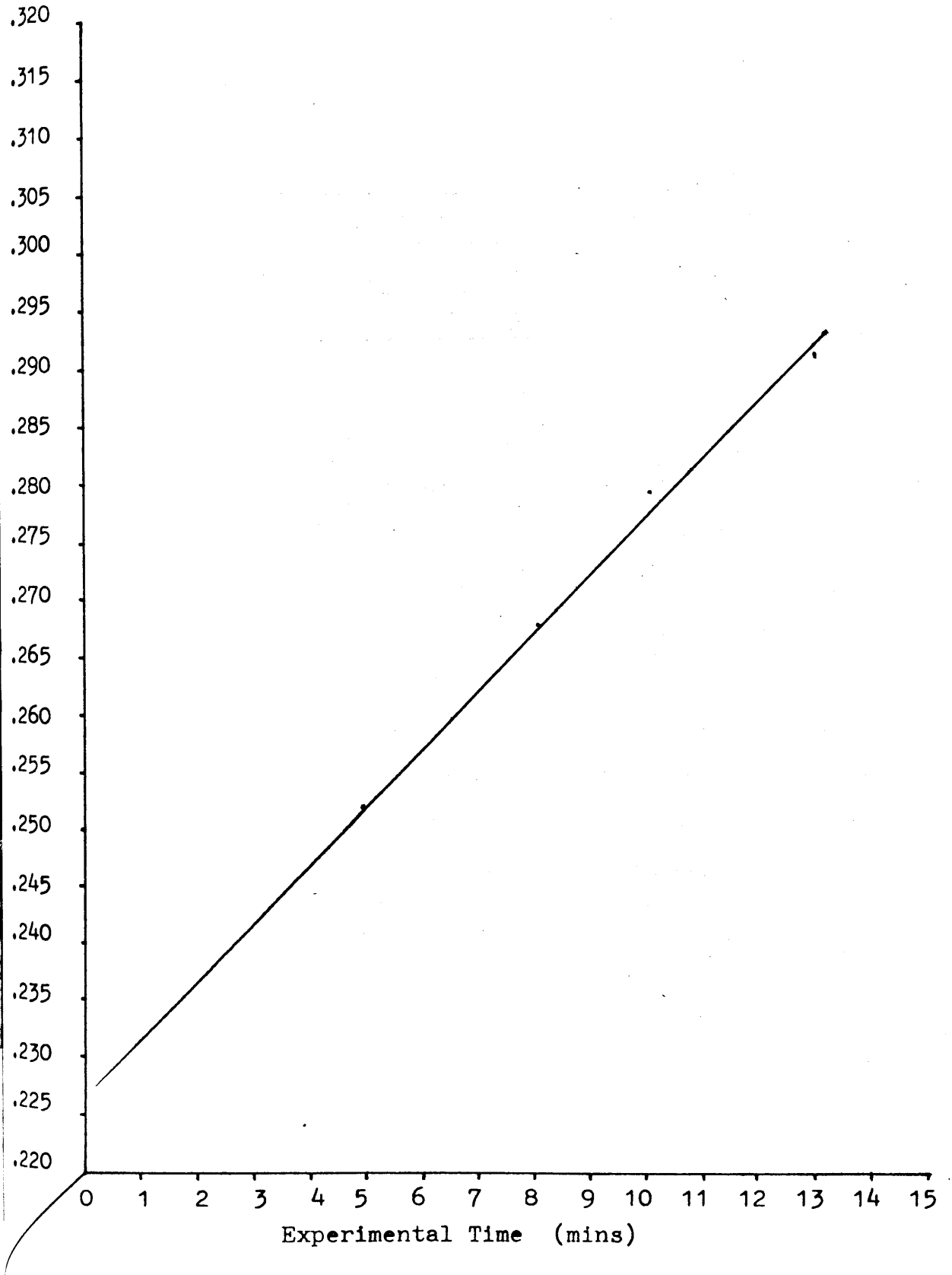

until 11 min into the reaction involving the dehydrochlorination of 1,1,1 trichloroethane owing to the small partial pressure of hydrogen chloride in the early stages of the reaction. The intensity of the hydrogen chloride band grew slowly over the period of 4h.

5.2.15 The Fourier Transform Infrared Investigation of the Dehydrochlorination of 1,1,1 Trichloroethane with Carbon Tetrachloride promoted Condea γ-Alumina treated with Deuterium Oxide.

The experimental procedure for the above investigation is described in section 5.3.14. The investigation by infrared analysis in section 5.2.14 showed that a small partial pressure of hydrogen chloride was observed after 11 min of the dehydrochlorination reaction with 1,1,1 trichloroethane. Figure 5.11 showed that after 27 min of the dehydrochlorination of 1,1,1 trichloroethane at 296K the Fourier Transform Infrared spectrum showed the absorbance at 2895 cm^{-1} due to the presence of hydrogen chloride in the gas phase. The absorbance at 2080 cm^{-1} was due to the presence of deuterium chloride in the gas phase. The source of the deuterium chloride was the surface of the Degussa 'C' treated γ-alumina. It was shown that proton species on the surface of the catalyst are labile.

Figure 5.11

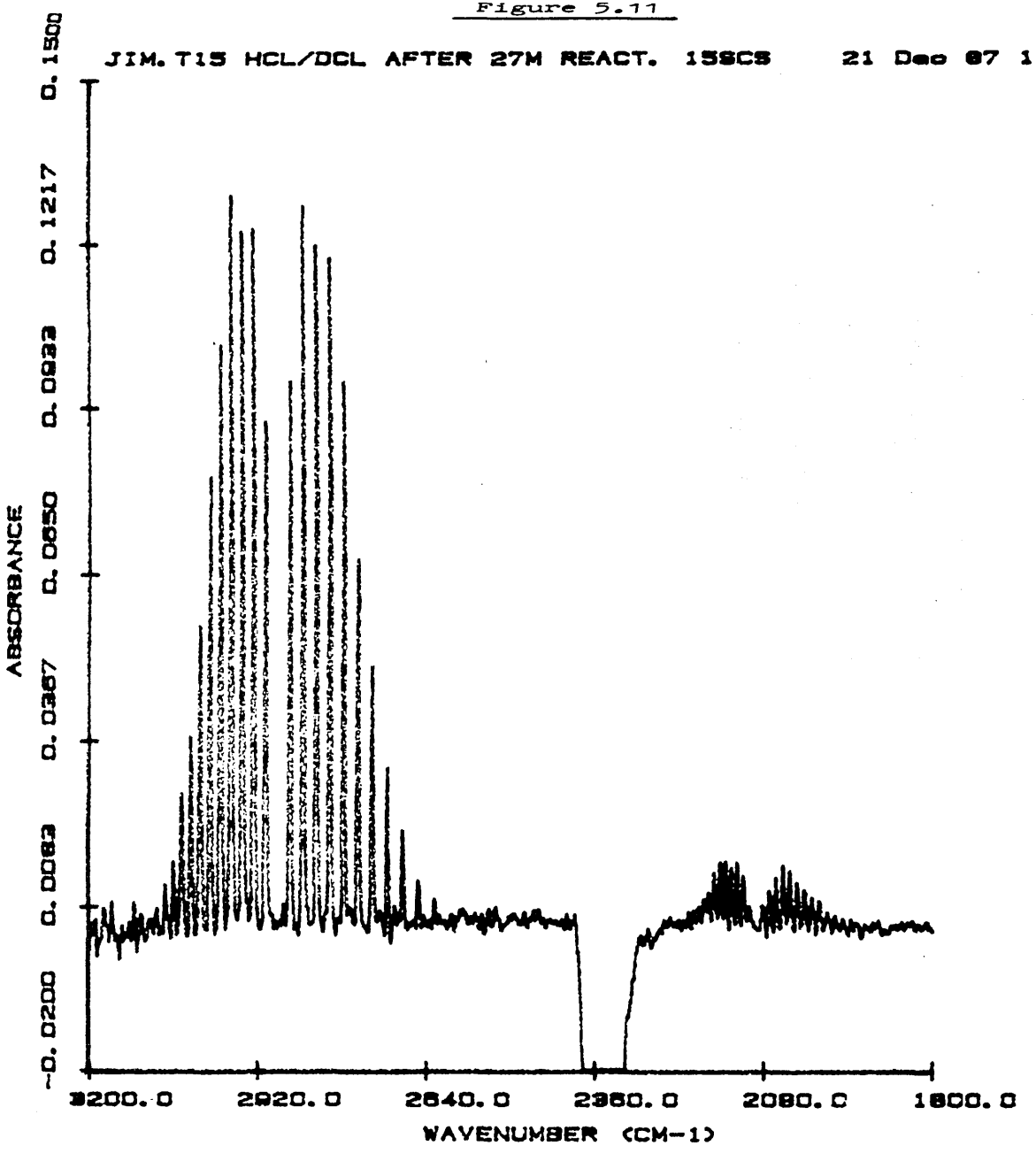
JIM.T15 HCL/DCL AFTER 27M REACT. 15SCS 21 Dec 87 14:00:34
ABSORBANCE
0.1500
0.1217
0.0933
0.0650
0.0367
0.0083
-0.0200
3200.0
2920.0
2640.0
2360.0
2080.0
1800.0
WAVENUMBER (CM-1)

5.2.16 Reaction of [^{36}Cl]-Chlorine labelled 1,1,1-Trichloroethane at 296K with Calcined Condea γ-Alumina previously treated with Carbon Tetrachloride.

The results of the above investigation are shown schematically in figure 5.12. The results showed that when [^{36}Cl]-chlorine labelled 1,1,1 trichloroethane was expanded into the counting cell which contained a sample of calcined Condea γ-alumina previously treated with carbon tetrachloride, a substantial increase in the surface count rate resulted. This rate of increase in the surface count rate slowed down after 97 min into the reaction. Figure 5.13 shows the total gas phase count rate with time. The results showed that the rate of depletion of the [^{36}Cl]-chlorine labelled 1,1,1 trichloroethane slowed down at 97 min into the reaction. The results were consistent with the deposition of labelled material from the gas phase which built up on the surface of the promoted γ-alumina sample. The product from the dehydrochlorination reaction of 1,1,1 trichloroethane, 1,1-dichloroethene, is known to polymerize on the surface of the chlorinated γ-alumina (Section 5.2.10) and the incorporation of a [^{36}Cl]-chlorine radiolabel into the 1,1 dichloroethene molecule would build up the surface count rate from the labelled polymer products. The production of [^{36}Cl]-chlorine labelled hydrogen chloride from the dehydrochlorination reaction of [^{36}Cl]-chlorine labelled 1,1,1 trichloroethane over the chlorine promoted γ-alumina sample would be available to exchange with labile surface chlorine to further increase the surface count rate.

Figure 5.12

Reaction of [^{36}Cl]-Chlorine labelled 1,1,1-Trichloroethane with Calcined Condea γ-Alumina treated with CCl_4.

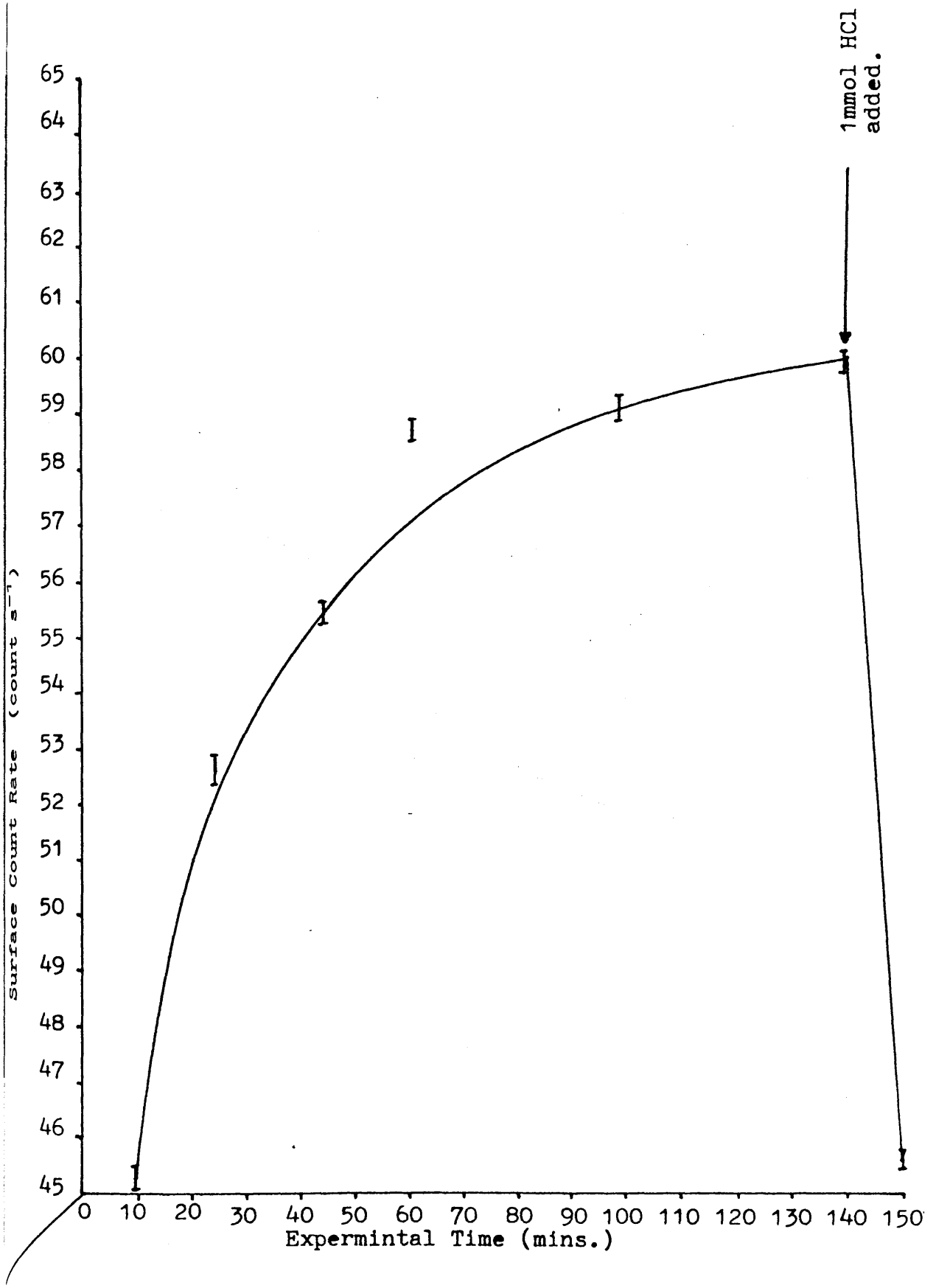

Figure 5.13

Total Gas Phase Count Rate from the dehydrochlorination of [^{36}Cl]-Chlorine labelled 1,1,1-Trichloroethane over CCl_4 treated Condea γ-Alumina.

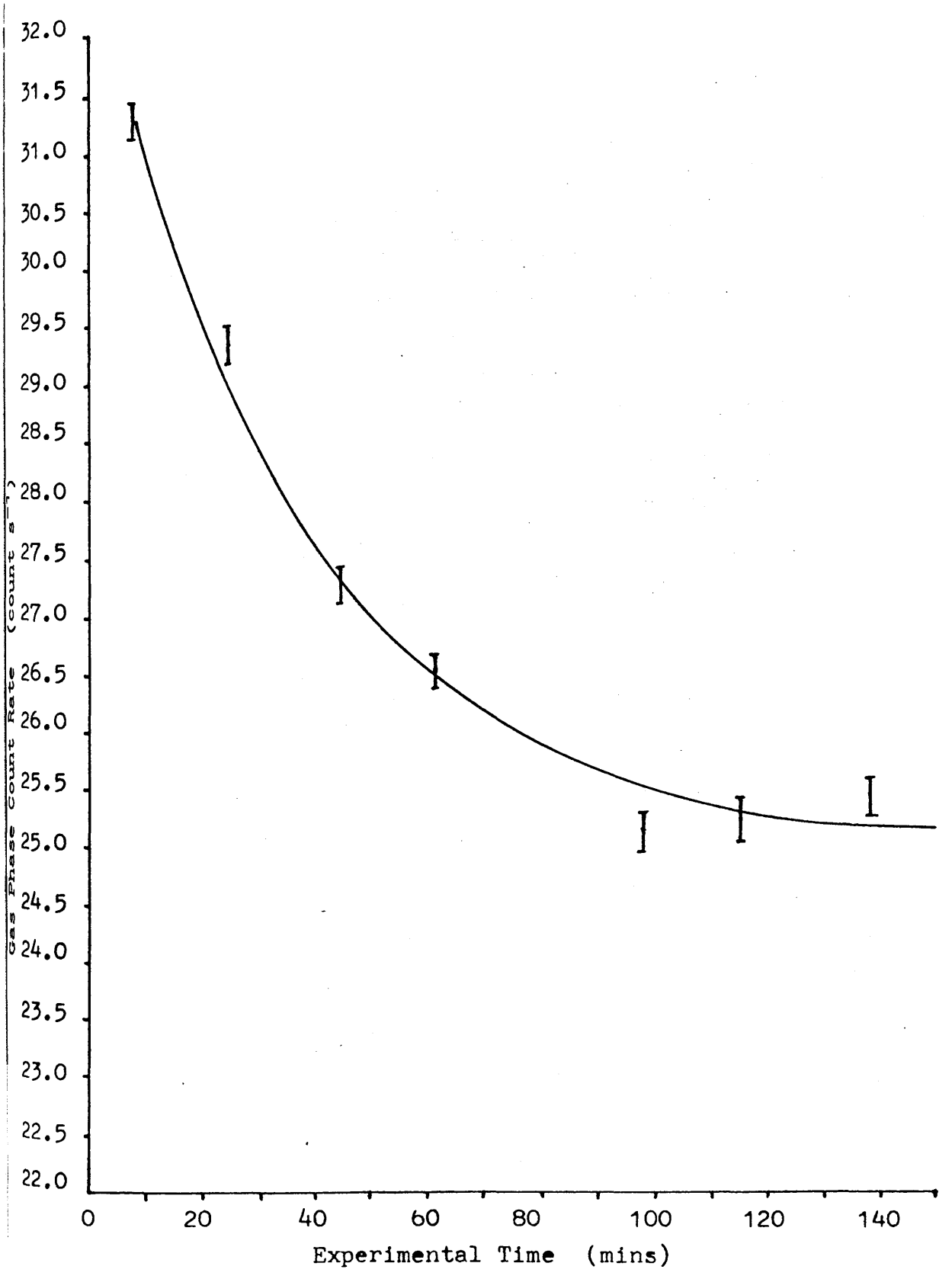

After 136 mins the solid sample was degassed and the exchange of the [^{36}Cl]-chlorine labelled surface with 1 mmol of anhydrous gaseous hydrogen chloride resulted in a 24.0% drop in the surface count rate.

5.2.17 Reaction of Uninhibited 1,1,1 Trichloroethane with Calcined Condea γ-Alumina treated with [^{36}Cl]-Chlorine labelled Carbon Tetrachloride.

The results of the above investigation are shown in figure 5.14 and figure 5.15.

The results from the surface activity had shown that when an aliquot of uninhibited 1,1,1 trichloroethane was expanded into the counting cell at 293K a drop in the surface activity resulted within the first 10 min of the reaction. This drop in the surface count rate was accompanied with an increase in the gas phase count rate (Figure 5.15). After this period of time the surface activity increased continuously through the following 5h of the investigation. The gas phase activity also increased slowly through the following 5h of the experiment. It was observed that the final surface activity of the solid was 31% greater than the initial surface activity observed at the start of the investigation. These results were reproducible using calcined Spence, and Degussa 'C' γ-alumina samples treated with [^{36}Cl]-chlorine labelled carbon tetrachloride.

Figure 5.14

Surface Count Rate from the Reaction of 1,1,1-Trichloroethane with Calcined Condea γ-Alumina treated with [^{36}Cl]-CCl_4

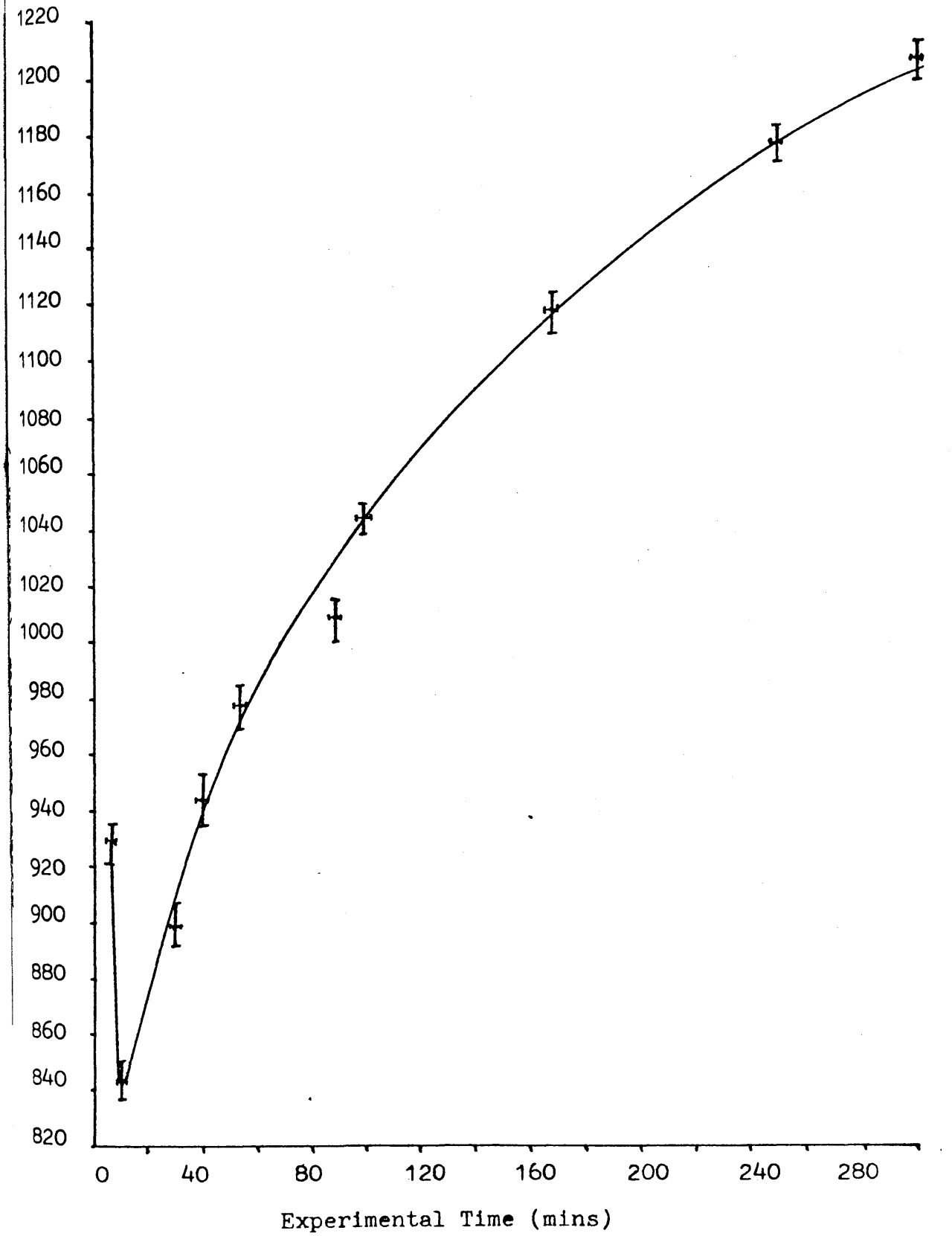

Figure 5.15

Gas Phase count rate from the reaction of 1,1,1-Trichloroethane with Calcined Condea γ-Alumina treated with [^{36}Cl]-CCl_4

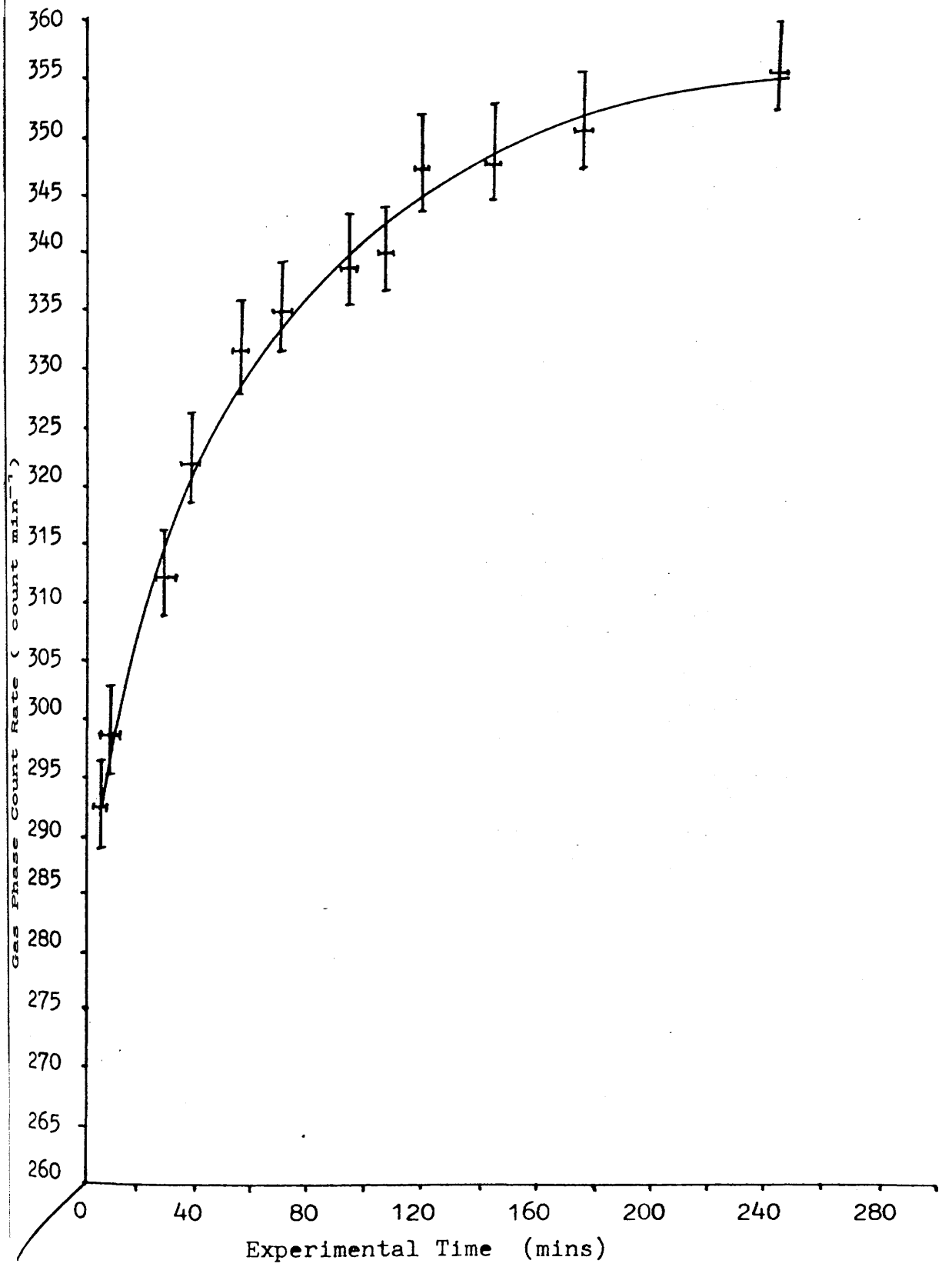

5.2.18 Reaction of Uninhibited 1,1,1 Trichloroethane with Calcined Condea γ-Alumina treated with Carbon Tetrachloride and [^{36}Cl]-Chlorine labelled Hydrogen Chloride Exchanged into the Solid.

The experimental procedure for the above investigation is described in section 5.3.17. The results of the surface activity with time are presented in figure 5.16 and the results of the gas phase activity are presented in figure 5.17.

When 1,1,1 trichloroethane (30.87 Torr; 2.24 mmol) was expanded into the counting cell at 293K a sharp reduction in the surface activity resulted in the first 10 min of the reaction (Figure 5.16). This reduction in the surface count rate was accompanied by an increase in gas phase count rate (Figure 5.17). The fall in the surface count rate gradually reduced with time over the 3h of investigation.

The activity that was removed from the surface was transferred into gas phase activity (Figure 5.17).

The reduction in the surface activity within the first 10 min of the reaction was observed as in the case of the dehydrochlorination reaction with [^{36}Cl]-chlorine labelled carbon tetrachloride (Section 5.2.17).

5.2.19 Reaction of 1,1,1 Trichloroethane at 296K with Calcined Degussa 'C' γ-Alumina treated with [^{36}Cl]-Chlorine labelled Carbon Tetrachloride followed by Anhydrous Gaseous Hydrogen Chloride.

The experimental procedure for the above investigation is described in section 5.3.18, and the results are presented

Figure 5.16

Surface Count Rate from $H^{36}Cl$ impregnated Calcined Degussa 'C' γ-Alumina treated with CCl_4 and reacted with 1,1,1-Trichloroethane.

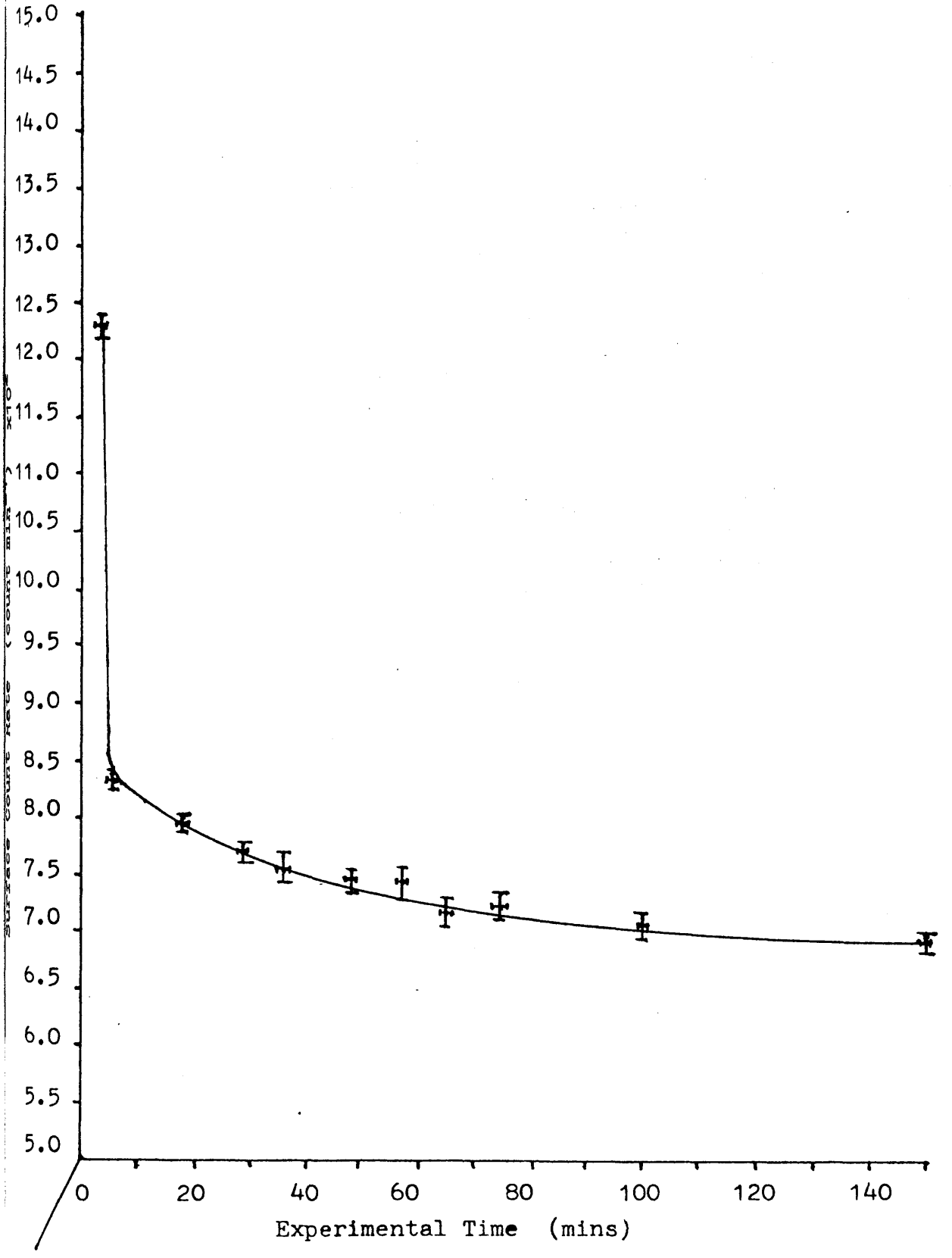

Figure 5.17

Gas Phase Count Rate of Reaction of 1,1,1-Trichloroethane with Degussa 'C' CCl_4/γ-Alumina and $H^{36}Cl$ exchanged into labile surface chlorine.

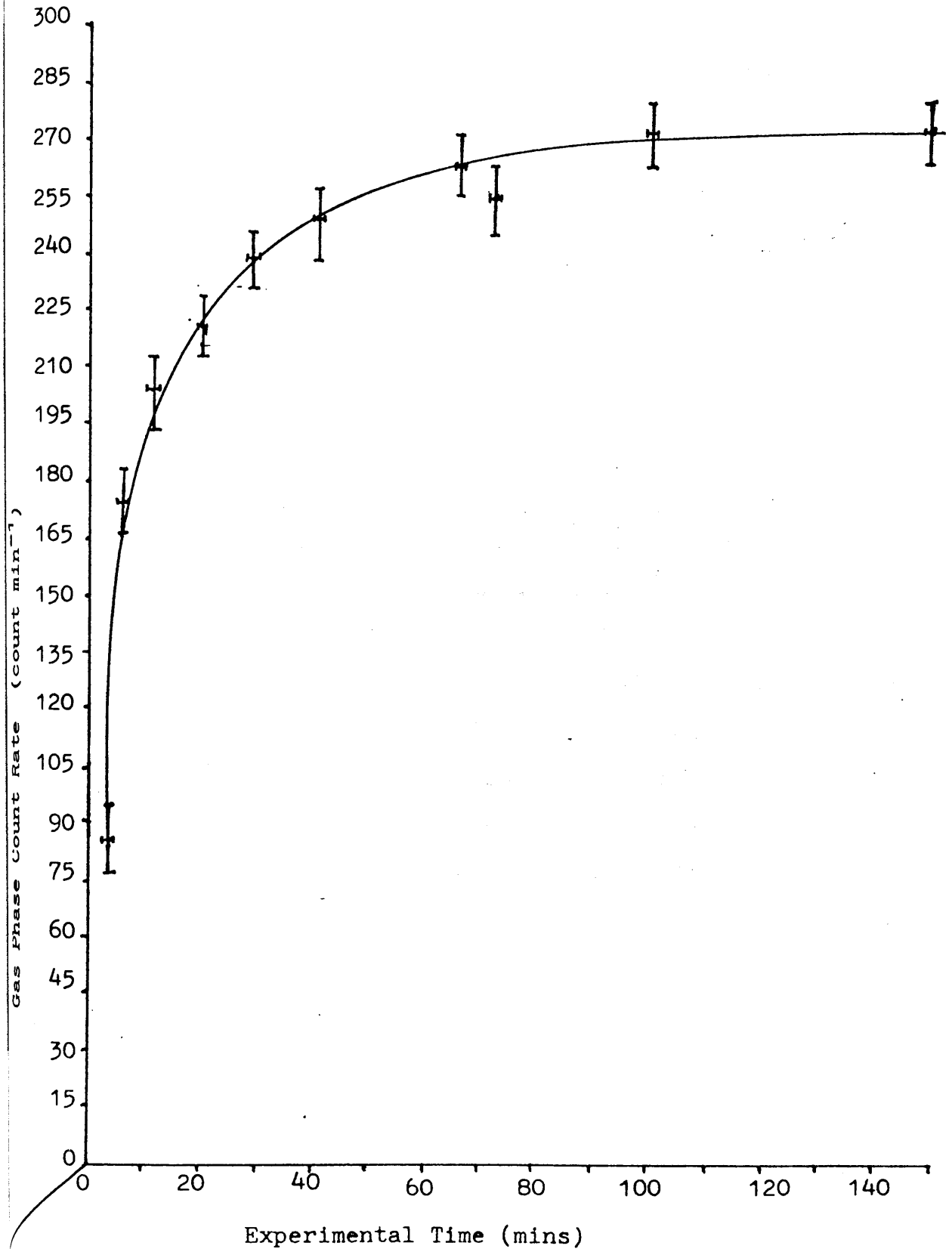

schematically in figure 5.18. The labile [^{36}Cl]-chlorine species from the [^{36}Cl]-chlorine labelled carbon tetrachloride treatment was exchanged out with eight aliquots of anhydrous gaseous hydrogen chloride (13.8 Torr; 1mmol) which left the [^{36}Cl]-chlorine label on the non-exchangeable chlorine site. The sample was degassed prior to the expansion of 1,1,1 trichloroethane (30.87 Torr; 2.2mmol) into the counting cell. There was no change in the surface count rate (Figure 5.18) or the gas phase count rate with time, which indicated that the [^{36}Cl]-chlorine on the surface of the γ-alumina was not removed during the dehydrochlorination of 1,1,1 trichloroethane.

5.3 EXPERIMENTAL

5.3.1 Determination of the Reaction Conditions Required for the Thermolytic Dehydrochlorination of 1,1,1 Trichloroethane with Calcined Spence γ-Alumina.

Spence γ-alumina (0.5234g; 3.97 mmol) was loaded in the dry box into a thick walled vacuum vessel. The vacuum vessel was transferred to a vacuum line, fitted with an infrared gas cell and degassed. The vacuum vessel was cooled to 77K and 1,1,1 trichloroethane (134.1 Torr; 3 mmol) was condensed into the vessel, which was then fitted with an electrical furnace and thermocouple. The contents of the vacuum vessel were allowed to warm to room temperature and were left to stand for 1h. Gaseous material was expanded into a manifold containing a gas cell and a gas phase i.r. spectrum obtained at 80 Torr. This procedure was repeated at 310K and at increments of 10K until 1,1 dichloroethene and hydrogen chloride were identified as gas phase products.

Figure 5.18

Dehydrochlorination of 1,1,1-Trichloroethane with Calcined Degussa 'C' γ-Alumina treated with $[^{36}Cl]$-CCl_4 with labile surface chlorine exchanged out with anhydrous Hydrogen Chloride.

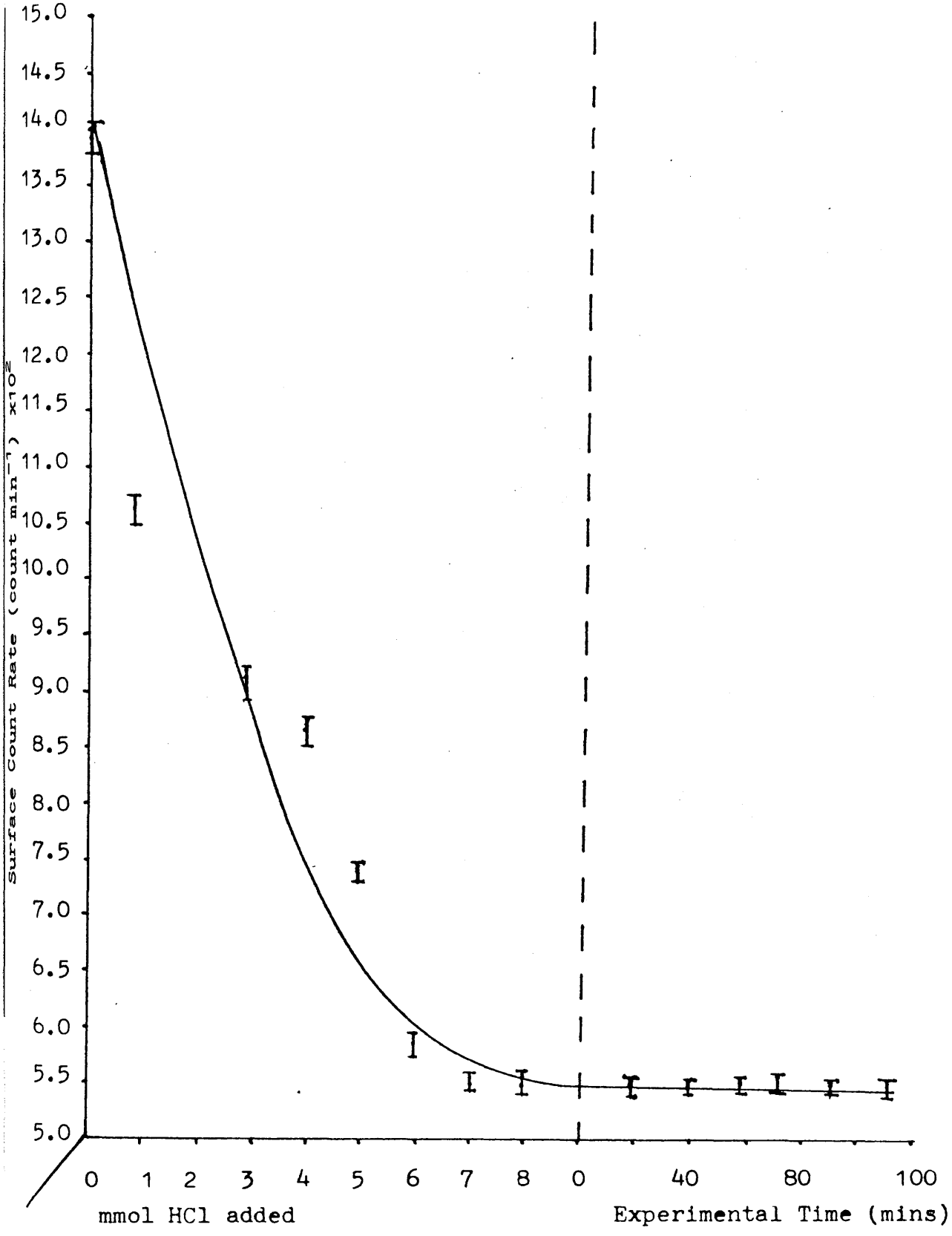

The infrared bands due to the presence of 1,1,1 trichloroethane and 1,1 dichloroethene were checked against calibration spectra that were run from pure standard samples of the respective compound. The bands obtained from the infrared spectra are listed (Table 2A; Section 2.3.3) and the calibration spectra are presented in figures 2.6 and 2.7 respectively.

5.3.2 Reaction of 1,1,1 Trichloroethane over Calcined Condea γ-Alumina treated with Anhydrous Hydrogen Chloride at 293K.

A sample of Condea γ-alumina (0.5197g; 3.93 mmol) was reacted with anhydrous hydrogen chloride (89.4 Torr; 2 mmol) for 90 mins at 293K. The solid sample was degassed by pumping prior to a sample of degassed dry 1,1,1 trichloroethane (90 Torr; 2.01 mmol) being condensed into the reaction vessel held at 77K. The system was allowed to warm up to 293K and left to react for 2h. The gas products were expanded into an infrared gas cell and a spectra obtained.

5.3.3 Reaction of 1,1,1 Trichloroethane with Calcined Degussa 'C' γ-Alumina treated with [^{36}Cl]-Chlorine labelled Anhydrous Gaseous Hydrogen Chloride.

A sample of Degussa 'C' γ-alumina (0.5536; 4.20 mmol) calcined to 523K was loaded into a dry dropping vessel in the dry box and was degassed by pumping prior to being fitted to the dry counting cell (Figure 2.11) The solid sample was dropped into the boat and manouvered under Geiger-Müller tube

No.2. An aliquot of anhydrous gaseous [^{36}Cl]-chlorine labelled hydrogen chloride (27.6 Torr; 2 mmol) was admitted into the counting cell and allowed to react with the calcined solid for 1h. The solid sample was degassed by pumping prior to expanding 1,1,1 trichloroethane (38 Torr; 2.75 mmol) into the counting cell at 293K. The surface activity and the gas phase activity were monitored for 2h.

5.3.4 Reaction of 1,1,1 Trichloroethane at 293K with Calcined Condea γ-Alumina treated with Anhydrous Gaseous Carbon Tetrachloride.

A sample of Condea γ-alumina (0.3271g; 2.47 mmol) was calcined to 523K and treated with anhydrous gaseous carbon tetrachloride. The solid sample was degassed by pumping. The carbon tetrachloride treated Condea γ-alumina was transferred in the dry box to a dry vacuum vessel prior to being transferred to a vacuum line which was fitted with an infrared gas cell. The vacuum vessel was cooled to 77K and an aliquot of 1,1,1 trichloroethane (100 Torr; 2.23 mmol) was condensed into the vacuum vessel. The vessel was warmed up to ambient temperatures and the system was reacted for 2h. The gas phase products were expanded into the manifold of the vacuum line and the infrared gas cell to a pressure of 80 Torr. The contents of the gas cell were analysed by infrared using a Perkin-Elmer 983 Grating Infrared Spectrometer.

5.3.5 Reaction of 1,1,1 Trichloroethane with Calcined Degussa 'C' γ-Alumina treated with 1,1 Dichloromethanone at 293K.

A sample of Degussa 'C' γ-Alumina (0.4793g; 3.63 mmol) was treated with an aliquot of 1,1 dichloromethanone (89.4 Torr; 2 mmol) at 293K as described in section 4.3.14.

After the treated sample was degassed by pumping an aliquot of uninhibited 1,1,1 trichloroethane (44.7 Torr; 1 mmol) was condensed into the vacuum vessel containing the phosgene treated Degussa 'C' γ-alumina which was held at 77K. The system was allowed to warm up to ambient temperature (293K) and the gaseous 1,1,1 trichloroethane contacted with the calcined phosgene treated Degussa 'C' γ-alumina sample for 1h. The gas phase was expanded into the manifold of the vacuum line which was fitted with an infrared gas cell to a pressure of 30 Torr. The gas phase contents were analysed by infrared using a Perkin-Elmer 983 Grating Infrared Spectrometer.

5.3.6 Reaction of 1,1,1 Trichloroethane with Calcined Degussa 'C' γ-Alumina treated with 1,1 dichloro-methanone at 500K.

A sample of Degussa 'C' γ-alumina (0.5271g; 3.99 mmol) was calcined to 523K and transferred in the dry box to a dry vacuum vessel. The treatment of the calcined γ-alumina sample with phosgene (89.4 Torr; 2 mmol) at 500K is described in section 4.3.15.

After the treatment of the solid by phosgene the

solid was degassed prior to condensing an aliquot of 1,1,1-trichloroethane (89.4 Torr; 2mmol) into the vacuum vessel at 77K. The system was warmed up to room temperature. The gaseous 1,1,1 trichloroethane was contacted with the calcined γ-alumina surface for 40 min. The gas phase was then expanded into the manifold of the vacuum line which was fitted with a gas cell to a pressure of 80 Torr. The contents of the gas cell were then analysed by infrared to identify the gaseous products using a Perkin - Elmer 577 Grating Infrared Spectrometer.

5.3.7 Reaction of 1,1 Dichloroethene and Anhydrous Gaseous Hydrogen Chloride at 296K Under Glass.

An aliquot of uninhibited 1,1 dichloroethene (100 Torr; 2.23 mmol) was condensed into a dry thick walled vacuum vessel which was held at 77K followed by an aliquot of anhydrous gaseous hydrogen chloride (100 Torr; 2.23 mmol). The system was warmed up to room temperature in the dark and left to interact for 24h. The gases were expanded into a dry manifold of the vacuum line which was fitted with an infrared gas cell to a pressure of 80 Torr. The gas cell was transferred to a Perkin - Elmer 577 Grating Infrared Spectrometer where the gas contents were analysed by infrared to identify the gas compounds.

5.3.8 Reaction of 1,1 Dichloroethene with Calcined Condea γ-Alumina treated with Anhydrous Gaseous Hydrogen Chloride.

A sample of Condea γ-alumina (0.5491g; 4.16 mmol) was treated with anhydrous gaseous hydrogen chloride using the procedure described in section 3.3.3.

After the sample had been treated with anhydrous hydrogen chloride (89.4 Torr; 2 mmol) for 180 min the solid sample was degassed by pumping. An aliquot of 1,1 dichloroethene (100 Torr; 2.23 mmol) was condensed into the vacuum vessel containing the treated γ-alumina sample, and warmed to room temperature and left to interact for 2h. The gas phase from the vacuum vessel was expanded into the manifold of the vacuum line which was fitted with an infrared gas cell to a pressure of 80 Torr. The gas contents of the infrared gas cell were analysed by infrared using a Perkin - Elmer 577 Grating Infrared Spectrometer.

5.3.9 Reaction of 1,1 Dichloroethene with Calcined Degussa 'C' γ-Alumina treated with Anhydrous Gaseous [^{36}Cl]-Chlorine labelled Hydrogen Chloride.

The experimental procedure for the treatment of Degussa 'C' γ-alumina (0.5536g; 4.20 mmol) calcined to 523K with anhydrous gaseous [^{36}Cl]-chlorine labelled hydrogen chloride (27.6 Torr; 2 mmol) is described in section 3.3.3. The treated γ-alumina sample was degassed by pumping and an aliquot of uninhibited 1,1 dichloroethene (13.8 Torr; 1 mmol) was expanded into the counting cell at 293K. The surface activity of the solid was monitored over a period of 104 min.

5.3.10 Reaction of 1,1 Dichloroethene with Calcined Condea γ-Alumina treated with Anhydrous Gaseous Carbon Tetrachloride.

A sample of Condea γ-alumina (0.5043g; 3.82 mmol) calcined to 523K was treated with an aliquot of anhydrous gaseous carbon tetrachloride (96.8 Torr; 2.17 mmol) as described in section 4.3.5, and transferred to a dry thick walled vacuum vessel in the dry box. After degassing the solid,an aliquot of 1,1 dichloroethene (44.7 Torr; 1 mmol) was condensed into the vacuum vessel held at 77K. The system was warmed up to room temperature and allowed to stand for 24h. The gas phase contents were expanded into the manifold of the vacuum line fitted with an infrared gas cell to a pressure of 50 Torr. The gas contents of the gas cell were analysed by infrared using a Perkin - Elmer 983 Grating Infrared Spectrometer.

5.3.11 Reaction of 1,1 Dichloroethene and Anhydrous Gaseous Hydrogen Chloride with Calcined Degussa 'C' γ-Alumina treated with Anhydrous Gaseous Carbon Tetrachloride.

A sample of Degussa 'C' γ-alumina (0.4291g; 3.25 mmol) was calcined to 523K and treated with carbon tetrachloride (89.4 Torr: 2 mmol). After the chlorination treatment the sample was degassed for 1h prior to its transfer to a dry thick walled vacuum vessel in the dry box. The vacuum vessel was transferred to a vacuum line fitted with an infrared gas cell. An aliquot of uninhibited 1,1 dichloroethene (49.7 Torr; 1 mmol) was condensed into the vacuum

vessel containing the chlorinated calcined γ-alumina sample held at 77K followed by an aliquot of anhydrous gaseous hydrogen chloride (44.7 Torr; 1 mmol). The contents of the vacuum vessel were warmed up to room temperature and reacted for 4h. The gas phase from the vacuum vessel was expanded into the manifold of the vacuum line and the infrared gas cell to a pressure of 50 Torr. The gas contents of the gas cell were analysed by infrared using a Perkin - Elmer 577 Grating Infrared Spectrometer.

5.3.12 Infrared Analysis of the Decomposition of 1,1,1 Trichloroethane at 296K with Calcined Condea γ-Alumina treated with Anhydrous Gaseous Carbon Tetrachloride.

The investigation of the rate of dehydrochlorination of 1,1,1 trichloroethane by the carbon tetrachloride treated γ-alumina sample was carried out using an 'in situ' infrared gas cell (Figure 2.5) from which a background infrared spectrum was collected and stored using a Perkin - Elmer 983 Grating Infrared Spectrometer connected to a workstation. The infrared spectrum was stored on a disk for reprocessing. A dry dropping vessel containing a small sample of calcined Condea γ-alumina treated with carbon tetrachloride (0.25g), and a sample of 1,1,1 trichloroethane (15 Torr) was reacted in the infrared gas cell. The reaction was carried out at room temperature.

The rate of dehydrochlorination of 1,1,1 trichloroethane was monitored by scanning the region 800 cm^{-1} to 700 cm^{-1} in order to observe the absorbance band at 720 cm^{-1} which was

specific for the 1,1,1 trichloroethane in that region (Section 2.3.3; Table 2A). The infrared scans were made every 59s in the first 25 min of the reaction followed by scanning every 5 min for the following 35 min and every 15 min for the following 3h. The scanned spectra were stored on disk for reprocessing. The reprocessing involved the removal of the background infrared signal from the blank gas cell and integrating the area under the 720 cm^{-1} peak for each infrared scan. The area under the 720 cm^{-1} peak is directly proportional to the partial pressure of 1,1,1 trichloroethane in the gas cell which was evaluated using the calibrating graph of the integrated area under the 720 cm^{-1} peak as a function of the pressure of 1,1,1 trichloroethane (Figure 2.6; Section 2.3.3).

The rate of dehydrochlorination of 1,1,1 trichloroethane was calculated by applying the method of empirical fit where the data was substituted into each of the rate laws in turn to find a straight line fit with time. The rate constant for the reaction was obtained from the slope of the plot which gave a straight line fit.

5.3.13 Infrared Analysis of the Concentration of 1,1 Dichloroethene at 296K with Calcined Condea γ-Alumina treated with Anhydrous Carbon Tetrachloride.

The experimental procedure was the same as that described for the infrared analysis of the decomposition of 1,1,1 trichloroethane that is described in section 5.3.12. This investigation was run in conjunction with the experiment

described in section 5.3.12, by scanning the region 1200 cm^{-1} to 1000 cm^{-1}. The concentration of 1,1 dichloroethene was analysed by observing the absorbance of the 1139 cm^{-1} which was specific to 1,1 dichloroethene (Section 2.3.3; Table 2.4) among the absorbances obtained from the presence of the gas phase contents of the infrared gas cell.

5.3.14 The Fourier Transform Infrared Investigation of the Dehydrochlorination of 1,1,1 Trichloroethane at 293K with Calcined Condea γ-Alumina treated with Carbon Tetrachloride.

A sample of Degussa 'C' γ-alumina (0.4792g; 3.63 mmol) was treated with Analar Deuterium Oxide (1ml; 0.056 mol) by the procedure described in section 4.3.13, and calcined at 523K. The sample was treated with anhydrous gaseous carbon tetrachloride by the procedure described in section 4.3.13. After the treatment with carbon tetrachloride the sample was degassed by pumping. The treated Degussa 'C' sample was transferred to a small dropping vessel and fitted to the infrared gas cell described in section 5.3.12 (Figure 2.5), and was evacuated prior to the expansion of uninhibited 1,1,1 trichloroethane to a pressure of 10 Torr into the gas cell. The infrared gas cell was fitted to a Nicolet 5DXC Fourier Transform Infrared Spectrometer. The decomposition of 1,1,1 trichloroethane was carried out with the Deuterium Oxide treated Degussa 'C' γ-alumina calcined to 523K and treated with carbon tetrachloride. The investigation of the dehydrochlorination of 1,1,1 trichloroethane with activated calcined γ-alumina (Section 5.2.14) had shown small

amounts of hydrogen chloride being generated. The purpose of this investigation was to see if the gas phase hydrogen chloride generated from the dehydrochlorination of 1,1,1-trichloroethane was available for exchange with the surface chlorine species as the results from section 4.2.9 had indicated.

5.3.15 Reaction of [^{36}Cl]-Chlorine labelled 1,1,1 Trichloroethane at 296K with Calcined Condea γ-Alumina treated with Carbon Tetrachloride.

A sample of Condea γ-alumina (0.5217g; 3.95 mmol) was calcined to 523K and treated with anhydrous gaseous carbon tetrachloride (89.4 Torr; 2 mmol) as described in section 4.3.5. The sample was degassed by pumping and transferred to the counting cell. An aliquot of [^{36}Cl]-chlorine labelled 1,1,1 trichloroethane (13.95 Torr; 1.08 mmol) (Section 2.2.4) was expanded into the counting cell. The gas phase and surface count rate was monitored with time. After the investigation had been carried out the sample was degassed prior to the expansion of anhydrous gaseous hydrogen chloride (13.80 Torr; 1 mmol) into the counting cell and exchanged with the solid at 296K. The final surface count rate was recorded after the exchange equilibrium had been established.

5.3.16 Reaction of Uninhibited 1,1,1 Trichloroethane with Calcined Condea γ-Alumina treated with [^{36}Cl]-Chlorine labelled Carbon Tetrachloride.

A sample of Condea γ-alumina (0.5961g; 4.51 mmol) was calcined at 523K, transferred to the counting cell and treated with [^{36}Cl]-chlorine labelled carbon tetrachloride (Section 4.3.10) after which the gas products were analysed by infrared for the production of phosgene, carbon dioxide and hydrogen chloride to ensure that chlorination of the solid had occurred. The solid was degassed by pumping prior to the expansion of uninhibited 1,1,1 trichloroethane (13.8 Torr; 1.00 mmol) into the counting cell. The gas phase and the solid count rates were monitored with time.

5.3.17 Reaction of Uninhibited 1,1,1 Trichloroethane with Calcined Degussa 'C' γ-Alumina treated with Carbon Tetrachloride and [^{36}Cl]-Chlorine labelled Hydrogen Chloride.

A sample of Degussa 'C' γ-alumina (0.4989g; 3.78 mmol) was calcined at 523K and transferred to the counting cell where it was treated with anhydrous gaseous carbon tetrachloride. The gaseous products were analysed by infrared after the reaction, for the presence of hydrogen chloride, carbon dioxide and phosgene. The sample was degassed by pumping prior to the expansion of anhydrous gaseous [^{36}Cl]-chlorine labelled hydrogen chloride (13.8 Torr; 1 mmol) into the counting cell and exchanged with the carbon tetrachloride treated γ-alumina solid for 90 min. The sample was degassed by pumping. An aliquot of uninhibited 1,1,1 trichloroethane (30.87 Torr; 0.24 mmol) was expanded into the counting cell

and reacted at 293K.

The gas phase and the solid count rate was monitored with time.

5.3.18 Reaction of 1,1,1 Trichloroethane at 296K with Calcined Degussa 'C' γ-Alumina treated with [^{36}Cl]-Chlorine labelled Carbon Tetrachloride and Anhydrous Gaseous Hydrogen Chloride.

A sample of Degussa 'C' γ-alumina (0.5429g; 4.11mmol) was calcined to 523K and transferred to the counting cell where it was treated with [^{36}Cl]-chlorine labelled carbon tetrachloride (Section 4.3.8). The sample was degassed and the labile surface activity was removed by the addition of sequential aliquots of anhydrous gaseous hydrogen chloride (Section 4.3.16) until no change in the surface activity was observed. The sample was degassed by pumping prior to the expansion of uninhibited 1,1,1 trichloroethane (18.00 Torr; 1.13 mmol) at 293K into the counting cell. The surface and gas phase count rate was monitored with time.

CHAPTER 6.

6.1 Molecular Orbital Approach to the Study of Chlorine Promoted γ-Alumina.

It has often been assumed that calcined γ-alumina possesses only Lewis acid sites since the observed hydroxyl groups which absorbed at 3680 cm^{-1} and 3745 cm^{-1} in the spectra have the same or even lower Brønsted acidity than those of silica (1) and consequently were not detected by pyridine adsorption (87,91,170). The use of stronger bases, primarily substituted pyridines (31,92) made it possible to detect very weak Brønsted acid sites at the γ-alumina surface. The absence of strong Brønsted acid sites had limited the use of γ-alumina in the commercial application to catalysis.

Several workers (171-174) have shown subsequently that fluorination or chlorination of γ-alumina created Brønsted acid sites thereby opening up its use for catalyzed carbonium reactions. It was generally accepted that the halogenation treatment removed the less acidic hydroxyl groups while strong acidic hydroxyl groups were created (175). The chlorination of γ-alumina with carbon tetrachloride removed most of the hydroxyl groups from the γ-alumina surface and these groups were replaced by chloride (22). Controversy exists as to the nature of the acid sites that are created on the surface of γ-alumina by treatment of the solid with either anhydrous gaseous hydrogen chloride or anhydrous gaseous carbon tetrachloride.

Solid state physics has provided substantial theoretical information regarding the bonding in crystals by using the periodicity of the lattice to simplify solutions of the wave equation (176). The band theory was extended to include solids that extend to infinity in all directions. However, bulk defects in the crystal give rise to difficulties since the defects lead to disruptions in the periodicity of the lattice. Progress has been made using models that assume infinite periodicity in two directions. Using this technique adsorption of a substrate by a crystal requires that the layer of adsorbed species has a periodicity related to that of the crystal in two dimensions and that a full monolayer of the substrate on the crystal is required to maintain the consistency of the model. This theoretical model is known as the periodic-surface-layer or solid state model (179).

Many practical catalysts are small clusters of atoms that can be better dealt with using the molecular orbital techniques that are used for organic molecules. These methods involve the calculation of the energy levels and bond strengths for a given small cluster of atoms and addition of other molecules to the outer crystal lattice emulates the formation of adsorbed species. This method is referred to as the cluster approximation method (179). Surfaces can be handled using this method, by isolating a small cluster of crystal atoms at the surface and solving for the energy levels and bond strengths for that group of atoms. An adsorbate can also be added to the cluster.

In this work cluster models have been employed. It was convenient from the catalytic viewpoint to consider that local states or localized orbitals are more important than band states or large orbitals spread over the cluster, when the discussion is focussed on the chemical reactivity of a particular active centre on the surface. Molecular orbital theoretical studies of the Brønsted acidity and basicity of silica alumina (177) have shown that the co-ordinate environment around the active site effects the acidity and basicity of the cluster. It is therefore important to develop representative cluster models on which the molecular orbital calculations are performed to obtain meaningful data illustrating the behaviour and structure of the acid sites.

6.2 Molecular Orbital Approach to Brønsted Acidity.

In this work the application of molecular orbital theory to the origin of Brønsted acidity in the γ-alumina system is based on Pauling (178) valence bond theory such that a protonated molecule H-O may be described as a resonance between two canonical structures i.e. covalent and ionic (Equ.6.1)

$$H\text{-}O \rightleftharpoons \{ H{:}O \longleftrightarrow H^{+}O^{-} \} \qquad \text{(Equ.6.1)}$$

In the usual case the more stable the ionic structure the stronger is the Brønsted acidity. Consider the following equilibrium (Equ; 6.2)

$$B + HO \rightleftharpoons BHO \rightleftharpoons BH^{+} + O^{-} \qquad \text{(Equ. 6.2)}$$

Assuming the fragment energies remain unchanged and the transition state BHO is stable, the reaction will proceed with no barrier to reaction and hence the energy of activation is zero. Therefore the Brønsted acidity is dominated by the free energy for the elimination of the proton from the cluster, E_H, so that

$$\Delta E_H = E_{H+} + E_{O-} - E_{H:O} \qquad \text{(Equ. 6.3)}$$

6.2.1 Derivation of the Energy Equation for a Protonated Cluster.

The ground state of the molecule H-O can be described using Valence Bond Theory (Equ. 6.4)

$$\Psi_{H-O} = C_{H:O}\,\Psi_{H:O} \pm C_{H^+O^-}\,\Psi_{H^+O^-} \qquad \text{(Equ. 6.4)}$$

To determine the energy and the co-efficients, matrix elements are introduced. In a system with two states, the matrix elements consist of:-

$$\int \psi_{H:O}\,\hat{H}\,\psi_{H:O}\,\delta\tau = \alpha \;;\quad \int \psi_{H^+O^-}\,\hat{H}\,\psi_{H^+O^-}\,\delta\tau = \gamma \;;$$

$$\int \psi_{H:O}\,\hat{H}\,\psi_{H^+O^-}\,\delta\tau = \beta \;;\quad \int \psi_{H:O}\,\psi_{H^+A^-}\,\delta\tau = S \;;$$

where :- $\delta\tau = r^2 \sin^2\theta\,\delta\phi$ and the Hamiltonian $\hat{H}$ incorporates the kinetic energy of the electron and its potential energy of attraction to nucleus O and to H (Figure 6.1), together with the repulsive energy between the nuclei. Thus we have (Equ 6.5):-

Figure 6.1

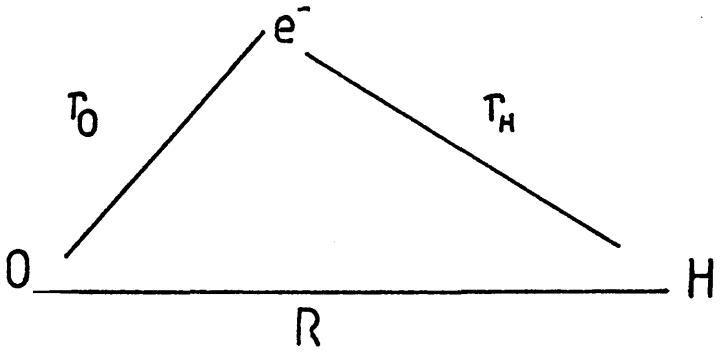

O = Oxygen atom

H = Hydrogen atom

e^- = associated electron

r_H = distance electron is from hydrogen atom.

r_O = distance electron is from oxygen atom.

R = interatomic distance.

$$\hat{H} = -\frac{1}{2}\nabla^2 - \frac{1}{r_o} - \frac{1}{r_H} + \frac{1}{R} \qquad \text{(Eq. 6.5)}$$

WHERE :-

$$-\nabla^2 = -\frac{\partial}{\partial r}\left(r^2 \frac{\partial \psi}{\partial r}\right) - \frac{1}{r^2 \sin\theta} \cdot \frac{\partial}{\partial \theta}\left(\sin\theta \frac{\partial \psi}{\partial \theta}\right)$$

$$- \frac{1}{r^2 \sin^2\theta} \cdot \frac{\partial^2 \psi}{\partial \phi^2} \qquad \text{(Eq. 6.6)}$$

Assuming the wavefunctions to be real (Ab = bA) so that,

$$\beta^* = \beta \quad \text{and} \quad S^* = S,$$

the eigenvalues of the matrix elements are obtained by solving the secular equation (Equ. 6.7) such that,

$$\sum_{ij} c_{ij}\left(H_{ij} - E s_{ij}\right) = 0 \qquad \text{(Equ. 6.7)}$$

The conditions for the existence of solutions are that the secular determinants should be zero, hence (Equ. 6.7i)

$$\det\left|H_{ij} - E S_{ij}\right| = 0. \qquad \text{(Equ. 6.7i)}$$

Evaluating H_{11}, H_{22}, H_{12}, H_{21} the matrix elements become (Eq. 6.8)

$$\det \begin{vmatrix} H_{11} - ES_{11} & H_{12} - ES_{12} \\ H_{21} - ES_{21} & H_{22} - ES_{22} \end{vmatrix} = 0 \qquad \text{(Eq.6.8)}$$

When the basis functions are orthogonalized (i.e. $\int \psi_A \psi_B \, d\tau = 0$) the overlap integrals S_{11} and $S_{22} = 1$ and the determinant reduces to (Equ. 6.9):—

$$\det \begin{vmatrix} H_{11} - E & H_{12} - ES_{12} \\ H_{21} - ES_{21} & H_{22} - E \end{vmatrix} = 0 \qquad \text{(Eq. 6.9)}$$

Substituting the matrix elements, the determinant now becomes (Eq. 6.10):—

$$\det \begin{vmatrix} \alpha - E & \beta - ES \\ \beta - ES & \gamma - E \end{vmatrix} = 0 \qquad \text{(Eq. 6.10)}$$

Expansion of the determinant gives the following quadratic equation in E:—

$$E^2(1 - S^2) - E(\alpha + \gamma - 2\beta S) + (\alpha\gamma + \beta^2) = 0 \qquad \text{(Eq. 6.11)}$$

The roots of this quadratic equation yield the lowest energy (Eq. 6.12):—

$$E_{H:A} = \frac{\alpha+\gamma - 2\beta S - \left\{(\gamma-\alpha)^2 + 4(\beta-\alpha S)(\beta-\gamma S)\right\}^{\frac{1}{2}}}{2(1-S^2)}$$

(Equ. 6.12)

6.2.2 Evaluation of the Coefficients.

On substitution of the matrix elements into the determinant (Eq. 6.10), the secular equations have the form

$$C_{H:A}\ (\alpha-E) + C_{H^+A^-}\ (\beta-ES) = 0 \qquad \text{(Eq. 6.13)}$$

and

$$C_{H:A}\ (\beta-ES) + C_{H^+A^-}\ (\gamma-E) = 0 \qquad \text{(Eq. 6.14)}$$

From Equ. 6.13:—

$$C_{H^+A} = -\frac{C_{H:A}\ (\beta-ES)}{\gamma-E} \qquad \text{(Equ. 6.15)}$$

Using normalised wavefunctions (i.e $n^2 \int \psi^2 \delta\tau = 1$) the energy coefficients are evaluated from Equ. 6.16:—

$$C^2_{H:A} + C^2_{H^+A^-} + 2C_{H:A}C_{H^+A^-}S = 1 \qquad \text{(Eq. 6.16)}$$

Substituting Equ. 6.15 into Equ. 6.16 the covalent wavefunction co-efficient can be obtained (Equ. 6.17):—

$$C_{H:A} = \frac{\gamma-E}{\gamma+\beta+E(1-S)+\left\{\gamma[-2E-2S(\beta-ES)]\right\}^{\frac{1}{2}}} \qquad \text{(Eq. 6.17)}$$

The ionic wavefunction co-efficient may be similarly obtained (Eq. 6.18):—

$$C_{H^+A^-} = \frac{\alpha-E}{\alpha+\beta+E(1-S)+\left\{\alpha[-2E-2S(\beta-ES)]\right\}^{\frac{1}{2}}} \qquad \text{(Eq. 6.18)}$$

6.2.3 The Brønsted Acidity Indicator.

In section 6.2 it was shown that the Brønsted acidity of a dissociating protonated molecule may be qualitatively determined by evaluating the deprotonation energy (ΔE_H) that is the formation of the anion from the protonated species. However the charge of the acidic hydrogen has been adopted as a quantum chemical measure of the Brønsted acidity by a number of workers (179-180). The magnitude of the Brønsted acidity relates to the deprotonation energy which in turn depends on the energy of the acidic hydrogen atom. The higher the energy of the acidic hydrogen, the smaller is the deprotonation energy and hence the stronger is the Brønsted acid. The deprotonation energy depends not only on the energy of the acidic hydrogen but also on the diatomic energy contribution from the associated oxygen atom E_{OH}, that comprises the hydroxyl group which is the source of the Brønsted acidity. The smaller the magnitude of E_{OH}, the weaker the O-H bond will be and hence the stronger the Brønsted acid character of the site. Using the charge on the acidic hydrogen as a measure of the Brønsted acidity means neglecting the effect of the O-H bond strength. The diatomic energy has contributions from the coulombic interaction (E_Q) and the exchange integral (E_J) from the proton and the associated anion.

The coulombic interaction is defined by Eq. 6.19:-

$$E_Q = \int \frac{\psi_0^2}{r_H} \delta\tau \qquad \text{(Eq. 6.19)}$$

where r_H is the distance the associated electron is from the proton (see fig 6.1).

The exchange integral is defined as:—

$$E_J = \frac{\int \psi_o \psi_H \delta\tau}{r_H} \qquad \text{(Eq.6.20)}$$

These energies are components of the covalent and ionic wavefunctions such that:—

$$\psi_{HOAl} = c_1 \psi_H \pm c_2 \psi_{OAl} \qquad \text{(Eq. 6.21)}$$

and

$$\psi_{H^+O^-Al} = c_3 \psi_{H^+} \pm c_4 \psi_{O^-Al} \qquad \text{(Eq. 6.22)}$$

to give the respective energies:—

$$E_{HOAl} = \frac{\int \psi_H \hat{H} \psi_H \delta\tau + \int \psi_{OAl} \hat{H} \psi_H \delta\tau}{1 + \int \psi_H \psi_{OAl} \delta\tau}$$

(Eq. 6.23)

and

$$E_{H^+O^-Al} = \frac{\int \psi_{H^+} \hat{H} \psi_{H^+} \delta\tau + \int \psi_{O^-Al} \hat{H} \psi_{H^+} \delta\tau}{1 + \int \psi_{H^+} \psi_{O^-Al} \delta\tau}$$

(Eq. 6.24)

These energies are the energies of the canonical structures described in section 6.2.1 as α and γ respectively. These

diagonal matrix elements α and γ can be approximately partitioned (181) to give:—

$$\alpha = E_H + E_O - E_Q + E_J \qquad \text{(Eq. 6.25)}$$

and

$$\gamma = E_{H^+} + E_{O^-} - E_{Q'} + E_{J'} \qquad \text{(Eq. 6.26)}$$

where E_Q and $E_{Q'}$ are the coulombic integrals of $E_{H:O}$ and $E_{H^+O^-}$ respectively E_J and $E_{J'}$, being the exchange integrals of H:O and H^+A^- respectively.

To enhance the Brønsted acidity of a cluster the energy of the ionic form must be lower than the energy of the covalent form, and the Brønsted acidity of the cluster can be measured by $\gamma-\alpha$ so that:—

$$\gamma-\alpha \approx (E_{H^+} + E_{O^-} - E_{Q'} - E_{J'}) - (E_H + E_O - E_Q - E_J)$$

$$\therefore \Delta E_H \approx (E_{H^+} - E_H) + (E_{O^-} - E_O) - (E_{Q'} - E_Q) - (E_{J'} - E_J). \qquad \text{(Eq. 6.25)}$$

Therefore the most reliable indicator of Brønsted acidity is the magnitude of the energy required to eliminate a proton from an associated cluster. The lower the value of ΔE_H for the cluster the stronger the Brønsted acid character of the acidic hydrogen. This deprotonation energy may be evaluated by calculating the difference in the total energy for the protonated cluster with the total energy of the deprotonated cluster.

6.3 Molecular Orbital Approach to the Lewis Acidity of Clusters.

It has been proposed that the exposed aluminium atoms on the surface of γ-alumina are the Lewis acid sites (182) (Section 1.7). The Lewis acidity is enhanced by treating the surface of the catalyst with chloromethanes (22) and the co-ordinative environment around the aluminium atom may be a significant factor in creating Lewis acidity (177). In view of this, the adsorption energy of a hydroxyl group on the aluminium atom ΔE_{OH} is expected to be the primary index for Lewis acidity, the greater this value, the stronger will be the Lewis acid character at the site. However it may not be exactly proportional to the acid strength since the hydroxyl anion is unique in that it is one of the strongest bases possessing negative charge. The orbital symmetry between a substrate and a reactant determines whether a bond can or cannot be formed (183-187). The strength of a bond is determined by the relative positions of energy levels of the interacting orbitals.

Consider two interacting orbitals of energy $E_{substrate}$ and $E_{catalyst}$ respectively. If $E_{substrate} = E_{catalyst}$ the bonding orbital will be at an energy of

$$E_{catalyst} - \int \psi_{substrate} \hat{H} \psi_{catalyst} \, d\tau \qquad \text{(Eq. 6.26)}$$

If the energy levels $E_{substrate}$ and $E_{catalyst}$ are separated by a value $E_{substrate} - E_{catalyst}$, where $E_{catalyst}$ is of lower energy than $E_{substrate}$, then the lowering of the bonding orbital energy with respect to $E_{catalyst}$ is

approximately equal to Equation 6.27:-

$$E_{cat\text{-}subs} = \frac{\int \psi_{substrate} \hat{H} \psi_{catalyst} \, d\tau}{E_{substrate} - E_{catalyst}} \quad \text{(Eq. 6.27)}$$

Hence the bond strength between the catalyst and the substrate rapidly decreases with the energy difference between the highest occupied molecular orbital (HOMO) and the lowest unoccupied molecular orbital (LUMO) of the interacting component orbitals. The importance of these interacting orbitals was first realised by Fukui who named them frontier orbitals (186). According to the frontier orbital theory (186,188) electron transfer between the HOMO and LUMO is a most important factor in intermolecular interactions. The HOMO-LUMO interaction is strong when their energy levels lie close together and their overlap is large. Envoking the Pauling Electroneutrality Principle (178), the electronic charge at the surface of the solid spreads out over the surface and into the bulk. This process reduces the ionic nature of the surface for a given structure depending on the electronegativity of the atoms surrounding the charged species, such that all the atoms are approximately neutral and no atom bears a charge of $+\frac{1}{2}$ or $-\frac{1}{2}$. This reducing potential at the surface results in the energy levels of the oxygen atoms, which includes the HOMO, being increased. The LUMO energy levels (centred over the aluminium atoms) at the surface are in turn lowered. Hence the electronic re-distribution through the cluster drives towards minimising

the HOMO and LUMO energy gap of the cluster. This results in Al-O species being more active at the surfaces, edges or corners than in the bulk of the crystallite material. The reducing potential of the surface is important if lattice defects are being discussed. In the study carried out an ideal model has been used, since dislocations or deformations in the sample cannot be wholly accounted. Therefore the indicator of maximum catalytic activity is a small difference between the energy level of the LUMO orbital and the HOMO orbital for a given local configuration of atoms. A small HOMO-LUMO gap will facilitate electron transitions to and from as well as within the catalyst. It has been shown that electron transitions to and from the catalyst are responsible for the enhancement or reduced catalytic activities of supported catalysts (189).

6.3.1 Lewis Acid Indicator.

To develop the Lewis acid indicator for a given cluster of atoms, consider the case where the Brønsted acid character of a proton associated with a hydroxyl group is dependent upon the Lewis acid character of a nearest neighbour aluminium atom. A strong Brønsted acid character would arise from the polarisation of electron density from the O-H bond to the O-Al bond the extreme case resulting in the ionic form Eq. 6.28:

$$HOAlO \rightleftharpoons H^{+}O^{-}AlO \qquad \text{(Eq. 6.28)}$$

The polarisation of electron density from the O-H bond would arise from the associated Lewis acid character of the nearest

neighbour aluminium atom.

In the case of the covalent AlO species where the singly occupied molecular orbital (SOMO), $3s^1$ lies low relative to the HOMO, $3s^2$ of the O^-Al species (Figure 6.2) The formation of the AlO^- bond is favoured by a lowering of the LUMO orbital of the aluminium atom (3px1) to overlap with the HOMO of the O^- atom, stabilizing the formation of the $3s^2$ M.O. The formation of the covalent AlO (SOMO; $3s^1$) would be unfavoured relative to the formation of the AlO^- species due to the better overlap with the higher energy $2py^1$ orbital from the O^- anion. A lowering of the LUMO orbital over the aluminium atom would further enhance the orbital overlap with the O^- anion and generate a stronger Brønsted proton. Therefore lowering the LUMO orbital is an indicator of stronger Lewis acid character of the aluminium atom. The Lewis acid character of the cluster is dominated by the LUMO orbital energy. The lower the LUMO orbital energy the greater the Lewis acidity of the cluster.

6.4 γ-Alumina Cluster Models.

The objectives of the molecular orbital calculations are to evaluate the absolute energy and the absolute energies of the HOMO and LUMO orbitals for the clusters shown in figures 7.1 to 7.4. The fully hydroxylated cluster models are CT1, C10, TT1,TO1 and OO1. The clusters studied contain terminal tetrahedral aluminium atoms, terminal octahedral aluminium atoms, a tetrahedral aluminium linked to a tetrahedral aluminium through a bridging oxygen atom, a

Molecular Orbital Diagram for the Formation of AlO^- and $AlO^{\cdot}$ Radical.

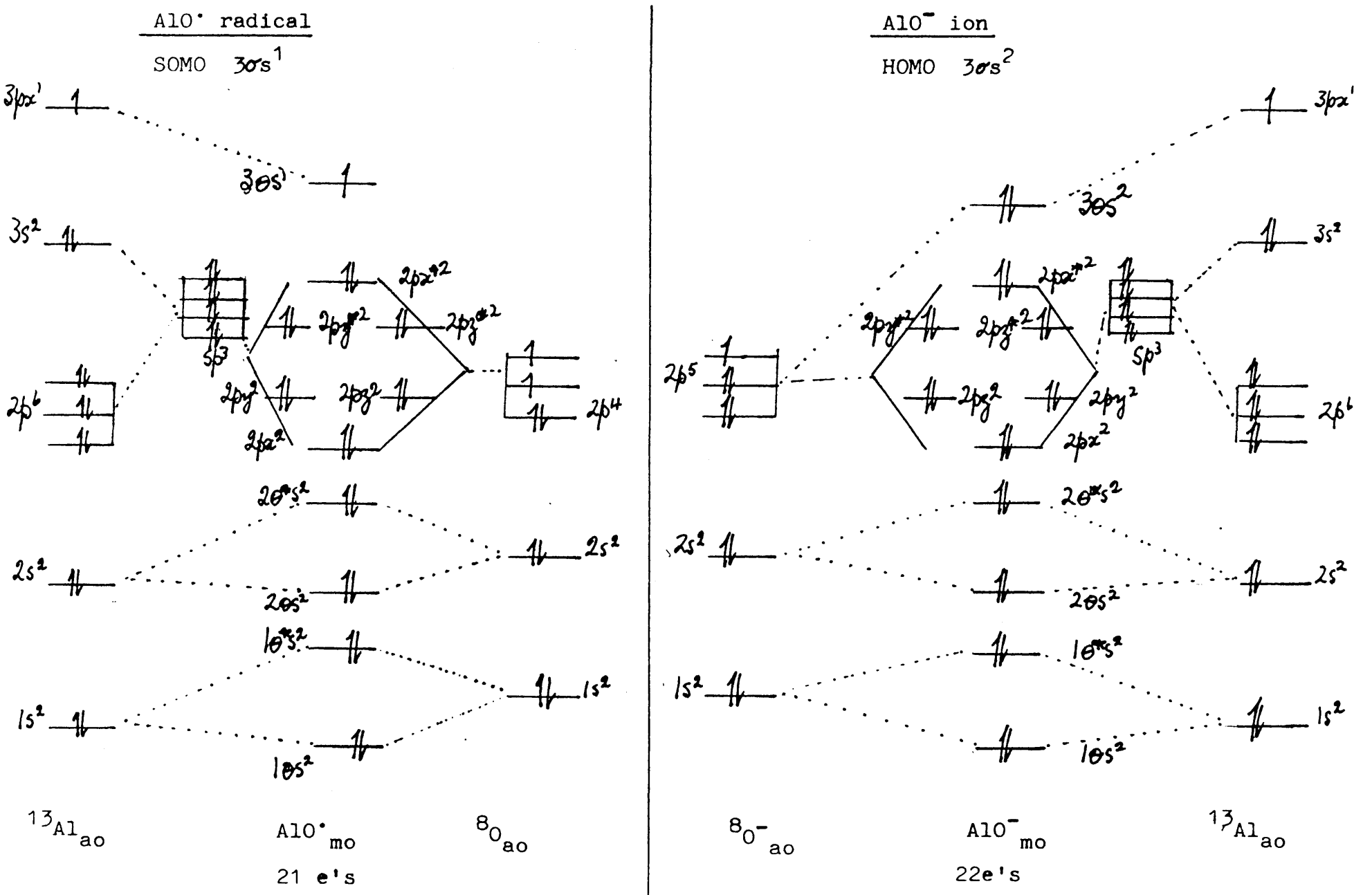

tetrahedral aluminium linked to an octahedral aluminium environment through a bridging oxygen, and an octahedral aluminium linked to another octahedral aluminium through two bridging oxygens. These aluminium environments are derived from an idealized spinel structure described in section 1.3. All aluminium lattice atoms and oxygen lattice atoms have the co-ordination (Al_{6c} and O_{6c}) in the case of octahedral aluminium environments, and (Al_{4c}, O_{6c}) in the case of tetrahedral aluminium environments. Low co-ordination sites or defect surfaces are represented by omitting the appropriate atoms.

For a given cluster structure a hydrogen atom is located at the end of each 'dangling' single bond with the AlOH angle fixed at 180°. Every tetrahedral aluminium-oxygen bond was fixed at 1.89 Å with the O-Al_{tet}-O angle at 109.8°, the octahedral aluminium-oxygen bond fixed at 2.19 Å, the O-Al_{oct}-O angle of 90° (Section 8.2.1). The surface Al-O-H angle was fixed at 110° with the O-H bond length fixed at 0.96 Å. Optimization of the interatomic distances was not undertaken as the cluster models are restricted to an idealized structure. Qualitative information regarding the acid behaviour was obtained from single point calculations. The electrostatic influence from the atoms around the cluster was neglected. It has been shown that the electrostatic potential does not effect the acid-base strength (191). The three dimensional Cartesian geometry for each atom in a cluster was calculated relative to a central aluminium atom based on the bond

distance and bond angle of the atom in question to the central aluminium atom. The resultant three dimensional positions of the atoms in the cluster were then used as a database which was accessed to carry out the Self Consistent Field-Unrestricted Hartree Fock calculations (SCF - UHF). SCF-UHF calculations were carried out on the fully hydroxylated, deprotonated, and dehydroxylated cluster models shown in figures 7.1 to 7.4. The removal of a proton, resulting in the deprotonated model or the removal of the hydroxyl group to give the dehydroxylated cluster model involved the removal of the surface orientated atoms. Calculations on these basic cluster models were extended to include a mono-chlorinated or a dichlorinated surface aluminium atom series which are also shown in figures 7.1 to 7.4. The chlorinated cluster models were produced by substituting a chlorine atom or atoms into the cluster in place of a hydroxyl group or groups. The aluminium-chlorine bond distance was fixed at 2.26 $\mathring{A}$.

Ab initio SCF-UHF single point calculations using the split-valence 3-21G basis sets (176,192) were carried out on the cluster models shown in figures 7.1 to 7.4. All the calculations were carried out using the GAMESS package (193) which is a development of the HONDO program (194). These programs have many features available in the ATMOL (195-196) and the Gaussian (197-198) series. The GAMESS package was run on the CDC CYBER 205 mainframe computer at the University of Manchester Regional Computer Centre (UMRCC).

CHAPTER 7.

Molecular Orbital Calculations:

7.1 The Molecular Orbital Theoretical Approach to the Study of Brønsted Acidity using Cluster Models of γ-Alumina Aluminium Environments.

The results of the investigation for the cluster models shown in figures 7.1 to 7.4 using the interatomic distances reported in section 8.1 are presented in table 7.2 and figure 7.8. The results showed that the fully hydroxylated tetrahedral aluminium clusters CT1 does not exhibit Brønsted acid character as a small destabilization of the cluster energy of 0.7919 Hartree had occurred on deprotonation from CT1 to CT2 (Table 7.2). The results for the octahedral aluminium cluster C10 also showed that a small destabilization of +0.9146 Hartree occurred when the cluster was deprotonated (C10 to C20). In both the models the substitution of chlorine into the cluster models C4T and C40 reduced to a small degree the destabilization energy that resulted from the deprotonation of the cluster. The results for the octahedral environments of aluminium were in good agreement with results obtained from the deprotonation of hydroxyl groups associated with the surface of α-alumina (177) in which deprotonation of the octahedral environment of aluminium resulted in destabilization of the cluster by +0.9041 Hartree.

The results from the Al_{tet}-O_b-Al_{tet}, clusters TT1 to TT7 showed that the fully hydroxylated cluster also

Figure 7.1

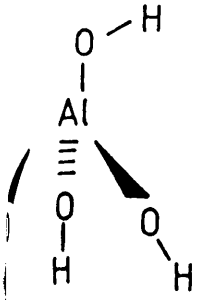

C1T

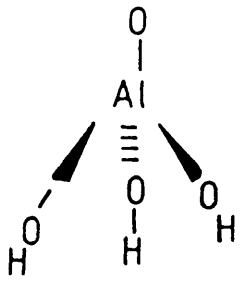

C2T

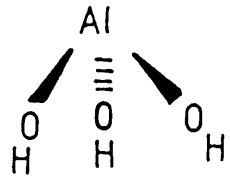

C3T

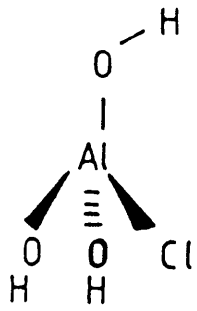

C4T

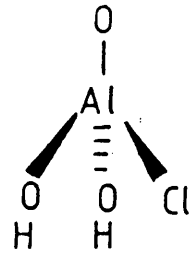

C5T

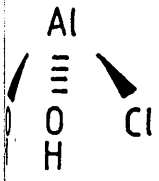

C6T

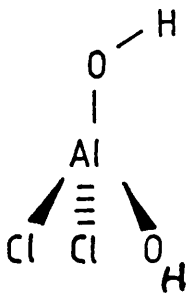

C7T

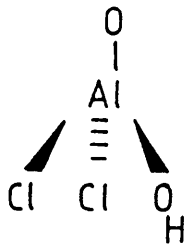

C8T

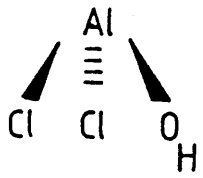

C9T

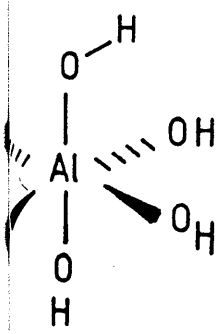

C10

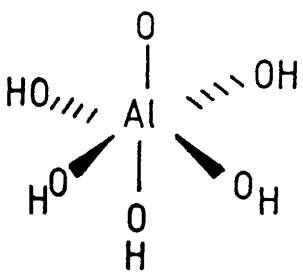

C20

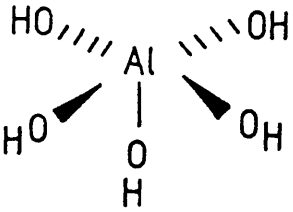

C30

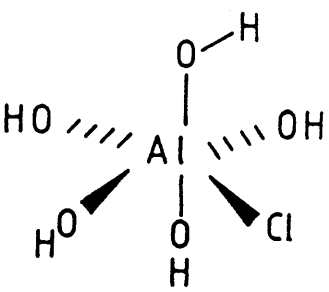

C40

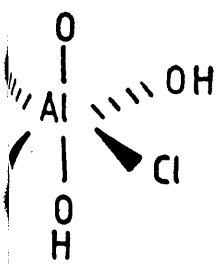

C50

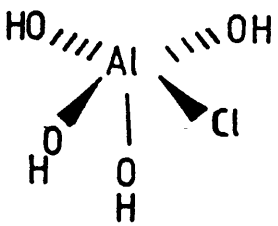

C60

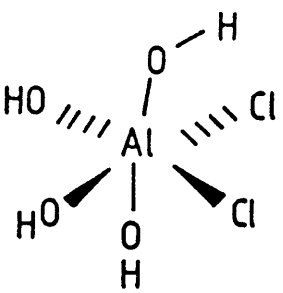

C70

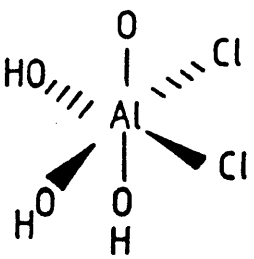

C80

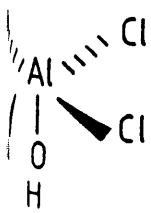

C90

Figure 7.2

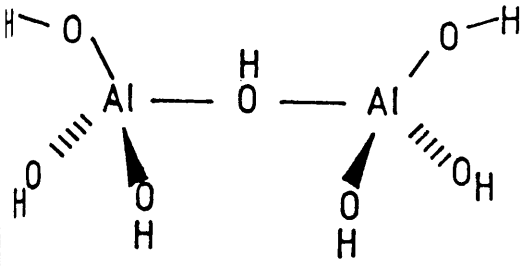

TT1

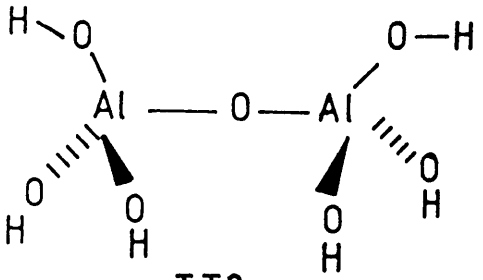

TT2

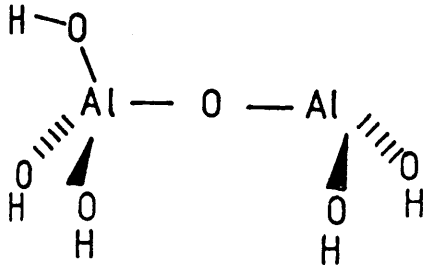

TT3

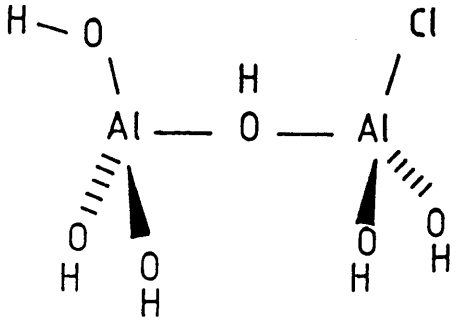

TT4

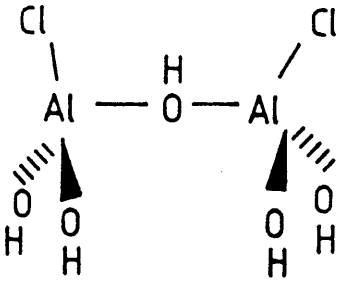

TT5

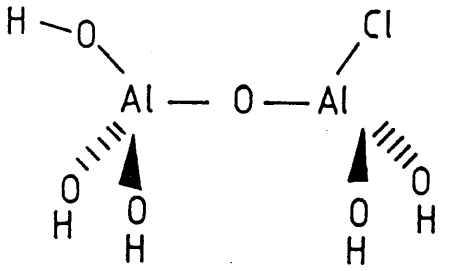

TT6

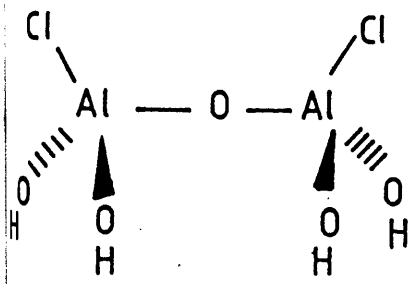

TT7

Figure 7.3

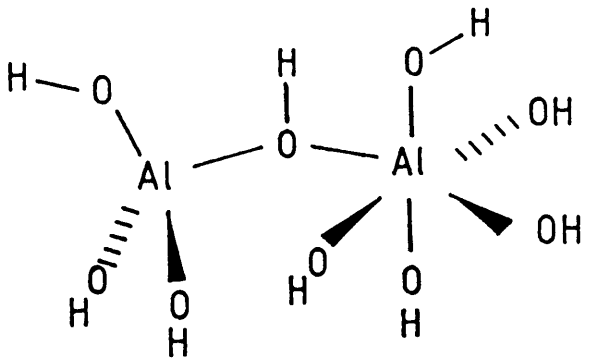

T01

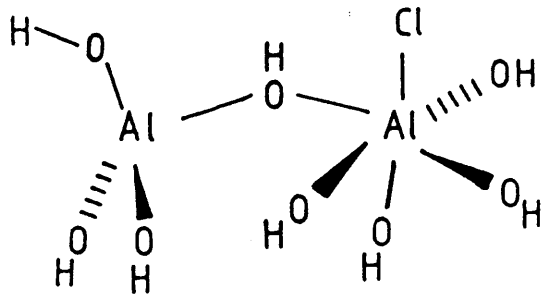

T02

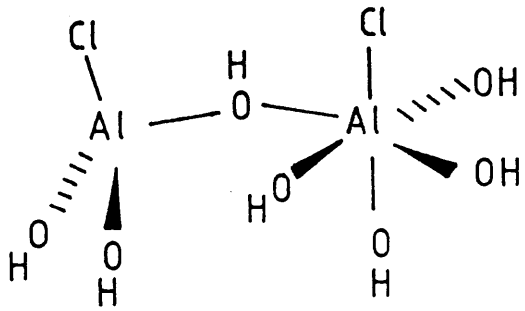

T03

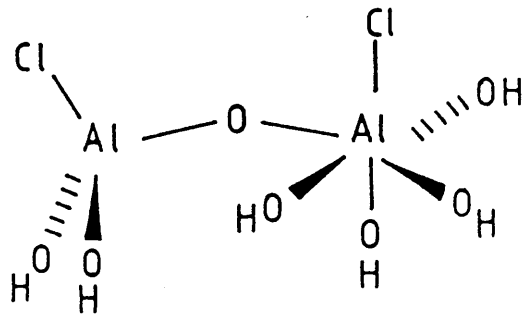

T04

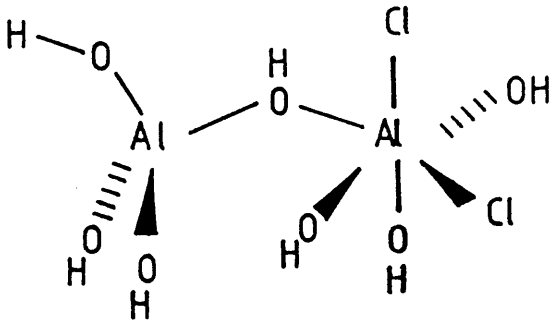

T05

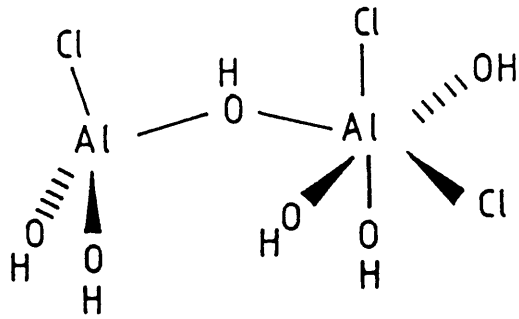

T06

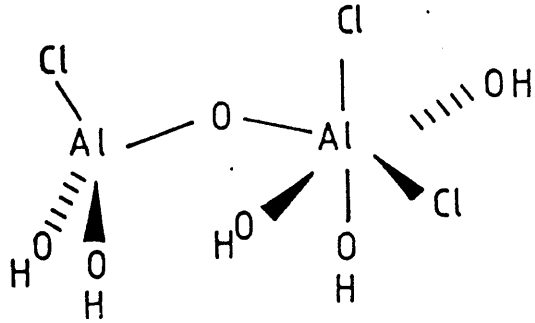

T07

Figure 7.4

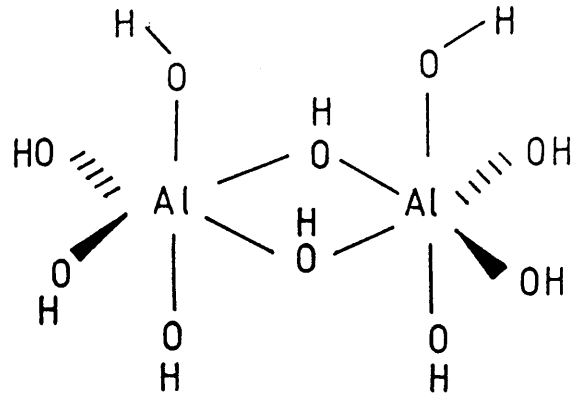

001

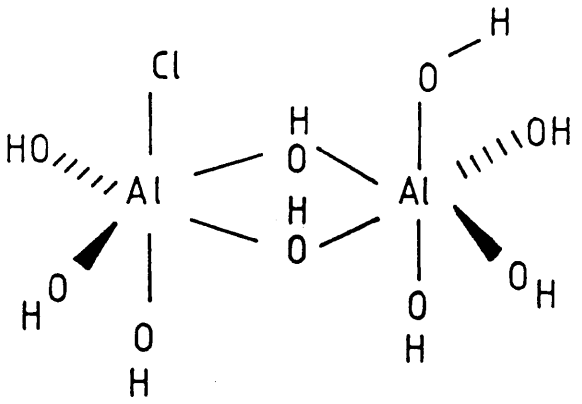

002

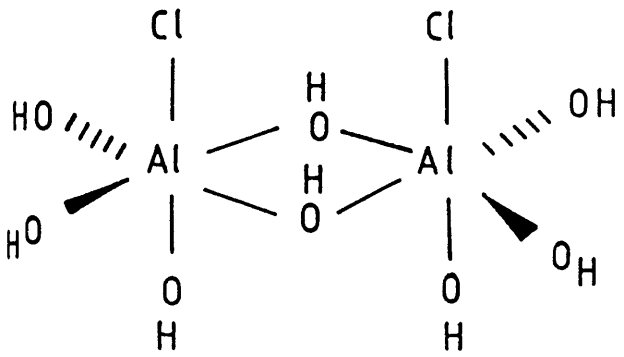

003

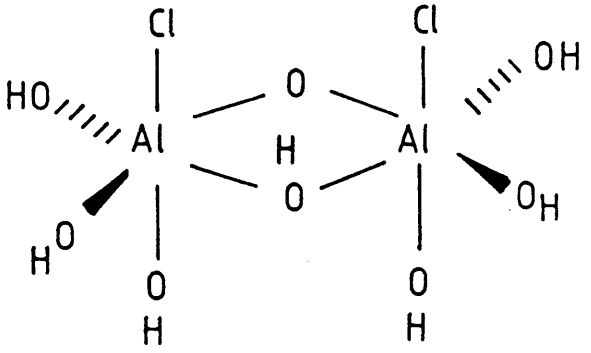

004

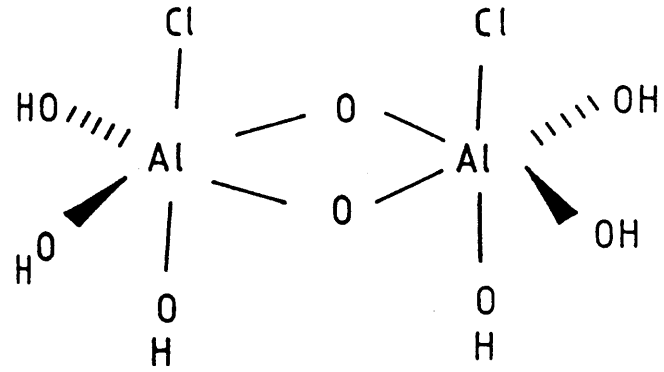

005

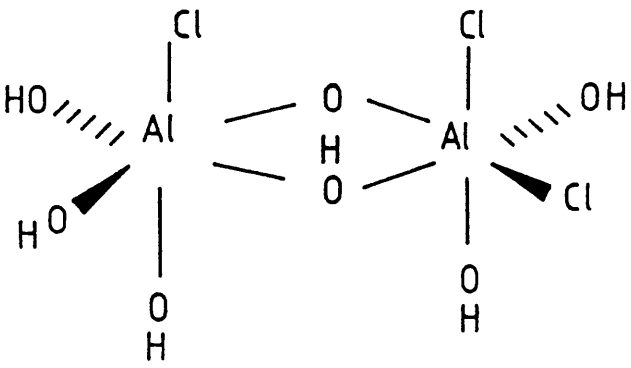

006

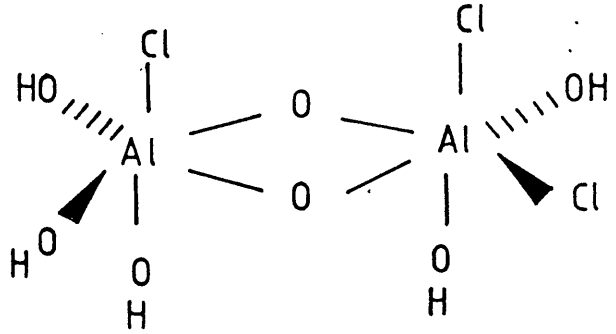

007

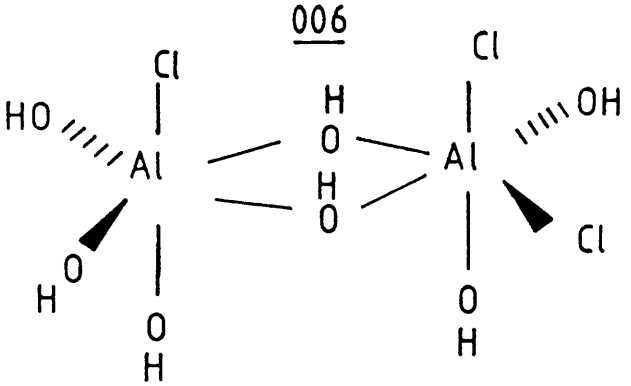

008

Table 7.2

Cluster Total Energy (Hartree).

Cluster	Protonated Precursor E_{AH}	Deprotonated Cluster Energy E_{A^-}	$E_A - E_{AH}$ E_H
TT1	-1005.9940		
TT2		-1005.1111	+0.8829
TT4	-1093.9938		
TT6		-1095.7085	-1.7147
TT5	-1196.6042		
TT7		-1438.9326	-242.3284
TO3	-1705.6905		
TO4		-1655.9858	+49.7047
TO6	-1786.3700		
TO7		-1847.5374	-61.1674
003	-1524.5236		
004	-1537.6125	-1537.6125	-13.0889
005		-1535.1498	+2.4627
008	-1783.5691		
006	-1799.8173	-1799.8173	-16.2482
007		-1975.2432	-175.4259
C1T	-538.9480		
C2T	-921.1819		
C3T	-1308.2429		
C4T		-538.1561	+0.7919
C5T		-920.4642	+0.7177
C6T		-1304.5109	+0.7320
C10	-690.6729		
C20	-1072.9714		
C30	-1455.2513		
C40		-689.7583	+0.9146
C50		-1072.0857	+0.8857
C60		-1454.4298	+0.8275

exhibited a small destabilization of +0.8829 Hartree when the bridging oxygen atom ($-O_b-$) was deprotonated. However incorporation of chlorine into the cluster does stabilize the deprotonation energy and hence Brønsted acid character from the chlorinated clusters is expected. Partial chlorination of the cluster stabilized the formation of a very weak Brønsted acid (TT4 to TT6) which produced a stabilization energy of -1.7147 Hartree for the deprotonated cluster. Monochlorination of the aluminium atoms in a cluster showed the strongest Brønsted acid character from the bridging oxygen proton with the deprotonated model (TT7) being more stable by 242 Hartree over the protonated precursor model.

The results from the $Al_{tet}-O_b-Al_{oct}$ cluster showed that deprotonation of the associated bridging proton was unfavoured (Figure 7.3, TO3 to TO4) with the anionic cluster being less stable by 49.70 Hartree. However, dichlorination of the octahedral aluminium environment (TO6 to TO7) favoured the formation of a Brønsted proton on the bridging oxygen by 61.16 Hartree.

The results from the deprotonation of the $Al_{oct}-O_b-Al_{oct}$ clusters (Figure 7.4, 001 to 007) showed that weak Brønsted acidity was shown by the monochlorinated cluster (003 to 004). The energy of deprotonation of the cluster was stabilized by 13.08 Hartree. The formation of a second Brønsted proton from the cluster was unfavoured for the monochlorinated cluster. When the cluster was incorporated with a dichlorinated aluminium environment the Brønsted

acid character of the second bridging proton was greatly improved resulting in the deprotonated cluster being more stable by 17.5 Hartree.

A Mulliken-Löwdin electron population analysis of the fully hydroxylated cluster models had shown that the charge on the surface proton was +0.395 ± 0.04. Chlorination of the clusters resulted in the charge over the surface proton of 0.371 ± 0.07. This result reinforced the hypothesis in section 6.2.3 that the deprotonation energy of the cluster is a more representative indicator of Brønsted acidity than the charge on the surface proton.

7.2 Molecular Orbital Approach to the Study of Lewis Acidity Using Cluster Models of γ-Alumina.

In section 6.3 it was shown that the Lewis acid indicator was the level of the LUMO orbital energy such that the lower the LUMO orbital energy obtained by a cluster the stronger the Lewis acid character of that cluster. This conclusion was confirmed by the molecular orbital calculations of the simple clusters comprising of octahedral environments of aluminium (Figure 7.1, clusters C10 to C90). The results are presented in table 7.3.

The results showed that the co-ordinatively unsaturated aluminium environments C30, C60 and C90 which contain no chlorine, monochlorinated and dichlorinated central aluminium atoms gave LUMO orbital energies where C30 = +0.001, C60 = -0.202 and C90 = -0.315 Hartree. The LUMO orbital energies of the deprotonated analogue cluster C20, C50 and

Table 7.3

Cluster	HOMO Energy (Hartree)	LUMO Energy (Hartree)	Egap HOMO-LUMO (Hartree)
TT1	-0.3962	+0.3579	0.7541
TT2	-0.3057	+0.0675	0.3732
TT3	-0 2938	+0.3665	0.6603
TT4	-2.7037	-2.6177	0.0860
TT5	-1.8890	-1.4919	0.3971
TT6	-2.8510	-2.7348	0.1162
TT7	-1.9253	-1.8518	0.0735
TO1	-0.2980	-0.0081	0.2899
T02	-2.7459	-2.5152	0.2307
T03	-0.8946	-0.7403	0.1543
T04	-2.2994	-2.1969	0.1025
T05	-3.1334	-2.8667	0.2668
T06	-2.2287	-2.0588	0.1699
T07	-1.8544	-1.7134	0.1410
001	-0.2319	+0.0924	0.3243
002	-0.3686	-0.1937	0.1749
003	-3.3277	-3.2416	0.0861
004	-3.1771	-3.0894	0.0876
005	-2.7990	-2.6831	0.1159
006	-2.7769	-2.5811	0.1958
007	-2.1779	-2.1047	0.0732
008	-2.7734	-2.6740	0.0995
C10	-0.2666	-0.0140	0.2526
C20	-0.3038	+0.2039	0.5077
C30	-0.3510	+0.0010	0.3500
C40	-0.2879	-0.1553	0.1326
C50	-0.3619	+0.1079	0.4698
C60	-0.3912	-0.2021	0.1891
C70	-0.7745	-0.5540	0.2205
C80	-0.3301	+0.2107	0.5408
C90	-0.7608	-0.3147	0.4461
C1T	-0.3950	+0.0835	-0.4786
C2T	-0.4131	+0.0924	-0.5054
C3T	-0.4090	+0.2875	-0.6964
C4T	-0.4140	-0.1756	-0.2384
C5T	-0.4379	-0.2060	-0.2319
C6T	-0.3864	-0.2217	-0.1747
C7T	-0.8595	-0.6878	-0.1717
C8T	-0.8616	-0.7078	-0.1538
C9T	-0.3896	-0.1286	-0.2609

Figure 7.5

Tetrahedral Al-bridging oxygen-tetrahedral Al cluster models.

SCF-UHF orbital energies (HOMO;LUMO;HOMO-LUMO plots)

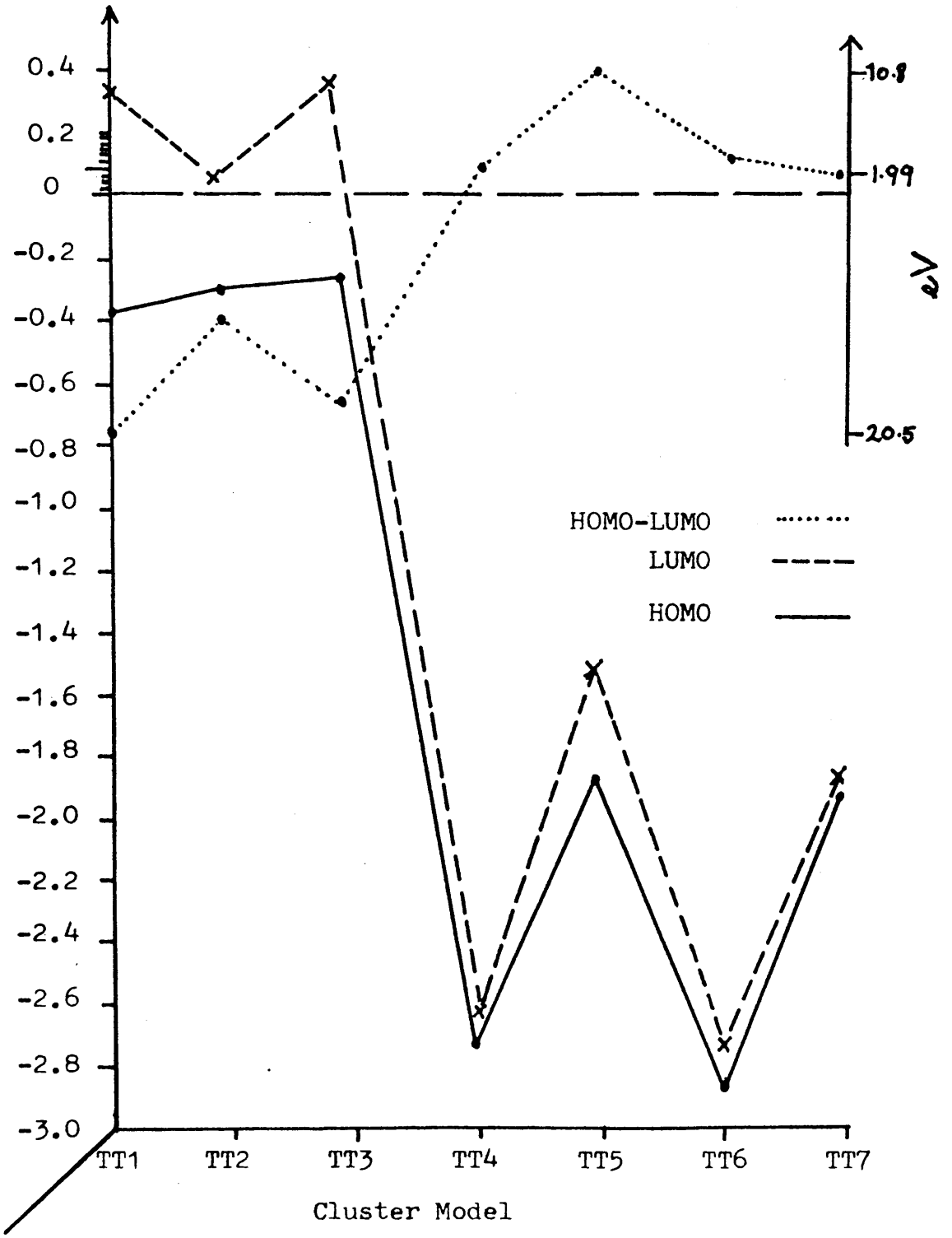

Figure 7.6

Tetrahedral Al-bridging oxygen-octahedral Al cluster models.

SCF-UHF orbital energies (HOMO;LUMO;HOMO-LUMO plots)

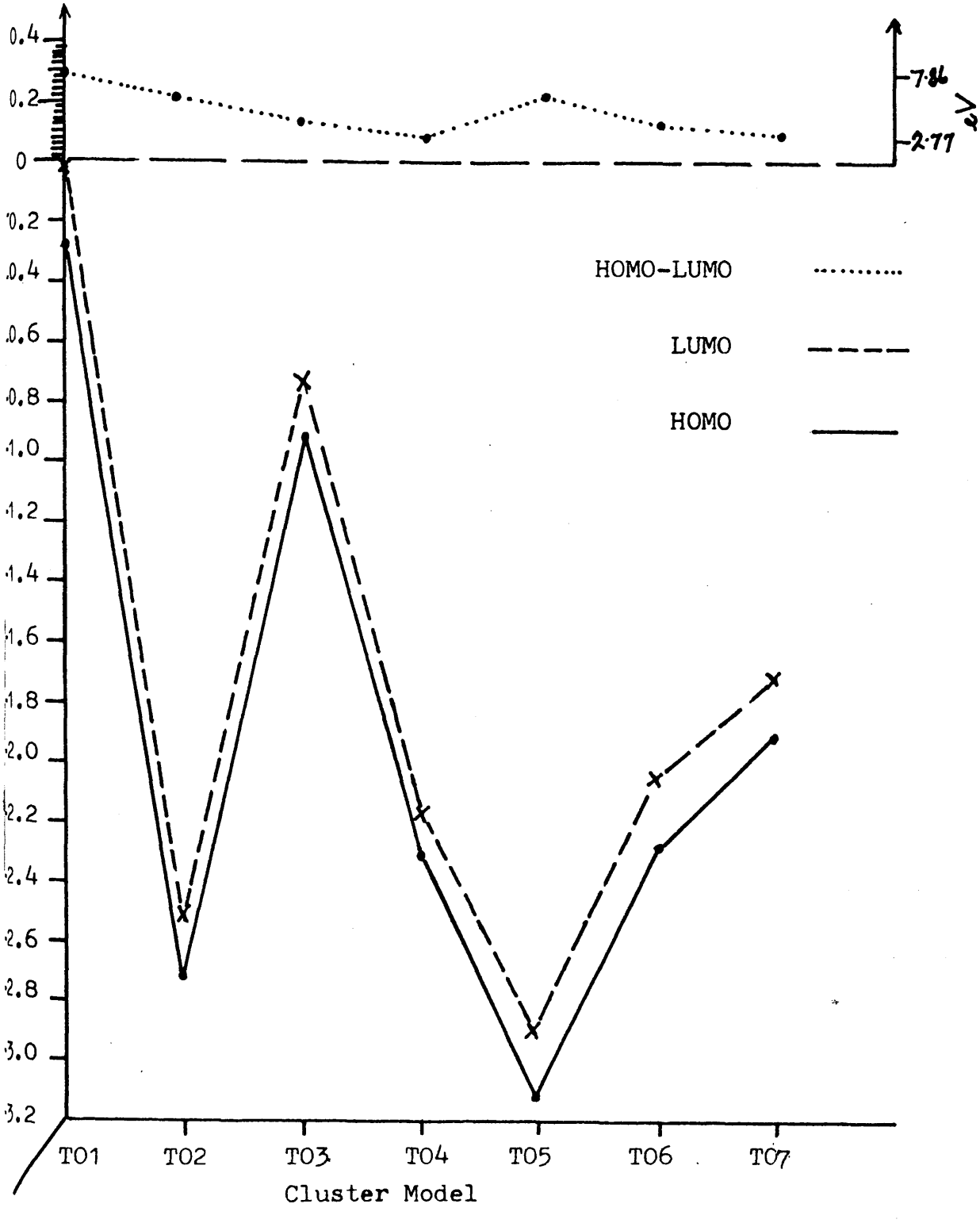

Figure 7.7

Octahedral Al-bridging oxygen-octahedral Al cluster models.
SCF-UHF orbital energies (HOMO;LUMO;HOMO-LUMO plots)

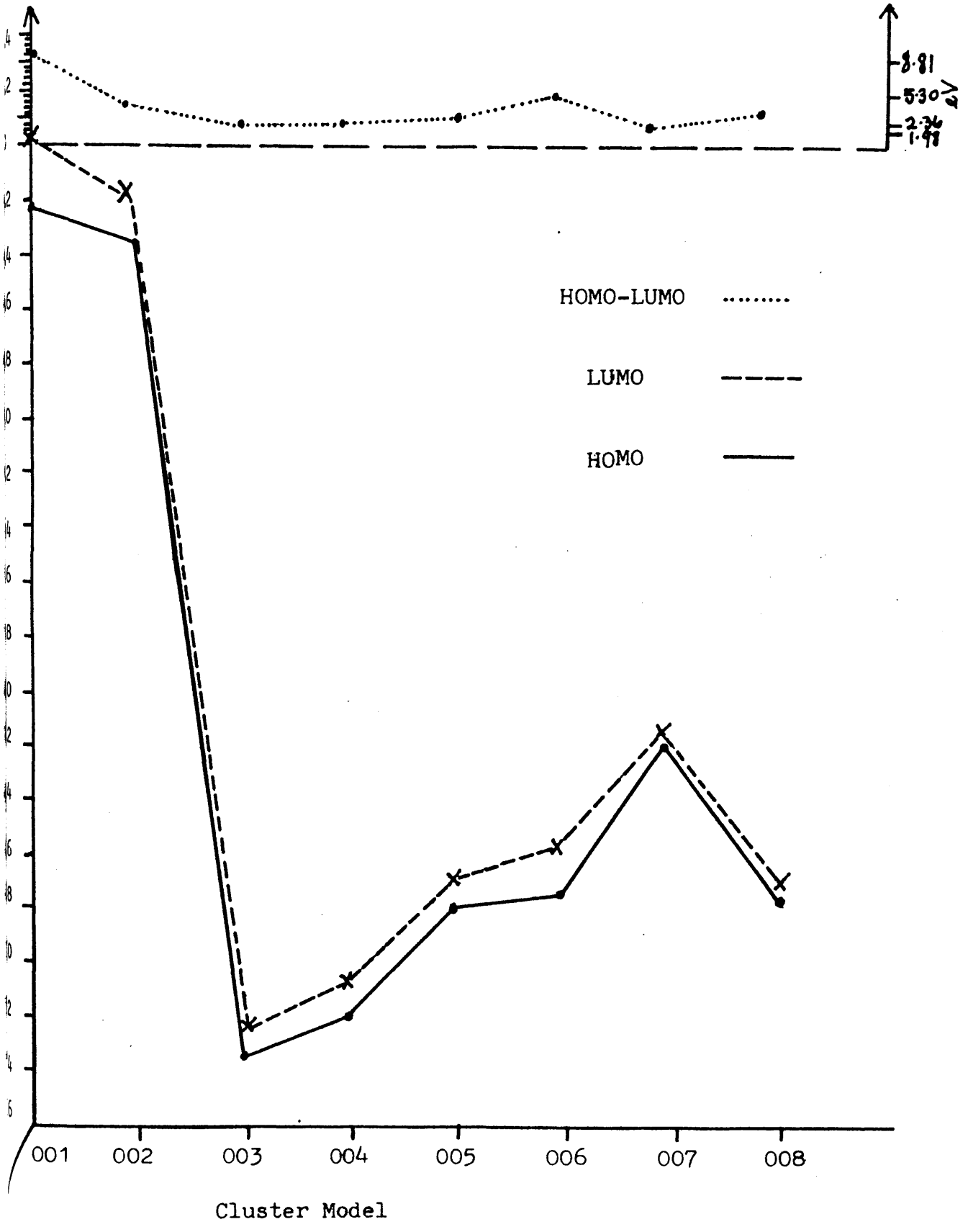

Figure 7.8

Brønsted Acidity

(Energy difference of anionic cluster and protonated precursor cluster.) Absolute energy calculated from SCF UHF single point calculation .

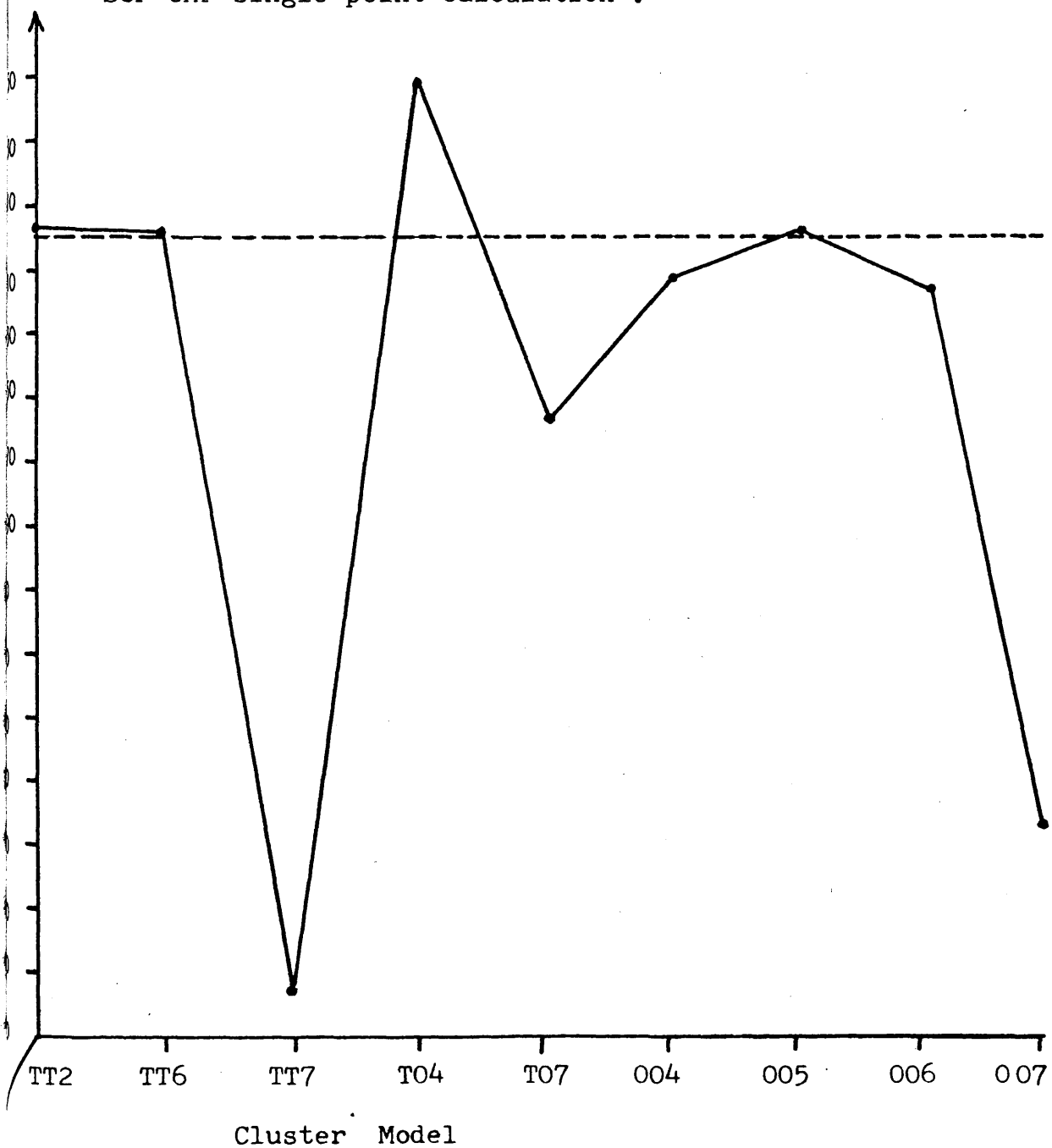

C80 showed positive or destabilized values for the LUMO orbital energies for the deprotonated cluster. This was consistent with the Lewis base character of these clusters containing a deprotonated terminal oxygen atom.

The results from the Al_{tet}-O_b-Al_{tet} clusters (Figure 7.2, TT1 to TT7) showed that Lewis acid character is not conferred on the cluster until chlorine had been incorporated into the model (Figures 7.2, 7.5). The incorporation of chlorine into the cluster resulted in stabilization of the LUMO from +3 6649 to -2.61770 Hartree (TT3 to TT4). Further chlorine incorporation into the cluster model resulted in a small reduction of the Lewis acid character of the cluster.

Stabilization of the Al_{tet}-O_b-Al_{oct} clusters (Figure 7.3, 7.6, Table 7.3) by the incorporation of chlorine into the model was also observed. The LUMO orbital energy for the cluster was lowered from -0.008 Hartree to -2.515 Hartree by monochlorinating the octahedral aluminium (T01 to T02). Incorporation of a second chlorine into the tetrahedral environment (T03) destabilizes the LUMO orbital energy of the cluster from -2.515 Hartree to -0.740 Hartree. However dichlorination of the octahedral aluminium environment maintained the strong Lewis acidity of the cluster (T05) when the LUMO orbital energy of -2.867 Hartree was obtained. Further chlorination of this cluster by incorporating a chlorine atom into the tetrahedral aluminium environment (T06) and deprotonation of the bridging oxygen atom (T07) destabilized the LUMO orbital energy of this cluster.

The results from the Al_{oct}-O_b-Al_{oct} cluster models (Table 7.3, Figure 7.7) showed that chlorinating the cluster enhanced the Lewis acidity as shown by a lowering of the LUMO orbital energy of the cluster. The LUMO orbital energy of the fully hydroxylated cluster (001) at +0.092 Hartree was in good agreement with the value of +0.107 Hartree reported for a similarly structured cluster in an α-alumina study (177). Substitution of additional chlorine into the cluster (006 to 008) maintained the low LUMO orbital energy of the cluster.

In all the cluster models studied the LUMO orbital energy co-efficient was centred over one of the aluminium atoms in the cluster. A Mulliken-Löwdin electron population analysis of the clusters showed that the charge over the aluminium atom in the fully hydroxylated clusters was +1.365 ± 0.25 increasing to +1.472 ± 0.11 for the chlorinated cluster models. This result indicated that 7.27% of the electron density initially associated with the aluminium atom was redistributed over the cluster when chlorine was added to the model.

7.3 HOMO - LUMO Energy Gap for the γ-Alumina Cluster Models.

The results for the investigation of the energy gap between the HOMO and LUMO orbital for a given cluster are presented in table 7.3 and figures 7.5 to 7.7. The energy gap results show that the Al_{oct}-O_b-Al_{oct} and the Al_{tet}-O_b-Al_{tet} energy gaps were 8.82 eV and 7.87 eV for the clusters CO1 and TO1 respectively. This value was in good

agreement with conductivity experiments (201) which showed that γ-alumina was an electrical insulator with an Egap > 8eV. The incorporation of chlorine into the cluster had the effect of reducing the calculated Egap. Chlorination of the clusters 001 to 002 to 003 resulted in narrowing the Egap from 8.82eV to 4.75eV to 2.34eV respectively. The Egap was further reduced if chlorination of the cluster together with deprotonation had occurred. In the clusters 006 to 007 the Egap was reduced from 5.33eV to 1.99eV. The smallest Egaps were achieved by the chlorinated deprotonated clusters TO4 at 2.79eV, T07 at 3.84eV, TT7 at 1.99eV, TT6 at 3.16eV and 007 at 1.99eV.

CHAPTER 8.

Characterization of the γ-Alumina Crystallite Material.

Prior to the construction of the cluster models for quantum mechanical analysis the interatomic bond distances were required to be evaluated for the γ-alumina crystallite material. This was achieved by using x-ray powder diffraction methods on the crystallites that comprise the calcined γ-alumina samples. The information obtained from the analysis of the solid by x-ray diffraction together with the derivation of the aluminium environments from the [110] face of the spinel unit cell led to the construction of the cluster models on which the SCF-UHF single point molecular orbital calculations were performed.

8.2.1 The X-Ray Powder-Diffraction of Spinel γ-Alumina Calcined to 523 K.

The results of the x-ray diffraction from a CuKα source (1.5405 Å) are presented in table 8.1. From the small number of absorption bands obtained from the γ-alumina sample it was shown that γ-alumina has a face centred cubic lattice (the $h^2+k^2+l^2$ series is specific for F.C.C) with a length 12.456±0.19 Å. According to the Rooksby classification of aluminas (41) d-spacings of 1.971 Å and 1.415 Å are specific to γ-alumina, hence the sample calcined to 523 K had retained the γ-phase. From figure 1.b it was shown that the γ-alumina spinel structure consisted of an outer face centred cubic lattice with inner cubes consisting of alternating octahedrally arranged

Table 8.1.

2θ	θ	$\sin^2\theta$	Empirical	$(h^2+k^2+l^2)$	$\frac{\lambda}{2\sin\theta}$	Cl_o
12.4	6.2	0.0117	1	3[100]	7.13	12.34
13.8	6.9	0.0144	1.23	4[200]	6.41	12.82
28.4	14.2	0.0612	5.23	16[400]	3.14	12.56
38.1	19.5	0.1065	9.20	27[333]	2.36	12.26
46.0	23.0	0.1527	13.05	40[620]	1.971	12.46
47.8	23.9	0.1641	14.02	43[533]	1.90	12.46
65.9	32.95	0.2958	25.28	76[662]	1.415	12.29

$$Cl = 12.456 \pm 0.19 \text{ Å}$$

aluminium and tetrahedrally arranged aluminium atoms. The [200] plane of the unit cell cuts through the face centred aluminium atoms at 6.228 Å and hence the octahedrally arranged aluminium cube is contained in a volume of 18.339 Å^3. The base of this cube has the Miller indices of [161] and hence the d-spacing for this face was at 2.02 Å from the [100] face. Similarily all the faces of the cube were sited 2.02 Å in from the [100] or [200] faces resulting in the dimensions of the octahedral cube being 2.188 Å cubed. Therefore the octahedral Al-O bond distance in the cube was 2.188 Å. The tetrahedral aluminium cube had sides of the same dimension which resulted in the tetrahedral Al-O bond length of 1.89 Å. The bond distance from the aluminium atoms that made up the face centred cubic unit cell to the oxygen atoms at the corners of the inner cubes are contained in the [660] plane and resulted in a d-spacing for this face of 1.467 Å, making this Al-O bond distance of 2.49 Å.

In the cluster model study the tetrahedral Al-O bond lengths used to determine cluster atom co-ordinates were 1.89 Å and 2.19 Å for the octahedral Al-O bond distance.

8.2.2 ^{27}Aluminium MAS-NMR Study of Calcined γ-Alumina and Chlorine promoted γ-Aluminas.

The ^{27}Al MAS-NMR spectra are presented in figures 8.1 to 8.7. The results had shown (Figure 8.1) that the ^{27}Al MAS-NMR produced a main broad peak at 6.944 ppm attributed to the octahedral aluminium environments of

Figure 8.1

^{27}Al MAS NMR of Al_2O_3 Calcined at 523K Single Pulse Decoupled.

Spin Rate 2950 Hz

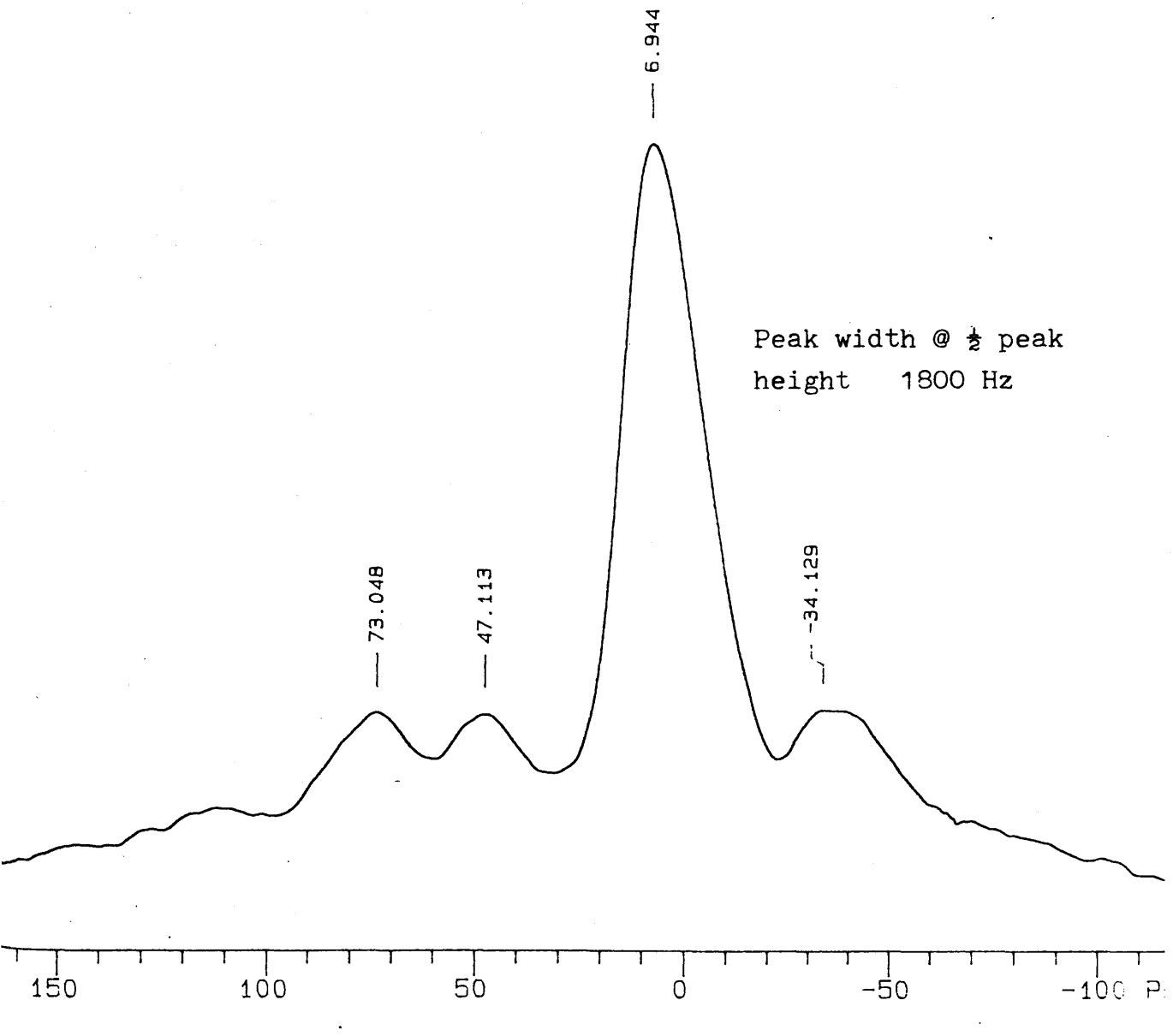

calcined γ-alumina. A smaller broad peak at 73.1 ppm was attributed to the tetrahedral aluminium environments. Both these peaks were consistent with the values reported for the octahedral and tetrahedral environments of γ-alumina (199). Spinning side bands at 47.1 ppm and 34.1 ppm were observed and were shifted when the spin rate was raised to 4000 Hz (Figure 8.5). The γ-alumina sample calcined to 523 K produced a peak width at half peak height for octahedral aluminium environments of 1800 Hz.

The ^{27}Al MAS-NMR for the γ-alumina sample calcined to 523 K and treated at 293 K with anhydrous gaseous hydrogen chloride (uptake of HCl = 2.05 ± 0.02 mmol g^{-1}) is presented in figure 8.2. The peak attributed to the octahedral aluminium environment was found at 5.4 ppm which was upfield from the comparable signal obtained from calcined material. The peak attributed to the tetrahedral aluminium environment was also shifted upfield to 69.8 ppm. The shift upfield had indicated that the ^{27}Al environments had been shielded by the chlorine treatment. The peak attributed to the octahedral aluminium environment produced a peak width at half peak height of 2200 Hz for the hydrogen-chloride treated material.

The ^{27}Al MAS-NMR obtained from the γ-alumina sample treated with anhydrous gaseous carbon tetrachloride at 500 K is presented in figure 8.3. The peak due to the octahedral aluminium environment was recorded at 5.2 ppm and the tetrahedral aluminium environments recorded a peak at 69.8 ppm. The peak due to the octahedral aluminium environment recorded a peak width of half peak height of 2450 Hz.

Figure 8.2

^{27}Al MAS NMR of Anhydrous Hydrogen Chloride treated Calcined Al_2O_3 Single Pulse Decoupled.

Spin Rate 3000 Hz

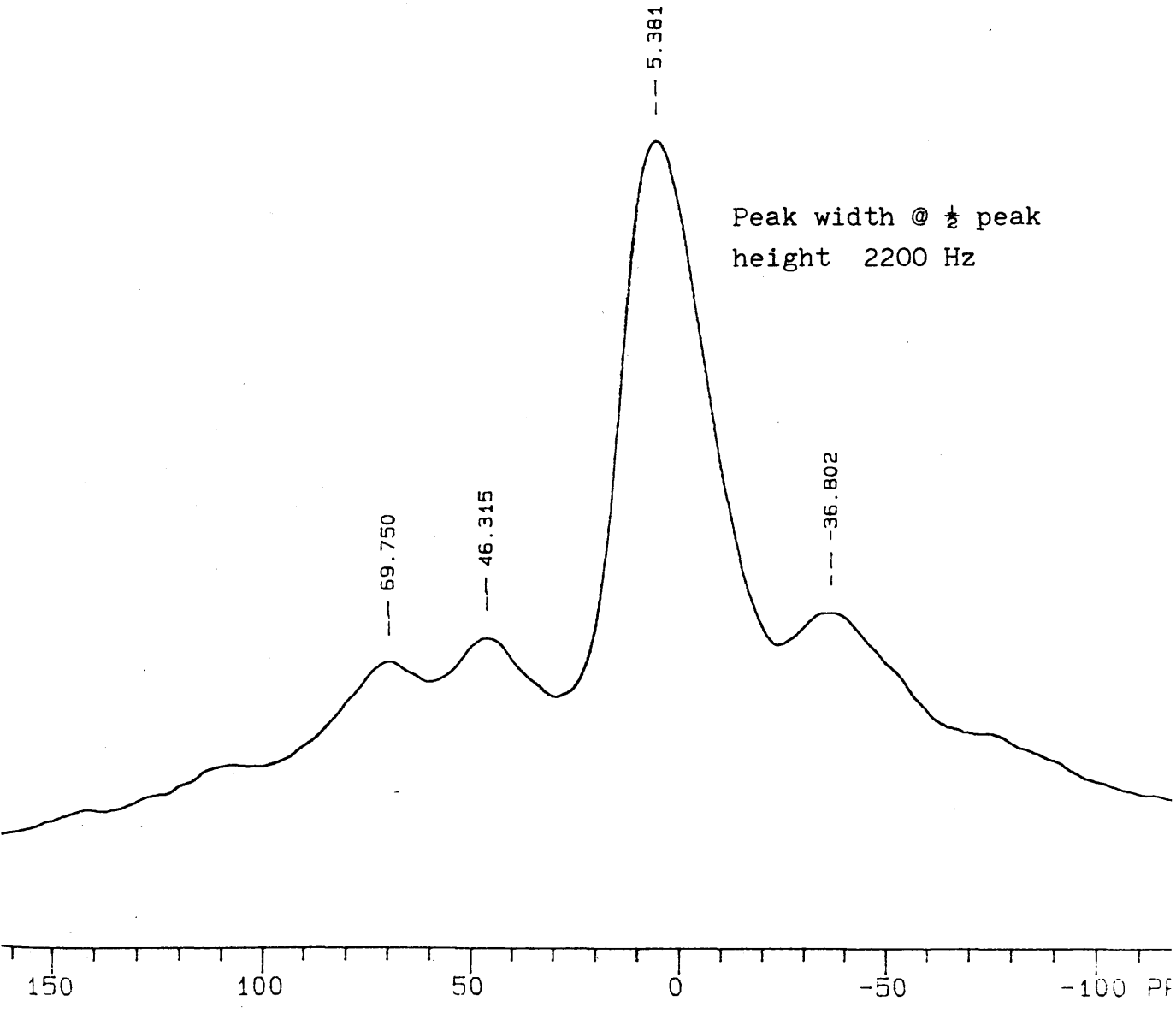

Figure 8.3

^{27}Al MAS NMR for carbon tetrachloride treated Al_2O_3 Single Pulse Decoupled.

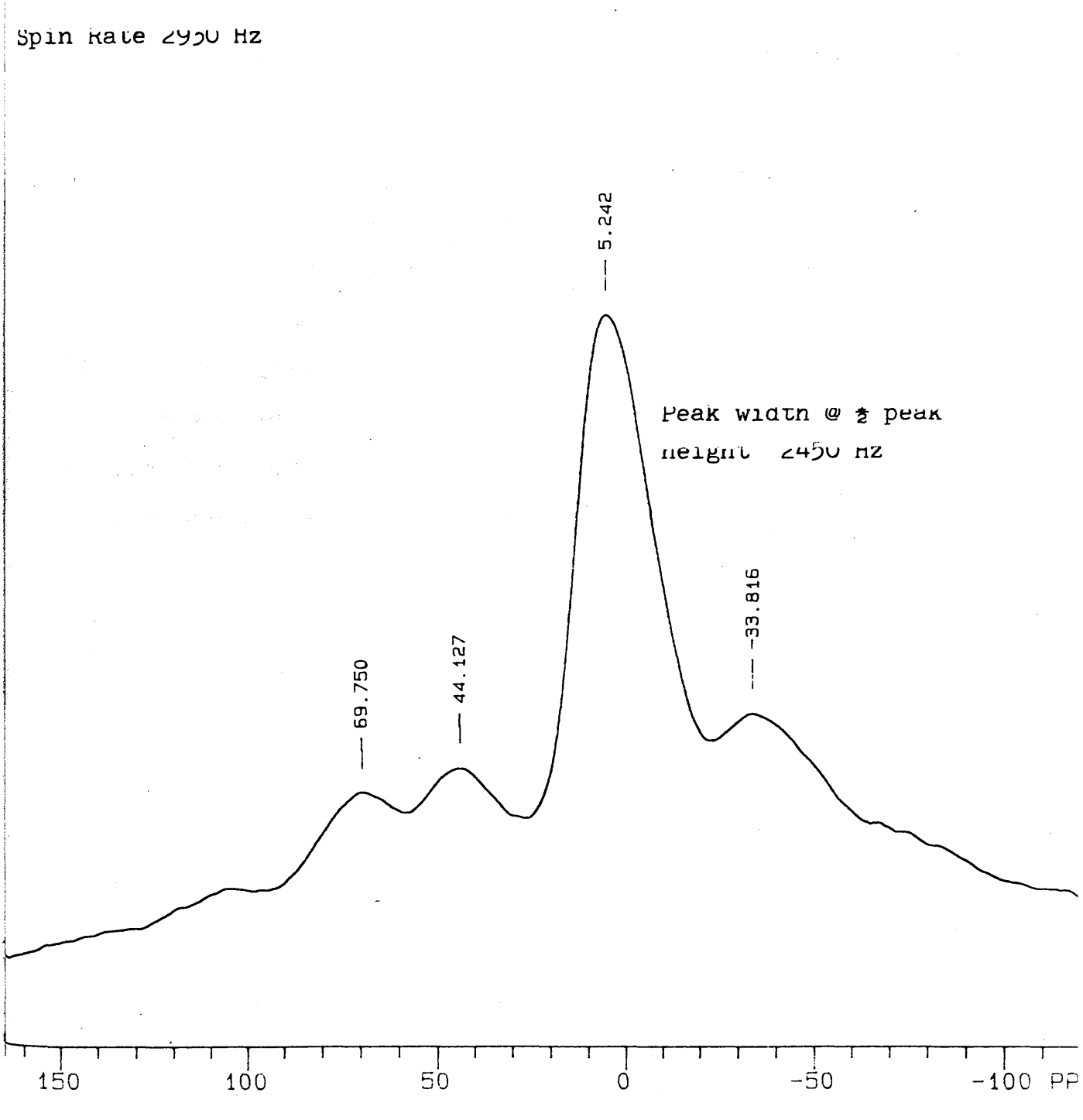

The ^{27}Al MAS-NMR spectra for anhydrous aluminium trichloride is presented in figure 8.4. The sample possessed exclusively octahedral aluminium environments and the sharp peak recorded at -1.250 ppm gave a peak width at half peak height of 300 Hz which indicated the high degree of long and short range order in the sample.

The results of the chlorinated γ-alumina samples showed that shielding of the ^{27}Al environments had occurred with the chlorination treatment and was consistent with the formation of Al-Cl bonds. The increase in the half peak height from 1800 Hz to 2200 Hz and to 2450 Hz for the calcined material, hydrogen chloride treated material and carbon tetrachloride treated material respectively had shown that a breakdown in the short and long range order of the sample had occurred, with the carbon tetrachloride treatment creating the greatest electronic asymmetry in the ^{27}Al environments.

Figure 8.4

^{27}Al MAS NMR of Anhydrous $AlCl_3$

Spin Rate 3225 Hz

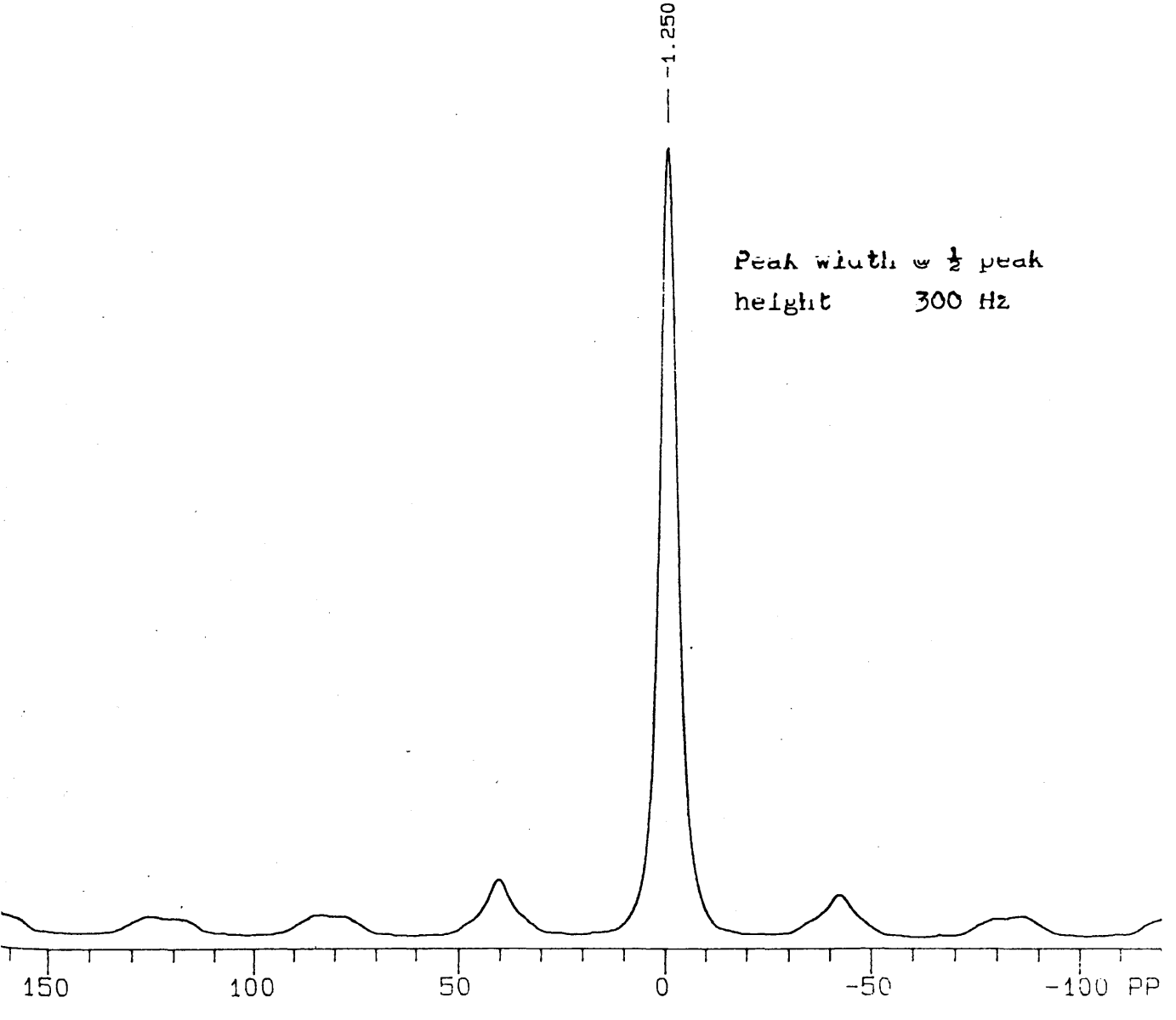

Figure 3.5

^{27}Al MAS NMR of Al_2O_3 Calcined at 523K Single Pulse Decoupled

Spin Rate 5700 Hz

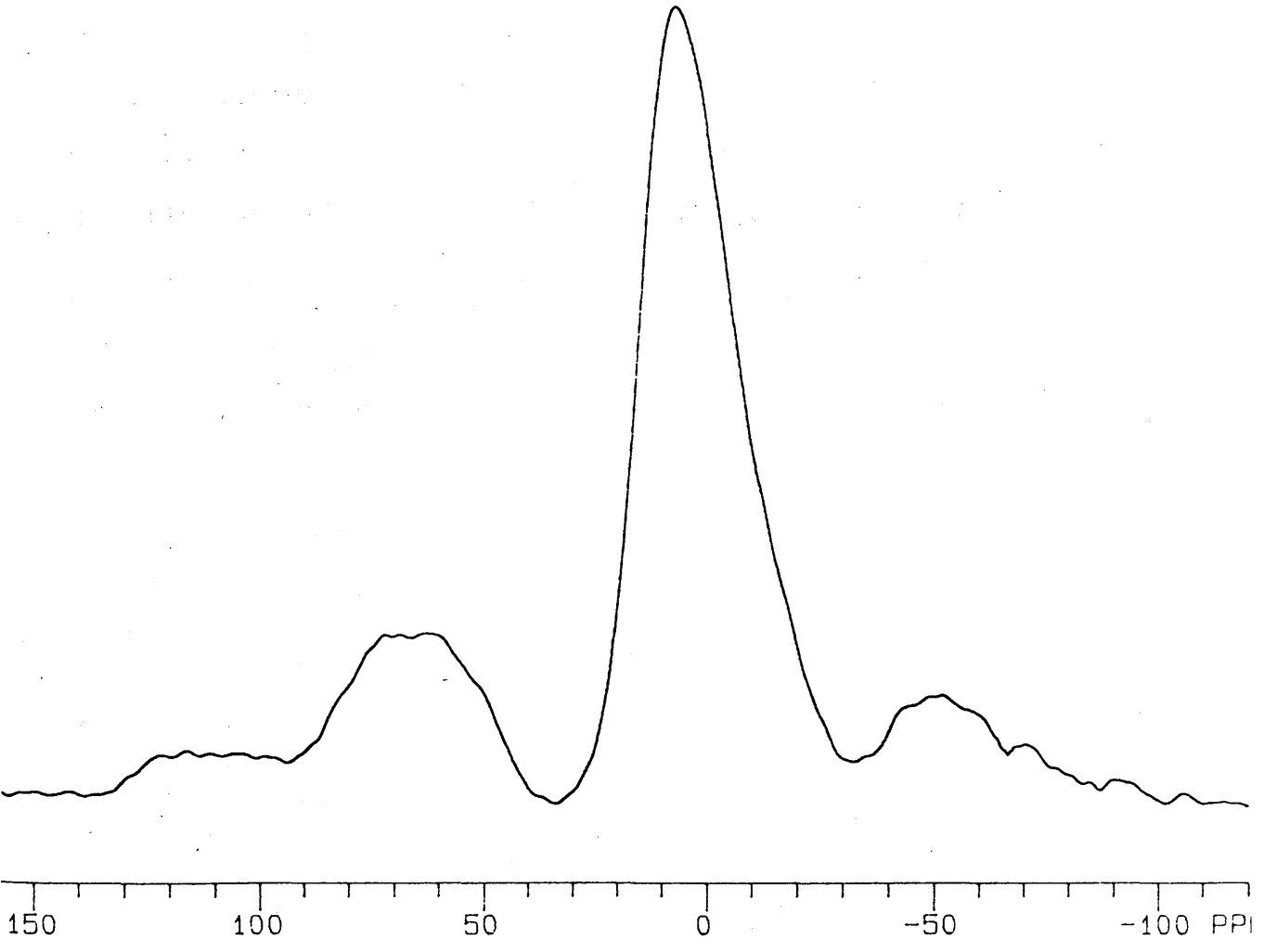

CHAPTER 9.

DISCUSSION.

The experimental chapters have shown that the calcination of γ-alumina samples resulted in an increase in the B.E.T area of the material whilst the subsequent chlorination of the calcined γ-alumina samples reduced the B.E.T area of the calcined material across the calcination range 293K to 523K. Treatment of the γ-alumina samples using anhydrous hydrogen chloride resulted in labile surface chlorine species and the formation of an inactive catalyst species towards the catalytic dehydrochlorination at 293K of 1,1,1 trichloroethane. Treatment of the calcined γ-alumina material with CCl_4 produced both labile and non-labile surface chlorine species together with an active catalyst towards the dehydrochlorination of 1,1,1 trichloroethane at 293K.

The B.E.T areas of the calcined γ-alumina samples show a uniform reduction with anhydrous hydrogen chloride treatment of the calcined γ-alumina samples in the calcination temperature range 293K to 523K (Table 3.1) for both the Spence and Condea γ-alumina samples. The extent of the reduction in the B.E.T area for a chlorinated sample is shown by the ratio of the B.E.T area of the chlorinated sample to the B.E.T area of the precalcined sample (Figure 3.4). The ratio of the extent of surface reduction owing to the chlorination, to the B.E.T area of the calcined material as a function of the calcination temperature, is the same as the individual correlation of the calcination temperature with:-

i) The B.E.T area of the calcined γ-alumina samples and

ii) The B.E.T area of the treated anhydrous hydrogen chloride calcined γ-alumina samples.

This continuity in the correlation of the B.E.T areas as a function of the calcination temperature is consistent with the treatment of the γ-alumina samples with anhydrous hydrogen chloride being limited to the surface, with no detectable diffusion of chlorine into the bulk of the γ-alumina crystallite material.

The surface density of chlorine at saturation uptake levels on the γ-alumina sample which had been calcined at 293K was found to be 13.27±0.75 chlorine atoms nm^{-2} (Table 3.1). This value is in good agreement with the surface density of hydroxyl groups on γ-alumina of 12-16 hydroxyl groups nm^{-2} (37). The surface density of chlorine at saturation uptake levels on γ-alumina which had been calcined at 373K is found to be 8.82±1.15 chlorine atoms nm^{-2} and this value is in exact agreement with the surface density of hydroxyl groups on γ-alumina calcined at 373K (69).

The results of the ^{27}Al MAS-NMR (Section 8.2.2) of solid γ-alumina samples treated with anhydrous hydrogen chloride shows that shielding of the aluminium environment occurs with a shift upfield of the signals arising from the tetrahedral environment of ^{27}Al from 73.048 ppm to 69.750 ppm (Figure 8.2). The chemical shifts for octahedral environment of ^{27}Al was moved upfield from 6.94 ppm to 5.38 ppm for the treated anhydrous hydrogen chloride calcined γ-alumina sample. The shielding of ^{27}Al is consistent with bonding between the surface chlorine and the surface aluminium atom.

The hydrogen chloride treatment of γ-alumina results in a breakdown in the long range order of the sample. The peak width at half peak height for the octahedral ^{27}Al environment is increased from 1800 Hz in the calcined γ-alumina sample to 2200 Hz for the sample treated with anhydrous hydrogen chloride. The peak width is an indicator of the extent of long range order in the sample as exemplified by the peak width at half peak height of 300 Hz for the highly ordered $AlCl_3$ sample (Figure 8.4).

The adsorption of hydrogen chloride by the γ-alumina surface is consistent with the proposed schemes shown in figure 9.1 using the Al_{oct}-O_b-Al_{oct} arrangement from figure 1F. Figure 9.1i represents a possible mechanism for the displacement of a weakly bound hydroxyl group by hydrogen chloride to form water and a monochlorinated co-ordinatively saturated aluminium environment. In the case where a terminal hydroxyl group is strongly bound to the surface, owing to the local configuration of atoms conferring strong Lewis acidity on the aluminium environment (Section 7.2), the hydrogen chloride may be hydrogen bonded to the γ-alumina surface. This process would result in an equilibrium being established between the hydrogen bonded species and the formation of an ion pair (Figure 9.1ii). During the calcination process, when water has been desorbed from the surface to form a deprotonated bridging oxygen atom and an exposed aluminium atom on the γ-alumina surface, the dissociative adsorption of hydrogen chloride can occur to produce a monochlorinated coordinatively saturated aluminium and a reprotonated bridging oxygen (Figure 9.1.iii). The

Figure 9.1

Chlorination of the γ-Alumina Surface by Anhydrous Gaseous Hydrogen Chloride.

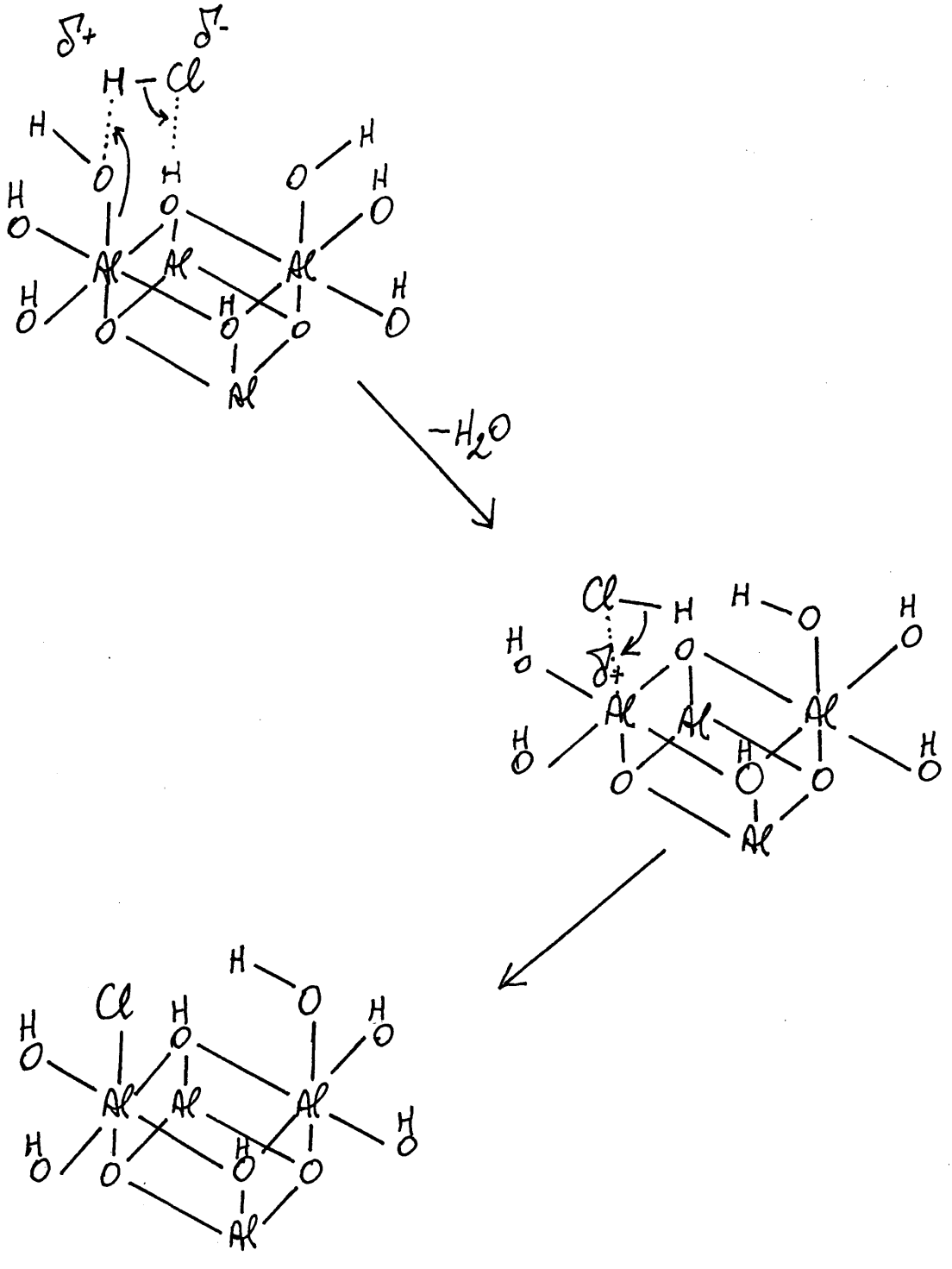

Displacement of a surface hydroxyl group by hydrogen chloride.

Figure 9.1 (continued)

ii)

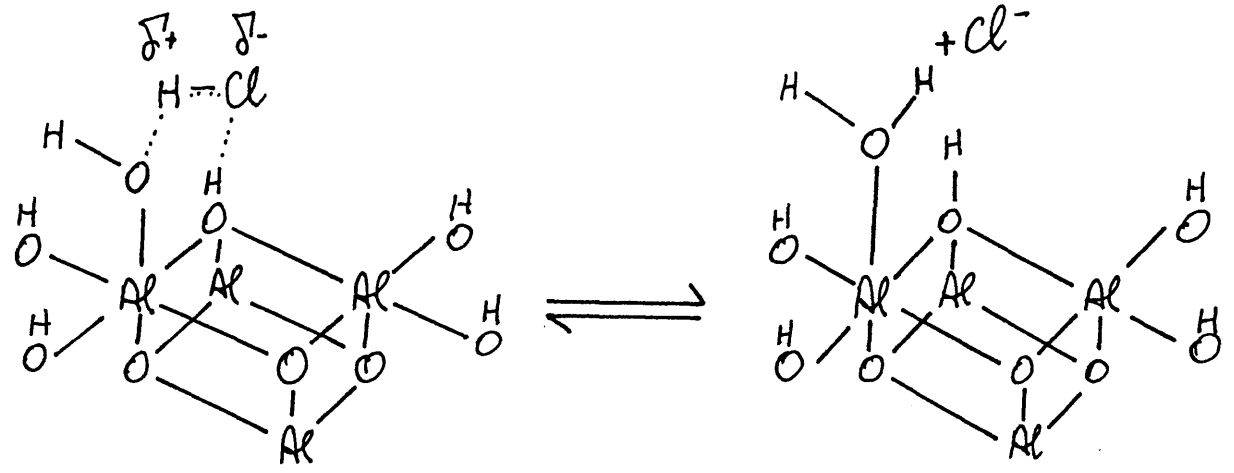

Complex formation where the hydroxyl group is strongly bound to the surface.

iii)

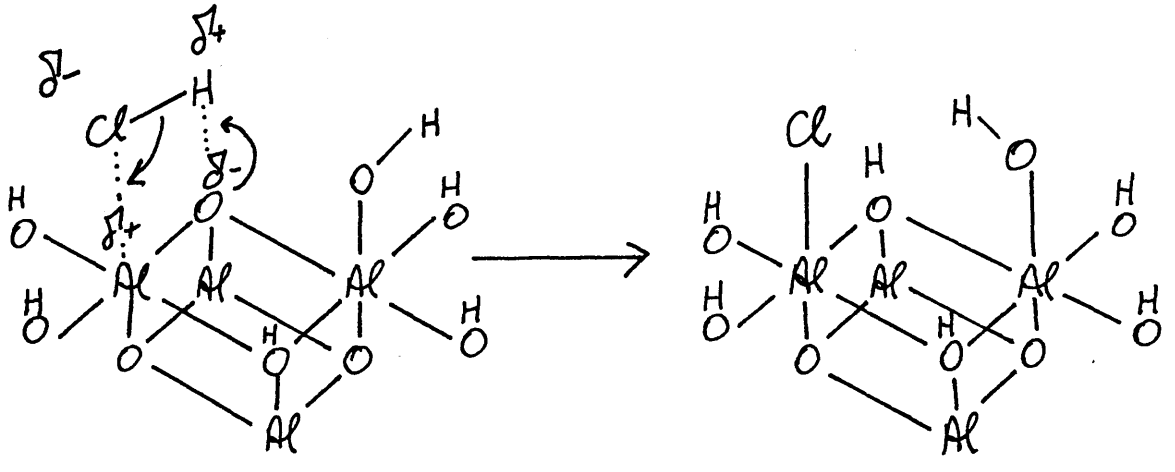

Dissociative adsorption of hydrogen chloride at a co-ordinatively unsaturated surface aluminium.

protonated bridging oxygen can be better regarded as an oxonium moiety and the source of Brønsted acidity.

The exchange reactions of the hydrogen chloride treated γ-alumina surface with anhydrous [^{36}Cl]-chlorine labelled hydrogen chloride showed that exchange of the surface chlorine occurs with no uptake of chlorine by the γ-alumina sample. Hence the chlorine adsorbed by the γ-alumina surface from the hydrogen chloride treatment is labile at ambient temperatures (Section 3.2.6, Table 3.4, Figure 3.7). When anhydrous deuterium chloride was used as the chlorinating reagent for the calcined γ-alumina and the treated surface was exchanged with anhydrous hydrogen chloride, deuterium chloride was found in the equilibrium gas phase mixture which shows that there was exchange of DCl for HCl or that the hydrogen was also labile (Section 3.2.9) thus exhibiting Brønsted acid character. The proposed exchange reactions at 293K are presented in figure 9.2. Figure 9.2.i shows schematically the exchange reaction between the γ-alumina surface treated with anhydrous hydrogen chloride and a [^{36}Cl]-chlorine labelled hydrogen chloride molecule. As the gas phase molecule approaches the exchange site, coulombic attraction arising from hydrogen bonding minimises the conformational energy between the chlorinated surface and the substrate. When alignment of the hydrogen chloride molecule is achieved a concerted exchange mechanism results. It is proposed that the reverse reaction is possible when the hydrogen on the bridging oxygen is a strong Brønsted acid (Figure 9.2.ii). The deprotonated bridging oxygen is then reprotonated by dissociative adsorption of the hydrogen chloride associated

Figure 9.2

Exchange @293K of HCl with the γ-Alumina Surface treated with Anhydrous Hydrogen Chloride.

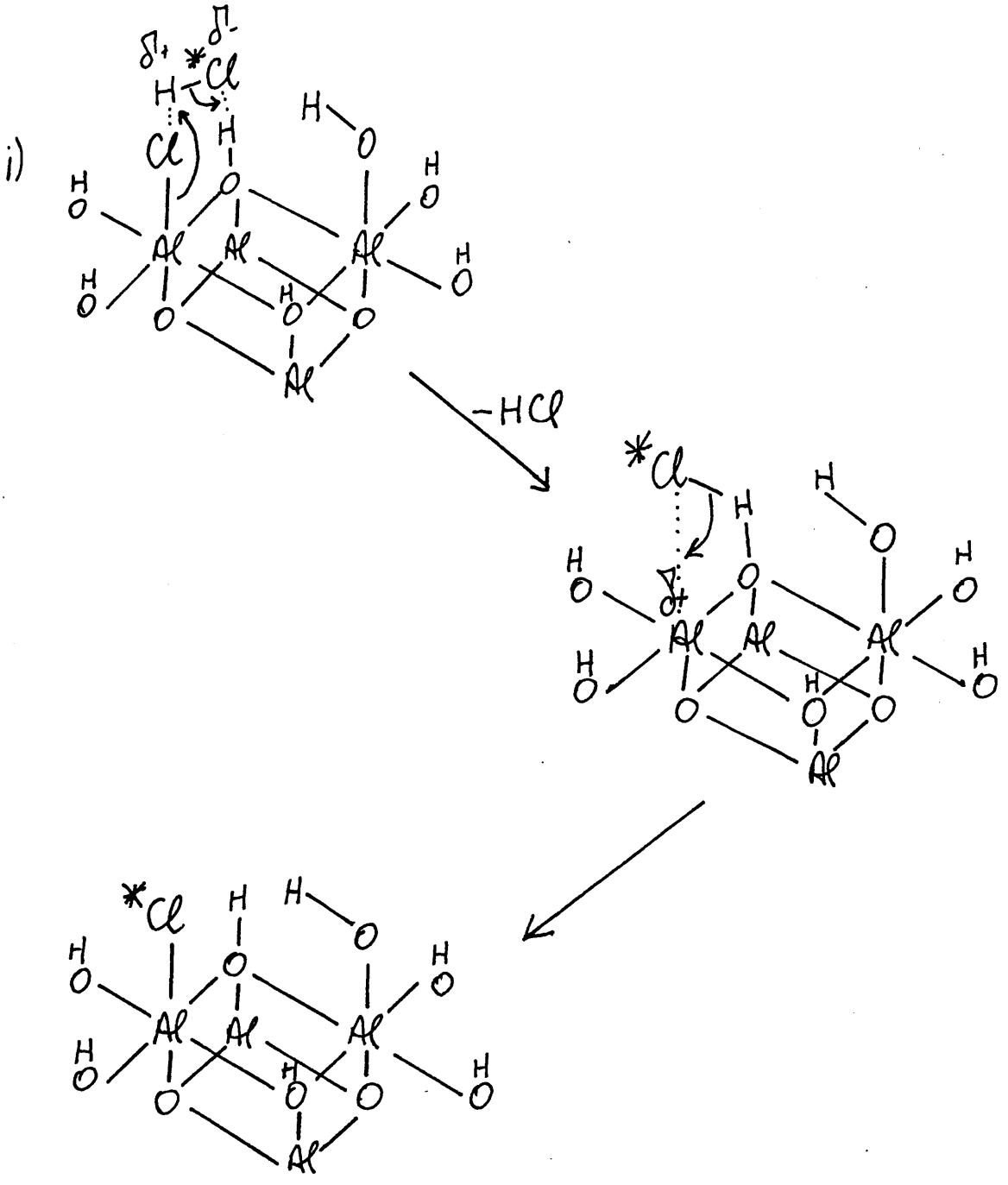

Figure 9.2 (cont.)

ii)

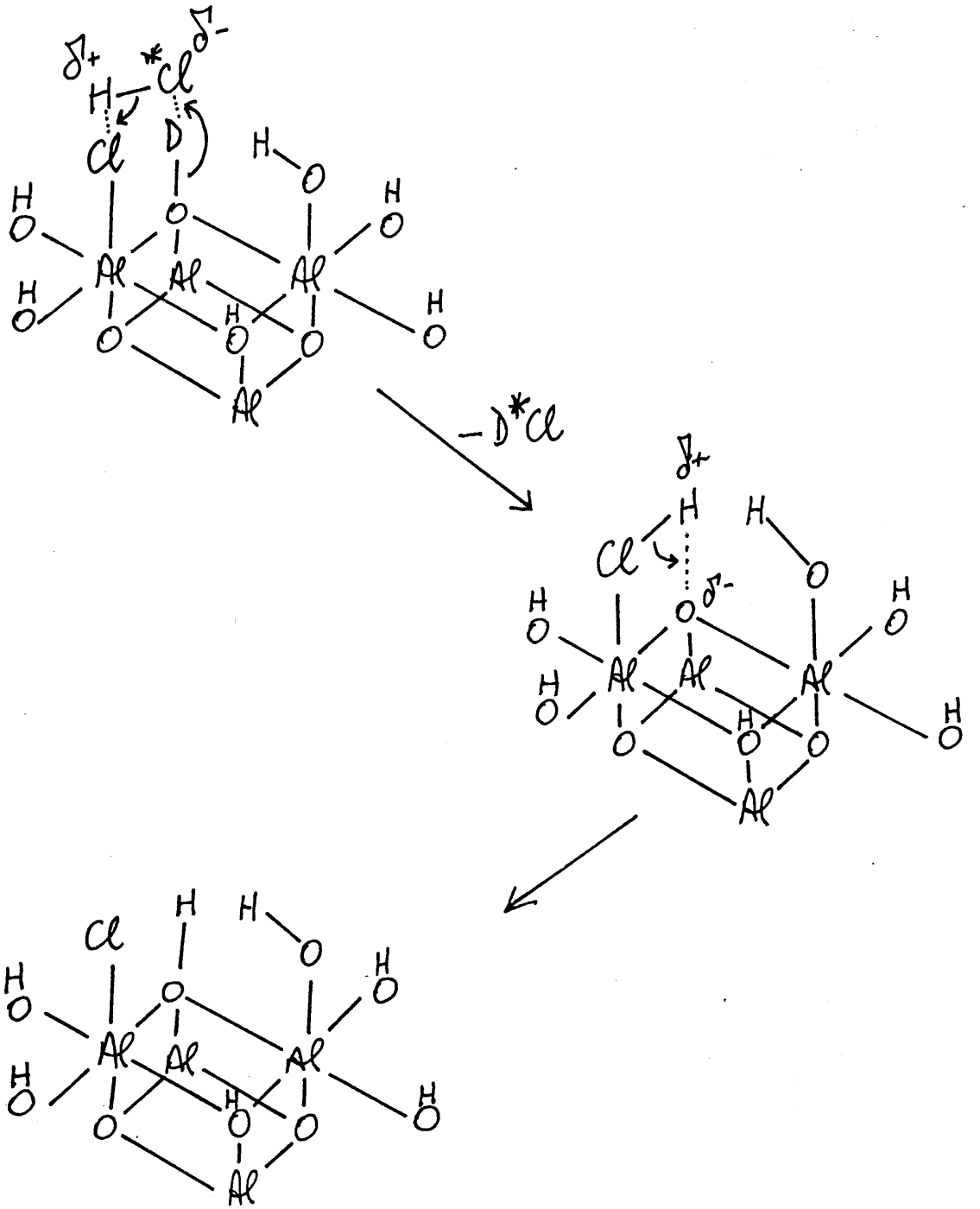

with the aluminium atom at the exchange site.

The γ-alumina treated with anhydrous hydrogen chloride did not exhibit catalytic activity towards the dehydrochlorination of 1,1,1 trichloroethane at 293K (Section 5.2.2) or towards the polymerization of the product of dehydrochlorination of 1,1,1 trichloroethane, that is 1,1 dichloroethene (Section 5.2.8) which, in the context of Lewis acid catalysts requires a strong co-ordinatively unsaturated acid site to initiate it (23).

There was no reaction at 293K leading to the reformation of 1,1,1 trichloroethane from an equimolar mixture of anhydrous hydrogen chloride and 1,1 dichloroethene (Section 5.2.8) or exchange of chlorine between 1,1 dichloroethene and the γ-alumina surface treated with [^{36}Cl]-chlorine labelled hydrogen chloride (Section 5.2.8). The surface site which is produced from the treatment of γ-alumina by anhydrous hydrogen chloride is named the G-site.

Chlorination of the γ-alumina surface by gaseous carbon tetrachloride requires a minimum reaction temperature of 423K and at this temperature CO_2, $COCl_2$, HCl and H_2O were formed (Section 4.2.2). Chlorination of the surface using 1,1 dichloromethanone at 500K also produces an active catalyst for the low temperature dehydrochlorination of 1,1,1 trichloroethane (Section 5.2.6) and the gas products CO_2, HCl and H_2O (Section 4.2.15). The chlorination of the γ-alumina surface by carbon tetrachloride proceeds via the formation of $COCl_2$ and CO_2 (Section 1.8) with no detectable carbon laydown from the carbon tetrachloride treatment (Section 4.2.12). The

1,1 dichloromethanone that is produced during the γ-alumina chlorination process reacts with a surface hydroxyl group (Section 4.2.15) or by a gas phase reaction with water vapour to produce hydrogen chloride and carbon dioxide (202). The hydrogen chloride thus produced can then react with the γ-alumina surface to form a G-site. The production of $COCl_2$ and CO_2 from the carbon tetrachloride is consistent with the deposition of two chlorine atoms being exchanged for one oxygen atom from the surface of γ-alumina. The neutron activation analysis results shows that the treatment of γ-alumina by carbon tetrachloride results in a greater surface density of chlorine compared with the treatment with hydrogen chloride (compare Table 4.3 with Table 3.1). The carbon tetrachloride treatment of the calcined γ-alumina results in a chlorine content of 7.6 - 10.8% w/w chlorine compared with 6.5 - 7.0% w/w chlorine from the hydrogen chloride treatment. The results show that up to 50% more chlorine was retained by the surface from the carbon tetrachloride treatment of γ-alumina.

The chlorination of the γ-alumina by carbon tetrachloride results in a reduction in the B.E.T area of the chlorinated material as compared with the calcined sample (Table 4.2, Figure 4.3). The relationship between the extent of the reduction in the B.E.T area and the calcination temperature is the same as that for the:

i) B.E.T area of the calcined material.

ii) B.E.T area of the carbon tetrachloride treated material

as a function of the calcination temperature between 293K and 473K. A small deviation from the extent of the B.E.T area

reduction for the chlorinated material as a function of calcination temperature is observed for the γ-alumina material calcined at 523K (Figure 4.3). This result suggests that the carbon tetrachloride treatment is effecting an attack on the bulk of the γ-alumina crystallite. The chlorination of the γ-alumina by carbon tetrachloride involving the removal of the bridging oxygen atoms can lead to sintering of the catalyst, under severe conditions, with the formation of $AlCl_3$ (100). The results from the B.E.T area determinations are consistent with the CCl_4 chlorination process being limited to the surface up to the reaction temperature of 473K.

The ^{27}Al-MAS NMR from a CCl_4 treated γ-alumina sample is consistent with the presence of an Al-Cl bond. The signal from the octahedral environment of aluminium was shifted upfield in the case of the CCl_4 treated material (Figure 8.3) to 5.24 ppm from 6.94 ppm recorded for the calcined γ-alumina sample (Figure 8.1). The shielding of the ^{27}Al environment from the CCl_4 treated γ-alumina material was not significantly increased from that observed for the hydrogen chloride treated material which gave a signal for the octahedral environment of aluminium at 5.38 ppm (Figure 8.2). The small change was due to the small number of CCl_4 chlorinated sites present on the surface of $\sim$ 8% of the total ^{27}Al content in the crystallite γ-alumina material, compared to $\sim$ 20% of total ^{27}Al content chlorinated by the hydrogen chloride treatment. Significantly, the peak width at half peak height for the octahedral environment of aluminium has increased to 2450 Hz from 1800 Hz in the calcined material compared with 2200 Hz for the hydrogen chloride treated

material (Figures 8.1 to 8.3). These results show that a further breakdown in the long range order of the crystallite material had occurred as a result of the carbon tetrachloride treatment. Together these factors lead to the proposed chlorination of γ-alumina by CCl_4 shown in figure 9.3.

It is proposed that during the calcination stage dehydration of the surface by the dehydroxylation process (Section 1.7) results in exposed aluminium atoms on the surface and deprotonated bridging oxygen atoms. It can be considered that coulombic forces presents the CCl_4 molecule at the surface where the small charge differential over the carbon atom (due to the inductive effect from the bonded chlorine atoms) attracts electron density from the thermally activated bridging oxygen atom to produce $COCl_2$. The chlorine atoms from the CCl_4 are available to chlorinate each of the aluminium atoms that are present on each side of the bridging oxygen atoms. When the chlorination of the γ-alumina surface has occurred the 1,1 dichloromethanone formed is able to desorb from the surface. The exact mechanism for the chlorination process was not studied in this work. However, no carbon laydown was observed from [^{14}C]-carbon labelled CCl_4 studies (Section 4.2.12), whereas chlorine laydown was observed from [^{36}Cl]-chlorine labelled CCl_4 studies (Figure 4.8) together with the formation of 1,1 dichloromethanone. The result of the removal of the bridging oxygen is that the chlorinated aluminium atom formed is not co-ordinatively saturated as was the proposed case for the hydrogen chloride treatment. The further removal of any residual activated deprotonated bridging

Figure 9.3

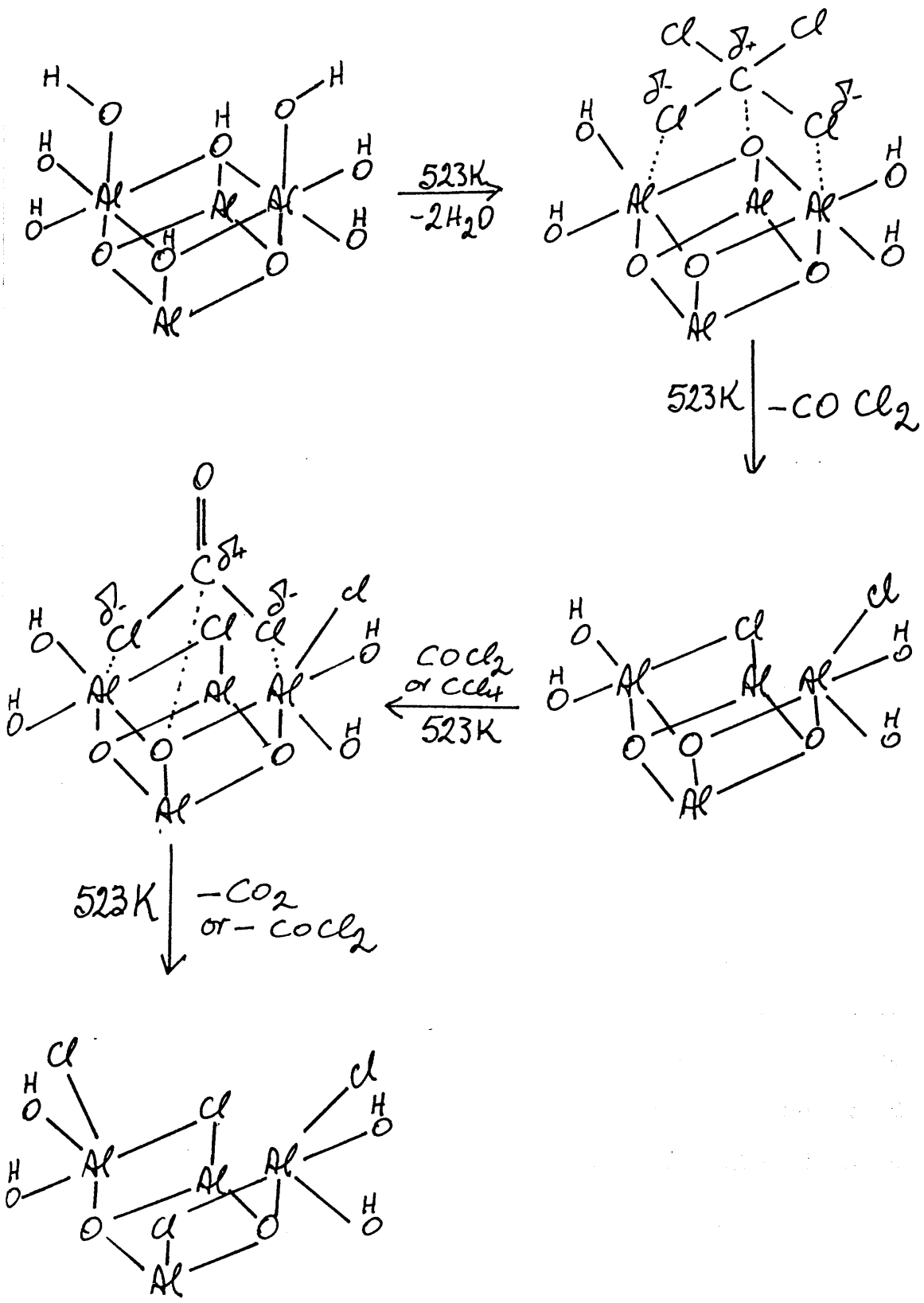

oxygen by the reaction with $COCl_2$ or another CCl_4 molecule will lead to the production of a co-ordinatively unsaturated dichlorinated aluminium site. Hence, the chlorination of γ-alumina by CCl_4 can result in two types of chlorination processes occurring:-

i) The production of co-ordinatively unsaturated aluminium by the reaction of CCl_4 or $COCl_2$ on the surface of γ-alumina at 500K.

ii) The production of co-ordinatively saturated chlorinated aluminium from the reaction of the hydrogen chloride by-product from the reaction of 1,1 dichloromethanone with surface bound water or hydroxyl groups and/or the gas phase reaction with water vapour. In order to distinguish the two types of sites, the site produced by the reaction of CCl_4 or $COCl_2$ with the surface of γ-alumina is called the J-site, and, as mentioned earlier, the site produced by the reaction of HCl the G-site.

The exchange of anhydrous [^{36}Cl]-chlorine labelled hydrogen chloride with carbon tetrachloride treated γ-alumina results in between 61-77% of the chlorine content of the γ-alumina being labile (Table 4.5). This labile chlorine is shown to originate from the chlorination of γ-alumina with hydrogen chloride, namely the G-site. The residual 23-39% of non-exchangeable chlorine associated with the J-site is shown to be non-exchangeable at 293K with CCl_4 (Section 4.2.10) anhydrous gaseous HCl (Section 4.2.5) and 1,1 dichloromethanone (Section 4.2.19). Figure 9.4 summarizes the ratio of J-site chlorine retained by the surface from the carbon tetrachloride treatment to the total chlorine content.

Figure 9.4

Removal of surface activity of $H^{36}Cl$/γ-alumina treated @ 523 K and $[^{36}Cl]$ -CCl_4/γ-alumina treated @ 523 K and each exchanged out with HCl

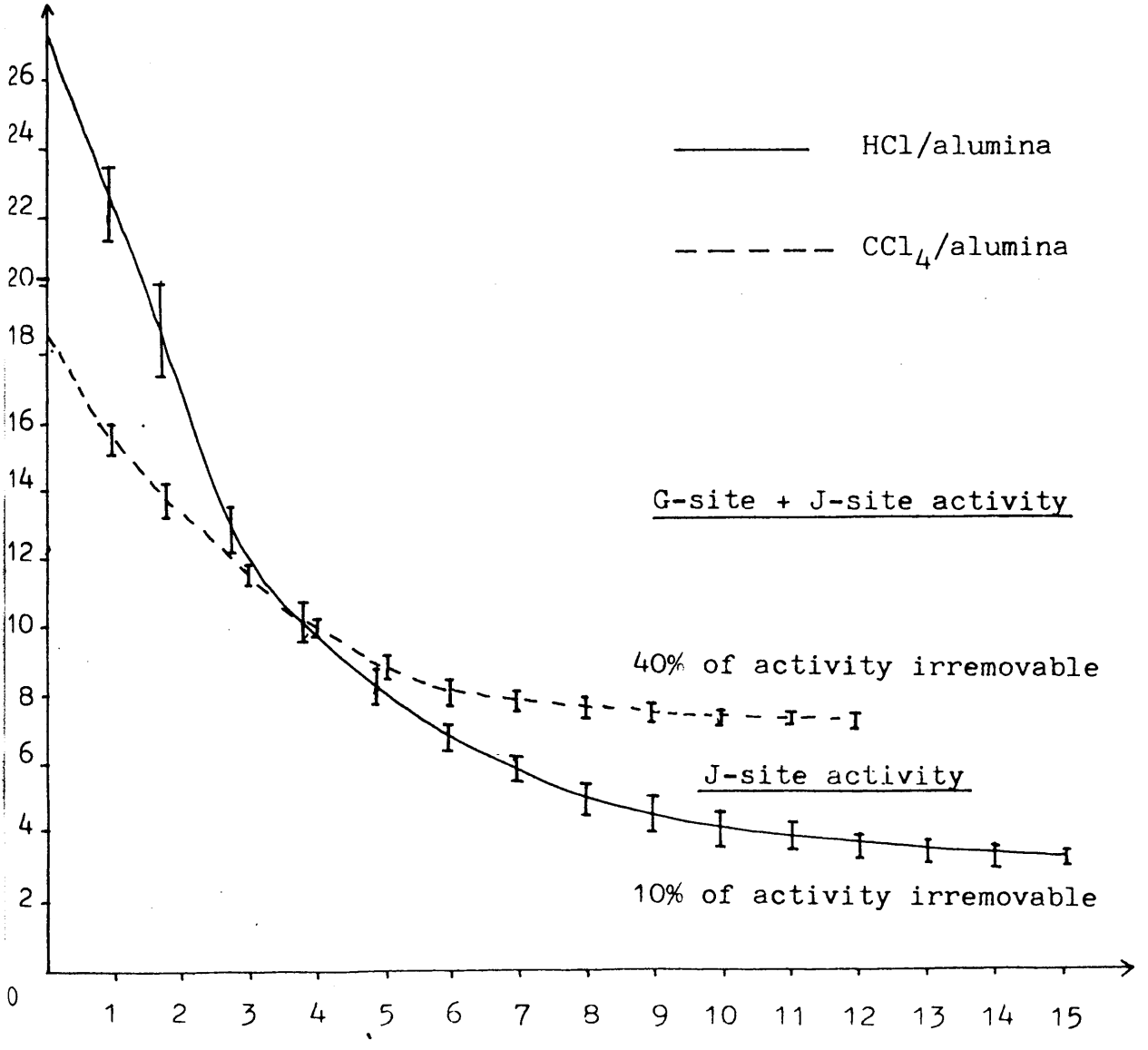

The labile chlorine originating from the G-site made it possible to selectively label either the G-site or the J-site. If the G-site was to be specifically labelled, treatment of the γ-alumina surface with carbon tetrachloride followed by exchanging in [^{36}Cl]-chlorine labelled hydrogen chloride incorporated the [^{36}Cl]-chlorine label into the G-site. Conversely, if the catalyst surface was treated with [^{36}Cl]-chlorine labelled carbon tetrachloride, the [^{36}Cl]-chlorine label on the G-site can be exchanged out by anhydrous hydrogen chloride leaving the label specifically at the J-site. The reactions of carbon tetrachloride with γ-alumina can be summarized as follows:-

i) $(O\text{-}Al\text{-}OH)_{2(s)} \xrightarrow[\text{calcination}]{500K} (O\text{-}Al\text{-}O_b\text{-}Al\text{-}O)_{(s)} + H_2O\ (g)$

ii) $(O\text{-}Al\text{-}O_b\text{-}Al\text{-}O)_{(s)} + CCl_{4(ads)} \xrightarrow{500K} 2(O\text{-}Al\text{-}Cl)_{(s)} + COCl_{2(g)}$

iii) $(O\text{-}Al\text{-}O_b\text{-}Al\text{-}O)_{(s)} + COCl_{2(ads)} \xrightarrow{500K} 2(O\text{-}Al\text{-}Cl)_{(s)} + CO_{2(g)}$

iv) $COCl_{2(g)} + H_2O_{(g)} \longrightarrow 2HCl_{(g)} + CO_{2(g)}$

v) $COCl_{2(ads)} + (O\text{-}Al\text{-}OH)_{2(s)} \longrightarrow (O\text{-}Al.Cl\text{-}OH\text{-}Al\text{-}O)_{(s)} + CO_{2(g)} + HCl_{(g)}$

vi) $(O\text{-}Al\text{-}O_b\text{-}Al\text{-}O)_{(s)} + HCl_{(ads)} \longrightarrow (O\text{-}Al.Cl\text{-}OH\text{-}Al\text{-}O)_{(s)}$

vii) $(O\text{-}Al.Cl\text{-}O_b\text{-}Al.Cl\text{-}O)_{(s)} + CCl_{4(ads)} \xrightarrow{500K} 2(O\text{-}AlCl_2)_{(s)} + COCl_{2(g)}$

viii) $(O\text{-}Al.Cl\text{-}O_b\text{-}Al.Cl\text{-}O)_{(s)} + COCl_{2(ads)} \xrightarrow{500K} 2(O\text{-}AlCl_2)_{(s)} + CO_{2(g)}$

In contrast to the treated hydrogen chloride γ-alumina surface where there was no detectable interaction between 1,1,1 trichloroethane or 1,1 dichloroethene and the surface at 293K, the carbon tetrachloride treated γ-alumina material catalyses the dehydrochlorination reaction at ambient temperatures (Section 5.2.4). Treatment of the γ-alumina surface with 1,1 dichloromethanone at 500K also produced a surface that was active towards the dehydrochlorination of 1,1,1 trichloroethane at 293K (Section 5.2.6). This active catalyst produced by carbon tetrachloride or 1,1 dichloromethanone treatment at 500K produced a light blue/purple hue in the material, this colour change was observed in all cases from the pure white colour of the untreated or hydrogen chloride treated γ-alumina samples.

The observed decomposition of 1,1,1 trichloroethane in the presence of J-sites at 293K was shown to be second order overall (Section 5.2.13). The rate of consumption of 1,1 dichloroethene that is produced from the dehydrochlorination of 1,1,1 trichloroethane over the active surface was also found to be second order overall (Section 5.2.14). The hydrogen chloride produced from the dehydrochlorination of 1,1,1 trichloroethane during the reaction is able to exchange with the chlorine retained at the G-site (Section 5.2.15). Where the G-site contained a radiolabelled [^{36}Cl]-chlorine anion the exchange reaction released [^{36}Cl]-chlorine labelled hydrogen chloride into the gas phase (Section 5.2.15). In the presence of J-sites, 1,1 dichloroethene and hydrogen chloride reacts to form 1,1,1 trichloroethane (Section 5.2.12). Therefore when [^{36}Cl]-labelled hydrogen chloride was present

in the gas phase this reaction led to the formation of [^{36}Cl]-chlorine labelled 1,1,1 trichloroethane (Section 5.2.17). Subsequent dehydrochlorination of the [^{36}Cl]-chlorine labelled 1,1,1 trichloroethane at the J-site produced [^{36}Cl]-chlorine labelled 1,1 dichloroethene. The [^{36}Cl]-chlorine labelled 1,1 dichloroethene then polymerized at a J-site and this resulted in a build up of surface activity (Section 5.2.17, Figure 5.14) owing to the incorporation of the [^{36}Cl]-chlorine into the polymer.

The treatment of γ-alumina at 500K with [^{36}Cl]-chlorine labelled carbon tetrachloride produces labelled G-sites and J-sites. When 1,1,1 trichloroethane was reacted over the activated surface a sharp reduction in the surface count rate was observed in the first 10 minutes of the reaction (Figure 5.14). By selectively labelling the G-site with [^{36}Cl] (Section 5.2.18, Figure 5.16), this sharp decrease in the surface count rate is consistent with the G-site chlorine leaving the surface of the [^{36}Cl]-chlorine labelled carbon tetrachloride treated γ-alumina surface. By exclusively labelling the J-site with [^{36}Cl]-chlorine no change in the surface activity of the solid during the dehydrochlorination of 1,1,1 trichloroethane at 293K is observed (Section 5.2.19, Figure 5.18). Thus it may be concluded that the chlorine retained by the surface at the J-site is not involved in the dehydrochlorination reaction by an intermolecular process.

The 1,1 dichloroethene produced from the dehydrochlorination of 1,1,1 trichloroethane at the J-site was desorbed from the surface (Section 5.2.14, Figure 5.7) and was removed from the gas phase to a small extent via the

reformation of 1,1,1 trichloroethane (Section 5.2.12) from hydrogen chloride. The depletion of 1,1 dichloroethene from the gas phase by the polymerisation process was slow and 1,1 dichloroethene was observed in the gas phase in the presence of activated γ-alumina for periods of up to 3 hours (Figure 5.8). The presence of Lewis acid J-sites are required to polymerise 1,1 dichloroethene (Section 5.2.10). During the polymerisation process of 1,1 dichloroethene at the J-site the colour of the solid changed from the light blue/purple colour associated with the activated γ-alumina surface to a blue/black colour as the polymerisation process progressed. The solid phase retained free running properties and there were no obvious tarring characteristics that had been observed during the polymerisation of 1,1 dichloroethene on $AlCl_3$ (23). The reactions of 1,1,1 trichloroethane and 1,1 dichloroethene at 293K in the presence of carbon tetrachloride treated γ-alumina are summarized in figure 9.6.

The study of the dehydrochlorination of 1,1,1 trichloroethane over $AlCl_3$ suggests that the dehydrochlorination route was effectively concerted and intramolecular but difficulties in surface labelling with [^{36}Cl]-chlorine resulted in the work being inconclusive (23). To account for the solution phase dehydrochlorination of 1,1,1 trichloroethane by $AlCl_3$ it was proposed that the 1,1,1 trichloroethane molecule was adsorbed at a co-ordinatively unsaturated aluminium ion, and the abstraction of chlorine from the 1,1,1 trichloroethane occurred to initiate the dehydrochlorination mechanism via the formation of the 1,1 dichloroethyl carbocation moiety (200).

In the present work it was shown that the chlorine retained by the surface of γ-alumina at the J-site was not removed from the surface in the dehydrochlorination reaction (Section 5.2.19). Thus the chlorine that is associated with the 1,1,1 trichloroethane molecule and adsorbed at the surface is non-equivalent to the chlorine that comprises the J-site. The non-equivalence of the chlorine originating from the 1,1,1 trichloroethane is the key to understanding the dehydrochlorination mechanism with the activated γ-alumina surface.

It is proposed that the treatment of the γ-alumina surface with carbon tetrachloride removes the bridging oxygen anion with the deposition of a chlorine anion on each of the aluminium atoms adjacent to the bridging oxygen, resulting in the surface structure shown in figure 9.3. This structure has one of the chlorine atoms of the dichlorinated aluminium ions bridging with a co-ordinatively unsaturated aluminium ion in the sublayer leaving a singly bonded chlorine atom on the surface co-ordinatively unsaturated aluminium. This singly bonded chlorine atom is not equivalent to the chlorine species from the 1,1,1 trichloroethane because it does not desorb from the surface (Section 5.2.19). Thus the dehydrochlorination mechanism of 1,1,1 trichloroethane in the presence of J-sites is not consistent with the formation of a singly bonded chlorine anion by the abstraction of chlorine from the 1,1,1 trichloroethane, which would be expected to be equivalent to other surface chlorine. The evidence is consistent with a concerted intramolecular dehydrochlorination mechanism

involving a transition state in which the 1,1,1 trichloroethane is adsorbed at the J-site structure of the activated γ-alumina (Figure 9.5). Such a concerted intramolecular mechanism requires that the chlorine which binds to the surface from the $-CCl_3$ group of the 1,1,1 trichloroethane molecule is non-equivalent to the surface bound chlorine that originates from the carbon tetrachloride treatment. The 1,1 dichloroethene and the hydrogen chloride formed from the reaction desorbs from the surface after the dehydrochlorination reaction.

It has been shown that the presence of Lewis acid J-sites are required to polymerize the 1,1 dichloroethene produced by the dehydrochlorination reaction (Section 5.2.10). During the dehydrochlorination reaction of 1,1,1 trichloroethane both the 1,1,1 trichloroethane and 1,1 dichloroethene substrates are present in the gas phase and hence there is competition between them for the available J-sites. It is considered that when a 1,1,1 trichloroethane molecule is adsorbed at a J-site, the site is not available to participate in the polymerisation of 1,1 dichloroethene. When the J-site is free and a 1,1 dichloroethene molecule becomes adsorbed at the J-site, transfer of π electrons from the double bond to the Lewis acid aluminium atom occurs (Figure 9.7) to begin the cationic polymerisation process (23). It is thought that this site is involved exclusively in the polymerisation process at the surface. The polymerisation of 1,1 dichloroethene on the activated catalyst was very slow (Figure 5.8) indicating that the system under study differs from the polymerisation of 1,1 dichloroethene on $AlCl_3$ (23), in which

Figure 9.5

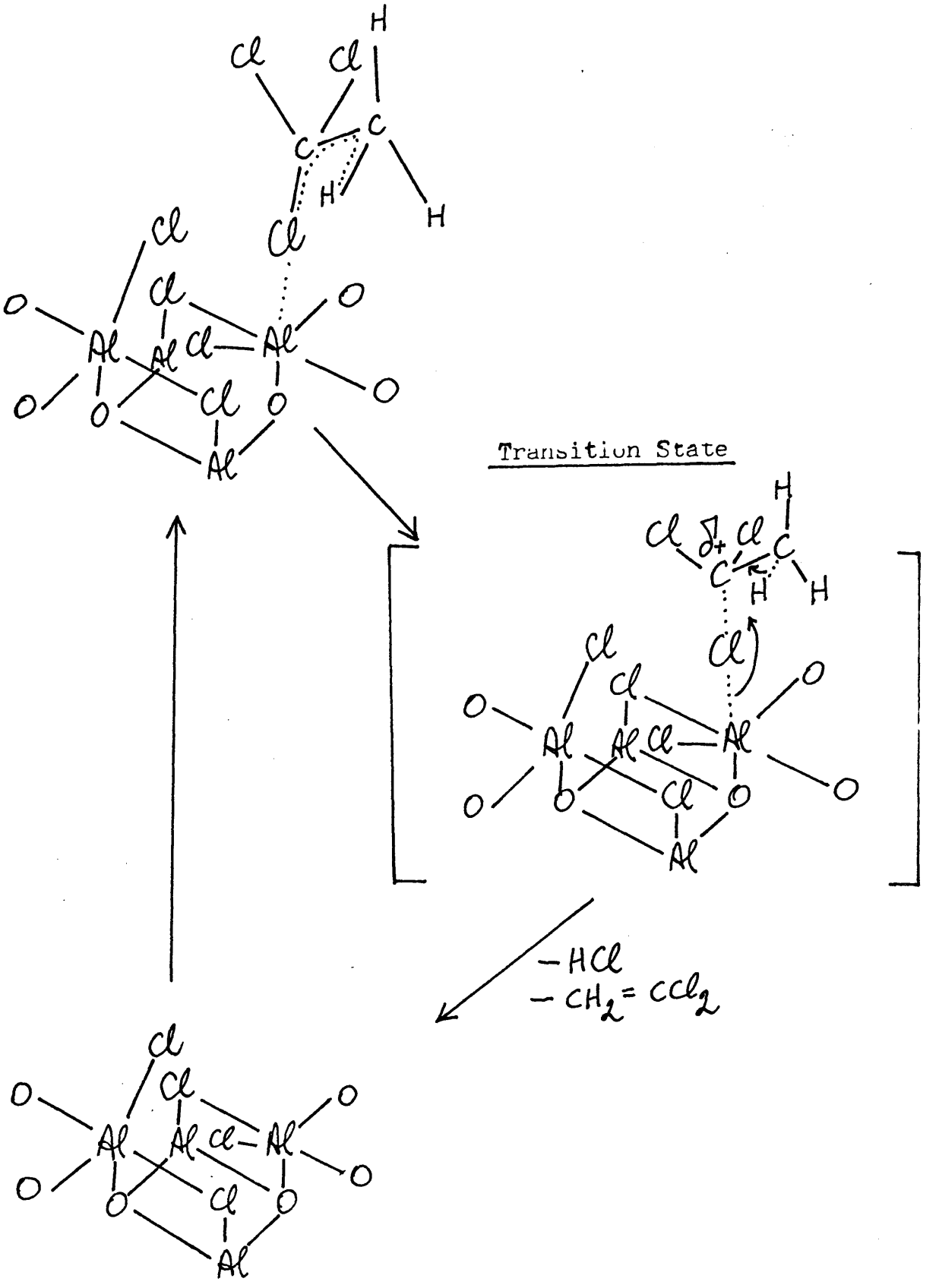

Figure 9.6

Reactions of 1,1,1-trichloroethane over CCl_4/alumina (calcined to 523K); reactions carried out at 293K.

1) $CCl_3CH_3\ (g) \xrightarrow[CCl_4/\text{alumina}]{k1} CCl_3\text{-}CH_3\ (ads)$

2) $CCl_3\text{-}CH_3\ (ads) \xrightarrow[\text{J-site}]{k2} CCl_2{=}CH_2\ (ads) + HCl\ (ads)$

3) $CCl_2{=}CH_2\ (ads) + HCl\ (ads) \xrightarrow[\text{J-site}]{k3} CCl_2{=}CH_2\ (g) + HCl\ (g)$

4) $CCl_2{=}CH_2\ (ads) + HCl\ (ads) \xrightarrow[\text{J-site}]{k-2} CCl_3\text{-}CH_3\ (ads)$

5) $CCl_3\text{-}CH_3\ (ads) \xrightarrow[\text{J-site}]{k-1} CCl_3\text{-}CH_3\ (g)$

6) $HCl\ (g) \xrightarrow[\text{G-site}]{k4} H^*Cl\ (g)$

7) $H^*Cl\ (g) + CCl_2{=}CH_2\ (g) \xrightarrow[\text{J-site}]{k-3} CCl_2{=}CH_2\ (ads) + H^*Cl\ (ads)$

8) $CCl_2{=}CH_2\ (ads) + H^*Cl\ (ads) \xrightarrow[\text{J-site}]{k-2} CCl_2{}^*Cl\text{-}CH_3\ (ads)$

9) $CCl_2{}^*Cl\text{-}CH_3\ (ads) \xrightarrow[\text{J-site}]{k1} CCl^*Cl{=}\ CH_2\ (ads) + H^*Cl\ (ads)$

10) $CCl_2{=}CH_2\ (g) \xrightarrow[\text{J-site}]{k5} CCl_2{=}CH_2\ (ads)$

11) $CCl^*Cl{=}CH_2\ (g) \xrightarrow[\text{J-site}]{k5} CCl^*Cl{=}CH_2\ (ads)$

12) $CCl_2{=}CH_2\ (ads) \xrightarrow[\text{J-site}]{k6} (CCl_2\text{-}CH_2)_n\ (ads)$

13) $CCl^*Cl{=}CH_2\ (ads) \xrightarrow[\text{J-site}]{k6} (CCl^*Cl\text{-}CH_2)_n\ (ads)$

Figure 9.7

Proposed Polymerization of 1,1 Dichloroethene over J-site

Structure of CCl_4 treated γ-Alumina @ 500K.

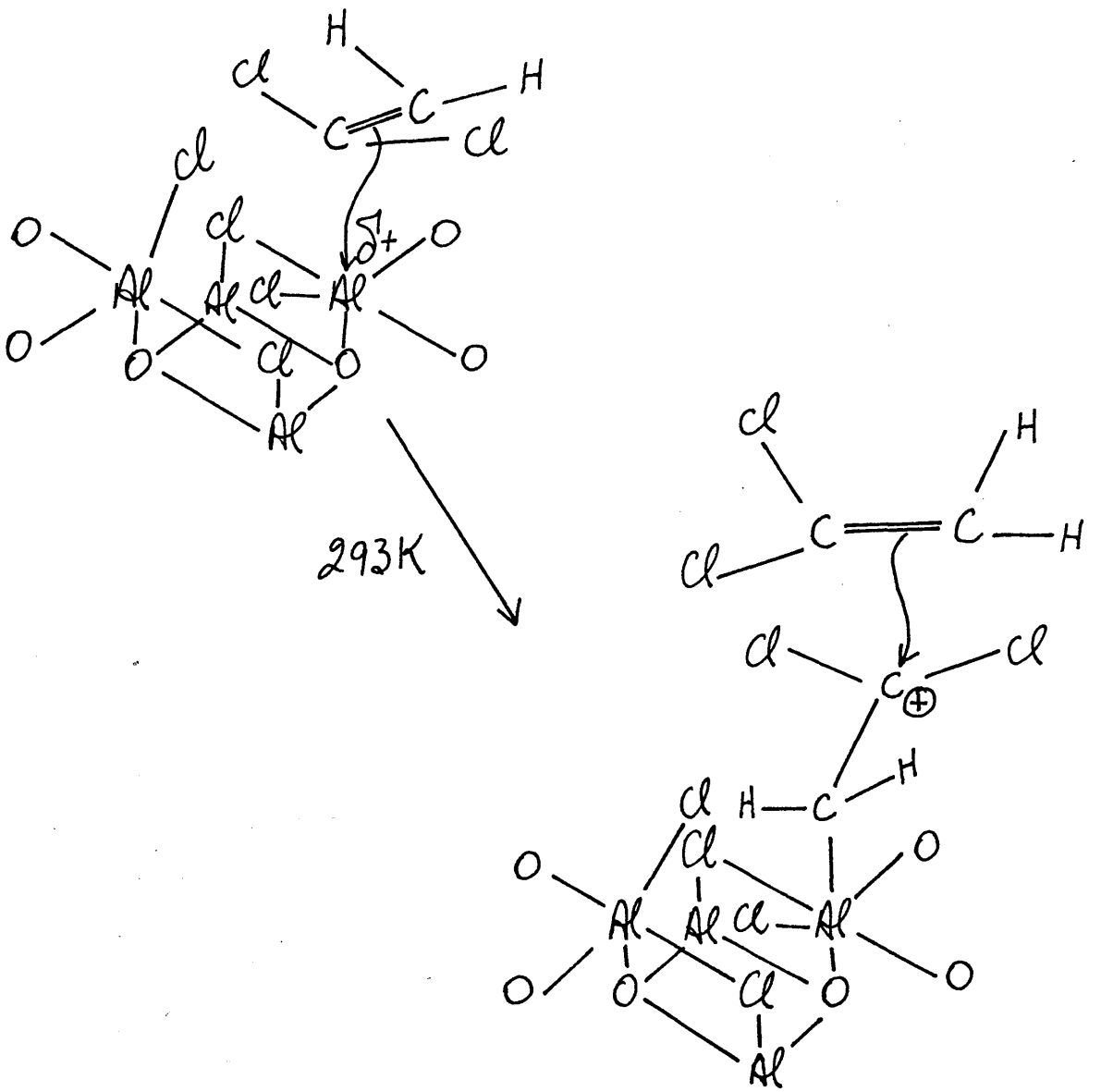

the rate of polymerisation of 1,1 dichloroethene was very fast.

As was noted earlier the γ-alumina material consists of a defect Spinel structure (Section 1.3) of aluminium and oxygen atoms in which approximately 20% of the total Al^{III} ions are present at the surface (62) and are bonded to terminal hydroxyl groups that are localised on distinct sites (69) or water molecules. The probable surface site geometries of the hydroxyl groups can be determined given that the Spinel structured crystallites are bound by the low index plane (Section 1.3, Figure 1E). From this study six distinct aluminium environments of terminal hydroxyl groups can be identified (Figure 1F). Thus from structural considerations alone the γ-alumina surface contains at least six potential Brønsted acid protons, the strength of each being dependent upon the local environment of the hydroxyl group at the surface. These individual environments of the hydroxyl groups can result in differing bonding energies of the adsorbed hydroxyl species (Section 7.1). The differing bonding energies of the adsorbed hydroxyl groups give rise to the range of infrared bands observed from sterically hindered adsorbed Lewis base probe molecules on the surface of γ-alumina (Section 1.4).

From the structural configuration of the local environment of atoms surrounding the hydroxyl group the calcination process will dehydroxylate heteroenergetically the surface of γ-alumina, where the more weakly bonded hydroxyl groups will be the first to be removed at a given calcination

temperature. The removal of the residual hydroxyl groups will require a continuously increasing enthalpy of dehydration owing to the greater affinity of the residual hydroxyl groups for the surface as the calcination process proceeds (73). The B.E.T area results show that a higher surface area resulted as the calcination temperature of the γ-alumina was increased (Table 3.1, Figure 3.1). This increase in the surface area is consistent with the removal of surface species from the sample. Two main regions were observed during the calcination process (Figure 3.1). The region from 293K to 373K is consistent with the desorption of physisorbed water molecules together with the dehydration from the surface of weakly bound hydroxyl groups. The region from 373K to 523K is attributed to the loss of chemisorbed water from the surface together with the loss of water by the dehydroxylation process. The continuously increasing enthalpy of dehydration renders a finite number of hydroxyl groups to be desorbed from the solid at a specific calcination temperature resulting in a decreasing surface density of hydroxyl groups. Conversely the dehydroxylation process will create a finite number of exposed aluminium ions at the surface which gives rise to the Lewis acid sites.

The Lewis acid sites are primarily created from the environment of atoms which make up the weak Al-OH bond strengths, and as the calcination process proceeds, are created through continuously increasing Al-OH bond strengths. Evoking the hard/soft - acid/base formalism of Pearson (77) and given that the hydroxyl groups are strong bases, the Lewis acid sites that are created through the desorption process of hydroxyl groups are

initially weak Lewis acid sites. As the calcination process progresses through the increasing Al-OH bond energies, the newly created Lewis acid sites will be continuously increasing in strength. Hence the Lewis acid strength of an exposed aluminium atom is strongly dependent upon the local environment of atoms around the site. Treatment of the γ-alumina surface with anhydrous hydrogen chloride or carbon tetrachloride may alter the relative strength of the Lewis acid site at the surface of γ-alumina, since oxygen atoms or a hydroxyl group in a near neighbour position is replaced by chlorine atoms. This would have the effect of establishing electronic asymmetry in the region of the Lewis acid site. The electronic asymmetry caused by the chlorination of the γ-alumina material by hydrogen chloride or carbon tetrachloride treatment is shown from the ^{27}Al-MAS NMR results (Section 8.2). An increase in the width of the peak for the octahedral environment of ^{27}Al at half peak height was observed from 1800 Hz for the calcined material to 2200 Hz for the hydrogen chloride treated material to 2450 Hz for the carbon tetrachloride treated material.

Based on an idealized model of γ-alumina the effects of the environments of oxygen and chlorine on the Lewis acidity and Brønsted acidity using cluster model approximations were studied (Section 7.2). The results of the ab-initio molecular orbital single point calculations of tetrahedral and octahedral environments of aluminium clusters confirm that the LUMO orbital energy of a cluster is critically dependent upon the environment of the aluminium atoms in the cluster. The position of the LUMO orbital energy was shown

to be an indicator of Lewis acid character (Section 7.2). The ab-initio molecular orbital calculations of the dehydroxylated tetrahedral aluminium cluster (C7T, Table 7.3) resulted in a lower LUMO orbital energy compared to the equivalent octahedral environment of aluminium (C7O, Table 7.3) which is consistent with the co-ordinatively unsaturated tetrahedral aluminium environment being a stronger Lewis acid site than the co-ordinatively unsaturated octahedral environment. The relative high levels of the LUMO orbital energies of the fully hydroxylated clusters are consistent with the amphoteric properties of the aluminium hydroxides. The acidity of the OH groups present on the surface of γ-alumina can be enhanced markedly by the proximity of chlorine ions for which the electronic asymmetry set up draws electron density from the O-H bond increasing the acidity of the group (92).

The ab-initio molecular orbital calculations using cluster models of monochlorinated co-ordinatively saturated aluminium clusters were consistent with that observation. The results showed that a protonated bridging oxygen which is adjacent to the monochlorinated co-ordinatively saturated aluminium will have strong Brønsted acid character (Section 7.1). The LUMO orbital energy of the aluminium cluster is low lying and situated at the aluminium atom signifying strong Lewis acid character of the aluminium atom (Section 6.3). The cluster model TT4 (Figure 7.2) results in a LUMO orbital energy at -2.62 Hartree, TO2 (Figure 7.3) at -2.52 Hartree and OO2 (Figure 7.4) at -1.19 Hartree (Section 7.2, Table 7.3).

The aluminium environments that are generated by the carbon tetrchloride treatment are strong Lewis acid centres in as much as they catalyse the dehydrochlorination reaction of 1,1,1 trichloroethane and polymerize 1,1 dichloroethene. The ab-initio molecular orbital calculations of such dichlorinated aluminium clusters are consistent with the strong Lewis acid character generated by the J-site. The ab-initio M.O calculations showed that the clusters 006, 007 008 (Figure 7.4) gave LUMO orbital energies of -2.59, -2.10, -2.67 Hartree compared to the starting value of +0.09 Hartree for the fully hydroxylated cluster 001 (Section 7.2, Table 7.3). Dichlorination of the aluminium atom in the cluster has the effect of narrowing the HOMO-LUMO energy gap from a starting value of ca. 8eV to ~2eV (Table 7.3). The catalytic activity in crystallite materials is enhanced where there are increased density of corners and edges (204-205). It is proposed that there is a minimumisation of the energy gap at the corners or edges (Section 6.3) of the crystallite material. The narrowing of the energy gap has the effect of lowering the Fermi level of the cluster, and the position of the Fermi level for a configuration of atoms is critical in determining the catalytic activity (204).

It is proposed that the treatment of the γ-alumina surface with carbon tetrachloride has the effect of enhancing the Lewis acidity by the formation of the J-site structure together with a lowering of the Fermi level for the cluster of atoms that comprises the J-site. The enhanced Lewis acid character of the co-ordinatively unsaturated aluminium attracts electron rich regions of a gas phase molecule to

initiate chemisorption of the substrate. The narrow energy gap enables the flow of electron density from the substrate through the cluster comprising the active site to assist the catalytic reaction to proceed. Desorption of the products reconstitutes the Lewis acid character and energy gap of the J-site.

CHAPTER 10.

Conclusions.

The chlorination of γ-alumina by gaseous hydrogen chloride resulted in surface chlorine which was chemically bound to the surface and was labile to exchange with anhydrous hydrogen chloride at 293K. This treatment of γ-alumina with hydrogen chloride produced a surface which possessed no catalytic activity towards the dehydrochlorination of 1,1,1 trichloroethane or towards the polymerization of 1,1-dichloroethene at room temperature. The surface site produced by the hydrogen chloride treatment of γ-alumina is known as the G-site. The chlorination of the γ-alumina surface via the carbon tetrachloride treatment at 500K resulted in two forms of chlorine on the surface. One form of the surface chlorine was produced by the hydrogen chloride by-product producing the G-sites. The other form of surface chlorine was not labile to exchange with hydrogen chloride,1,1-dichloromethanone or carbon tetrachloride and was found to be catalytically active towards the low temperature dehydrochlorination of 1,1,1 trichloroethane. This site possessed strong Lewis acid character also envoked the polymerization of 1,1 dichloroethene. This site is known as the J-site and was produced by the exchange of a thermally activated deprotonated bridging oxygen with the deposition of two chlorine atoms from carbon tetrachloride or from 1,1 dichloromethanone. It was possible to selectively label either the G-site or the J-site with [^{36}Cl]-chlorine to follow the role of a particular site in the catalytic dehydrochlorination of 1,1,1 trichloroethane. Using this technique the

dehydrochlorination reaction of 1,1,1 trichloroethane was found to occur at the J-site and the degradation process was consistent with a concerted intramolecular dehydrochlorination mechanism. The observed rate order for the depletion of 1,1,1 trichloroethane at 293K from the gas phase in the presence of J-sites was found to be second order overall. The polymerization of 1,1 dichloroethene also occurred at a J-site and the observed rate order for the depletion of 1,1 dichloroethene from the gas phase was found to be second order overall.

From structural considerations of the γ-alumina surface based on the [110] face of an idealized defect Spinel crystallite structure, the surface of γ-alumina contains six Brønsted acid protons. Using the interatomic distances obtained from an X-ray diffraction analysis of calcined γ-alumina, ab-initio molecular orbital calculations using cluster model approximations based on the probable site geometries of the aluminium environments of terminal hydroxyl groups and their chlorinated analogues suggest that the strength of each Brønsted proton is dependent upon the local configuration of atoms surrounding the terminal hydroxyl groups present at the surface. The calcination process dehydroxylates heteroenergetically the surface of γ-alumina creating co-ordinatively unsaturated aluminium atoms. These exposed aluminium atoms are considered to be the source of Lewis acidity, the strength of which is also dependent upon the local configuration of atoms surrounding the Lewis acid site. The ab-initio calculations indicated that the LUMO orbital energy was a good indicator

of Lewis acid character for a given cluster of atoms in that the lower the LUMO orbital energy the stronger was the Lewis acid character of the cluster of atoms. The magnitude of the deprotonation energy was found to be a good indicator of Brønsted acid character for a given protonated cluster and the ab-initio molecular orbital calculations suggest that a good Brønsted acid site would possess a strong Lewis acid species in an near neighbour position to the Brønsted proton. The incorporation of chlorine into the cluster models enhanced both the Lewis acid character of the dehydroxylated cluster and the Brønsted acid character of a hydroxylated cluster and this observation was in good agreement with the experimental findings. It was also observed from the ab-initio SCF calculations that the HOMO-LUMO energy gap for a given cluster was reduced by the incorporation of chlorine into the cluster. The narrowing of the energy gap being synonomous with a lowering of the Fermi level of the cluster of atoms.

REFERENCES

1. H. Knözinger and P. Ratnasamy, Catal. Rev. Sci., Eng., 1978, 17, 31.
2. F.S. Stone, 'Chemistry and Chemical Engineering of Catalytic Processes', ed. R. Prins and G.C.A. Schuit, (Nato Adv. Study E39, 1980).
3. B.C. Gates, J.R. Katzer and G.A. Schuit, 'Chemistry of Catalytic Processes', McGraw - Hill Chemical Engineering Series, 1979, 184.
4. P.C.H. Mitchell, Catalysis, 1977, 1, 204.
5. H. Topscoe, R. Candia, N.Y. Topscoe and B. Clausen, Bull.Soc.Chim.Belg., 1984, 93, 783.
6. T. Pasryjczak and P. Zienlinski, React. Kinet. Catal. Lett., 1982, 20, (3-4), 357.
7. J.M. Zowtiak, G.D. Weatherbee and C.H. Bartholomew, J. Catal., 1983, 82, 230.
8. G.D. Weatherbee and C.H. Bartholomew, J. Catal., 1984, 87, 55.
9. G.D. Weatherbee, J.L. Rankin and C.H. Bartholomew, Appl. Catal., 1984, 11, 73.
10. K. Lu and B.J. Tatarchuk, J. Catal., 1987, 106, pp166-175.
11. F.M. Dautzenberg and H.B.M. Wolters, J. Catal., 1978, 51, 26.
12. G.J. Den Otter and F.M. Dautzenberg, J. Catal., 1978, 53, 116.
13. L. González Tejuca, K. Alka, S. Namba and J. Turkevich, J. Phys. Chem., 1977, 81, 1399.
14. P.G. Menon and G.F. Froment, J. Catal, 1979, 59, 138.

15. P.G. Menon and G.F. Froment, Appl. Cat., 1981, 1, 31.

16. Z. Paál and P.G. Menon, Catal. Rev. Sci. Eng., 1983, 25 (2), 229.

17. C.R. Apesteguia, T.F. Garetto and A. Borgna, J. Catal., 1987, 106, pp73-84.

18. C.S. John and M.S. Scurrell, Catalysis Vol.1, Specialist Report, Chem . Socy, London, 1977, 136.

19. B.C. Gates, J.V. Boegel and G.A. Fuentes, J. Catal, 1982, 78, 436.

20. J.H. Sinfelt, Adv. Chem. Eng., 1964, 5, 37.

21. F.G. Ciapetta and D.N. Wallace, Catal. Rev., 1971,5,67.

22. A.G. Goble and P.A. Lawrance, Proc. Int. Congr. Catal., 3rd Amsterdam, 1964, p320.

23. D.G. McBeth, Ph.D Thesis, University of Glasgow, 1987.

24. W.L. Archer, Ind. Eng.Chem.Prod.Res.Dev., 1982, 21, 670.

25. T. Draper, Ph.D Thesis, University of Glasgow, 1980.

26. U. Steinike, Z. Anorg. Allg. Chem., 1965, 338, 78.

27. V.A. Dzis'ho, M. Kolovertnova, T.S. Vinnikóva and Y.O. Bulgakova, Kinet. Katal., 1966, 7, 655.

28. J.H. deBoer, J.M.H. Fortuin, B.C. Lippens and W.H. Meys, J. Catal., 1963, 2, 1.

29. K. Pohl and G. Rubentisch, Chem. Technol., 1966, 18, 496.

30. J.B. Peri, J. Phys. Chem., 1965, 69, 231.

31. H. Dunken, P. Fink and E. Pilz, Chem. Technol., 1966, 18, 490.

32. G.M. Schwab and H. Kral, Proc. 3rd Congr. Catal., Vol.1, 1965, p433.

33. B.D. Flockhart, C. Naccacke, J.A.N. Scott and R. Pink, J. Chem.Soc., Chem. Commun., 1965, 238.

34. J.A.N. Scott, B.D. Flockhart and R.C. Pink, Proc. Chem. Soc., 1964, 139.

35. N.D. Parkyns and B.C. Patterson, J. Chem. Soc., Chem. Commun., 1965, 30.

36. F.A. Cotton and G. Wilkinson 'Advanced Inorganic Chemistry', J. Wiley & Sons, 4th Ed., 1980, 329.

37. J.J. Kipling, D.B. Peakall, J. Chem. Socy., 1957, 834.

38. F.C. Frany, Ind. Eng. Chem., 1946, 38, 129.

39. H.C. Stumpf, A.S. Russel, J.W. Newsome and C. Tucker, Ind. Eng. Chem., 1950, 42, 1398.

40. H. Thibon, J. Charrier and R. Tertian, Bull. Soc. Chim., Fr., 1951, 384.

41. H.P. Rooksby, 'X-Ray Identification and Crystal Structure of Clay Minerals', The Mineralogical Socy., London, 1951.

42. K.B. Day and V.J. Hill, Nature, 1952, 170, 539.

43. K.B. Day and V.J. Hill, J. Phys. Chem., 1953, 57, 946.

44. J.F. Brown, D. Clark and W. Elliot, J. Chem. Soc., 1953, 84.

45. H. Krishner, Ber. dt. keram. Ges., 1966, 43, 479.

46. B.C. Lippens, 'Structure and Texture of Aluminas', Thesis,Delft University of Technology, The Netherlands, 1961.

47. H. Saalfeld, Neues Jb. Miner Abh., 1960, 95, 1.

48. L.L. van Reijen, Thesis, Technical University of Eindhoven, The Netherlands, 1964.

49. L.E. Oomes, J.H. deBoer and B.C. Lippens, 'Reactivity of Solids', Editor J.H. deBoer, Elsevier, Amsterdam, 1961, pp317-320.

50. B.C. Lippens, Chem. Weekbl., 1966, 62, 336.

51. J.H. deBoer, J.M.H. Fortuin and J.J. Steggerda, Proc. K. ned. Akad. Wet, 1954, B57, 170, 434.

52. J.J. Steggerda, Thesis, Delft University of Technol, The Netherlands, 1955.

53. R. Tertian and D. Papée, J. Chim. Phys., 1958, 55, 341.

54. E.J.W. Verwey Z. Kristallogr, 1935, 91, 37.

55. R.C. Evans, 'Crystal Chemistry', 2nd Ed., Cambridge Univ. Press, 1966, 174.

56. A.F. Wells, 'Structural Inorg. Chem., 3rd Ed., Oxford Press, London, 1962, 556.

57. H. Jagodszinski and H. Saalfeld, Z. Kristallogr, 1958, 110, 197.

58. J.M. Cowley and A.L.G. Rees, Rep. Prog. Phys., 1958, 21, 165.

59. R.A. van Nordstrand, Proc. Symp. Techniques Catalyst Prep., Dallas, Texas, 1956, p43.

60. H. Saalfeld and B.B. Mehrotra, Ber. dt. keram. Ges., 1965, 42, 161.

61. J.H. de Boer and G.M.M. Houben ,'Proceedings 2nd Int. Symp. Reactive Solids', Gothenburg, 1952.

62. S. Soled, J. Catal., 1983, 81, pp252-257.

63. H. Knözinger and P. Ratnasamy, Catal. Rev. Sci. Eng., 1978, 17(1), 31.

64. D.S. McIver, H.H. Tobin and R.T. Barth, J. Catal., 1963, 2, 485.

65. J.H. de Boer, J.M.H. Fortuin, B.C. Lippens and W.H. Meys J. Catal., 1963, 2, 1.

66. J. B. Peri and R.B. Hannan, J. Phys. Chem., 1960, 64, 1526.

67. M.R. Basila, Appl. Spectros. Rev., 1968, 1(2), 289.

68. M.L. Bair, 'Infrared Spectroscopy in Surface Chemistry Chpt. V, Dekker, N.Y., 1967.

69. J.B. Peri, J. Phys. Chem, 1965, 69, 211.

70. J.B. Peri, J. Phys. Chem., 1965, 69, 220.

71. J.K. Lee and S.W. Weller, Anal. Chem., 1958, 30, 1057

72. H.P. Boehm, Adv. Catal. Relat. Subj., 1966, 16, 179.

73. E.B. Cornelius, T.H. Milliken, G.A. Mills, and A.G. Oblad, J. Phys. Chem., 1955, 59, 809.

74. D.M. Brouwer and H. Hogeveen, Prog. Phys. Org. Chem., 1972, 9, 179.

75. J.N. Brønsted, Z. Phys. Chem., 1924, 108, 185.

76. J.N. Brønsted and R.P. Bell, Proc. Roy. Soc., 1934, 143A, 377.

77 R.G. Pearson, J. Chem. Educ., 1968, 45, 581, 643.

78. B.D. Flockhart and R.C. Pink, J. Catal., 1967, 8, 293.

79. M.S. Goldstein, "Experimental Methods in Catalytic Research", Ed., R.B. Anderson, Academic Press, N.Y., 1968, p361.

80. K. Tanabe, "Solid Acids and Bases", Academic Press, N.Y., 1970.

81. F. Forni, Catal. Rev., 1973, 8, 69.

82. H.H. Voge, Catalysis, 1958, 6, 407.

83. F.E. Condon, Catalysis, 1958, 6, 43.

84. R.M. Kennedy, Catalysis, 1958, 6, 1.

85. G.A. Olah, "Friedel-Crafts Chemistry", Wiley, N.Y., 1973, p43.

86. A.G. Oblad, G.A. Mills and H. Heinemann, Catalysis, 1958, 6, 341.

87. E.P. Parry, J. Catal., 1963, 2, 371.

88. H. Pines and W.O. Haag, J. Am. Chem. Soc., 1960, 82, 2471.

89. W.K. Hall, F.E. Lutinski and H.R. Gerberich, J. Catal., 1964, 3, 512.

90. M.R. Basila and T.R. Kanter, J. Phys. Chem., 1967, 71, 467.

91. T.R. Hughes and H.M.White, J. Phys. Chem., 1967, 71, 2192.

92. J. Dewing, G.T. Monks and B. Youll, J. Catal., 1973, 44, 226.

93. H.A. Benesi, J. Catal, 1973, 28, 176.

94. A. Corma, C. Rodellas and V. Fornés, J. Catal, 1984, 88, 374.

95. P.A. Jacobs and C.F. Heylen, J. Catal, 1974, 34, 267.

96. E.R.A Matulewicz, F.P.J.M. Kerkof, J.A.Moulijn and H.J. Reitsma, J. Colloid. Int. Chem., 1980, 77, 110.

97. M.W. Tamele, L.B. Ryland, L. Rampino and W.G. Schlaffer, 3rd World Pet. Congr. Proc., 1951, 4, 98.

98. A.E. Hirschler, J. Catal., 1963, 2, 428.

99. M. Tanaka and S. Ogasawara, J. Catal., 1970, 16, 157.

100. A. Melchor, E. Garbowski, M.V. Mathieu and M. Primet, J. Chem. Soc. Faraday Trans I, 1986, 82, 1893.

101. D.J. Milne, Ph.D. Thesis, University of Newcastle, Australia, 1974.

102. G. Blumenthall, R. Luck and G. Wegner, Freiberg Forschungsh A., 1981, 653, 101.

103. T. Bertoti, A. Toth, I.S. Pap and T. Szekely (Editor W. Henninger), Thermal Analysis, Proc. 6th I.C.T.A, Bayreuth, 1980, Birkhauser, Verleig, Bawel, 1980, p235.

104. J. Basset, M.V. Mathieu and M. Prettre, Rev. Chim. Miner, 1968, 5, 879.

105. D.J. Milne and L.J. Wibberly, A.I.M.E., 1978, 147.

106. H.P. Alder, H. Geisser, A. Baiker and W. Richarz, A.I.M.E, 1979, 336.

107. A. Toth, I. Bertoti and T. Szekely, Thermochim. Acta., 1982, 52, 211.

108. I. Bertoti, A. Toth, T. Szekely and I.S. Pap, Thermochim. Acta, 1981, 44, 325.

109. F. Seon, G. Picard and B. Tremillon, Electrochim. Acta, 1983, 28, 209.

110. H.P. Alder, H. Geisser, A. Baiker and W. Richarz, Light Metals, 1979, 3, 337.

111. A. Landsberg, Metall. Trans. B., 1975, 6B, 207.

112. A. Bergholm, Trans. Metall. Soc., A.I.M.E., 1961, 221, 1121.

113. D.J. Milne and L.J. Wibberley, Light Metals, 1978, 2, 147.

114. G.A. Olah, "Friedel-Crafts Chemistry", Wiley, 1973, 420.

115. D.J. Milne, Proc. Australas. Inst. Min. Metall., 1976, 260, 23.

116. R.P. Raval and S.J. Dixit, J. Chem. Tech. Biotechn., 1979, 29, 107.

117. I. Bertoti, B. Podor, J. Mink, I.S. Pap, A. Szabo and T. Szekely, "Alumine Alum", 1982, 17, 185.

118. I. Barin and W. Schuler, Metall Trans B, 1980, 11B, 199.

119. M. Stern and H.H. Uhlig, J. Electrochem. Soc., 1952, 99, 381.

120. M. Stern and H.H. Uhlig, J. Electrochem Soc., 1953, 100, 543.

121. J.D. Minford, M.H. Brown and R.H. Brown, J. Electrochem. Soc., 1959, 106, 185.

122. W.L. Archer and M.K. Harter, Corrosion, 1978, 35(5), 159.

123. W.L. Archer and E.L. Simpson, Ind. Eng. Chem. Prod. Res. Dev., 1977, 16, 158.

124. I. Mochida and Y. Yoneda, J. Catal, 1967, 8, 223.

125. Z.A. Foroulis and M.J. Thubrickar, J. Electrochem. Soc , 1975, 122(10), 1296.

126. I. Mochida, J. Take, Y. Saito and Y. Yoneda, J. Organic Chem., 1967, 32, 3894.

127. I. Mochida, A. Uchino, H. Fujitsu and K. Takeshita, J. Catal., 1976, 43, 264.

128. I. Mochida, Y. Anju, A. Kato and T. Seizama, Bull. Chem. Soc. Japan., 1972, 45, 1635.

129. I. Mochida, Y. Anju, A. Kato and T. Seizama, J. Org. Chem., 1974, 39, 3785.

130. H. Knözinger, H. Bull, and K. Kochloefl, J. Catal., 1972, 24, 57.

131. I. Mochida, Y. Anju, A. Kato and T. Seizama, Bull. Chem. Soc. Japan., 1970, 43, 2245.

132. I. Mochida, A. Uchino, H. Fujitsu and K. Takeshita, J. Catal., 1978, 51, 72.

133. G. Engelhardt, U. Lohse, A. Samoson, M. Mägi, M. Tarmak and E. Lippmaa, Zeolites,1982, 2, pp59-62.

134. E. Lippmaa, M. Mägi, A. Samoson, G. Engelhardt and A.H.R. Grimmer, J. Am. Chem. Soc., 1980, 102, 4889.

135. I.E. Maxwell, W.A. van Erp, G.R. Hays, T. Couperus, R. Huis and A.D.H. Clague, J. Chem. Soc., Chem. Commun., 1982, 523.

136. S. Ramdas, J.M. Thomas, J. Klinowski, C.A. Fyfe and J.S. Hartman, Nature, 1981, 292, 228.

137. M.J. Melchior, D.E.W. Vaughan and A.J. Jacobson, J. Am. Chem. Soc., 1982, 104, 4859.

138. J.M. Thomas, C.A. Fyfe, S. Ramdas, J. Klinowski and G.C. Gobbi, J. Phys. Chem., 1982, 86, 3061.

139. M.J. Melchior, D.E.W. Vaughan, R.H. Jarman and A.J. Jacobson, Nature, 1982, 298, 455.

140. C.A. Fyfe, G.C. Gobbi, J.S. Hartman, J. Klinowski and J.M. Thomas, J. Phys. Chem., 1982, 86, 1247.

141. F. Fairbrother and J.F. Nixon, J. Chem. Soc., 1958, 3224.

142. G. Brauer, "Handbook of Preparative Inorganic Chemistry", Vol. 1, Academic Press (London)Ltd., London, 2nd Edn., 1965.

143. A.J. Vogel, Textbook of Prac. Organic Chem., Longmans, 1962, pp 179-180.

144. R.N. Maxson, Inorg. Synth., 1939, 1, 147.

145. H.A. Taylor and W.E. Hanson, J.Chem.Phys., 1939,7,418.

146. G. Friedlander, J.W. Kennedy and J.M. Miller, "Nuclear and Radiochemistry", 2nd Ed., J. Wiley and Sons Inc., N.Y., pp146-148.

147. C.M. Lederer and V. Shirley, editors, "Table of Isotopes", 7th Ed., Wiley Interscience, N.Y. (1978).

148. G. Friedlander, J.W. Kennedy and J.M. Miller, 'Nuclear and Radiochemistry', 2nd Ed., J. Wiley and Sons Inc., N.Y., pp171-175.

149. K.A. Brownlee "Statistical Theory and Methodology in Science and Engineering", Wiley, N.Y. 1960.

150. C.A. Bennet and N.L. Franklin, "Statistical Analysis in Chemistry and Chemical Industry", Wiley, N.Y., 1954.

151. E. Breitenberger, "Scintillation-Spectrometer Statistics", Progress in Nuclear Physics, Vol. 4., (O.R. Frisch, Ed.),

Pergamon, London, 1955, pp56-94.

152. A.S. Al-Ammar and G. Webb, J. Chem. Soc., Faraday Trans I, 1978, 74, 195.

153. G.A. Kolta, G. Webb and J.M. Winfield, Appl. Catal., 1982, 2, 257.

154. R. Belcher and A.J. Nolk, "Quantitative Inorganic Analysis", Butterworth and Co., Ltd., London, 3rd Ed., 1970, p56.

155. Nuclear Data Sheets, Ed. by the Nuclear Data Group of the National Academy of Sciences- National Research Council, Washington D.C., Vol.5, No. 3.

156. K.W. Dixon, Ph.D. Thesis, University of Glasgow 1986.

157. Brunauer, Emmet and Teller, J.A.C.S., 1938, 60, 309.

158. G.D. Halsey, Disc. Faraday Soc., 1950, 8, 54.

159. D.R. Stranks and R.G. Wilkins, Chem. Rev., 1957, 57, 743.

160. F. Joliot and I. Curie, Nature, 1934, 133, 201.

161. M.F.A. Dove and D.B. Sowerly, "Halogen Chemistry", Editor V. Gutman, Academic Press, 1967, 1, 41.

162. G.T. Seaborg, Chem. Rev., 1940, 27, 199.

163. S.J. Thomson and G. Webb, "Heterogeneous Catalysis", Oliver and Boyd, 1968.

164. H.A.C. McKay, Nature, 1938, 142, 997.

165. Halogen Chemistry, Ed. Gutmann, Academic Press, 1967, Vol. 1, 52.

166. K. Clusuis and H. Haimerl, Z. Physik Chem., 1942, 51B, 347.

167. I.M. Pearson and C.S. Garner, J. Chem. Phys., 1960, Vol. 32, 4, 1214.

168. D.R. Stull, Ind. Eng. Chem., 1947, 39, 57.

169. J. Langmuir, J. Am. Chem. Soc., 1916, 38, 2221.

170. T.R. Hughes, H.M. White and R.J. White, J. Catal., 1969, 13, 58.

171. A.N. Webb, Ind. Eng. Chem., 1963, 49, 261.

172. P. Strand and M. Kraus, Coll. Czech. Chem. Com., 1965 30, 1136.

173. K. Matsuura, T. Watnanabe, A. Suzuki and M. Itoh, J. Catal, 1972, 26, 127.

174. V.V. Yushechenki and T.V. Antipina, Kinet. Katal., 1970, 11, 134.

175. P.O. Scokart, S.A. Selim, J.P. Damon and P.G. Rouxhet, J. Coll. Int. Chem., 1979, 70, 209.

176. J.S. Binkley, J.A. Pople and W.J.Hehre , J.Am. Chem. Soc., 1980, 102, 939.

177. H. Kawakami, S. Yoshida and T. Yonezawa, J. Chem. Soc., Faraday Trans. 2, 1984, 80, 205.

178. L. Pauling, The Nature of the Chemical Bond, Cornell Univ. Press, Ithaca, 3rd Edn., 1960.

179. B.C. Gates, J.R. Katzer and G.A. Shuit, 'Chem. of Catal. Proc', McGraw Hill Chem. Eng., Series, 1979, 227.

180. W. Grabowski, M. Misono and Y. Yonoda, J. Catal., 1980, 61, 103.

181. K. Tukui and H. Fuzimoto, Bull of the Chem. Soc Japan, 1968, 41, 1989.

182. J.H. Lunsford, L.W. Zingery and M.P. Rosynek, J. Catal, 1975, 38, 179.

183. L. Salem and J.S. Wright, J.Am.Chem.Soc., 1969, 91, 5947.

184. R.G. Pearson Theor. Chim. Acta, 1970, 16, 107.

185. R.G. Pearson, Acta. Chem. Res., 1971, 4, 152.

186. K. Fukui, Bull. Chem. Soc. Jap., 1968, 39, 498.

187. R.F. Bader, Can. J. Chem., 1962, 40, 1164.

188. H. Fujimoto and K. Fukui, 'Chemical Reactivity and Reaction Paths', Ed. G.Klopman, (J.Wiley, N.Y., 1974)

189. F.D. Mango, "Advances in Catalysis", Editors D.D.Elsey, H. Pines and P.B. Weisz, Vol. 20, 291, Academic Press, N.Y., 1969.

190. R. Hoffman and R.B. Woodward, Accounts Chem. Res., 1968, 1, 17.

191. H. Kawakami and S. Yoshida, J. Chem. Soc., Faraday 2, 1984, 80, 205.

192. M.S. Gordon, J.S. Binkley, J.A. Pople, W. Pietro and W.J. Hehre, J.Am.Chem.Soc., 1982, 104, 2797.

193. M. Dupuis, D. Spangler, J.J. Wendoloski, N.R.C.C. Program QG01 (1980).

194. M. Dupuis, J. Rys and H.F. King, HONDO5, QCPE 13, (1981), 401.

195. V.R. Saunders, M.F. Guest, ATMOL 3 Part 9, RL-76-106 (1976)

196. M.F. Guest and V.R. Saunders, Mol. Phys, 1974, 28, 819.

197. W.J. Hehre, W.A. Lather, R. Ditchfield, M.D. Newton and J.A. Pople, GAUSSIAN-70 program No. 236, Q.C.P.E., Indiana University, 1973.

198. J.S. Binkley, R.A. Whiteside, R. Krishman, R. Seeger, D.J. De Frees, H.B. Schlegel ,S. Topial ,L.R. Kahn, J.A. Pople; GAUSSIAN 80, Q.C.P.E. 13, 406 (1980)

199. D. Müller, G. Scheler, Chem. Phys. Lett. , 1979, No.1, 59.

200. N. Winterton; I.C.I. Internal Report.

201. C.J. Drewitt, R.D. Shannon, D.B. Rogers, A.W. Sleight, Inorg. Chem., 1969, 8, 1985.

202. 'Organic Chemistry", L. Finar, 4th Ed., Longmans (1964) 382.

203. "Introduction to Quantum Electronics", P. Hlawiczka, Academic Press, 1971, 114.

204. G. Somorjai; Cat. Rev., 1973, 7, 87.

205. R.W. Joyner, B. Lang, G.A. Somorjai, J. Catal., 1972, 27, 405.

206. Th. Wolkenstein, J. Phys. Chem. (USSR), 1958, 32, 2383.